Robust Filtering

Garry Allan Einicke, B.E., M.E.

Thesis submitted as a requirement for the degree of Doctor of Philosophy

June, 1995

THE UNIVERSITY OF ADELAIDE

DEPARTMENT OF ELECTRICAL AND
ELECTRONIC ENGINEERING
SOUTH AUSTRALIA

Abstract

This study is concerned with filters that are robust to uncertainties in either the signal models or the noise statistics. The thesis begins with some extensions to an interpolation approach to solving a continuous-time, linear, stationary H_∞ filtering problem. The generalisations include specified noise variances, coloured observation noise, frequency weighted estimation error and the discrete-time case. The well known continuous-time, game-theoretic results are then presented and a comparison is drawn with the interpolation approach. A refinement for the accommodation of additive and multiplicative model uncertainty is proposed and it is shown that the robust H_∞ solution is sufficient for the original uncertain filtering problem. The arguments used in the development of the continuous-time, game-theoretic H_∞ filter are applied to specialise the discrete-time control results to filtering. It turns out that the game-theoretic H_∞ filter possesses the structure of the Kalman filter and the gain calculation is the same, the only difference arises in the quadratic term of the Riccati equation. Although all the theory may be known, the same is not true of the cost benefits. To this end, the Kalman and H_∞ solutions for output estimation and equalisation problems are compared. Both known and uncertain signal models are considered. Nonlinear filtering is introduced subsequently where nonlinear observers are designed using false algebraic Riccati equations. This technique trades off optimality for error stability and some demodulation examples are presented to demonstrate an advantage compared to the extended Kalman filter (EKF). This work culminates in the development of a robust EKF, where the truncation of the Taylor series terms is motivated as a model uncertainty problem. The extension to nonlinear direct feedthrough functions is also described. Finally, the results of simulation studies are presented to illustrate benefits when the problems are sufficiently nonlinear.

Preface

I am indebted to Bruce Davis, Marie-Antoinette Poubelle, Michael Green and Lang White. "Most of the ideas are theirs, while all the misinterpretations and prejudices are mine", [Kokotovic, IEEE Cont. Sys. Mag., Jun. 1992]. Another's acknowledgement is used to emphasise that the work reported herein has indeed been a collaborative effort.

I am grateful to Associate Professor Bruce Davis for being my supervisor. Bruce helped me to decipher two key papers [Shaked, IEEE Trans. AC, May 1990; Limebeer, Green and Walker, CDC, 1989] and showed me how to solve algebraic Riccati equations.

The Cooperative Research Centre for Robust and Adaptive Systems (CRASYS) has been a great influence. It has been an inspiration to rub shoulders with the highly motivated people in Systems Engineering, ANU. Thanks to Marie-Antoinette Poubelle for putting so much energy into CRASYS. M^{elle} Poubelle also suggested the use of the false algebraic Riccati equation in the construction of nonlinear observers.

I spent my first year barking up the wrong tree, with a frequency domain approach to filtering - Brian Anderson suggested how one might proceed in the nonlinear case, but it all seemed too hard. Fortunately, I bumped into Michael Green at the bar during a CRASYS function, who proceeded to map out the virtues of the four block problem on the back of a coaster. Michael then gave a course on H_∞ control which made the mud clearer for me. The method used to accommodate model uncertainty was based on advice from Michael.

I am privileged to have Lang White as my external supervisor, who provided the research topic, directed my work, kept me motivated and on track. This thesis culminates in the development of a robust EKF. The very idea of using a H_∞ design to provide robustness against linearisation errors was suggested by Lang. Quite a few weeks were then spent running simulations, until almost by accident the EKF was observed to produce an outlier in one realisation of a thousand, whereas the robust version did not.

I do claim however to have independently discovered two optimal filters: the short circuit for high SNR filtering and the open circuit for low SNR non-minimum phase equalisation.

In addition, thanks to Neil Bryans for giving me the nod to go ahead, the members of Signals Analysis Discipline who have aided me in rewriting my explanations and anglicising this thesis. Most importantly of all, I thank Marise, Jak and Chloe for their moral support.

This work has been supported by three institutions: Communications Division, Defence, Science and Technology Organisation, CRASYS and the Department of Electrical and Electronic Engineering, University of Adelaide. I am grateful to the individuals concerned.

Finally, I hereby declare that this work contains no material which has been accepted for the award of any other degree or diploma in any university or other tertiary institution and, to the best of my knowledge and belief, contains no material previously published or written by another person, except where due reference has been made in the text. I give consent to this copy of my thesis, when deposited in the University Library, being made available for loan and photocopying.

Garry Einicke
30th June, 1995.

Contents

Chapter 1

Introduction

This thesis is a study of robust filters. The problem is motivated in Section 1.1 where it is argued that erroneous problem assumptions occur quite naturally and that robust filters are desirable. Some preliminary notation is defined in Section 1.2, the treatment is brief and the readers are referred to texts such as [DV, F, GL] for a full account. Robust filters are introduced in Section 1.3 and subsequently a historical perspective of robust filter theory is set out in Section 1.4. An overview of the contributions are listed in Section 1.5.

1.1 Motivation - a perceived need for robustness.

The notion of robustness is certainly not new. In hardware design it is a good practice to ensure that a circuit can tolerate specified varations in the supply voltages. In the design of software it is prudent to accommodate unlikely input conditions. Similarly it is desirable that filters have some robustness to errors in the underlying assumptions.

The very nature of engineering is to proceed with some simplifying assumptions and deliver a cost benefit. Clearly the errors introduced by the assumptions represent a cost. More often than not, there are errors present in the filtering problem assumptions. Errors can arise by approximation, ignorance or out of economic considerations. For example, nonlinear systems are frequently approximated by linear systems. The dynamics of the applications at hand may not be well understood. There may be many phenomena at play, which are lumped together via stochastic models bearing little or no resemblence to the physics of the underlying processes. The price of real time implementation may constrain one to using simplified models.

Most traditional solutions to signal processing problems are based on minimum variance methods. For example, in classical approaches to filtering, it is assumed that the models are exact and that the exogenous signals are white processes. These assumptions are

implicit in the formulation of signal processing toolboxes within design packages such as *Matlab*®, *Matrix-X*®, *Xmath*® and *Entropic*®. A concern is that there may be a tendency for engineers to routinely enter in the parameters of the problem and place too much trust in the conventional design. Arguably it is important to ask "What happens if the signal models are in error and the noises are not white ?" It is this question that has motivated the work described herein. It turns out that when the inputs are white, the variances are known and the models are exact then it is difficult to "improve" on the minimum variance techniques. The term "improve" refers to exhibiting some robustness at the expense of increased error variance. However the performance of classical methods can degrade severely when uncertainties are present, whereas robust designs can sometimes yield performance benefits. Arguably, it can be advantageous for design engineers have some familiarity with the robust toolboxes that are emerging in the marketplace.

The scope is obviously limitless. Every signal processing solution relying on linear gaussian assumptions is a potential candidate for robustness. The possible filtering applications would no doubt include estimation, demodulation and identification. Robust designs promise to accommodate both uncertainties in the exogenous inputs and uncertainties in the signal models. There are countless permutations of modelling errors and non-ideal signals that could be considered. Consequently the range of interest addressed here is narrowed down considerably.

The objectives of this study include

- Focus on the communications applications of output estimation and equalisation.
- Explain how robust methods may be applied to both continuous-time and discrete-time filtering problems.
- Investigate the consequences of modelling errors when there is either implicit or explicit robustness built in the design to accommodate the uncertainties.
- Even though robust designs promise to accommodate uncertainties in the inputs, undertake performance comparisons with the Kalman filter when inputs are in fact Gaussian.
- Explore the application of robust techniques to the nonlinear filtering problems of demodulating frequency or phase modulated signals.
- Identify the cost benefits of robust designs.

1.2 Preliminary notation.

1.2.1 Continuous-time systems.

Linear systems. This study is mostly concerned with finite dimensional, linear, time-invariant systems. Continuous-time systems may be represented in state space form as

$$\dot{x}(t) = A(t)x(t) + B(t)w(t)$$
$$y(t) = C(t)x(t) + D(t)w(t). \qquad (1.1)$$

The $A(t)$, $B(t)$,$C(t)$ and $D(t)$ are time varying matrices of dimensions n x n, n x l, p x n and p x l respectively. The n vector $x(t)$ denotes the system state, the l vector $w(t)$ the system input, and the p vector $y(t)$ the system output at time t. For convenience (1.1) is often abbreviated by $\begin{bmatrix} A(t) & B(t) \\ C(t) & D(t) \end{bmatrix}$. The system (1.1) may also be denoted as a linear map $G : w \rightarrow Gw$ defined as $(Gw)(t) = \int_0^t g(t-\tau)w(\tau)d\tau$.

Inner product. Consider two continuous, integrable, complex functions of time t, denoted by $u(t)$ and $v(t)$, then $\langle u,v \rangle = \int_0^\infty u(t)^H v(t)dt$ defines the inner product [S, p. 246; R, p. 78], where $u(t)^H$ denotes the Hermitian conjugate of $u(t)$.

Norms. The 2-norm of $u(t)$, denoted by $\|u\|_2$, equals the non-negative square root of $\langle u,u \rangle$ [S, p. 244; R, p. 76]. The set of all vectors defined above having a finite 2-norm is known as the Lebesgue space $\mathbf{L_2}$ [R, p. 78]. The p-norm of $u(t)$ is $\|u\|_p = \left(\int |u(t)|^p dt \right)^{1/p}$, $1 \le p < \infty$, the corresponding normed space is called the Lebesgue space $\mathbf{L_p}$ [DV, p. 12].

Adjoint systems. Let $F : X \rightarrow Y$ be a linear operator between two Hilbert spaces X and Y. Then $F^H : Y \rightarrow X$, the adjoint of F, is the unique linear operator such that for all $w \in X$ and $y \in Y$, $\langle y, Fw \rangle = \langle F^H y, w \rangle$ [LAKG, p. 270; IG, p. 1042]. In terms of the system (1.1), the adjoint G^H may be described by the system

$$\dot{\lambda}(t) = -A^T(t)\lambda(t) + C^T(t)y(t)$$
$$\Gamma(t) = -B^T(t)x(t) + D^T(t)y(t), \qquad (1.2)$$

a proof is given in [LAKG, p. 270]. The system (1.2) is often written as $\begin{bmatrix} -A^T(t) & C^T(t) \\ -B^T(t) & D^T(t) \end{bmatrix}$. For example, the adjoints of systems are used in the calculating the spectra of linear time-invariant systems. While adjoints pertain to operators or systems, Hermitians are less general - they apply to matrices. For convenience the notation F^H is used to denote the adjoint of F when F is an operator and, denote the Hermitian of F when F is a transfer function matrix (defined below).

Transfer function matrices. Consider a causal, linear time-invariant system having an impulse response denoted by $g(t)$ [K, p.23]. The output of system having an inpulse response $g(t)$ and having an input vector $w(t)$, is given by the well known convolution integral $y(t) = \int_0^\infty g(\tau)w(t-\tau)d\tau$ [K, p. 24]. The Laplace transform of $g \in \mathbf{L_1}$, denoted by $G(s)$, is known as the transfer function of the system, which is defined for $\mathrm{Re}\{s\} > 0$ and s

is the Laplace transform variable defined in [K, p. 25]. If the state-space parameters of (1.1) are time-invariant, the transfer function matrix is defined and is given by

$$G(s) = C(sI - A)^{-1}B + D, \tag{1.3}$$

a derivation is presented in [K, p. 68]. The transfer function of the adjoint system is defined by $G^H(s) = G^T(-s)$ which yields

$$G^H(s) = B^T(-sI - A^T)^{-1}C^T + D^T. \tag{1.4}$$

The Hardy space $\mathbf{H}_\infty$, is defined as the set of all complex-valued functions $G(s)$ which are bounded and analytic in the open right half plane. The least such bound is called the $\mathbf{H}_\infty$-norm of $G(s)$, denoted by $\|G\|_\infty$. Equivalently

$$\|G\|_\infty = \sup_{\mathrm{Re}s>0} |G(s)| = \sup_{\omega \varepsilon \mathbf{R}} |G(j\omega)| \tag{1.5}$$

The right-hand-side of (1.5) follows via the so-called *maximum-modulus principle* [D]. The induced $\mathbf{L}_2$ norm is defined as

$$\|G\| = \sup_{w \neq 0} \frac{\|Gw\|_2}{\|w\|_2} \tag{1.6}$$

and may be interpreted as the maximum of the ratio of the output signal energy to the input signal energy. The induced norm is defined equivalently as $\|G\| = \sup_{\|w\|_2 = 1} \|Gw\|_2$ [DV, p. 20]. The induced norm from $\mathbf{L}_2 \rightarrow \mathbf{L}_2$ of the time-invariant linear map is

$$\|G\| = \max_{\omega \varepsilon R} |\hat{g}(j\omega)| = \|G\|_\infty, \tag{1.7}$$

where $\hat{g}(j\omega)$ denotes the Fourier transform of the impulse response $g(t)$ [DV, Thm. 7, p. 25; F, Thm. 2, p. 13]. Thus the induced norm of the (time-invariant) linear map is equivalent to the maximum modulus of the system transfer function.

1.2.2 Discrete-time systems.

The discrete-time counterpart to (1.1) is

$$\begin{aligned} x_{k+1} &= A_k x_k + B_k u_k \\ y_k &= C_k x_k + D_k u_k. \end{aligned} \tag{1.8}$$

Consider two sequences of complex numbers $u = \{u_1, u_2, \ldots, u_n\}$ and $v = \{v_1, v_2, \ldots, v_n\}$ with all $u_i, v_i \in \mathbf{C}$. Let u^H denote the complex-conjugate transpose of u, then $\langle u,v \rangle = \sum_{k=1}^{n} u_k^H v_k$ defines the inner product [S, p. 245; R, p. 77]. Once again, the 2-norm of u, denoted by $\|u\|_2$ is the non-negative square root of $\langle u,u \rangle$ and the set of all sequences having a finite 2-norm is known as the Lebesgue space l_2. The p-norm of u is defined as

$\|u\|_p = \left(\sum_{k=1}^{n} |u_k|^p \right)^{1/p}$, where $1 \le p < \infty$, the corresponding normed space is called the Lebesgue space l_p [DV, p. 11].

The adjoint of the system (1.8) is

$$\begin{aligned} \lambda_k &= A_{k-1}^T \lambda_{k-1} - C_{k-1}^T y_{k-1} \\ \Gamma_{k-1} &= -B_{k-1}^T \lambda_{k-1} + D_{k-1}^T y_{k-1}, \end{aligned} \tag{1.9}$$

A discrete-time analogy to the continuous-time proof of [LAKG, p. 270] may be used to verify that (1.9) is the adjoint of (1.8). In the case of time-invariant systems, the output is related to the input via a convolution summation [O, pp. 180-181]; the z-transform of the impulse response $g(t)$ is known is the transfer function matrix and is denoted by $G(z)$. If the state-space parameters of (1.8) are time-invariant, then the transfer function matrix is defined and is given by

$$G(z) = C(zI - A)^{-1}B + D. \tag{1.10}$$

The transfer function matrix of the adjoint system is defined by

$G^H(z) = G^T(z^{-1})$ which yields

$$G^H(z) = G^T(z^{-1}) = B^T(z^{-1}I - A^T)^{-1}C^T + D^T. \tag{1.11}$$

1.3 What is a robust filter ?

The Kalman filter calculates minimum variance state estimates, given noisy measurements of a linear system and is the optimum estimator over all possible linear ones [AM, p. 108]. A Kalman filter relies implicitly on the assumptions that the noises are gaussian, having known statistics, the (linear) signal model is known and the initial conditions are known. When these assumptions are erroneous, the Kalman filter performance can degrade and a filter is said to be robust if it offers a comparative performance improvement (such as a reduction in the maximum of the magnitude of the error spectrum). For example, a filter that exhibits desirable properties when a modelling error is present, is robust with respect to model uncertainty. The cost is that the robust design may not perform as well as the Kalman filter when no uncertainties are present.

The two methods of designing robust filters under consideration arise via the so-called fake algebraic Riccati equation (ARE) and from H_∞ control. The fake ARE technique is comparatively simpler and is introduced first.

1.3.1 The fake ARE technique.

Consider the filtering problem where it is required to estimate the output of a known time-invariant, SISO plant from noisy observations. Referring to the model (1.1), assume

that $w(t)$ is a white Gaussian noise process of known covariance Q and the observations may be modelled as $z(t) = y(t) + v(t)$, where $v(t)$ is a white Gaussian noise process of known covariance R. For simplicity assume also that $B = 1$ and $D = 0$. The solution is the well known Kalman-Bucy filter [AM2, Sec. 7.3] and has the structure depicted in Figure 1.1 where the time-varying filter gain is calculated as

$$K(t) = \tilde{P}(t)C^T R^{-1} \tag{1.12}$$

and $\tilde{P}(t)$ arises via the Riccati differential equation (RDE)

$$\dot{\tilde{P}}(t) = A\tilde{P}(t) + \tilde{P}(t)A^T - \tilde{P}(t)C^T R^{-1} C\tilde{P}(t) + Q. \tag{1.13}$$

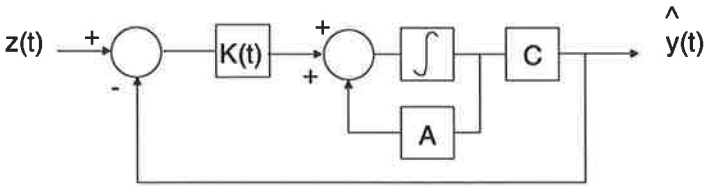

Fig. 1.1. The structure of the optimal continuous-time filter.

Now consider the filter design problem when there is some uncertainty associated with process noise power. A solution that was conceived for problems possessing an unknown Q is the fake ARE technique [PPGB,BTP,PBG,BGW,BG]. The key idea is to masquerade the RDE (1.13) as a fictitious or fake ARE by solving

$$0 = A\overline{P} + \overline{P}A^T - \overline{P}C^T R^{-1} C\overline{P} + \overline{Q}, \tag{1.14}$$

requiring the choice of a $\overline{Q} \geq 0$. The gain is calculated in the usual way via (1.12) and the filter possesses the structure of Figure 1.1. If the pair (C,A) is completely observable then the resulting error system is asymptotically stable [PPGB, Thm. 1].

In the case of discrete-time, consider $B_k = 1$ and $D_k = 0$ in (1.8). The Kalman filter has the structure depicted in Figure 1.2 where the gain is calculated from

$$K_k = A\tilde{P}_k C^T (C\tilde{P}_k C^T + R)^{-1} \tag{1.15}$$

and $\tilde{P}_k$ arises recursively via the Riccati difference equation (also denoted as a RDE)

$$\tilde{P}_{k+1} = A\tilde{P}_k A^T - A\tilde{P}_k C^T (C\tilde{P}_k C^T + R)^{-1} C\tilde{P}_k A^T + Q. \tag{1.16}$$

An uncertainty in the process noise power may similarly be accommodated by proceeding with some $\underline{Q} \geq 0$ via a false ARE

$$\underline{P} = A\underline{P}A^T - A\underline{P}C^T (C\underline{P}C^T + R)^{-1} C\underline{P}A^T + \underline{Q} \tag{1.17}$$

and calculating the gain from (1.15). It turns out [BTP] that the resultant filter can offer some robustness to observation noise at the cost of convergence rate. Consider the case in which the Q is known. Denoting P_k as the estimation error variance exhibited by the fake ARE filter and $\tilde{P}_k$ as the (optimal) error variance resulting from the Kalman filter, then $P_k \geq \tilde{P}_k$. Thus any robustness offered by the fake ARE technique is achieved at the cost of increased MSE.

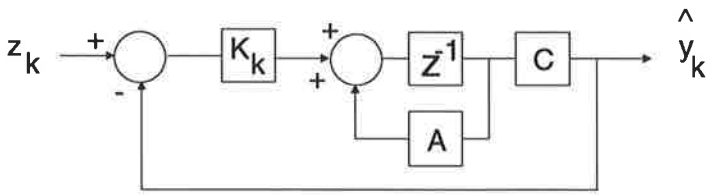

Fig. 1.2. The structure of the optimal discrete-time filter.

The application of the fake ARE technique to linear filtering problems (in which the Q is known) is reported in [BTP]. The fake ARE method may be applied to more general problems where optimality is traded off for error stability. In Chapter 6 it is shown how the fake ARE technique may be exploited in the design of nonlinear observers for the demodulation of frequency or phase modulated signals. Compared to the conventional EKF solution [SM, pp. 439-440], the claimed advantages of the fake ARE approach include some robustness to amplitude uncertainty and to initial conditions.

1.3.2 H_∞ optimisation.

Although the subject of H_∞ optimisation is deeply entrenched in mathematics and has been the subject of considerable research, the H_∞ filter is not dissimilar to the Kalman filter. The continuous-time H_∞ filter for the previously mentioned problem has the structure depicted in Figure 1 with the gain calculated via (1.12), the only difference is in the quadratic term of the RDE, viz.

$$\dot{P}(t) = AP(t) + P(t)A^T - P(t)(C^T R^{-1} C - \gamma^{-2} C^T C)P(t) + Q. \tag{1.18}$$

Here the γ is a scalar to be minimised whilst ensuring that $P(t) > 0$. In particular if $\gamma = \infty$ then it follows that $P(t) = \tilde{P}(t)$, that is the H_∞ filter reverts to the Kalman filter. The discrete-time H_∞ filter has the structure depicted in Figure 1.2, the gain calculated via (1.15) and the RDE is

$$P_{k+1} = AP_kA^T - AP_k\begin{bmatrix} -C^T \\ C^T \end{bmatrix}\begin{bmatrix} CP_kC^T - \gamma^2 I & CP_kC^T \\ CP_kC^T & CP_kC^T + R \end{bmatrix}^{-1}[-C \quad C]P_kA^T + Q \tag{1.19}$$

and it is shown in Chapter 4 that $P_k = \tilde{P}_k$ at $\gamma = \infty$. The optimal γ needs to be determined iteratively by successively decreasing candidate values and testing that the solution to the

RDE is positive definite. (If γ is too small so that the RDE solution is not positive, then the resulting filter will be unstable.)

So the fake ARE and H_∞ designs offer some robustness with respect to input uncertainties, by choosing a $P_k \geq \tilde{P}_k$ in an appropriate way. The first approach is somewhat *ad hoc*, there is no guidance as to how the Q in fake ARE may be chosen and how this affects the filter performance. The design method is iterative, candidate filters need to be assessed from error spectra when the plant is time-invariant, otherwise error statistics need to be gathered from trials. In H_∞ design, one proceeds more formally and the theoretical aspects are well understood. The H_∞ objective is equivalent to minimising the induced norm of a linear map from the inputs to the error. If the 2-norm of the inputs is normalised to unity, from (1.6) it is seen that the H_∞ filter seeks to minimise the energy of the error. This compares with the Kalman filter which minimises the variance or power of the error. When the problem is time-invariant, an intuitively pleasing interpretation of the H_∞ optimality criterion follows; from (1.7) it is seen that the peak of the error spectrum is minimised. The capacity to minimise the maximum of the error spectrum is attained at the expense of MSE since $P_k \geq \tilde{P}_k$. In practice, γ may be used as a parameter to control the trade-off between MSE and peak error.

When uncertainties exist in the plant models, a common approach [J, GA] is to design with an increased measurement noise variance and then look at the residuals in order to evaluate filter performance. Such procedures tend to rely heavily on heuristics. It is contended that the problem is more tractable in a H_∞ framework. The problem possessing a model uncertainty is tackled similarly by considering an extra ficticious input *in lieu* of the uncertainty. However it is found that H_∞ designs are rather conservative and it can be advantageous to consider less pessimistic (fictitious) inputs.

Now that robust filters have been introduced, it is fitting to review to evolution of the theoretical developments that have made it all possible.

1.4 A historical perspective.

The development of the fake ARE technique began with [PPGB,PBG], where the stability properties of a Kalman filter were connected with the solution of an ARE. The first application is detailed in [BTP] where *covariance setting* is described as "the approach of explicitly adding state noise to the signal model leads to positive definite estimation error covariances and hence stabilising gains." The subject of fake AREs is discussed in detail within the texts [BGW, BG].

The H_∞ approach has evolved in order to accommodate problems where model uncertainties exist and the inputs were not necessarily stochastic. In linear H_∞ filtering, the objective is to minimise the H_∞ norm of an error transfer function. The problem is quite general,

indeed filtering is the dual to control and the origin of H_∞ filtering is entrenched in the robust control literature. For example, H_∞ filtering can be cast in a generalised regulator framework or in a model matching setting. Classical approaches to solving H_∞ optimisation problems are based on Nevanlinna-Pick interpolation [ZF], see the books by Vidyasagar where filtering is addressed explicitly [V] and by Francis where model matching and tracking problems are discussed [F]. However interpolation approaches are problematic, as they rely on the cancellation of polynomial factors, which is numerically intractable. This obstacle was overcome by Petersen who obtained the solution to the H_∞ optimisation problem via an ARE equation [P]. Subsequently Doyle *et al.* stated the filter for the continuous time output estimation problem in terms of the solution of an ARE [DGKF], and, a great deal of work has been published since. Iglesias *et al.* have derived some analogous discrete-time results, namely a minimum entropy controller, where some conditions are imposed on the plant [IG] and for the more general case, where the solution is stated in terms of two dual Riccati difference equations and a coupling condition [IMG]. Stoorvogel details an alternate minimum entropy solution for the discrete-time measurement feedback problem in terms of two different RDEs [St]. Khargonekar and Nagpal have reported on the conditions for the existence of solutions for continuous-time filtering and smoothing problems [KN,NK]. Most H_∞ optimisation problems can be cast in the form of the four block problem, a characterisation of all solutions for the continuous-time case was worked out by Glover *et al.* [GLDKS]. Limebeer *et al.* rediscovered the connection between optimal H_∞ control and differential game theory, where the optimal strategy arises as a saddle point condition due to the worst case inputs [LAKG]. Green and Limebeer have summarised the game theoretic derivations for the continuous-time H_∞ controller and filter [GL]. The game theoretic derivations for the the discrete-time controller were formulated by Limebeer, Green and Walker in [LGW] and by also by Basar and Bernhard [BB]. Other approaches have evolved independently, Grimble solved a stationary discrete-time filtering problem using a polynomial systems approach [GE]. Shaked *et al.* used spectral factorisation approaches for solving stationary filtering problems [Sh,Sh2,YS]. A continuous-time H_∞ filter has been obtained by solving a model matching problem [Hu].

The theory is all standard now, however surprisingly little is understood of the cost benefits. Indeed Stoorvogel laments that "we still need to make the step from basic understanding to design (how to apply all this nice theory in practice)" [St].

1.5 Contributions to the field of robust signal processing.

This study is neither theoretical, nor is it applications oriented; it is somewhere in between. For practical filtering applications it is not uncommon to find (say) 20th order models in use. In stark contrast, here the approach is to investigate the application of robust filtering

for scalar examples and, where possible, an analysis is attempted so that something may be inferred about higher order problems. Inevitably, the conclusions that result tend to be anecdotal rather than precise. The work outlined herein is tendered as a contribution, however many open questions remain. Briefly, the contributions include:

- The development of a discrete-time analogy to the solution of a linear, stationary H_∞ filtering problem of [Sh2] and the observation of some benefits.
- Refining a method for designing filters that are robust with respect to model uncertainty and are guaranteed to solve the H_∞ filtering problems possessing the modelling error.
- The use of the arguments in [GL] to simplify the results of [LGW] for the discrete-time, game-theoretic H_∞ filter.
- The identification of performance trends for continuous-time and discrete-time problems of H_∞ output estimation and equalisation.
- The application of the fake ARE technique in the design of nonlinear observers for signal demodulation.
- Combining the discrete-time H_∞ filter with the linearisation akin to the extended Kalman filter (EKF) resulting in a filter which, with the aid of examples, is demonstrated to exhibit some robustness to linearisation errors.
- Developing an EKF for an adjoint system which is used in the construction of an extended Kalman smoother.

Some extensions to an interpolation solution due to [Sh2] for the continuous-time, linear, stationary filtering problem, have been reported in [EW] and are detailed in Chapter 2. This approach uses spectral factorisation and vector interpolation [Sh3]. The H_∞ filter formulation is generalised to include non-unity noise powers, frequency weighted error spectra and an analogous formulation is set out for the discrete-time case. The results of simulations are presented to illustrate that the H_∞ filter can be advantageous compared to the Wiener filter for the problems of linear filtering and linear pre-equalisation.

The third chapter describes the continuous-time game-theoretic H_∞ filtering results of [GL]. It is noted that the filter can be scaled to exhibit all-pass error and a comparison is drawn with the interpolation solution of [Sh2]. A method of accommodating additive and multiplicative model uncertainty is proposed, which guarantees that the solution satisfies the original H_∞ problem containing the model error.

Chapter 4 is concerned with the discrete-time game-theoretic H_∞ filter. The application of the bilinear transform to a strictly proper continuous-time plant usually yields plant possessing a non-zero direct feedthrough term. Consequently the Kalman filter results are reviewed for plants having a feedthrough. It is confirmed that the Kalman filter reverts to

the Wiener filter in the stationary case. Despite the fact that H_∞ filters have been addressed either explicitly or inadvertantly in the literature, yet another formulation is described and presented in [EW2]. The approach of [GL] is followed to specialise the H_∞ control results [LGW] to filtering in terms of the solution of a game theoretic RDE. It possesses precisely the structure of the Kalman filter and so is applicable to nonstationary problems. The formulation reduces to that of [BB] when the plants are strictly proper. The H_∞ predictor and filter have the structure of the so called *a priori* and *a posteriori* filters that arise via a spectral factorisation approach [YS].

The performance aspects of H_∞ filters are discussed in Chapter 5 and in [EW2]. Scalar continuous-time and discrete-time output estimation examples are presented in order to demonstrate what happens at various signal to noise ratios (SNRs). In the case of channel equalisation, the conventional minimum MSE solution is a Wiener formulation [KP] which is limited to stationary problems. Here equalisers are obtained via the solution of the so-called general regulator problem [GL]. Performance comparisons of Kalman and H_∞ equalisers are undertaken when the channel model is known and is either minimum phase, non-minimum phase or uncertain.

Non-linear filtering is introduced in Chapter 6, where the problem of demodulating frequency and phase modulated signals is addressed. An observer structure possessing a linear transition matrix and non-linear gain terms is derived so that the fake ARE technique may be used to advantage. This results in an adaptive phase-locked loop with an amplitude dependent gain that is different to the EKF. A stability analysis is carried out and the results of simulation studies are presented to demonstrate some benefits compared to the extended Kalman filter (EKF). This work is reported in [EW3,EW4].

This study culminates in the development of the so-called extended H_∞ filter [EW4, EW5], where the discrete-time H_∞ filter derived in Chapter 4 is combined with the linearisation akin to the EKF and applied to the demodulation problems of Chapter 6. The details are set out in Chapter 7. Briefly, the approach is to treat the truncated terms of the Taylor series expansion as a model uncertainty problem. Compared to the EKF, the performance benefit of the extended H_∞ filter is most significant when the problem is profoundly non-linear. This arises because in highly non-linear problems, the linearisation tends to be unsuccessful and so an allowance for the truncated terms can be beneficial. The extended H_∞ filter tends to be beneficial at high SNR. A technique which can sometimes offer a benefit at low SNR, is the extended Kalman smoother, which is detailed in an appendix.

The conclusion begins by highlighting the recent achievements. The status quo is then summarised. Namely, the problems where robust filtering is advantageous are listed and

the work that supports the claims are cited. Finally some unsolved problems, namely noncausal filtering and nonlinear smoothing, are remarked upon.

REFERENCES

[AM] Anderson, B. D. O. and J.B. Moore, *Optimal Filtering*, Prentice Hall, Englewood Cliffs, N.J., 1979.

[AM2] Anderson, B. D. O. and J.B. Moore, *Optimal Control*, Prentice Hall, Englewood Cliffs, N.J., Sec. 7.3, 1989.

[BB] Basar, T. and P. Bernhard, *H_∞-optimal control and related minimax design problems. A dynamic game approach.*, Birkhauser, Boston, 1991.

[BG] Bitmead, R. R. and M. Gevers, "Riccati difference and differential equations: convergence, monotonicity and stability", in: S. Brittanti, A. J. Laub, J. C. Willems, Eds, *The Riccati Equation*, Springer Verlag, ch. 10.8.1, 1991.

[BGW] Bitmead, R. R., M. Gevers and V. Wertz, *Adaptive optimal control*, Prentice Hall, Sydney, pp. 86-87, 1990.

[BTP] Bitmead, R. R., A. -C. Tsoi and P. J. Parker, "Kalman filtering approach to short time Fourier analysis", *IEEE Trans. Acoustics, Speech and Signal Processing,* v. 34, no. 6, pp. 1493-1501, 1986.

[DGKF] Doyle J.C., K. Glover, P.P. Khargonekar and B.A. Francis, "State space solutions to standard H_2 and H_∞ control problems", *IEEE Trans. Automat. Contr.,* vol. 34, no. 8, pp. 831-847, Aug. 1989.

[D] Dorato, P. (editor), *Robust Control*, IEEE Press, NY, 1987.

[Do] Doyle, J. C. "Analysis of feedback systems with structured uncertainty", *IEE Proc.*, pt. D, no. 6, pp. 242-250, Nov. 1982.

[DV] C. A. Desoer and M. Vidyasagar, *Feedback Systems: Input - Output Properties*, Academic Press, N.Y., 1975.

[EW] Einicke, G. A. and L.B. White, "The use of H_∞ filters for linear demodulation and equalisation", *IEEE Int. Symp. CAS.*, San Diego, CA, vol. 4, pp. 1721-1724, May 1992.

[EW2] Einicke, G. A. and L. B. White, "Performance comparison of H_∞ and Kalman filters", submitted for publication.

[EW3] Einicke, G. A. and L. B. White, "Estimation of frequency and phase modulated signals using false algebraic Riccati techniques", *Proc. 3rd ISSPA*, Gold Coast, Aust., vol. 2, pp. 339-343, Aug. 1992.

[EW4] Einicke, G. A. and L. B. White, "A class of nonlinear filters for periodic signals", *IEEE Int. Symp. CAS.*, Chicago, IL, vol. 1, pp. 144-147, May 1993.

[EW5] Einicke, G. A. and L. B. White, "The extended H_∞ filter - a robust EKF", *Proc. ICASSP*, Adelaide, vol. 4, pp. 181-184, Apr. 1994.

[EW6] Einicke, G. A. and L. B. White, "Robust nonlinear filtering using a H_∞ performance criterion", submitted to *Automatica.*

[F] Francis, B. A., *A course in H_∞ control theory*, Lecture notes information and in control and information sciences, vol. 88, Springer-Verlag, Berlin, 1987.

[FdSX] Fu, M., C.E. de Souza and L. Xie, "H_∞ estimation for uncertain systems", *Technical Report EE9039*, Department of Electrical Engineering and Computer Science, University of Newcastle, NSW, Australia, May 1990.

[FHZ] Francis, B. A., J.W. Helton and G. Zames, "H_∞-optimal feedback controllers for linear multivariable systems", *IEEE Trans. Automat. Contr.,* vol. 29, no. 10, pp. 888-899, Aug. 1984.

[GA] Grewal, M. S. and A. P. Andrews, *Kalman filtering. Theory and practice*, Prentice Hall, Englewood Cliffs, NJ, Sec. 7.2, 1993.

[GE] Grimble, M. J. and A. El Sayed, "Solution of the H_∞ optimal linear filtering Problem for discrete-time systems", *IEEE Trans. Acoust., Speech, Signal Processing*, vol. 38, no. 7, pp. 1092-1104, Jul. 1990.

[GL] Green, M. and D.J.N. Limebeer, *Robust Linear Control*, , Prentice-Hall, Englewood Cliffs, N.J., 1993.

[GLDKS] Glover, K., D.J.N. Limebeer, J.C. Doyle, E.M. Kasenally and M.G. Safonov, "A characterization of all solutions to the four block general distance problem", *SIAM J. Control Optim.*, vol. 29, no. 2, pp. 283-324, Mar. 1991

[Glo] Glover, K., "All optimal Hankel-norm approximations of linear multivariable systems and the L_∞-error bounds", *Int. J. Cont.*, vol. 39, no. 6, pp. 1115-1193, 1984.

[Gre] Grewal, M. S. and A.P. Andrews, *Kalman Filtering*, Prentice Hall, NJ USA, pp. 279-285, 1993

[HB] W.M. Haddad and D.S. Bernstein, "On the gap between H_2 and entropy performance measures in H_∞ control design", *Systems Control Lett.*, vol. 14, pp. 113-120, 1990.

[HB2] Haddad, W. M. and D.S. Bernstein, "Generalized Riccati equations for the full- and reduced-order mixed norm H_2 / H_∞ standard problem", *Systems Control Lett.*, vol. 14, pp. 185-197, 1990.

[Hu] Hung, Y. S., "H_∞ filtering and model matching", *IFAC World Congress*, Sydney, vol. 2, pp. 39-41, 1993.

[IG] Iglesias, P. I. and K. Glover, "State space approach to discrete-time H_∞ control", *Int. J. Cont.*, vol. 54, no. 5, pp. 1031-1073, 1991.

[IMG] Iglesias, P. A., D. Mustafa and K. Glover, "Discrete-time H_∞ controllers satisfying a minimum entropy criterion", *Sys. Contr. Lett.*, vol. 14, pp. 275-286, 1990.

[J] Jazwinski, A. H., *Stochastic processes and filtering theory*, Academic Press, San Diego, Sec. 8.4, 1970.

[K] Kailath, T., *Linear systems*, Prentice-Hall, Englewood Cliffs, NJ, pp. 23-25, 68, 1980.

[KN] Khargonekar P. P. and K. M. Nagpal, "Filtering and smoothing in an H^∞ setting", *Proc. 28th IEEE CDC,* Tampa, FL, vol. 1, pp. 415-420, Dec. 1989.

[KP] Kassam, S. A. and H.V. Poor, "Robust techniques for signal processing: A survey", *Proc. IEEE*, vol. 73, no. 3, pp. 433-481, Mar. 1985.

[LAKG] Limebeer, D. J. N., B.D.O. Anderson, P.P. Khargonekar and M. Green, "A game theoretic approach to H^∞ control for time-varying systems", *SIAM J. Control Optim.*, vol. 30, no. 2, pp. 262-283, Mar. 1992.

[LGW] Limebeer, D. J. N., M. Green and D. Walker, "Discrete-time H^∞ control", *Proc. IEEE CDC*, Tampa, FL, vol. 1, pp. 392-396, Dec. 1989.

[LS] Limebeer, D. J. N. and U. Shaked, "Minimax terminal state estimation and H_∞ filtering", submitted to *IEEE Trans. Automat. Contr.,* 1992.

[MN] McLaughlin, S. W. and D.L. Neuhoff, "Achievable data and bit densities in digital magnetic recording", *Conf. Inf. Sciences and Sys.*, Princeton, N.J., 1992.

[MG] McFarlane, D. C. and K. Glover, *Robust controller design using normalized coprime factor plant descriptions*, Lecture notes in control and information sciences, vol. 38, Springer-Verlag, Berlin, 1989.

[NK] Nagpal, K. M. and P.P. Khargonekar, "Filtering and smoothing in an H^∞ setting", *IEEE Trans. Automat. Contr.,* vol. 36, no. 2, pp. 152-166, Feb. 1991.

[O] Ogata, K., *Discrete-time control systems*, Prentice-Hall, Englewood Cliffs, New Jersey, pp. 180-181, 1987.

[P] Petersen, I. R., "Disturbance attenuation and H^∞ optimization: a design method based on the algebraic Riccati equation", *IEEE Trans. Automat. Contr.,* vol. 32, no. 5, pp. 427-429, May 1987.

[PBG] Poubelle, M. -A., R. R. Bitmead, M. Gevers, "Fake algebraic Riccati techniques and stability", *IEEE Trans. Automatic Contr.*, vol. 33, pp. 379-381, 1988.

[PPGB] Poubelle, M. -A., I. R. Petersen, M. R. Gevers and R. R. Bitmead, "A Miscellany of Results on an equation of Count J. F. Riccati", *IEEE Trans. Automatic Contr.*, vol 31, no. 7, pp. 651-654, Jul., 1986.

[R] Rudin, W., *Real and complex analysis*, McGraw-Hill Book Co., Singapore, pp. 77-78, 1987.

[S] Simmons, G. F., *Introduction to topology and modern analysis*, McGraw-Hill Book Co., Singapore, pp. 245-246, 1963.

[Sa] Sarason, D., "Generalised interpolation in H_∞", *Trans. AMS.*, vol. 127, pp. 179-203, 1967.

[Sh] Shaked, U., " The explicit structure of inner matrices and its application in H_∞-optimization", *IEEE Trans. Automat. Contr.*, vol. 34, no. 7, pp. 734-738, Jul. 1989.

[Sh2] Shaked, U., " H_∞-minimum error state estimation of linear Stationary Processes", *IEEE Trans. Automat. Contr.*, vol. 35, no. 5, pp. 554-558, May 1990.

[SM] Sage, A.P. and J.L. Melsa, *Estimation theory with applications to communications and control,* McGraw-Hill, N.Y., 1973.

[St] Stoorvogel, A., *The H_∞ control problem. A state space approach*, Prentice Hall, N.Y., 1992.

[Str] Strejc, V., *State Space Theory of Discrete Linear Control, Wiley*, Chichester, pp. 257-258, 1983.

[V] Vidyasagar, M., *Control systems synthesis: a factorization approach*, MIT Press, Camb., Mass., 1985.

[VT] Van Trees, H. L., *Detection, Estimation, and Modulation Theory*, Part I, John Wiley & Sons, N.Y., p. 533, 1968.

[Vis] Vishwanath T.G., D.R. Campbell and T.J. Moir, "A real-time implementation of an IIR adaptive line enhancer", *Int. J. Adapt. Cont. and Sig. Proc.*, vol. 3, pp. 293-303, 1988.

[YS] Yaesh I. and U. Shaked, "Game theory approach to optimal linear estimation in the minimum H_∞-norm sense", *Proc. 28th IEEE Conf. Decision and Control*, Tampa, FL., pp. 415-420, Dec. 1989.

[ZF] Zames G., B.A. Francis, "Feedback, minmax sensitivity, and optimal robustness", *IEEE Trans. Automat. Contr.*, vol. 28, pp. 585-600, May 1983.

Chapter 2

A frequency domain approach to H_∞ filtering

This chapter addresses the solution of stationary filtering problems. It could well be argued that this subject is uninteresting, since the game-theoretic approaches used herein have far wider application, namely non-stationary (and stationary) problems. Consequently the theoretical aspects are relegated to the appendices, the emphasis here is on application and performance issues.

The contributions of this chapter are :

- Some generalisations to an interpolation solution for the continuous-time, linear, stationary, H_∞ filtering problem. In particular the approach of [Sh2] is generalised to include specified noise covariances, coloured observation noise and frequency weighted estimation error.
- The formulation of a discrete-time analogy to the H_∞ filter of [Sh2].
- Establishing some benefits in output estimation and equalisation applications.

The problem is defined in Section 2.2. The Wiener and H_∞ solutions are stated in Sections 2.3 and 2.4 respectively. Some remarks concerning the choice of frequency weighting are made in Section 2.5. Finally, the application and performance of the H_∞ filter to output estimation and equalisation is introduced in Section 2.6.

2.1 Background.

The pioneering contributions to the solution of H_∞ optimization problems no doubt includes the work of Zames and Francis [ZF,FZ] where the Nevanlinna-Pick algorithm is used to solve the interpolation problem of designing an inner function that cancels non-causal plant zeros. An extensive survey of the developments that have led to and followed on from

[ZF,FZ] is given in [Dor]. A problem confronting newcomers to H_∞ filtering is that the majority of the contributions cited in [Dor] tend to focus almost entirely on theoretical developments. Amongst the first papers that explicitly address H_∞ filtering and show how the theory may be applied in examples are [GE] and [Sh]. Grimble uses an approach due to [Ku] and casts the discrete-time stationary filtering problem in terms of coprime polynomial matrices and the solution of coupled diophantine equations [GE]. Coloured noise and frequency weighting are built into the problem formulation, and it is illustrated that the maximum magnitude of the error spectra exhibited by the H_∞ filter is less than or equal to that of the Kalman filter. Shaked [Sh] uses a vector extension of the scalar Pick-Nevanlinna interpolation [Ki] to derive a closed-form, state-space formulation of an inner matrix [Sh]. The vector interpolation is then used in the solution of a continuous-time, stationary, filtering problem [Sh2]. An example is then used to compare the interpolation solution with dual to the optimal controller of [DGKF].

Here, the approach of [Sh2] is generalised to include specified noise covariances, coloured observation noise and frequency weighted estimation error. An analogous formulation for the discrete-time case is then described. Two key applications are discussed: state estimation in the presence of coloured noise and, equalisation. It is argued that an ad hoc procedure can be employed to appropriately choose the frequency weighting function. Both continuous-time and discrete-time examples are described and, finally, the results of simulations are reconciled with the H_∞ optimality criterion.

2.2 Problem definition.

Consider the continuous-time filtering problem shown in Figure 2.1 where $G_1(s)$, $G_2(s)$, $N(s)$ and $W(s)$ are the transfer function matrices of linear-time invariant systems. The objective is to design the optimal, linear, causal filter $H(s)$ that estimates the output of $G_1(s)$ from the output of $G_2(s)$ corrupted by coloured noise, to minimize the error $z(t)$, in an optimum way. The plants $G_1(s)$, $G_2(s)$ and $W(s)$ are assumed to stable, $W(s)$ is also assumed to be minimum phase.

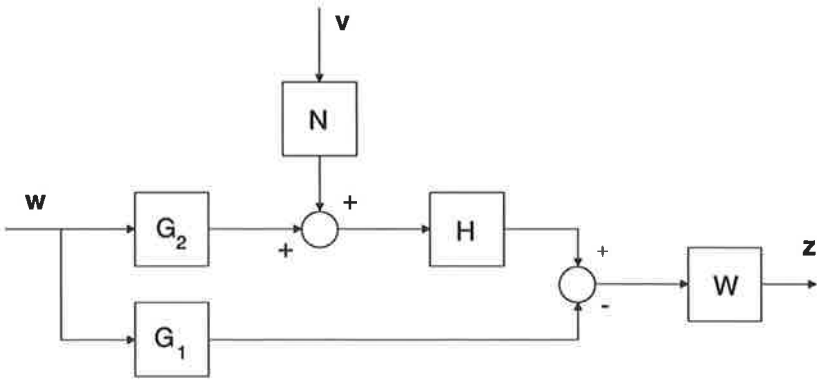

Fig. 2.1. The filtering problem.

Many filtering problems of interest can be cast into the configuration of Figure 2.1, in which G_2 is the actual plant under consideration and G_1 specifies the quantity to be estimated. When $G_1 = G_2$, the objective is to estimate the output of the plant, this is known as *output estimation.* A *state estimation* problem is where G_1 specifies all the states, (rather than a linear combination of the states) of G_2. When $G_1 = I$, the objective is to estimate the input to the plant, this problem is commonly referred to as *equalisation*, because the task is to equalise or to undo the effect of the plant.

In this chapter, the attention is confined exclusively to stationary problems. The notation of [Sh4,YS] is adopted, where transfer function matrices rather than operators are used throughout. The approach is to construct the error transfer function matrix and then seek to minimise the maximum of the error power spectrum matrix.

It is assumed that $w(t) \in \mathbf{R}^l$ and $v(t) \in \mathbf{R}^p$ are zero mean, uncorrelated white noise processes with covariance matrices $E\{w(t)w^T(\tau)\} = Q\,\delta(t-\tau)$, $E\{v(t)v^T(\tau)\} = R\delta(t-\tau)$. The covariances may be factored into the plant transfer function matrices by defining $\tilde{G}_1 = G_1Q^{1/2}$, $\tilde{G}_2 = G_2Q^{1/2}$ and $\tilde{N} = NR^{1/2}$. The estimation error of Figure 2.1 can be written as

$$z = R_{zv}v + R_{zw}w, \tag{2.1}$$

where $R_{zv} = WH\tilde{N}$ and $R_{zw} = W(H\tilde{G}_2 - \tilde{G}_1)$ are the transfer function matrices from $v(t)$ to $z(t)$, and from $w(t)$ to $z(t)$ respectively. For convenience, the inputs to the problem are jointly denoted as $d(t) = \begin{bmatrix} v(t) \\ w(t) \end{bmatrix}$ so that the error power spectral density matrix may be denoted as

$$R_{zd}R_{zd}^H = R_{zn}R_{zn}^H + R_{zw}R_{zw}^H. \tag{2.2}$$

By expanding out (2.2) and completing the square, it can be found that

$$R_{zd}R_{zd}^H = W(H\Delta - \tilde{G}_1\tilde{G}_2^H\Delta^{-H})(\Delta^H H^H - \Delta^{-1}\tilde{G}_2\tilde{G}_1^H)W^H + \Phi_1, \tag{2.3}$$

where Δ is a stable, minimum phase spectral factor of the observations power spectral density matrix

$$\Delta\Delta^H = \tilde{N}\tilde{N}^H + \tilde{G}_2\tilde{G}_2^H, \tag{2.4}$$

Δ^H is the adjoint or Hermitian of Δ, and

$$\Phi_1 = W\tilde{G}_1(I + \tilde{G}_2\tilde{N}^{-H}\tilde{N}^{-1}\tilde{G}_2)\tilde{G}_1^H W^H. \tag{2.5}$$

It is seen from (2.3) that $R_{zd}R_{zd}^H$ has two components. The first component includes the filter and therefore can be minimised according to a chosen optimality criterion, whereas (2.5) is constant and represents a lower bound for $R_{zd}R_{zd}^H$.

An insight to the problem solutions can be gleaned by contemplating the negligible noise and high noise cases. Consider $W = 1$, G_2 is a minimum phase, single-input-single-output (SISO) plant and suppose that $\sigma_v^2 \approx 0$. Then $R_{zd} \approx (H - I)G_2\sigma_w$ for the output estimation problem, hence the solution $H \approx 1$ minimises $R_{zd}R_{zd}^H$. Thus, the filter for the noiseless output estimation problem approaches a short circuit. Also, $R_{zd} = (HG_2 - 1)\sigma_w$ for the noiseless equalisation problem and the solution $H = G_2^{-1}$ minimises $R_{zd}R_{zd}^H$. Now suppose instead, that $\sigma_v^2 >> \sigma_w^2$ so that $R_{zd} \approx H\sigma_v$. Clearly for high noise problems the solution $H \approx 0$ (that is, an open circuit) minimises $R_{zd}R_{zd}^H$. These short circuit, exact inverse and open circuit solutions are indeed an oversimplification. Obviously in practical applications the noises are not negligible and the filter is somewhere between a short circuit and an open circuit.

2.3 The Wiener filter.

The Wiener filter minimises the cost function

$$tr \frac{1}{2\pi j}\int_{-j\infty}^{j\infty} R_{zd}R_{zd}^H(s)\, ds, \tag{2.6}$$

which, in the case of SISO plants, is equivalent to minimising the area under a plot of the magnitude of the error spectrum. Numerous versions appear in the literature, see [AM,Pa,Sh,Sh2,SM] for example. In Appendix A, it is shown that the result follows immediately from a completion of squares argument, and the various formulations are in fact equivalent. For the problem of Figure 2.1, the Wiener filter is

$$\tilde{H} = W^{-1}\left\{\tilde{G}_1\tilde{G}_2^H\Delta^{-H}\right\}_+\Delta^{-1}, \tag{2.7}$$

where the causal part, denoted by $\{\,.\,\}_+$, is calculated differently for continuous-time and discrete-time cases (see Appendix A).

2.4 An optimal discrete-time H_∞ filter.

The H_∞ objective is to minimise $\sup_{\omega\in\mathbf{R}} |R_{zd}R_{zd}^H(j\omega)|$. The solution for the H_∞ filter is clearly not unique since an error transfer function can be multiplied by any of an infinite number of different inner functions and not affect the spectral maximum. In [GE,Sh2] the approach is to seek an all-pass error, that is

$$R_{zd}R_{zd}^H = \gamma^2 I, \tag{2.8}$$

where γ is a scalar to be minimised. In the case of SISO plants, this objective is equivalent to finding a minimum γ so that the magnitude of the error spectrum of $R_{zd}R_{zd}^H$ is flat and equal to γ^2.

An optimal H_∞ filter for the continuous-time filtering problem with the simplifications $N = W = I$ and $Q = R = I$ is detailed in [Sh4]. A H_∞ filter for the more general problem of Figure 2.1 is of the form

$$H = \tilde{H} + W^{-1}\left\{\tilde{G}_1\Delta_2 U\tilde{\Delta}^H\Delta^{-H}\right\}_+\Delta^{-1}, \tag{2.9}$$

where Δ_2 is a stable, minimum-phase spectral factor and U is an inner matrix which may be found using the continuous-time, vector interpolation method of [Sh3]. The role of the inner function and the interpolation results are discussed in Appendix B. Briefly, U is required to cancel the poles of Δ^{-H}, or equivalently the zeros of Δ^H. Alternatively from (2.9), the H_∞ filter may be thought of as a sum of a Kalman filter and a transfer function which ensures that the noncausal part of $H\Delta - \tilde{G}_1\tilde{G}_2^H\Delta^{-H}$ is cancelled.

When the plants have discrete-time representations, the H_∞ filter is also given by (2.9) except that a discrete-time inner needs to found. The use of the bilinear transform together with the results of [Sh3] in the solution of the discrete-time interpolation problem is described in Appendix B.

2.5 Choosing the weighting function.

The use of weighting functions allows the magnitude of the spectrum of either a so-called "sensitivity function" [ZF] or an error transfer function [GE] to be minimised in a particular part of the frequency band. The weighting function may well be specified by the application at hand. From (2.9) it is seen that the inverse of the weighting function is a factor of the H_∞ filter and therefore the performance benefits of frequency weighting (if any) must be reconciled with the expense of a higher order filter. In this section, it is assumed that the inverse of the weighting function is proper and stable but otherwise may be chosen freely to yield a performance benefit.

The idea behind a frequency weighted H_∞ design is to reduce the magnitude of the error spectrum (say) in the vicinity of the plant bandwidth at the expense of increased error elsewhere in the frequency band. From (2.8), the frequency weighted error spectrum for a H_∞ filter is designed to be $\gamma^2 I$ and, from (2.3), it follows that the actual error spectrum is $\gamma^2 W^{-H}W^{-1}$. That is to say, frequency weighting allows the shape of the error spectrum to be chosen *a priori.*

Consider the problem of filtering a band-pass signal in white noise and applying a range of candidate weighting functions. Attempts to weight the estimation error out to progressively higher frequencies will be at the expense of an increased γ^2. Eventually the error within the signal bandwidth will exceed that for the unity weighted case. Conversely, shifting the error weighting to progressively lower frequencies will be at the expense of increased inband error. It is claimed here that W can be chosen in an *ad hoc* manner by

seeking to satisfy some optimality criterion appropriate to the application. In the examples that follow, a search is conducted for a weighting function that is optimum in the sense of minimising (2.6) over the bandwidth of the plant.

2.6 Performance.

This section begins with a discussion of a continuous-time output estimation example. The approach in [GE] is followed, where an indication of performance follows by comparing the Wiener and H_∞ error spectra. Subsequently, the results of simulation studies for discrete-time equalisation problems are presented, where an energy ratio and the bit error rate (BER) serve as performance indicators.

Example 2.1. Signal demodulation is an output estimation problem where the objective is to extract a message from a noisy radio frequency (RF) signal. For a linear modulation scheme such as AM double sideband suppressed carrier (AM-DSB/SC), a nonstationary Kalman filter can serve as an optimum demodulator [Sn,SM]. A suboptimum demodulator may be realised by mixing the modulated signal with a phase-locked local oscillator and filtering the result. It is assumed that the double frequency product term will not pass through the low-pass filter. An arbitrary numerical example was selected to comply with a state space canonical form for AM-DSB/SC [Sn], which resulted in the plant

$$G_2(s) = (3s^2 + 12s + 21)[(s+1)(s+2)(s+3)]^{-1}. \tag{2.10}$$

For $\sigma_w^2 = 1$, $\sigma_n^2 = 1$, coloured observation noise $N(s) = (s+3)(s+6)^{-1}$, and unweighted error ($W = 1$), a solution to the H_∞ problem was found at $\gamma^2 = 0.304$. The solution procedure is detailed in Appendix B. The magnitudes of the H_∞ and Wiener filters and the error spectra are shown in Figure 2.2 and 2.3 respectively. It is seen that the Wiener filter has a low-pass response, whereas the spectrum of the H_∞ filter is rather flat. (In fact it turns out that if the SNR is increased sufficiently, the resulting H_∞ filter possesses negligible dynamics, that is, it becomes a *do nothing filter* or a short circuit.) Figure 2.2 shows that the H_∞ filter minimises the peak error, the error spectrum is all-pass with a magnitude equal to γ^2. The Wiener filter is designed to minimise the cost function (2.6) which is the average error power or MSE. It is well known from theory (see Chapters 3 and 4) that compared to the Wiener filter, the H_∞ filter exhibits an increase in MSE. This can be observed from the area under the magnitude of the error spectrum in Figure 2.3, which is infinite for the (all-pass) H_∞ error spectrum. For this example it is seen that an improvement within the plant bandwidth is accompanied by a larger degradation at high frequencies. While the Wiener filter has greater susceptability to peak error within the signal bandwidth, it does minimise the MSE and therefore can be better on average. The H_∞ filter, by virtue of having a flatter response, is less able to reject any high frequency interference.

Example 2.2. An additional performance benefit can arise via the use of an appropriate weighting function. In the case of a first order low-pass function

$$W_1(s) = b(s+a)[a(s+b)]^{-1}, \tag{2.11}$$

the task is to search for a suitable constants $a > b > 0$. It turns out for Example 2.1 that good choices are $b = 3.34$, $a = 6.76$. This was obtained by alternately perturbing the pole and the zero of $W_1(s)$, recalculating the H_∞ filter via the solution procedure of Appendix B, numerically integrating the resulting error spectra (within the 3 dB bandwidth of the plant) and searching for a minimum. A H_∞ design arises at $\gamma^2 = 0.768$, so compared to the unity weighted case it is apparent that the penalty is an increase in peak error. The filter magnitudes and error spectra that result are shown in Figures 2.4 and 2.5 respectively. It can be seen that the use of the low-pass frequency weighting enables the magnitude of the low frequency error to be reduced even further by trading off the high frequency error.

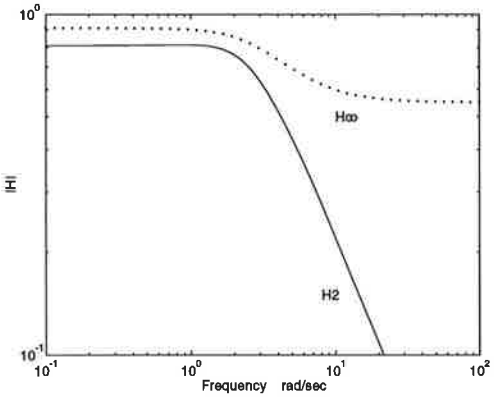

Fig. 2.2 Filter magnitudes for Example 2.1.

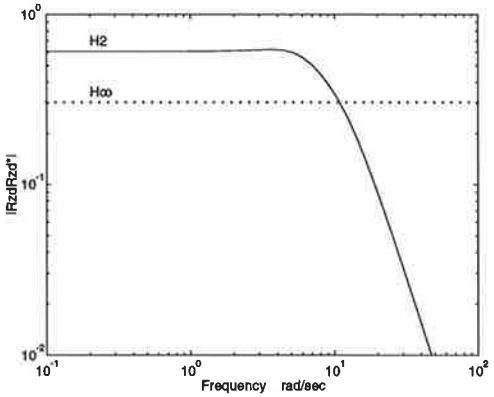

Fig. 2.3 Error spectra for Example 2.1.

The first order weighting function (2.11) may not be entirely satisfactory, since it is evident from Figures 2.4 and 2.5 that the frequency weighted H_∞ filter is rather sensitive to high frequency noise. This can be alleviated by choosing instead a weighting function possessing an additional high frequency zero, such as

$$W_2(s) = b(s+a)(s+10a)[10a^2(s+b)]^{-1}, \tag{2.12}$$

so that the filter magnitude has a high frequency roll-off. The filter magnitudes and error spectra that result from $b = 3.34$, $a = 6.76$ in (2.12) are also shown in Figures 2.4 and 2.5 respectively. Once again it can be seen that the reduction in the peak of the error spectrum magnitude is accomplished at the expense of MSE.

A disadvantage of frequency weighting is that the order of the problem is increased, which exacerbates design difficulties. The calculation of the optimal H_∞ filter (2.9) requires spectral factorisations to determine the Δ, Δ_2 and the cancellation of polynomial factors common to $U(s)$ and $\Delta^{-H}(s)$. It has been found that spectral factorisation and common

factor cancellation tend to be more error prone as the order of the problem increases (see Appendix B). The overhead in calculating the $U(s)$ increases dramatically with higher order problems because a symbolic matrix inversion is required (see Appendix B). Furthermore, the pursuit of polynomial weighting function that is somehow optimal, requires large number of candidates to be tested, which can become computionally expensive.

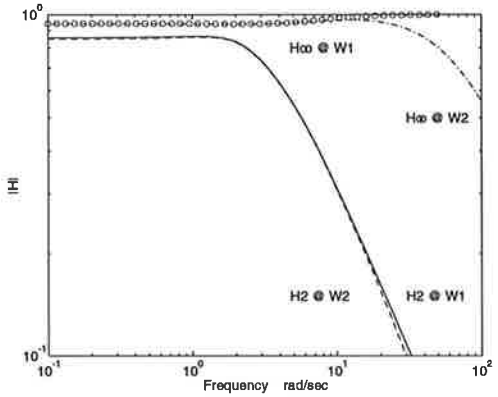

Fig. 2.4 Filter magnitudes for Example 2.2.

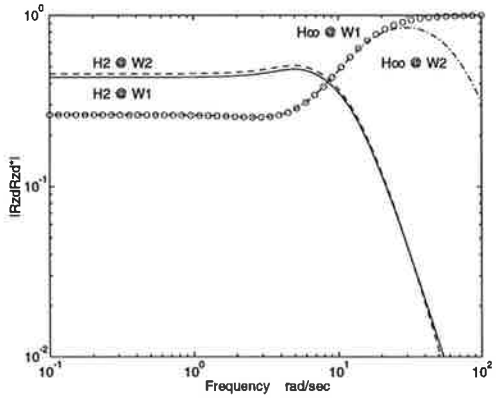

Fig. 2.5 Error spectra for Example 2.2.

Example 2.3. A commonly encountered filtering problem arises when the spectrum of the communications channel is low-pass and the cutoff frequency occurs within the signal bandwidth. The objective is to design H to mitigate the low-pass filtering of the signal by the channel. This equalisation problem can be modelled by choosing $G_2 = CG_1$ where G_1 and C are the transfer functions of the signal and channel models respectively.

Consider the low-pass signal model and channel models

$$G_1(z) = -2.33(z+1)(z-0.333)^{-1}, \quad C(z) = (1.4z-0.2)(z-0.6z)^{-1}, \tag{2.11}$$

which are the bilinear transforms of $G_1(s) = -7(s+1)^{-1}$ and $C(s) = (s+1.5)(s+0.5)^{-1}$ respectively. Denoting the output of CG_1 as y, from simulations it has been observed that $\sigma_w^2 = 1$ results in $\sigma_y^2 = 77.3$. It is desired to compare the performance of the unity weighted filters for high noise ($\sigma_n^2 = 77.3$, ie. 0 db SNR) and low noise ($\sigma_n^2 = 0.773$, ie. 20 dB SNR) cases. It turns out that the H_∞ solutions arise with $\gamma^2 = 13.6$ and $\gamma^2 = 0.57$ at 0 dB and 20 dB SNR respectively.

Since the H_∞ filter is designed to minimise the worst case bound of the ratio

$$\left(\frac{\sum_{k=1}^{n} |z_k|^2}{\sigma_w^{-2} \sum_{k=1}^{n} |w_k|^2 + \sigma_n^{-2} \sum_{k=1}^{n} |v_k|^2} \right) < \gamma^2, \tag{2.12}$$

it is expected that the observed energy ratio is bounded by γ^2. Simulations were conducted and the histograms of the energy ratios calculated for a 1000 realisations of 1000 data points each, are shown in Figures 2.6 and 2.7. It is seen that in both cases the energy ratios are distributed well below γ^2, indicating that the H_∞ design is rather conservative. For example at 20 dB SNR, the maximum observed energy ratio is 0.32, whereas H_∞ filter is designed for a worst case energy ratio of $\gamma^2 = 0.57$. It is conjectured that either the worst case realisations may occur rarely or they may occur for quite different combinations of input sequences, since H_∞ design makes no assumptions about probability distributions. Figure 2.7 illustrates that the H_∞ solution is extremely conservative. At 0 dB SNR, the maximum energy ratio of 6.7 exhibited by the H_∞ solution is less than $\gamma^2 = 13.6$ but is greater than 5.03 which was observed for the Wiener design.

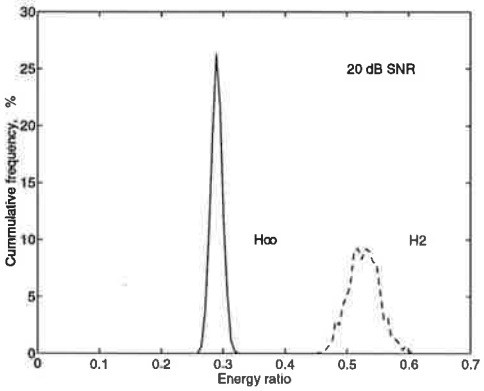

Fig. 2.6 Error histogram at 20 dB SNR.

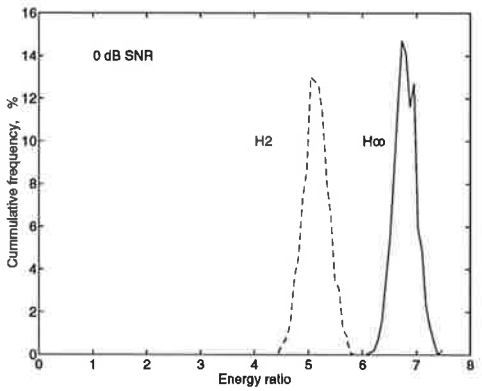

Fig. 2.7 Error histogram at 0 dB SNR.

For this example it is seen at 20 dB SNR, on average the error of H_∞ filter is about 2.5 dB less than the corresponding Wiener filter. When the SNR is decreased to 0 dB SNR, the Wiener equaliser is seen to be preferable. Evidently from this example, as the SNR is reduced, a design that provides robustness to worst case inputs can be too conservative. Thus if an equalisation problem is dominated by measurement noise and the (noise) statistics are known exactly, then it is best to proceed with a Wiener design.

Example 2.4. The application of discrete-time equalisation with binary data can be demonstrated via the configuration of Figure 2.8. The data w_t is an identically independently distributed (iid) binary sequence which is distorted by the channel. The effect of a low-pass channel on binary data is to smear the state transitions which is known as intersymbol interference (ISI). Here an equaliser serves to mitigate the channel distortion, which is followed by a limiter that quantises the equaliser output to [± 1].

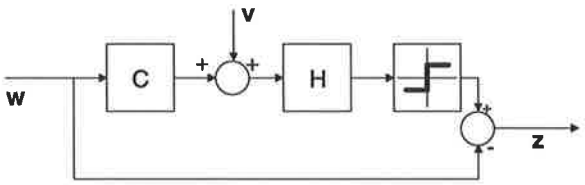

Fig. 2.8 The ISI problem.

Consider the low-pass channel model

$$C(z) = 0.214(z+1)(z+0.111)[(z+0.333)(z+0.1223)]^{-1}, \tag{2.13}$$

then from simulations it was observed that $\sigma_w^2 = 1$ results in $\sigma_y^2 = 0.198$. The Wiener and H_∞ equalisers were designed for 10 dB SNR ($\sigma_v^2 = 0.0198$) and 0 dB SNR ($\sigma_v^2 = 0.198$). The histograms of the bit error rate (BER) were calculated for 1000 realisations of 1000 data points each, these are shown Figures 2.9 and 2.10. At 10 dB SNR it is seen that the mean BER of the H_∞ equaliser is about 1.5 dB less than that exhibited by the Wiener equaliser, whereas at 0 dB SNR they perform similarly.

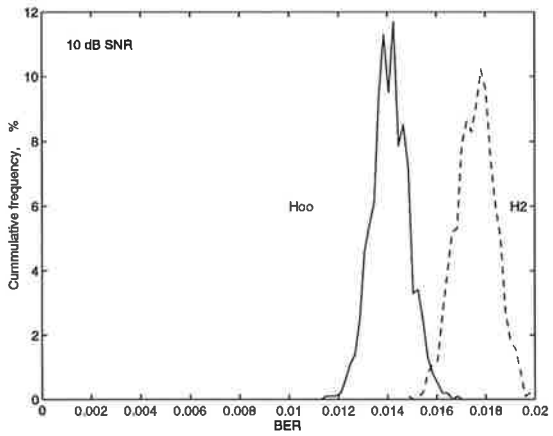

Fig. 2.9 BER at 10 dB SNR.

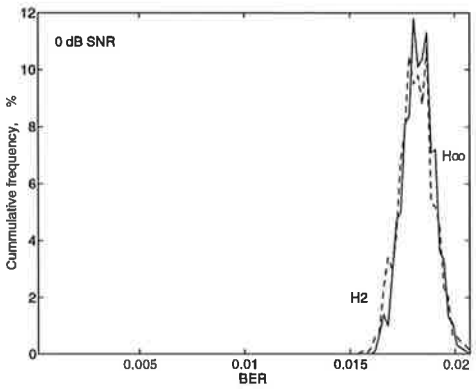

Fig. 2.10 BER at 0 dB SNR.

It has been illustrated that H_∞ designs can sometimes be advantageous, provided that the SNR is sufficiently high. When the SNR is reduced so that the problem becomes dominated by gaussian white noise, then it has been observed that the Wiener filter performs better. Performance trends are investigated in detail within Chapter 5.

2.7 Conclusions.

This chapter has introduced the filtering problems of output estimation and equalisation, and described some generalisations to a frequency domain solution. The frequency domain approach has two major disadvantages. Firstly, the problems are restricted to being stationary. Secondly, the method of solution suffers from computational difficulties. Both of these limitations are overcome by the game theoretic solutions which are the subject of subsequent chapters.

However in the stationary case, the H_∞ optimality criterion does have an intuitively pleasing interpretation, namely minimising the peak of the error spectrum magnitude. Furthermore, the solution of stationary problems is interesting because performance appraisals follow quite naturally from error spectra.

A few examples and the results of simulations studies have been presented to demonstrate that H_∞ filtering can beneficial. In particular it has been observed that,

- In an output estimation problem, if the SNR is sufficiently high the H_∞ filter approaches a short circuit.
- From the plots of the error spectrum magnitude, it can be seen that a reduction in the peak of the error spectrum is attained at the cost of an increase in MSE.
- The benefits (and costs) are most profound when there is an interest in certain parts of the spectrum, such as output estimation when the measurement noise is coloured, equalisation problems and where frequency weighting is applied.
- From the histograms of the energy ratios, it is apparent that H_∞ designs are extremely conservative at high SNR. Therefore it may be beneficial to proceed with a $\gamma > \gamma_{min}$ and thus trade-off peak error for MSE.
- If in an equalisation problem, the signal model and the noise statistics are known, then a H_∞ solution can be advantageous provided that the SNR is sufficiently high (see Examples 2.3 and 2.4). However when the problem is dominated by white measurement noise (see Examples 2.3 and 2.4 at 0 dB SNR), the robust equaliser can be too conservative, and it is preferable to proceed with a Wiener equaliser.

REFERENCES

[AM] Anderson, B.D.O. and J.B. Moore, *Optimal Filtering*, Prentice Hall, Englewood Cliffs, N.J., 1979.

[D] Dorato, P. (editor), *Robust Control*, IEEE Press, NY, 1987.

[DGKF] Doyle, J. C., K. Glover, P.P. Khargonekar and B.A. Francis, "State space solutions to standard H_2 and H_∞ control problems", *IEEE Trans. Automat. Contr.*, vol. 34, no. 8, pp. 831-847, Aug. 1989.

[EW] Einicke, G. A. and L.B. White, "The use of H_∞ filters for linear demodulation and equalisation", *IEEE Int. Symp. Circuits and Sys.*, vol. 4, pp. 1721-1724, May 1992.

[FZ] Francis, B.A. and G. Zames, "On H_∞-optimal sensitivity theory for SISO feedback systems", *IEEE Trans. Automat. Contr.*, vol. 29, no. 1, pp. 9-16, 1984.

[GE] Grimble, M. J. and A. El Sayed, "Solution of the H_∞ optimal linear filtering Problem for discrete-time systems", *IEEE Trans. Acoust., Speech, Signal Processing*, vol. 38, no. 7, pp. 1092-1104, Jul. 1990.

[Ki] Kimura, H., "Directional interpolation approach to H_∞-optimisation and robust stabilisation", *IEEE Trans. Automat. Contr.,* vol. 32, no. 12, pp. 1085-1093, Dec. 1987.

[Ku] Kucera, V., *Discrete linear control: The polynomial equation approach*, Wiley, Chichester, 1979.

[Pa] Papoulis, A., *Probability, random variables and stochastic processes*, McGraw-Hill, 2nd Ed., ch. 13, 1989.

[Sh] Shaked, U., "A general transfer-function approach to the steady-state linear quadratic Gaussian stochastic control problem", *Int. J. Control*, vol. 24, no. 6, pp. 771-800, 1976.

[Sh2] Shaked, U., "A transfer function approach to the linear discrete stationary filtering and the steady-state discrete optimal control problems", *Int. J. Control*, vol. 29, no. 2, pp. 279-291, 1979.

[Sh3] Shaked, U., "The explicit structure of inner matrices and its application in H_∞-optimization", *IEEE Trans. Automat. Contr.,* vol. 34, no. 7, pp. 734-738, Jul. 1989.

[Sh4] Shaked U., "H_∞-minimum error state estimation of linear Stationary Processes", *IEEE Trans. Automat. Contr.,* vol. 35, no. 5, pp. 554-558, May 1990.

[SM] Sage, A.P. and J.L. Melsa, *Estimation theory with applications to communications and control,* McGraw-Hill, N.Y., 1973.

[Sn] Snyder, D.L., *The State-variable Approach to Continuous Estimation*, Massachusetts, M.I.T. Press, pp. 50-53, 1969.

[YS] Yaesh, I. and U. Shaked, "A transfer function approach to the problems of discrete-time system: H_∞-optimal linear control and filtering", *IEEE Trans. Automat. Contr.*, vol. 36, no. 11, Nov. 1991.

[ZF] Zames G., B.A. Francis, "Feedback, minmax sensitivity, and optimal robustness", *IEEE Trans. Automat. Contr.,* vol. 28, pp. 585-600, May 1983.

Chapter 3

A continuous-time, game-theoretic H_∞ filter

In order to differentiate between interpolation solutions to H_∞ optimisation problems and those that arise by solving Riccati equations, the qualifier *game-theoretic* is used here; this also emphasises that the H_∞ solution is designed for the worst case inputs. The game-theoretic H_∞ filter has far wider application than the interpolation methods discussed in Chapter 1 for the reasons that follow.

- The solution is applicable to both non-stationary and stationary problems.
- Solving Riccati equations can avoid the numerical problems associated with spectral factorisation and the cancellation of common factors in polynomial fractions.
- the filter representation formula is a parameterisation of all linear filters meeting the H_∞ bound, whereas in the interpolation method of Chapter 2, the error spectrum is specified (to be all-pass) *a priori*.
- In particular, the filter representation formula includes the minimum entropy solution which exhibits a reduced MSE compared to an all-pass error solution.

Although the continuous-time, game-theoretic results have been reported extensively, it appears that the H_∞ filter is still not widely known and the cost benefits are not well understood. The contributions of this chapter include a comparison of minimum entropy and all-pass solutions and a proposal for a procedure that accommodates model uncertainty. The minimum entropy and all-pass solutions are stated in Section 3.2 and their merits are discussed in Section 3.3. The accommodation of model uncertainties is introduced in Section 3.4.

3.1 Background.

Arguably, [DGKF] is the first account of a continuous-time H_∞ filter requiring the solution of an ARE. In the development of the Kalman-Bucy filter [AM], the solution of an output estimation problem can be formulated by considering the dual of a regulator problem. Similarly the H_∞ filter can be found by exploiting a duality relationship with perfect information H_∞ control.

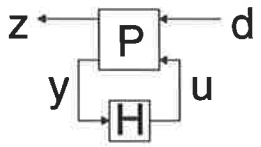

Fig. 3.1. A linear fractional transformation.

The basic block diagram used in [DGKF] is known as a linear fractional transformation (LFT) and is shown in Figure 3.1. The LFT represents a means of standardising a wide variety of feedback problems. The various plant models are combined into a single partitioned matrix $P(s) = \begin{bmatrix} P_{11} & P_{12} \\ P_{21} & P_{22} \end{bmatrix}(s)$ and $H(s)$ is a controller or filter to be found and this is known as the four block problem [GLDKS]. The LFT of the partitioned matrix P and the matrix H is defined as $F(P,K) = P_{11} + P_{12}H(I - P_{22}H)^{-1}P_{21}$ [MG,LG] and from Figure 3.1 it is seen that $z(s) = F(P,K)d(s)$. In H_∞ optimisation, the objective is to design a suitable $H(s)$ which minimises $\|F(P,K)\|_\infty$.

In [DGKF] the plant is assumed to be time-invariant and the representation formula for the H_∞ filter is based on the solution of an ARE. In the time-varying case, a Riccati differential equation is required and a derivation of the formulas appears in [LAKG]. The results of [LAKG] are also reported in [LS], they have since formed the basis of a course [Gr] and a book [GL].

An interesting by-product of the work in [LAKG] is the connection between the H_∞ filtering problem and game theory. The H_∞ optimisation problem is a zero-sum, leader-follower, dynamic game where the u-player (the filter designer) seeks to minimise the energy in $z(t)$ and the d-player (nature) maliciously tries to maximise it. The optimum filter satisfies a saddle point condition which arises as a function of the worst case inputs. A discussion of the dynamic game aspects of H_∞ control are detailed in [BB]. The theory is all known, the objective here is to provide concise statements of the results of [LAKG,Gr] and to show how filtering problems may be explicitly solved.

It is assumed that $P(s)$ has a time-varying, state-space realisation given by

$$P(s) \stackrel{s}{=} \begin{array}{c} \\ n \\ p \\ q \end{array} \begin{array}{c} \begin{array}{ccc} n & l & m \end{array} \\ \begin{bmatrix} A & B_{11} & B_{12} \\ C_{11} & D_{11} & D_{12} \\ C_{21} & D_{21} & D_{22} \end{bmatrix} \end{array}(t). \tag{3.1}$$

The formulation (3.1) is known as a generalised regulator problem [Gr]. Often the simplifications $D_{11}= 0$, $D_{22}= 0$ are assumed [LAKG,Gr]. An approach to tackle problems in which $D_{11}\neq 0$ and $D_{22}\neq 0$ is set out in [GLDKS]. For example, consider the general filtering problem of Figure 3.2 in which the plants G_2, $G_1 : \mathbf{R}\rightarrow\mathbf{R}$ have state space realisations denoted by $\begin{bmatrix} A_2 & B_2 \\ C_2 & 0 \end{bmatrix}$ and $\begin{bmatrix} A_1 & B_1 \\ C_1 & 0 \end{bmatrix}$ respectively. Then the components of (3.1) are $A=\begin{bmatrix} A_2 & 0 \\ 0 & A_1 \end{bmatrix}$, $B_{11}=\begin{bmatrix} 0 & B_2\sigma_w \\ 0 & B_1\sigma_w \end{bmatrix}$, $B_{12}=\begin{bmatrix} 0 \\ 0 \end{bmatrix}$, $C_{11}= [0\ -C_1]$, $C_{21}= [C_2\ 0]$, $D_{11}= [0\ 0]$, $D_{12}= 1$, $D_{21}= [\sigma_v\ 0]$ and $D_{22}= 0$. The objective is to design a filter denoted by the operator H, that estimates $\{\hat{G_1 w}\} = H\{y\}$ and yields $\|z\|^2 \leq \gamma^2(\sigma_w^{-2}\|w\|^2 + \sigma_v^{-2}\|v\|^2)$.

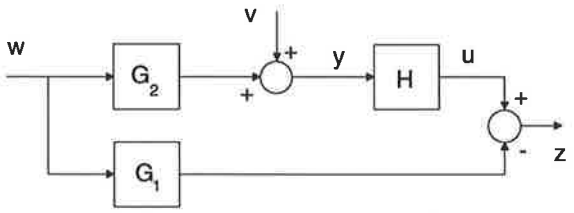

Fig. 3.2. The general filtering problem.

3.2 A statement of solutions.

The attention is confined to problems which can be written as

$$\begin{bmatrix} \dot{x} \\ z \\ y \end{bmatrix}(t) \overset{s}{=} \begin{matrix} n \\ p \\ q \end{matrix}\begin{bmatrix} \overset{n}{A} & \overset{l}{B_{11}} & \overset{m}{B_{12}} \\ C_{11} & 0 & D_{12} \\ C_{21} & D_{21} & 0 \end{bmatrix}(t)\begin{bmatrix} x \\ d \\ u \end{bmatrix}(t). \tag{3.2}$$

If both D_{12} and D_{21} are identity matrices, the plant is invertible and the controller or filter does not require the solution of an ARE and, this is known as a *problem of the first kind* [LAKG, Gr]. A so-called *problem of the second kind* [LAKG,Gr] arises if either D_{12} or D_{21} is an identity matrix. If $D_{21}= I$, a control ARE needs to be solved. In filtering problems, typically $D_{12}= I$ and an observation ARE needs to be solved. A *problem of the third kind* [LAKG,Gr] is defined as one where neither D_{12} nor D_{21} is an identity matrix, in which case the solution of two AREs is required.

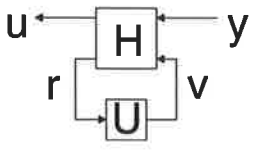

Fig. 3.3. The H_∞ filter.

In filtering problems where $D_{12}= I$ and $D_{21} = [I\ 0]$, the solution is not unique. It actually has the structure of Figure 3.3, in which $\gamma^{-1}U$ is a causal, contractive, free operator. The H_∞ filter is defined below.

Suppose that

$$\begin{bmatrix} \dot{x} \\ z \\ y \end{bmatrix}(t) \overset{s}{=} \begin{matrix} n \\ p \\ q \end{matrix}\begin{matrix} \begin{matrix} n & l & m \end{matrix} \\ \begin{bmatrix} A & B_{11} & B_{12} \\ C_{11} & 0 & I \\ C_{21} & D_{21} & 0 \end{bmatrix} \end{matrix}(t)\begin{bmatrix} x \\ d \\ u \end{bmatrix}(t), \tag{3.3}$$

is given with $D_{21} = [I \ 0]$, then a filter exists such that $\|R_{zd}\|_\infty < \gamma$ if and only if the ARE

$$(A - B_{11}D_{21}^T C_{21})P + P(A - B_{11}D_{21}^T C_{21})^T - P(C_{21}^T C_{21} - \gamma^{-2}C_{11}^T C_{11})P + B_{11}D^T{}_\perp D_\perp B_{11}^T = \dot{P}, \tag{3.4}$$

with $P(0) = 0$ has a positive definite solution on [0,T] and, the set of all filters with the property $\|R_{zd}\|_\infty < \gamma$ is parametrized by [LAKG, Thm. 3.2, p. 275]

$$\begin{bmatrix} \dot{\hat{x}} \\ u \\ v \end{bmatrix}(t) \overset{s}{=} \begin{bmatrix} A - B_{12}C_{11} & B_{11}D_{21}^T C_{21} - PC_{21}^T C_{21} & -B_{11}D_{21}^T - PC_2^T & -\gamma^{-2}PC_{11}^T \\ C_{11} & 0 & I \\ C_{21} & I & 0 \end{bmatrix}(t)\begin{bmatrix} \hat{x} \\ y \\ r \end{bmatrix}(t), \tag{3.5}$$

$$v(t) = (\mathsf{U}r)(t), \tag{3.6}$$

in which $\gamma^{-1}\mathsf{U}$ is a causal, contractive operator. Causality is discussed in Appendix A. An operator U is contractive if $\|\mathsf{U}\|_\infty \leq 1$ [LG, p. 296].

The $D_\perp$ is any matrix such that $[D^T{}_\perp \ D_{21}^T]^T$ is nonsingular and $D_\perp \ [D^T{}_\perp \ D_{21}^T]^T = [I \ 0]^T$, here $D_\perp = \begin{bmatrix} 0 \\ I \end{bmatrix}$. See [GLDKS, LAKG, Gr] for a discussion of orthogonal extensions. It turns out that setting the free operator, U, in (3.6) to zero (the ultimate contraction) is an optimum choice because it minimises the entropy for R_{zd} [LS, Thm. 3.9, p21]. The result is known as a minimum entropy filter and it is the filter which minimises the 2-norm of R_{zd} from the set of filters that minimises the ∞-norm of R_{zd} [St, p. 229].

Suppose for example, that the plants are strictly proper with $G_2 \overset{s}{=} \begin{bmatrix} A & B \\ C_2 & 0 \end{bmatrix}$, $G_1 \overset{s}{=} \begin{bmatrix} A & B \\ C_1 & 0 \end{bmatrix}$ and the noise covariances are unity. Then one may proceed with $B_{11} = [0 \ B]$, $C_{11} = -C_1$, $C_{21} = C_2$ and $B_{11}D_{21}^T = 0$. Since there is no path from the filter output to the plant, $B_{12} = 0$. Although in Figure 3.2 the error is defined as $z = u - G_1 w$, often it is more conventional to consider instead $\bar{z} = G_1 w - u$. Therefore, the negative of the state of (3.5) may be assumed. Thus the minimum entropy ($\mathsf{U} = 0$) H_∞ filter is

$$\begin{bmatrix} \dot{\hat{x}} \\ u \end{bmatrix}(t) \overset{s}{=} \begin{bmatrix} A - PC_2^T C_2 & PC_2^T \\ C_1 & 0 \end{bmatrix}(t)\begin{bmatrix} \hat{x} \\ y \end{bmatrix}(t). \tag{3.7}$$

The formulation (3.6) is also discussed in [Gr,LS]. Instead of minimising the entropy, it is possible to construct a H_∞ filter that yields an all-pass error.

Suppose that the plant in (3.2) is time-invariant, then scaling the input and output of U by γ and choosing $U=\gamma^{-1}$ ensures that $R_{zd}R_{zd}^H=\gamma^2 I$. This is shown in Appendix C.

The all-pass error version of (3.6) is given by

$$\begin{bmatrix}\dot{\hat{x}}\\ u\end{bmatrix}(t) \overset{s}{=} \begin{bmatrix}A-PC_2^TC_2-\gamma^{-1}PC_1^TC_2 & PC_2^T+\gamma^{-1}PC_1^T\\ C_1-\gamma C_2 & \gamma\end{bmatrix}(t)\begin{bmatrix}\hat{x}\\ y\end{bmatrix}(t). \tag{3.8}$$

The virtue of attaining an all-pass error is the subject of a subsequent section. In applications the noise variances are not likely to be unity and the plant may possess a direct feedthrough term. Defining $R=I\sigma_v^2$ and $Q=I\sigma_w^2$, $G_1 \overset{s}{=}\begin{bmatrix}A & B_1\\ C_1 & D_1\end{bmatrix}$ and $G_2 \overset{s}{=}\begin{bmatrix}A & B_2\\ C_2 & D_2\end{bmatrix}$, then a standard correlated noise argument (see Appendix D) may be used to obtain

$$\begin{bmatrix}\dot{\hat{x}}\\ u\end{bmatrix}(t) \overset{s}{=} \begin{bmatrix}A-KC_2 & K\\ C_1 & 0\end{bmatrix}(t)\begin{bmatrix}\hat{x}\\ y\end{bmatrix}(t), \tag{3.9}$$

where

$$K=(PC_2^T+B_2QD_2^T)R^{-1}, \tag{3.10}$$

is the filter gain and the RDE is

$$\begin{aligned}\dot{P}=&(A-B_2QD_2^TR^{-1}C_2)P+P(A-B_2QD_2^TR^{-1}C_2)^T-P(C_2^TR^{-1}C_2-\gamma^{-2}C_1^TC_1)P\\ &+B_2(Q-D_2Q^{1/2}R^{-1}Q^{1/2}D_2^T)B_2^T.\end{aligned} \tag{3.11}$$

Compared to the Kalman filter [SM], clearly the H_∞ filter has the same structure (3.8) and the gain calculation (3.9) is the same. The only difference arises in the quadratic term the RDE (3.10). Since the RDE (3.11) reverts to the Kalman RDE at $\gamma=\infty$, obviously the H_∞ filter (3.9) reverts to the Kalman filter at $\gamma=\infty$.

3.3 Some properties.

3.3.1. Increased error covariance upper bound.

Consider the output estimation problem where the plant model and noise statistics are known. It is shown here that if the initial RDE solution is set equal to (or greater than) the initial state error covariance, then the state error covariance is bounded above by the RDE solution.

For a linear filter of the form (3.9), it is easily shown that the state estimation error may be written as $\dot{e}=(A-KC)e+w-Kv$ (see Appendix G or [AM, p. 189]). Then the error covariance $\Sigma(t)=E\{e(t)e^T(t)\}$ is defined by (see [V, Prop. 14, p. 533])

$$\dot{\Sigma}=(A-KC)\Sigma+\Sigma(A-KC)^T+Q+KRK^T. \tag{3.12}$$

Let $\Sigma(t)$ denote the estimation error variance for the H_∞ filter where the gain is given by $K = PC^TR^{-1}$ in which

$$\dot{P} = AP + PA^T - PC^T(R^{-1} - \gamma^{-2}I)CP + BQB^T. \tag{3.13}$$

Subtracting (3.12) from (3.13) yields

$$\dot{P} - \dot{\Sigma} = (A - KC)^T(P - \Sigma) + (P - \Sigma)(A - KC)^T - (P - \Sigma)C^TR^{-1}C(P - \Sigma) + q, \tag{3.14}$$

where

$$q = \Sigma C^TRC\Sigma + PC^TRCP + \gamma^{-2}PC^TCP. \tag{3.15}$$

Clearly $q > 0$ from (3.15). From the monotonicity properties of Riccati differential equations [BG, Th. 10.11], if $P(t) \geq \Sigma(t)$ for some t, then $P(t) \geq \Sigma(t)$ for all subsequent times. Thus, provided that RDE is initialised appropriately, then the state error covariance is bounded above by the Riccati equation solution. Since the Kalman error covariance, denoted by $\tilde{P}(t)$, is the optimal error covariance, then by definition $\Sigma(t) \geq \tilde{P}(t)$. It follows that $P(t) \geq \Sigma(t) \geq \tilde{P}(t)$. Hence the price of robustness is an increase in the upper bound of the state error covariance.

3.3.2. Monotonicity.

Consider the known plant $\left(G \overset{s}{=} \begin{bmatrix} A & B \\ C & 0 \end{bmatrix}\right)$, known noise statistics, output estimation problem and suppose that a $\gamma_i > 0$ has been found so that the H_∞ RDE (3.13) has a positive definite solution. Then for a $\gamma_j > \gamma_i$, as $\gamma_j^{-2} \to 0$, the solution of the H_∞ RDE monotonically approaches the solution of the Kalman RDE. This can be seen by writing (3.13) as

$$\dot{P}_i = AP_i + P_iA^T - P_iC^TR^{-1}CP_i + Q_i. \tag{3.16}$$

in which $Q_i = BQB^T + \gamma_i^{-2}P_iC^TCP_i > 0$. It follows that $\gamma_j > \gamma_i \Rightarrow Q_j < Q_i$ and from the monotonicity results of RDEs [BG, Th. 10.11], if $P_j(t) \leq P_i(t)$ for some t, then $P_j(t) \leq P_i(t)$ for all subsequent t.

3.4 The equivalence of interpolation and game-theoretic solutions.

The purpose of this section is to briefly draw a comparison between the interpolation and game-theoretic approaches to solving stationary filtering problems.

The process of arriving at the optimal γ is remarkably similar because performing a spectral factorisation is equivalent to solving an ARE. In the task of partitioning the roots of a polynomial into those having positive and negative real parts, if γ is less than the optimum value, a pair will be located on the imaginary axis. In the case of attempting to partition the eigenvalues of the Hamiltonian (associated with the ARE) into those having positive and negative real parts, if γ is too small, a pair will be similarly located on the imaginary

axis. With both procedures, after having iteratively determined the minimum possible γ, in order to avoid numerical problems it is often necessary to increase γ slightly.

The interpolation solution of [Sh] is designed to have an all-pass error, whereas in the game-theoretic approach, it is usual to to assume a minimum entropy solution which results in a low-pass error. Two examples are presented to demonstrate that a minimum entropy filter is, in fact, preferable.

Example 3.1. Consider the stationary filtering problem of [Sh] where the plants are $G_2 = -50[(s+1)(s+2)(s+3)]^{-1}$, $G_1 = 25(s^2+2s+7)[(s+1)(s+2)(s+3)]^{-1}$ and $\sigma_v^2 = 1$, $\sigma_w^2 = 1$. At $\gamma = 9.375$, the interpolation solution (2.9) and the game-theoretic all-pass error solution (3.9) yield identically

$$H^\infty = \frac{-\gamma(s+1.648)(s+3.554)}{(s+4.122\pm 2.4j)}. \tag{3.17}$$

The minimum entropy filter (3.6) is

$$H^\infty = \frac{-\gamma 3.7e5(s+1.648)(s+3.554)}{(s+3.7e5)(s+4.122\pm 2.4j)}. \tag{3.18}$$

The minimum entropy filter has the same response at dc but has a reduced magnitude at high frequencies. The error spectra that result for the minimum entropy and all-pass error filters are shown in Figure 3.4. The minimum entropy filter is seen to exhibit the same peak error (since γ is unchanged) and the same performance over the bandwidth of the plant. The high frequency pole occurs well beyond the plant dynamics, so the minimum entropy filter has less sensitivity to high frequency noise.

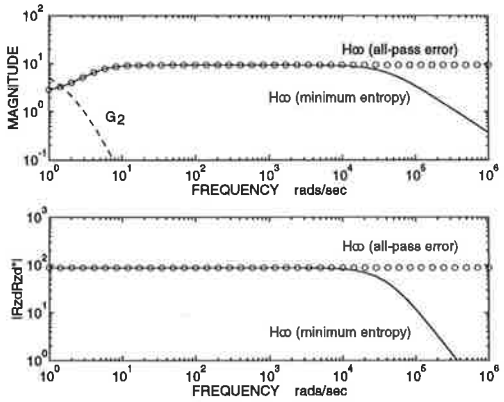

Fig. 3.4. Filter and error spectra for Example 3.1

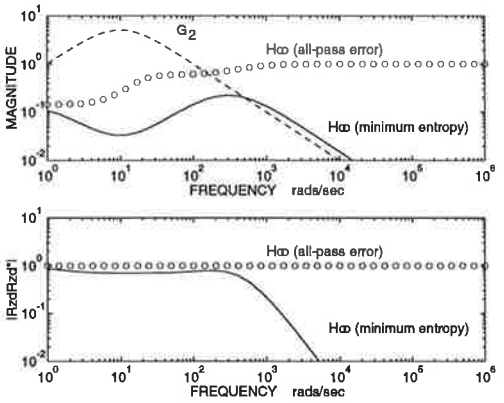

Fig. 3.5. Equaliser and error spectra for Example 3.2

Example 3.2. It is not at all surprising that a (low-pass) minimum entropy solution is advantageous in a low pass filtering problem. Now the task of equalising a band-pass channel is examined where it is, perhaps, less obvious how the minimum entropy solution

would perform. Continuous-time equalisation is discussed in Chapter 5. Consider the channel $G_2 = 100(s+0.1)(s+10)^{-2}$, together with $G_1 = 500(s+500)^{-1}$, $\sigma_v^2 = 1$ and $\sigma_w^2 = 1$. The equaliser and error spectra are shown in Figure 3.5. The equaliser is required to invert the channel and needs to assume a high magnitude at high frequencies. It can be seen from Figure 3.4 that the minimum entropy equaliser actually constructs a better inverse within the channel bandwidth. For this example the peak error occurs at dc, since the all-pass error solution maintains that error over the entire band, it exhibits greater mean square error (the area under the error spectrum). Once again it can be seen that the roll off exhibited by the minimum entropy solution occurs sufficiently beyond the plant dynamics. The only possible advantage offered by the all-pass error solution is that the shape of the error spectrum is known *a priori*. However as no applications are known where this is beneficial, it is concluded here that there is no virtue in all-pass error designs.

3.5 Model uncertainty.

The H_∞ filters of Section 3.3 rely implicitly on the assumption that the plant models are known. The contribution of this section is to outline a procedure that enables some model uncertainty to be accommodated.

Early methods of compensating for model errors in a H_2 framework are reported in [J,GA]. When model uncertainties exist, a common approach is to consider an alternate problem having additional measurement noise in lieu of the uncertainties. Such procedures tend to be *ad hoc* and rely on heuristics. There is no guidance on how much noise to add and whether the ensuing filter will even be satisfactory. More recently, uncertainties have been parametrized as additive perturbations to the plant state space parameters; in [GC,WHLHJ,XS], the parametric uncertainties are translated into tuning parameters within an extra term of a Riccati equation.

Filtering problems containing model uncertainties are accommodated quite naturally in a H_∞ framework. There is a rationale for scaling the noises and the robust filter is guaranteed to meet a worst case performance bound. Typically [FdSX,MHB], structured uncertainties are considered which leads to a higher dimension state vector. For example an uncertain plant could be modelled by

$$\dot{x} = (A + A_\Delta)x + (B + B_\Delta)w, \quad y = Cx. \tag{3.19}$$

This requires the uncertainty to be well characterised. Rather than parametrise the uncertainty, a more general approach [Gr] is to assume that the uncertainty is unstructured but has a known H_∞-norm bound. Here it is argued that the two approaches are equivalent. For example the model uncertainty may be additive as represented in Figure 3.6. In addition, if estimates are available for the dynamics of Δ, this then leads to a frequency

weighted uncertainty problem. In particular, the assumption $\Delta \overset{s}{=} \begin{bmatrix} A_\Delta & B_\Delta \\ C & 0 \end{bmatrix}$ leads precisely to the plant structure (3.19).

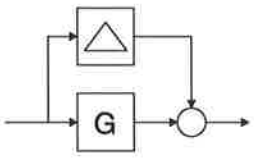

Fig. 3.6. Additive model uncertainty.

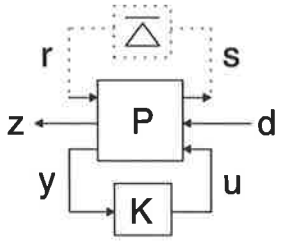

Fig. 3.7. Model uncertainty problem.

The approach adopted here follows on from M. Green's suggestion [Gr2] that a sufficient solution to a problem possessing an uncertainty Δ can be obtained by solving the H_∞ problem depicted in Figure 3.7. The scaled uncertainty $\bar{\Delta}$ is defined such that $\| \bar{\Delta} \|_\infty < \gamma^{-1}$. The input and output of the uncertainty are deemed to be exogenous. Suppose that the auxiliary H_∞ problem has been solved, then a γ has been found such that

$$\begin{aligned} \|z\|^2 + \|s\|^2 &< \gamma^2 (\|d\|^2 + \|r\|^2) \\ &< \gamma^2 (\|d\|^2 + \gamma^{-2}\|s\|^2) \\ \Rightarrow \|z\|^2 &< \gamma^2 \|d\|^2 \end{aligned}$$

The second inequality arises from the assumption $\| \bar{\Delta} \|_\infty^2 < \gamma^{-2}$, so that $\|r\|^2 < \gamma^{-2}\|s\|^2$. Thus modelling error may be accommodated by regarding the inputs and outputs of the uncertainties as inputs and outputs to an auxiliary H_∞ problem. Formal solutions for problems having additive or multiplicative uncertainty are defined below.

Lemma 3.1. (Additive model uncertainty) *Consider the filtering problem of Figure 3.8. Suppose that the actual plant comprises $G_2 \pm \Delta$ where G_2 is the nominal plant and Δ is an additive model uncertainty having a H_∞ norm bounded by δ, that is $\|\Delta\|_\infty \leq \delta$. Then (i) The solution of the auxiliary H_∞ problem of Figure 3.9 where $c_r^{-1} = \gamma\delta$, is a sufficient solution to the original problem of Figure 3.8. In particular, it is guaranteed that the induced norm of the map from the inputs through to the error will be bounded by γ.*
(ii) The solution to the scaled auxiliary H_∞ problem of Figure 3.10, in which $c_w^{-2} = \gamma^2(\gamma^2 - 1)^{-1}$, is sufficient for the solution of the original problem.

Proof. (i) Since $\|\Delta\|_\infty = \delta$ then $\|r\|^2 < \delta^2\|s\|^2$. Let $r' = c_r r$ and denote $d = \begin{bmatrix} v \\ w \end{bmatrix}$. By solving the H_∞ minimization problem of Figure 3.9, a γ is required to satisfy

$$\begin{aligned} \|s\|^2 + \|z\|^2 &< \gamma^2(\|d\|^2 + \|r'\|^2) \\ &= \gamma^2(\|d\|^2 + c_r^2\|r\|^2) \end{aligned}$$

$$\begin{aligned} &\leq \gamma^2(\|d\|^2 + c_r^2\delta^2\|s\|^2) \\ &= \gamma^2\|d\|^2 + c_r^2\gamma^2\delta^2\|s\|^2) \end{aligned} \tag{3.20}$$

Substituting $c_r = \dfrac{1}{\gamma\delta}$ into (3.20) yields $\|z\|^2 < \gamma^2\|d\|^2$.

(ii) From Figure 3.9 it can be recognised that $s = w$ and therefore $\|r\|^2 < \delta^2\|w\|^2$. By solving the H_∞ minimization problem of Figure 3.10, a γ is required to satisfy

$$\begin{aligned} \|z\|^2 &< \gamma^2(\|v\|^2 + \|w'\|^2 + \|r'\|^2) \\ &= \gamma^2(\|v\|^2 + \frac{\gamma^2-1}{\gamma^2}\|w\|^2 + \frac{1}{\gamma^2\delta^2}\|r\|^2) \end{aligned} \tag{3.21}$$

Expanding out (3.21) yields $\|z\|^2 < \gamma^2\|d\|^2$. ∇

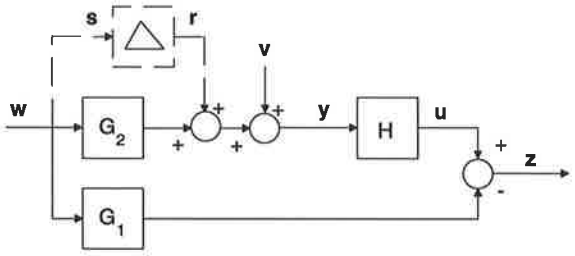

Fig. 3.8. Uncertain filtering problem.

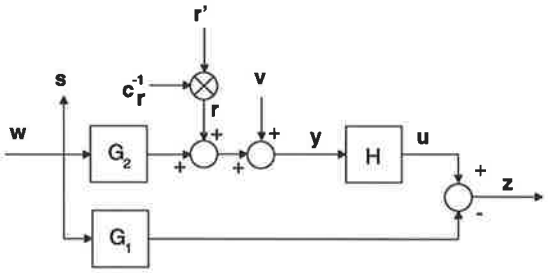

Fig. 3.9. Auxiliary filtering problem.

The first part of Lemma 3.1 is a direct application of M. Green's suggestion [Gr2]. In the auxiliary problem of Figure 3.8 there is a second output which is a little cumbersome. The second part of Lemma 3.1 shows how scaling may be applied to convert the two output problem into a one output problem. Hence an additive uncertainty can be accommodated by simply scaling the process noise and adding observation noise to an auxiliary problem which does not have any model uncertainty.

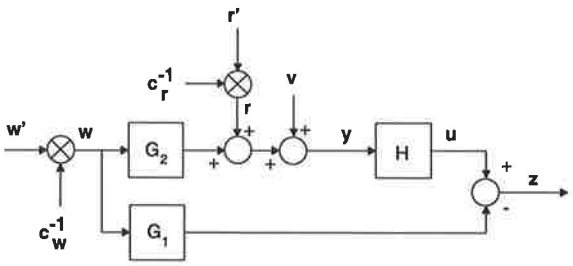

Fig. 3.10. Scaled filtering problem.

Lemma 3.2. (Multiplicative model uncertainty). *Consider a H_∞ filtering problem in which the actual plant comprises $G_2 \pm \Delta G_2$ where G_2 is the nominal plant and Δ is a model uncertainty and the H_∞-norm of ΔG_2 is bounded by δ, that is $\|\Delta G_2\|_\infty \leq \delta$. Then*
(i) The solution of an auxiliary H_∞ minimisation problem possessing an extra input scaled by $c_r = \gamma\delta$, is a sufficient solution to problem possessing the uncertainty.

(ii) The solution to a scaled auxiliary H_∞ minimisation problem, where the process noise is scaled by $c_w^2 = 1 - \gamma^{-2}\|G_2\|_\infty^2$, is sufficient for the solution of the problem possessing the uncertainty.

Proof. (i) Same as for Lemma 3.1(i).

(ii) Define $r' = c_r r$, $w' = c_w w$ and recognise that $s = G_2 w$. By solving the abovementioned scaled auxiliary H_∞ minimization problem, a γ is required to satisfy

$$\begin{aligned} \|z\|^2 &< \gamma^2(\|v\|^2 + \|w'\|^2 + \|r'\|^2) \\ &= \gamma^2(\|v\|^2 + \frac{\gamma^2 - \|G_2\|_\infty^2}{\gamma^2}\|w\|^2 + \frac{1}{\gamma^2\delta^2}\|r\|^2) \end{aligned} \tag{3.22}$$

Expanding out (3.21) yields $\|z\|^2 < \gamma^2\|d\|^2$. ∇

Remark 3.1. Regarding filters that are designed to offer some robustness to model uncertainty, clearly it is important not to overestimate δ otherwise the design observation noise power will be overly pessimistic. In addition, the designs arising via use of Lemma 3.1 and 3.2 are rather conservative, since the solution arises only out of sufficient conditions. Therefore it is prudent to explore the merits of filters that arise for a range of $\delta < \|\Delta\|_\infty$ and $\gamma > \gamma_{\min}$, although robustness may not be guaranteed.

Some numerical examples are presented in Chapter 5. Here a brief outline is given on how general problems may be solved. Suppose that the plants are SISO and an additive uncertainty exists with $G_1 \overset{s}{=} \begin{bmatrix} A_1 & B_1 \\ C_1 & 0 \end{bmatrix}$, $G_2 = G_0 \pm \Delta$, $G_0 \overset{s}{=} \begin{bmatrix} A_0 & B_0 \\ C_0 & 0 \end{bmatrix}$ and $\|\Delta\|_\infty = \delta$. Then a filter that offers some robustness to the model uncertainty can be found by solving the auxiliary problem of Figure 3.8 which may be represented by

$$\begin{bmatrix} \dot{x}_2 \\ \dot{x}_1 \\ z \\ y \end{bmatrix} \overset{s}{=} \begin{bmatrix} A_0 & 0 & 0 & 0 & B_0\bar{\sigma}_w & 0 \\ 0 & A_1 & 0 & 0 & B_1\bar{\sigma}_w & 0 \\ 0 & -C_1 & 0 & 0 & 0 & 1 \\ C_0 & 0 & \sigma_r & \sigma_v & 0 & 0 \end{bmatrix} \begin{bmatrix} x_2 \\ x_1 \\ r \\ v \\ w \\ u \end{bmatrix}, \tag{3.23}$$

where $\sigma_r = \gamma\delta$, $\bar{\sigma}_w = \frac{\gamma\sigma_w}{\sqrt{\gamma^2 - 1}}$. If the inputs are gaussian, the σ_v^2 and σ_w^2 correspond to the process variances, otherwise they may be interpreted as weights. In the case that the inputs are uncorrelated gaussian processes, then (3.23) may be simplified by proceeding with $\bar{\sigma}_v^2 = \sigma_v^2 + c_r^2$ in lieu of r. If an estimate is available for the dynamics of the uncertainty such as $\Delta \overset{s}{=} \begin{bmatrix} A_\Delta & B_\Delta \\ C_\Delta & 0 \end{bmatrix}$, then this leads to a coloured noise problem, viz

$$\begin{bmatrix} \dot{x}_0 \\ \dot{x}_1 \\ \dot{x}_\Delta \\ z \\ y \end{bmatrix} \overset{s}{=} \begin{bmatrix} A_0 & 0 & 0 & 0 & 0 & B_0\bar{\sigma}_w & 0 \\ 0 & A_1 & 0 & 0 & 0 & B_1\bar{\sigma}_w & 0 \\ 0 & 0 & A_\Delta & B_\Delta c_r & 0 & 0 & 0 \\ 0 & -C_1 & 0 & 0 & 0 & 0 & 1 \\ C_0 & 0 & C_\Delta & 0 & \sigma_v & 0 & 0 \end{bmatrix} \begin{bmatrix} x_0 \\ x_1 \\ x_\Delta \\ r \\ v \\ w \\ u \end{bmatrix}. \tag{3.24}$$

The H_∞ filter may be obtained by constructing the RDE (3.3) for the augmented blocks of (3.19) and calculating the gain in the usual way. Here $A = diag[A_0, A_1, A_\Delta]$, $C_{11} = [0\ -C_1\ 0]$, $C_{21} = [C_0\ 0\ C_\Delta]$, $B_{11} = \begin{bmatrix} 0 & 0 & B_0\bar{\sigma}_w \\ 0 & 0 & B_1\bar{\sigma}_w \\ B_\Delta\sigma_r & 0 & 0 \end{bmatrix}$. The filter is given by (3.9) where $K = PC_{21}^T\sigma_v^{-2}$ is the gain and P arises from the RDE (3.4).

Some examples are presented in Chapter 5.

Remark 3.2. The methods set out here for accommodating model uncertainty are conservative. One possible reformulation (in Lemma 3.4) is to introduce a new input ρr instead of r, resulting in $c_r^{-2} = \rho^{-2}\gamma^2\delta^2$, which allows a reduction in conservativeness of the design by appropriate choice of $\rho > 0$. While unstructured uncertainties are simpler to describe, the incorporation of plant structure, is expected in general, to result in a less conservative design. For example in an uncertain channel equalisation problem (of Section 5.4.5), the use of a structured uncertainty is crucial to the success of the design.

3.6 Conclusions.

The known results for the continuous-time H_∞ filter have been stated. The method of solution for H_∞ problems is the same as for H_2 problems. Namely the problem can to be formulated in a general regulator framework and a Riccati equation is then required to be solved. The gain calculation and filter structure remains unchanged. The only difference is that the quadratic term of the Riccati equation is a function of a scalar γ, the minimum value of which needs to be determined iteratively.

In the case of time-invariant plants, the value of γ corresponds to the peak of the error power spectral density. Since the H_∞ filter is designed to minimise the peak error for the worst case input conditions, it is rather conservative. It may be advantageous to pay less attention to the worse case peak error design by choosing γ greater than the minimum possible value. In the limit, if there is no interest in peak error whatsoever, at $\gamma = \infty$, the H_∞ filter reverts to the Kalman filter.

It has been shown that the estimation error variance for the H_∞ filter is greater than or equal to the optimal Kalman filter error variance. Thus the cost of minimising the maximum magnitude of the error spectrum is an increase in MSE.

The choice of γ^{-1} for the free operator in the open loop formulation of the H_∞ filter (3.5), (3.6) has been found to yield all-pass error.

It has been illustrated, via an example, that the interpolation approach and the all-pass game-theoretic solution can yield the same filter. Compared to an all-pass error solution, the minimum entropy solution can be advantageous for two reasons.

- The minimum entropy filter is that which minimises mean square error from the set which satisfies the H_∞ optimality criterion [St, p. 229]. Consequently the minimum entropy solution is strictly proper and exhibits reduced error beyond the plant bandwidth.
- If the peak error occurs at dc, (see Example 3.2 where a band-pass channel is equalised at high SNR,) then the minimum entropy design may exhibit reduced error within the plant bandwidth.

H_∞ filters can be designed to provide some robustness to modelling errors. This may be done by converting the problem possessing the modelling uncertainty into an auxiliary problem which has an additional input in lieu of the uncertainty. Design methods have been outlined for problems having either additive or multiplicative model uncertainties.

REFERENCES

[AM] Anderson, B. D. O. and J. B. Moore, *Optimal control. Linear quadratic methods.*, Prentice-Hall, Englewood Cliffs, NJ, pp. 178-205, 1989.

[BB] Basar, T. and P. Bernhard, *H_∞ optimal control and minmax design problems. A dynamic game approach.*, Birkhauser, Boston, pp. 13-103, 1991.

[BG] Bitmead, R. R. and M. Gevers, "Riccati difference and differential equations: convergence, monotonicity and stability", in: S. Bittanti, A. J. Laub, J. C. Willems, Eds., *The Riccati equation*, Springer-Verlag, sec. 10.6.2, 1991.

[DGKF] Doyle, J. C., K. Glover, P.P. Khargonekar and B.A. Francis, "State space solutions to standard H_2 and H_∞ control problems", *IEEE Trans. Automat. Contr.*, vol. 34, no. 8, pp. 831-847, Aug. 1989.

[FdSX] Fu, M., C.E. de Souza and L. Xie, "H_∞ estimation for uncertain systems", *Technical Report EE9039*, Department of Electrical Engineering and Computer Science, University of Newcastle, NSW, Australia, May 1990.

[GL] Green, M. and D. J. N. Limebeer, *Robust Linear Control*, Prentice-Hall, Englewood Cliffs, N.J., 1993.

[GLDKS] Glover, K., D. J. N. Limebeer, J. C. Doyle, E. M. Kasenally and M. G. Safonov, "A characterization of all solutions to the four block general distance problem", *SIAM J. Contr. Optim.*, vol. 29, no. 2, pp. 283-324, Mar. 1991

[Gr] Green, M., *Optimal H_∞ control course*, Faculty of Engineering and Information Technology, Dept. of Systems Engineering, Australian National University, 3rd - 7th Feb. 1992.

[Gr2] Green, M., Personal communication, Faculty of Engineering and Information Technology, Dept. of Systems Engineering, Australian National University, 29th Apr., 1992.

[Gu] Gu, K. and Y. H. Chen, "Uncertain systems: new uncertainty characterization for linear control design", *Proc. IEEE CDC,* Tampa, Florida, pp. 1508-1512, Dec. 1989.

[LAKG] Limebeer, D. J. N., B. D. O. Anderson, P. P. Khargonekar and M. Green, "A game theoretic approach to H^∞ control for time-varying systems", *SIAM J. Contr. Optim.*, vol. 30, no. 2, pp. 262-283, Mar. 1992.

[LG] Limebeer, D. J. N. and M. Green, "Parametric interpolation, H_∞-control and model reduction", *Int. J. Contr.*, vol. 52, no. 2, pp. 293-318, 1990.

[LS] D.J.N. Limebeer and U. Shaked, "Minimax terminal state estimation and H_∞ filtering", submitted to *IEEE Trans. Automat. Contr.,* 1992.

[MG] McFarlane, D. C. and K. Glover, *Robust controller design using normalised coprime factor plant descriptions*, Lecture notes in control and information sciences, vol. 38, Springer-Verlag, Berlin, 1990.

[MHB] Madiwale, A. N., W. M. Haddad and D. S. Bernstein, "Robust H^∞ control design for systems with structured parameter uncertainty", *Proc. IEEE CDC*, Austin, Texas, pp. 965-972, Dec. 1988.

[Sh] Shaked, U. "H_∞-minimum error state estimation of linear stationary processes", *IEEE trans. Automat. Contr.*, vol. 35, no. 5, pp. 554-558, May 1990.

[SM] Sage, A. P. and J. L. Melsa, *Estimation theory with applications to communications and control*, McGraw-Hill, NY, p. 304, 1973.

[St] Stoorvogel, A. *The H_∞ control problem, A state space approach,* Prentice-Hall, Englewood Cliffs, NJ, pp. 139-153, 1992.

[V] Van Trees, H. H. *Detection, estimation and modulation theory*, John Wiley & Sons, N.Y, p. 533, 1968.

[WKLHJ] Wang, S. D., T. S. Kuo, Y. H. Lin, C. F. Hsu and Y. T. Juang, "Robust control design for linear systems with uncertain parameters", *Int. J. Control*, vol. 46, no. 5, pp. 1557-1567, 1987.

Chapter 4

A discrete-time, game-theoretic H_∞ filter

The H_∞ filter is simply the solution to the dual of the control *problem of the second kind* [LAKG]. The controller for *problems of the third kind* [LAKG] requires the solution of two RDEs and the discrete-time game-theoretic results are reported in [LGW]. A derivation that is couched in terms of J-lossless coprime factorizations, which applies to both continuous-time and discrete-time systems, is detailed in [Gr]. The contribution of this chapter is the specialisation of [LGW] to filtering. On first inspection the H_∞ filter may seem enigmatic because it possesses a direct feedthrough term even when the plant does not, but in fact the Kalman filter does likewise. It is shown subsequently that the H_∞ filter reverts trivially to the Kalman filter when $\gamma = \infty$. The formulation derived here is the basis of the extended H_∞ filter discussed in Chapter 7.

The derivation of the game-theoretic discrete-time H_∞ filter discussed here follows the continuous-time case [LAKG,Gr2] and is presented in Section 4.2. Some properties of H_∞ filters and predictors are stated in Section 4.3.

4.1 Motivation.

It is seen in Chapter 3 that the continuous-time H_∞ filter is intimately related to the Kalman-Bucy filter - the only difference is that the quadratic term of the RDE is more complicated. The same is true for the discrete-time case and this has motivated the reformulation of the solutions in [LGW,Gr].

Arguably most signals that occur in nature are bandlimited and so it is quite reasonable that most texts confine their attention to plants that are strictly proper. However the application of the bilinear transform to a strictly proper continuous-time plant generally leads to a discrete-time model that possesses a direct feedthrough term. In some applica-

tions such as equalisation, there is a requirement to accommodate direct feedthroughs. This chapter addresses the problem where the two plants depicted in Figure 3.2 may be different and possess non-zero direct feedthrough terms. The exogenous inputs v_k and w_k, are assumed to be uncorrelated, zero mean, gaussian processes with known covariances $E\{v_k v_k^T\} = R$ and $E\{w_k w_k^T\} = Q$. For convenience of notation, the inputs are referred to jointly as $d_k = \begin{bmatrix} v_k \\ w_k \end{bmatrix}$. The plants are assumed to have state space representations denoted by $G_2 \triangleq \begin{bmatrix} A & B_2 \\ C_2 & D_2 \end{bmatrix}$ and $G_1 \triangleq \begin{bmatrix} A & B_1 \\ C_1 & D_1 \end{bmatrix}$. (If G_1 and G_2 have different dynamics one may proceed similarly by defining $\overline{A} = diag\ [A_1, A_2]$, $\overline{C}_1 = [0\ C_1]$ and $\overline{C}_2 = [C_2\ 0]$.)

The problem may be cast in a general regulator framework, that is

$$\begin{matrix} \\ n \\ p \\ l \end{matrix} \begin{bmatrix} x_{k+1} \\ z_k \\ y_k \end{bmatrix} \triangleq \begin{matrix} n & l & m \\ \multicolumn{3}{c}{} \end{matrix} \begin{bmatrix} A & B_{11} & 0 \\ C_{11} & D_{11} & D_{12} \\ 0 & D_{21} & 0 \end{bmatrix}_k \begin{bmatrix} x_k \\ d_k \\ u_k \end{bmatrix}. \tag{4.1}$$

A review of the Kalman solution is provided in Appendix D. The Kalman predictor is

$$\begin{bmatrix} \hat{x}_{k+1/k} \\ u_{k/k-1} \end{bmatrix} \triangleq \begin{bmatrix} A - \tilde{K} C_2 & \tilde{K} \\ C_1 & 0 \end{bmatrix}_k \begin{bmatrix} \hat{x}_{k/k-1} \\ y_k \end{bmatrix}, \tag{4.2}$$

where the output prediction is $u_{k/k-1} = C_1 \hat{x}_{k/k-1}$, in which $\hat{x}_{k/k-1}$ is the minimum variance estimate of x_k given the data $\{y_{k-1}, y_{k-2}, y_{k-3}, \ldots\}$. For convenience of notation, the k-dependence is not shown, except where confusion may arise. The one-step-ahead predictor gain is given by

$$\tilde{K}_k = (A\tilde{P}_k C_2 + B_2 Q D_2^T)\tilde{\Omega}_k^{-1}, \tag{4.3}$$

where $\tilde{\Omega}_k = C_2 \tilde{P}_k C_2^T + D_2 Q D_2^T + R$ and $\tilde{P}_k$ satisfies the RDE

$$\tilde{P}_{k+1} = A\tilde{P}_k A^T - \tilde{K}_k \tilde{\Omega}_k \tilde{K}_k^T + B_2 Q B_2^T. \tag{4.4}$$

The true Kalman filter that estimates $C\hat{x}_{k/k}$ (denoted by $u_{k/k}$) may be written as

$$\begin{bmatrix} \hat{x}_{k+1/k} \\ u_{k/k} \end{bmatrix} \triangleq \begin{bmatrix} A - \tilde{K}_k C_2 & \tilde{K}_k \\ C_1 - \tilde{D}_k C_2 & \tilde{D}_k \end{bmatrix}_k \begin{bmatrix} \hat{x}_{k/k-1} \\ y_k \end{bmatrix}, \tag{4.5}$$

in which

$$\tilde{D}_k = (C_1 P_k C_2^T + D_1 Q D_2^T)\tilde{\Omega}_k^{-1}. \tag{4.6}$$

(Alternatively, one can obtain a single recursion for $\hat{x}_{k/k}$ by combining (D.8) and (D.16) using the approach of [AM, p. 116].) Denoting the prediction error as $y_k - C_2 \hat{x}_{k/k-1}$ allows (4.2) and (4.5) to be expressed equivalently as

$$\begin{bmatrix} \hat{x}_{k+1/k} \\ u_{k/k-1} \\ u_{k/k} \end{bmatrix} \stackrel{z}{=} \begin{bmatrix} A & \tilde{K} \\ C_1 & 0 \\ C_1 & \tilde{D} \end{bmatrix}_k \begin{bmatrix} \hat{x}_{k/k-1} \\ y_k - C_2 \hat{x}_{k/k-1} \end{bmatrix}. \tag{4.7}$$

It will be shown subsequently that the game-theoretic H_∞ filter has precisely the forms of (4.2) and (4.7).

4.2 An evolution of the H_∞ filter.

The discrete-time game-theoretic H_∞ filter can be derived following the arguments for the continuous-time case [LAKG,Gr]. The objective is to design a filter, denoted by the operator H, that produces the sequence $\{u\} = \mathsf{H}\{y\}$ which is an estimate of $\mathsf{G}_1\{w\}$ so that the error sequence, denoted by z_k, satisfies

$$\|z\|^2 \leq \gamma^2 \sigma_d^{-2} \|d\|^2, \tag{4.8}$$

for any input sequence d_k and any filter output sequence u_k. In [LAKG,Gr2] it is recognised that solving a full information problem is connected with playing a leader-follower difference game in which the u-player (the controller designer) seeks to minimise the energy in z_k and the d-player (nature) maliciously seeks to maximise it. It turns out that the optimal strategy arises as a saddle point condition between the worst case input sequence d_k^* and the best case control sequence u_k^* and

$$\|z\|^2 - \gamma^2 \|d\|^2 = \|u - u^*\|^2 - \gamma^2 \|d - d^*\|^2. \tag{4.9}$$

The solution to problems of the third kind [LGW,Gr] can be simplified for filtering. The details are presented in Appendix E. Firstly the saddle point conditions are stated for the so-called *perfect information* problem where it is assumed that the inputs and the states are available. Then a state observer is developed (assuming that $D_{21} = I$) and combined with the perfect information control law as if the state reconstruction were perfect. The solution to the dual problem where $D_{12} = I$ is found via a standard inverse adjoint argument of [Gr2,IG].

Consider the following definitions: $\overline{B} = [B_{11}\ 0]$, $\overline{C} = \begin{bmatrix} C_{11} \\ C_{21} \end{bmatrix}$, $\overline{D} = \begin{bmatrix} D_{11}\ \mathrm{I_p} \\ D_{21}\ 0 \end{bmatrix}$, $J_{pl} = \begin{bmatrix} I_p & 0 \\ 0 & -\gamma^2 I_l \end{bmatrix}$ and $J_{ml} = \begin{bmatrix} I_m & 0 \\ 0 & -\gamma^2 I_l \end{bmatrix}$. The main result is stated below without proof.

Suppose for every sequence d_k there exists a $S_k > 0$ and a M_k such that $M_k S_k^{-1} M_k^T > 0$ for all k, where

$$S = \begin{bmatrix} S_1 & S_2 \\ S_2^T & S_3 \end{bmatrix} = \overline{D} J_{lm} \overline{D}^T + \overline{C} P_k \overline{C}, \tag{4.10}$$

$$M = \overline{B} J_{lm} \overline{D}^T + A P_k \overline{C}^T, \tag{4.11}$$

$$W=\begin{bmatrix} W_{11} & W_{12} \\ W_{21} & 0 \end{bmatrix} \text{ such that } S=WJ_{qm}W^T, \tag{4.12}$$

$$L=[L_1 \;\; L_2]=MW^{-T}J_{qm}^{-1}, \tag{4.13}$$

in which P_k satisifies the RDE

$$P_{k+1}=AP_kA^T-MS^{-1}M^T+\overline{B}J_{lm}\overline{B} \tag{4.14}$$

and $P_0=0$. Then the open loop filter

$$\begin{bmatrix} \hat{\underline{x}}_{k+1/k} \\ \underline{u}_k \\ j_k \end{bmatrix} \overset{z}{=} \begin{bmatrix} A-B_{12}C_{11}+B_{12}W_{11}W_{21}^{-1}C_{21}-L_1W_{12}^{-1}C_{21} & B_{21}W_{11}W_{21}^{-1}-L_1W_{21}^{-1} & \gamma(L_2-B_{12}W_{12}) \\ C_{11}-W_{11}W_{12}^{-1}C_{21} & -W_{11}W_{21}^{-1} & \gamma W_{12} \\ \gamma W_{21}^{-1}C_{21} & \gamma W_{21}^{-1} & 0 \end{bmatrix}_k \begin{bmatrix} \hat{\underline{x}}_{k/k-1} \\ y_k \\ i_k \end{bmatrix} \tag{4.15}$$

satisifies (4.9).

The minimum entropy solution is optimum [LS,St] and in filtering problems there is usually no path from the output to the state. Hence with $\boldsymbol{U}=0$ and $B_{12}=0$, (4.15) becomes

$$\begin{bmatrix} \hat{\underline{x}}_{k+1/k} \\ \underline{u}_k \end{bmatrix} \overset{z}{=} \begin{bmatrix} A-L_1W_{21}^{-1}C_{21} & -L_1W_{21}^{-1} \\ C_{11}-W_{11}W_{21}^{-1}C_{21} & -W_{11}W_{21}^{-1} \end{bmatrix}_k \begin{bmatrix} \hat{\underline{x}}_{k-1/k} \\ y_k \end{bmatrix}. \tag{4.16}$$

From [LGW, (2.41), p. 394] it follows that W may be obtained from S via

$$W_{12}W_{12}^T=\gamma^{-2}(S_2S_3^{-1}S_2^T-S_1), \quad W_{21}W_{21}^T=S_3, \quad W_{11}=S_2S_3^{-1}W_{21}=S_2W_{21}^{-T}, \tag{4.17}$$

and it is easy to verify (4.17) satisfies (4.12). The result $\begin{bmatrix} A & B \\ C & 0 \end{bmatrix}^{-1}=\begin{bmatrix} 0 & C^{-1} \\ B^{-1} & -B^{-1}AC^{-1} \end{bmatrix}$ leads to

$$(JW^T)^{-1}=\begin{bmatrix} 0 & -\gamma^{-2}W_{12}^T \\ W_{21}^T & \gamma^{-2}W_{21}^TW_{11}W_{12}^T \end{bmatrix}, \tag{4.18}$$

provided the inverses exist. Substituting $\overline{B}=[0 \;\; B_2Q^{1/2} \;\; 0]$, $\overline{C}=\begin{bmatrix} -C_1 \\ C_2 \end{bmatrix}$ and

$\overline{D}=\begin{bmatrix} 0 & -D_1Q^{1/2} & 1 \\ R^{1/2} & D_2Q^{1/2} & 0 \end{bmatrix}$ into (4.10) yields $S=\begin{bmatrix} C_1PC_1^T+D_1QD_1^T-\gamma^2I & -C_1PC_2^T-D_1QD_2^T \\ -C_2PC_1^T-D_2QD_1^T & C_2PC_2^T+D_2QD_2^T+R \end{bmatrix}$.

Then from (4.13), (4.17) the predictor gain may be written as

$$K_k=L_1W_{21}^{-1}=(B_2QD_2^T+AP_kC_2^T)S_3^{-1}=(B_2QD_2^T+AP_kC_2^T)(C_2P_kC_2^T+D_2QD_2^T+R)^{-1}. \tag{4.19}$$

The filter gain is

$$D_k=-W_{11}W_{21}^{-1}=-S_2S_3^{-1}=(C_1P_kC_2^T+D_1QD_2^T)(C_2P_kC_2^T+D_2QD_2^T+R)^{-1}. \tag{4.20}$$

Since it is more conventional to define the error as $-z_k=G_1w_k-u_k$, the negative of the state in (4.16) is assumed, hence a simplified minimum entropy H_∞ filter is

$$\begin{bmatrix} \hat{\underline{x}}_{k+1/k} \\ \underline{u}_{k/k} \end{bmatrix} \overset{z}{=} \begin{bmatrix} A-KC_2 & K \\ C_1-DC_2 & D \end{bmatrix}_k \begin{bmatrix} \hat{\underline{x}}_{k/k-1} \\ y_k \end{bmatrix}. \tag{4.21}$$

Clearly the H_∞ filter (4.21) has the same structure as the Kalman filter of (4.5). The predictor gain and feedthrough term calculations are the same, only the RDEs are different. This is perhaps more apparent when the plants are strictly proper in which case (4.14) becomes

$$P_{k+1}=AP_kA^T-AP_k\begin{bmatrix}-C_1^T\\ C_2^T\end{bmatrix}\begin{bmatrix}C_1P_kC_1^T-\gamma^2\mathrm{I} & -C_1P_kC_2^T\\ -C_2P_kC_2^T & C_2P_kC_2^T+R\end{bmatrix}^{-1}[-C_1\ \ C_2]P_kA^T+B_2QB_2. \quad (4.22)$$

Using the arguments of Appendix E, the H_∞ (one-step-ahead) predictor may similarly be defined by

$$\begin{bmatrix}\hat{\underline{x}}_{k+1/k}\\ \underline{u}_{k/k-1}\end{bmatrix}\overset{z}{=}\begin{bmatrix}A-KC_2 & K\\ C_1 & 0\end{bmatrix}_k\begin{bmatrix}\hat{\underline{x}}_{k/k-1}\\ y_k\end{bmatrix}. \quad (4.23)$$

To establish that the H_∞ filter reverts to H_2 filter at $\gamma=\infty$, it needs to be shown that (4.14) reverts to (4.4) when $\gamma=\infty$. The quadratic term in (4.4) is $-LJL^T=-L_1L_1^T+\gamma^2L_2L_2^T$. Since $-L_1L_1^T$ is the quadratic term in the H_2 RDE, it remains to be shown that $\gamma^2L_2L_2^T$ vanishes at $\gamma=\infty$. Clearly $L_2=(\bar{B}J\bar{D}^T+AP\bar{C}^T)\begin{bmatrix}-\gamma^{-2}W_{12}^{-T}\\ \gamma^{-2}W_{21}^{-T}W_{11}W_{12}^{-T}\end{bmatrix}$ from (4.13) and (4.18). It is easily seen that $\gamma^2L_2L_2^T$ is the sum of terms having the common factor $(S_2S_3^{-1}S_2^T-S_1)^{-1}$where $S_1=C_1PC_1^T+D_1QD_1^T-\gamma^2\mathrm{I}$. From the standard inverse result for Banach algebras [GG] that if $\|A\|<1$, then $I+A$ is invertable and $\|(I+A)^{-1}\|<(1-\|A\|)^{-1}$, so the result follows.

4.3 Some properties.

In this section it is noted that:

- The H_∞ filter's robustness is attained at the expense of an increased upper bound for the state error covariance;
- As $\gamma^{-2}\rightarrow 0$, the solution to the H_∞ RDE monotonically approaches the solution to the Kalman RDE;
- Filters outperform predictors; and,
- The choice $U=\gamma^{-1}$ (or any other scalar) does not result in all-pass error.

4.3.1 Increased error covariance upper bound.

Consider the output estimation problem in which the plant model and noise statistics are known. Once again, if the initial RDE solution is set equal (or greater than) the initial state error covariance, it is shown that the state error covariance is bounded above by the RDE solution.

For a linear filter of the form (4.21), it is easily shown that the state estimation error may be written as

$$e_{k+1} = (A - K_k C_2)e_k + Bw_k + K_k v_k, \tag{4.24}$$

(see Appendix G). Assuming that the $\tilde{x}_k$, w_k and v_k are independent and have zero mean, then the estimation error covariance Σ_k for $E\{e_k e_k^T\}$ is defined by

$$\Sigma_{k+1} = (A - K_k C_2)\Sigma_k(A - K_k C_2)^T + B_2 Q B_2^T + K_k R K_k^T - B_2 Q D_2^T K_k^T - K_k D_2 Q B_2^T. \tag{4.25}$$

The H_∞ RDE (3.5) may be written as

$$P_{k+1} = AP_kA^T - K_k(C_2P_kA^T + D_2QB_2^T) + BQB^T + \gamma^2 L_2 L_2^T \tag{4.26}$$

and subtracting (4.25) from (4.26) yields

$$P_{k+1} - \Sigma_{k+1} = (A - K_k C_2)(P_k - \Sigma_k)(A - K_k C_2)^T + \gamma^2 L_2 L_2^T. \tag{4.27}$$

It follows by induction that the first term of $P_{k+1} - \Sigma_{k+1}$ is non-negative and provided that $\gamma^2 L_2 L_2^T \geq 0$, then $P_{k+1} \geq \Sigma_{k+1}$. Thus, if the RDE is initialised appropriately, then the state error covariance is bounded above by the Riccati equation solution. Since the Kalman error covariance, denoted by $\tilde{P}_k$ is the optimal estimation error variance, then by definition $\Sigma_k \geq \tilde{P}_k$. It follows that $P_k \geq \Sigma_k \geq \tilde{P}_k$.

Thus the cost of H_∞ design is an increase in mean square error (MSE). However even if peak error is of prime concern, providing it is deemed to be an infrequent occurrence, it may be beneficial to proceed with a $\gamma > \gamma_{\min}$ and realise some improvement in MSE performance.

4.3.2 Montonicity.

Consider again a known plant, known noise statistics, output estimation problem. Suppose that a $\gamma_i > 0$ has been found so that $P_{k+1}^{(i)} = AP_k^{(i)}A^T - K_k(C_2P_k^{(i)}A^T + D_2QB_2^T) + Q_k^{(i)}$ has a positive definite solution, where $Q^{(i)} = BQB^T + \gamma^2 L_2^{(i)}(L_2^{(i)})^T > 0$. It follows that $\gamma_j > \gamma_i \Rightarrow Q_k^{(j)} < Q_k^{(i)}$ and from the monotonicity properties of RDEs [BGW], if $P_k^{(i)} \leq P_k^{(i)}$ for some k, then $P_k^{(i)} \leq P_k^{(i)}$ for all subsequent k. Thus as $\gamma_j^{-2} \to 0$, $P_k^{(j)}$ monotonically approaches the solution of the Kalman RDE.

4.3.3 Predictors.

Suppose that $G_1 = G_2$ are strictly proper SISO plants and a solution to the H_∞ RDE has been found such that $S \geq 0$, then

(i) The H_2 filter exhibits less MSE than the H_2 predictor; and,

(ii) The H_∞ filter exhibits less MSE than the H_∞ predictor.

The first result is well known result and is immediate from the (2,2) block of (D.5), that is

$$\tilde{P}_{k/k} = \tilde{P}_{k/k-1} - \tilde{P}_{k/k-1}C_2^T(C_2\tilde{P}_{k/k-1}C_2^T + \sigma_v^2)^{-1}C_2\tilde{P}_{k/k-1}. \tag{4.28}$$

The (2,2) partition of the H_∞version of (D.5) may similarly be found to be

$$P_{k/k} = P_{k/k-1} - P_{k/k-1}\begin{bmatrix} C^T \\ -C^T \end{bmatrix}\begin{bmatrix} CP_{k/k-1}C^T - \gamma^2 & -CP_{k/k-1}C^T \\ -CP_{k/k-1}C^T & CP_{k/k-1}C^T + \sigma_v^2 \end{bmatrix}^{-1}[C \ -C]P_{k/k-1}. \tag{4.29}$$

By assumption $P_{k/k-1} \geq 0$ and $\begin{bmatrix} C_2P_{k/k-1}C_2^T - \gamma^2 & -C_2P_{k/k-1}C_2^T \\ -C_2P_{k/k-1}C_2^T & C_2P_{k/k-1}C_2^T + R \end{bmatrix} \geq 0$, so the second result follows.

Also, it is clear from (4.28) and (4.29) that the improvement in MSE offered by the filter increases as σ_v^2 is reduced.

4.3.4 All-pass error.

In the case of continuous-time stationary plants it was shown that open loop H_∞ filter can be scaled to yield all-pass error and this led to the finding that $U = \gamma^{-1}$ ensures that the error exhibited by the closed loop filter is all-pass. The same strategy was attempted in the discrete-time case and did not prove fruitful. In particular it is claimed that:

(i) The open loop system of (4.15) is all-pass; and,

(ii) a scalar for U cannot be found which ensures that the same is true for the closed loop system of (4.16).

A proof is set out in Appendix F.

4.4 Conclusions.

The results of [LGW] have been used to derive a H_∞ filter for the problem where the plants may be different and possess a nonzero direct feedthrough term. However the formulation is believed to be known. For example in the case of equal plants that do not possess a feedthrough term, the RDE (4.22) is the same as [BB, (6.25b), p. 160].

It has been shown that the H_∞ filter has the same structure as the Kalman filter. The gain calculation is the same, the only difference arises in the quadratic term of the RDE. Similarly, the H_∞ predictor has the same structure as the Kalman predictor.

As in the continuous-time case, it has been demonstrated that the discrete-time H_∞ RDE reverts to the Kalman RDE when $\gamma = \infty$, and the H_∞ state estimation error covariance is greater than or equal to the Kalman state estimation error covariance.

It has been found that the so-called open loop filter (4.15) can be scaled to yield all-pass error but a scalar cannot be found for the free operator so that the closed loop filter is all-pass.

REFERENCES

[AM] Anderson, B. D. O. and J. B. Moore, *Optimal Filtering*, Prentice-Hall, Englewood Cliffs, N.J., 1979.

[BB] Basar, T. and P. Bernhard, *H_∞-optimal control and related minimax design problems. A dynamic game approach.*, Birkhauser, Boston, p. 160, 1991.

[BGW] Bitmead, R. R., M. Gevers and V. Wertz, *Adaptive optimal control*, Prentice Hall, Sydney, pp. 86-87, 1990.

[GG] Gohberg, I. and S. Goldberg, *Basic operator theory*, Birkhauser Verlag, Basel, 1981.

[Gr] Green, M., "H_∞ controller synthesis by J-lossless coprime factorization", *Siam J. Contr. Optim.*, vol. 30, no. 3, pp. 522-547, May 1992.

[Gr2] Green, M., *Optimal H_∞ control course* ,Faculty of Engineering and Information Technology, Dept. of Systems Engineering, ANU, 3rd - 7th Feb., 1992.

[IG] Iglesias, P. I. and K. Glover, "State space approach to discrete-time H_∞ control", *Int. J. Contr.*, vol. 54, pp. 1031-1073, 1991.

[LAKG] D.J.N. Limebeer, D. J. N., B. D. O. Anderson, P. P. Khargonekar and M. Green, "A game theoretic approach to H^∞ control for time-varying systems", *SIAM J. Contr. Optim.*, vol. 30, no. 2, pp. 262-283, Mar. 1992.

[LGW] D. J. N. Limbeer, M. Green and D. Walker, "Discrete-time H_∞ control", Proc. IEEE CDC, Tampa, FL, vol. 1, pp. 392-396, Dec. 1989.

[LS] Limebeer, D. J. N. and U. Shaked, "Minimax terminal state estimation and H_∞ filtering", submitted to *IEEE Trans. Automat. Contr.*, 1992.

[St] Stoorvogel, A. *The H^∞ control problem. A state space approach.* Prentice-Hall, N.Y. 1992.

Chapter 5

Performance

In the general filtering problem of Figure 3.2, the two plants are different and may be time-varying. This chapter addresses the two simplest permutations: when either the plants are the same and stationary or when one of them is an identity. Four problems are considered

- continuous-time output estimation,
- discrete-time output estimation,
- continuous-time equalisation, and
- discrete-time equalisation.

Although it is well known that the H_∞ filter minimises the peak of the error spectrum, it may not be clear when this is of any consequence. The contribution of this chapter is to provide an answer to "when is H_∞ filtering advantageous ?" The approach taken is to look at scalar examples so that something may be inferred about higher order problems. Some of the discrete-time aspects of this chapter have been summarised in [EW].

5.1 Continuous-time output estimation.

The objective of this section is to contribute to an understanding of when continuous-time H_∞ filters can be advantageous and how an advantage may arise. It is shown that the reduction in the peak of the error spectrum is only apparent when the SNR is sufficiently high and the cost is an increase in MSE. A stationary, scalar problem is discussed, where the value of γ can be determined *a priori* and some numerical examples are presented to demonstrate what happens at various SNRs.

Regarding the continuous-time, stationary, output estimation problem, when the inputs are gaussian, the noise statistics and the plant model are known, the following behaviour has been observed.

- The magnitude of the spectrum of the Kalman error component due to the process noise is always greater than that due to the observation noise.
- When the SNR is sufficiently high, the magnitude of the spectrum of the H_∞ error component due to the observation noise is greater than that due to the process noise.
- The magnitude of the H_∞ error spectrum is noticably less than that of the Kalman error spectrum, provided that the SNR is sufficiently high.

An attempt has been made to establish sufficient conditions for "when the SNR is sufficiently high", see Appendix G. Unfortunately the high SNR conditions of Appendix G are difficult to interpret and therefore some scalar examples are examined instead.

It can be argued (see Appendix G) that for SISO output estimation problems, the error components may be expressed as

$$R_{zv}(s) = -\sigma_v H(s), \tag{5.1}$$

$$R_{zw}(s) = -\sigma_w (H(s) - 1)G(s). \tag{5.2}$$

If the SNR is sufficiently high such that the spectrum of R_{zw} is insignificant compared to the spectrum of R_{zv}, then R_{zd} may be minimised by the choice of $H \approx 1$, in which case $R_{zd}R_{zd}^H \approx \sigma_v^2$ and therefore a convenient *a priori* choice for γ is $\gamma \approx \sigma_v$. Thus at very high SNR, the optimum H_∞ solution is a "do nothing filter". This is illustrated by the examples that follow.

Example 5.1. Consider the scalar low-pass plant $c(s-a)^{-1}$, $a < 0$, in which case the ARE (G.8) is the quadratic $-c^2p^2(\sigma_v^{-2} - \gamma^{-2}) + 2ap + \sigma_w^2 = 0$, having the solution

$$p = \frac{-a \pm \Delta}{-c^2\sigma_w^2(\sigma_v^{-2} - \gamma^{-2})}, \tag{5.3}$$

where $\Delta = \sqrt{a^2 + c^2\sigma_w^2(\sigma_v^{-2} - \gamma^{-2})}$. For $\Delta \geq 0$ it is required that $\gamma^2 \geq \sigma_v^2(1 + a^2\sigma_v^2c^{-2}\sigma_w^{-2})^{-1}$ which ensures that the denominator of (5.3) is positive. The choice $\Delta = 0$ yields the minimum $p = -\sigma_w^2 a^{-1}$ at which the optimal γ is given by $\gamma^2 = \sigma_v^2(1 + a^2\sigma_v^2c^{-2}\sigma_w^{-2})^{-1}$. This γ is clearly less than the *a priori* choice of Appendix G. The filter gain is $k = \frac{\sigma_w^2 c}{\sigma_v^2 a}$ which becomes large when $\sigma_w^2 >> \sigma_n^2$. The error spectrum is given by

$$r_{zd}r_{zd}^H(s) = \frac{c^2(\sigma_w^2 + k^2\sigma_v^2)}{(s-a+ck)(-s-a+ck)}. \tag{5.4}$$

Since $p > \tilde{p}$ (see Appendix G), then $k > \tilde{k}$ and it is seen from (5.4) that the poles of the H_∞ error spectrum occur at higher frequencies compared to those of the Kalman error spectrum. Therefore it is expected that the H_∞ filter will exhibit greater error at high frequencies. Thus, the H_∞ filter is

$$h(s) = \frac{\sigma_w^2 c^2}{\sigma_v^2 a}\left(s - a + \frac{\sigma_w^2 c^2}{\sigma_v^2 a}\right)^{-1}, \tag{5.5}$$

when $\frac{\sigma_w^2}{\sigma_v^2}$ becomes large, the pole of the H_∞ filter occurs at higher frequencies. The high SNR H_∞ filter (5.5) does nothing at dc because $h(0) \approx 1$. Since $\tilde{p} > p$, the Kalman filter may be thought of as the filter (5.3) designed with a $\tilde{\sigma}_w^2 < \sigma_w^2$. It follows from (5.5) in which $a < 0$, that $\tilde{h}(0) < h(0) \approx 1$. From (5.1) $r_{zw} r_{zw}^H(s) = [h(s)-1]^2 g^2(s)\sigma_w^2$, which is acutely sensitive to a $\tilde{h}(0) < 1$, so the high SNR observation (see Appendix G) that $\tilde{r}_{zw}\tilde{r}_{zw}^H > \tilde{r}_{zv}\tilde{r}_{zv}^H$ is not surprising.

Example 5.2. The error spectra for the low-pass plant $50(s+1)^{-1}$ at $\sigma_w^2 = 1$ and $\sigma_n^2 = \{100, 10, 1\}$ are calculated via (5.4) and shown in Figure 5.1. It can be seen that the H_∞ filter exhibits less peak error at the cost of higher out of band error. In addition it is evident that the reduction in peak error increases with higher SNR.

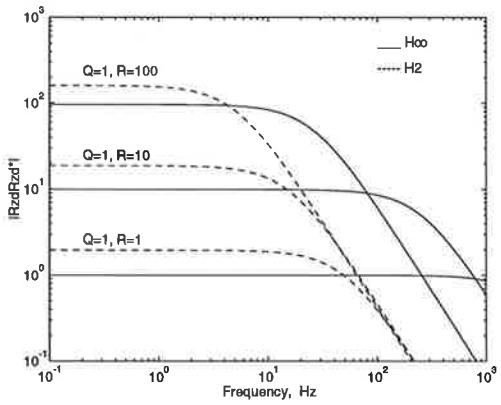

Fig. 5.1. Error spectra for Example 5.2.

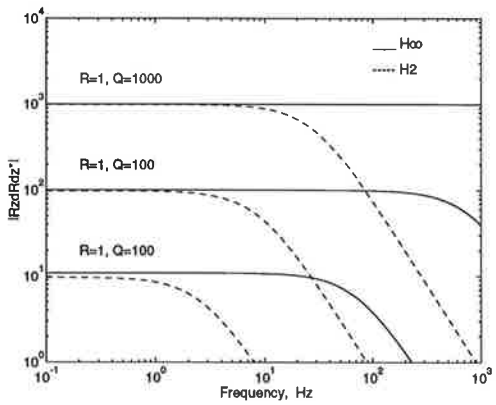

Fig. 5.2. Error spectra for Example 5.3

Example 5.3. Suppose that the scalar plant is given by $g(s) = cb(s-a)^{-1} + d$, then from (3.10) it can be shown that a real p requires that γ satisifies

$$\gamma^2 \geq c^2\left(\frac{c^2}{\sigma_v^2} + \frac{(a - bdc\sigma_v^{-2})^2}{b^2(\sigma_w^2 - d^2\sigma_v^{-2})}\right)^{-1}. \tag{5.6}$$

If $a - bdc\sigma_v^{-2} > 0$ and $\sigma_w^2 - d^2\sigma_v^{-2} > 0$, then

$$p = -b^2(\sigma_w^2 - d^3\sigma_v^{-2})(a - bdc\sigma_v^{-2})^{-1}. \tag{5.7}$$

The H_∞ filters for the band-pass plant $(s+0.1)(s+1)^{-1}$ at $\sigma_v^2 = 1$, $\sigma_w^2 = \{1000,100,10\}$ are calculated via (5.7) and the error spectra are shown in Figure 5.2. Once again, at higher SNR, the H_∞ filter becomes progressively flatter (a do nothing filter,) and exhibits less peak error than the Kalman filter at dc. Here the difference between the H_∞ and Kalman error spectra diminishes with increasing σ_w^2, because of the presence of the plant feedthrough term within R_{zw}.

5.2 Discrete-time output estimation.

The objective is this section is to contribute to an understanding of when discrete-time H_∞ filters can be advantageous and how a benefit may arise. The treatment follows the continuous-time counterpart. The general scalar problem is examined and a numerical example is described to compare the performance of Kalman and H_∞ predictors and filters. Examples are also presented to demonstrate that the H_∞ filter can be beneficial when the plant is either high-pass, unstable or uncertain.

Regarding the discrete-time, stationary, output estimation problem, when the noises are zero mean, white gaussian processes and the covariances are known, it has been observed that

- In the case of known, stable, low-pass plants, (a) the spectrum of the Kalman prediction error component driven by w is always greater than the spectrum of the component driven by v, (b) when the SNR is sufficiently high, the spectrum of the H_∞ prediction error component driven by v is greater than the spectrum of the component driven by w, (c) any advantage offered by the H_∞ predictor is not very significant and occurs at high SNR, and (d) the same is true of filters.
- In the case of known, stable, high-pass plants, the reduction in peak error offered by the H_∞ filter can be more significant compared to the Kalman filter.
- When the plant is known but unstable, the reduction in peak error offered by the H_∞ filter can be more significant compared to the Kalman filter.
- When the plant is uncertain, then the H_∞ filter designed to accommodate the uncertainty may reduce the worst case error, at the cost of an increased lower error bound.

These observations are illustrated via some examples.

5.2.2 Known, low-pass plants.

Example 5.4. Consider the scalar, low-pass plant $g(z) = cb(z-a)^{-1}$, $-1 < a < 0$. From (4.18), the quadratic term of (G.34) is $LJL^T = L_1L_1^T - \gamma^2 L_2L_2^T$ where $L_1 = \gamma^{-2}ap[c \;\; c]\begin{bmatrix} 0 \\ W_{21}^{-T} \end{bmatrix}$ and

$L_2 = \gamma^{-2} ap[c \quad c]\begin{bmatrix} -W_{12}^{-T} \\ W_{21}^{-T} W_{11} W_{12}^{-T} \end{bmatrix}$ in which $W = \begin{bmatrix} \frac{c^2 p}{\sqrt{c^2 p + \sigma_v^2}} & \frac{\sqrt{pc^2(1-\sigma_v^2\gamma^{-2}) + \sigma_v^2}}{\sqrt{c^2 p + \sigma_v^2}} \\ \sqrt{c^2 p + \sigma_v^2} & 0 \end{bmatrix}$. It has been argued (in Appendix G) that at high SNR it is reasonable to make the choice of $\gamma \approx \sigma_v$. It is easily verified that this yields $LJL^T = 0$, which results in

$$p = b^2\sigma_w^2(1-a^2)^{-1}. \tag{5.8}$$

The H_∞ filter is then given by

$$h(z) = \frac{\varepsilon}{\varepsilon + \frac{c^2 b^2}{1-a^2}}\left(z - a + \frac{\frac{ac^2b^2}{1-a^2}}{\varepsilon + \frac{c^2b^2}{1-a^2}}\right)^{-1}\frac{\frac{ac^2b^2}{1-a^2}}{\varepsilon + \frac{c^2b^2}{1-a^2}} + \frac{\frac{c^2b^2}{1-a^2}}{\varepsilon + \frac{c^2b^2}{1-a^2}}, \tag{5.9}$$

where $\varepsilon = \frac{\sigma_v^2}{\sigma_w^2}$. Clearly $\lim_{\varepsilon \to 0} h(0) = 1$, that is at high SNR the H_∞ filter possesses negligible dynamics and is a do nothing filter. Since $\tilde{p} < p$, the Kalman filter may be thought of a design with a $\tilde{\sigma}_w^2 < \sigma_w^2$ in (5.8) and (5.9). Conversely the H_∞ filter may be thought of as a Kalman filter design that is pessimistic about the observation noise. So when $\frac{\sigma_v^2}{\sigma_w^2}$ becomes small, both filters approach a short circuit. If the peak of the error spectrum magnitude is the only criterion of interest, then $h(z) = 1$ would be the ideal high SNR filter. The Kalman filter is concerned with the MSE and therefore needs to be low-pass. Similarly the minimum entropy H_∞ filter is cognisant of the MSE and is also low-pass. It can be seen from (5.9) that a $\tilde{\sigma}_w^2 < \sigma_w^2$ results in $\tilde{h}(z) < h(z) \approx 1$. The spectrum of the error is given by

$$r_{zd}r_{zd}^H(z) = h^2(z)\sigma_v^2 + [h(z)-1]^2 g^2(z)\sigma_w^2 \tag{5.10}$$

from (G.30) and (G.31). If $h(z)$ is sufficiently close to 1, then clearly (5.10) is dominated by $h^2(z)\sigma_v^2$; conversely, if $\tilde{h}(z)$ is sufficiently less than 1, then it can be deduced that $\tilde{r}_{zd}\tilde{r}_{zd}^H \approx [\tilde{h}(z)-1]^2 g^2(z)\sigma_w^2$ (see Appendix G).

An illustration is provided by the following numerical example.

Example 5.5. The Kalman and H_∞ error spectra for the plant $0.4(z-0.6)^{-1}$ at $T_s = 0.5$, with $\sigma_w^2 = 1$, $\sigma_v^2 = 0.001$ and $\sigma_v^2 = 100$ are shown in Figure 5.3. It can be seen that at $\sigma_v^2 = 0.001$ both the Kalman predictor and filter exhibit comparatively flat error. The filter error is dominated by R_{zv} and is over 20 dB less than the predictor error which is dominated by $\tilde{R}_{zw}$. This is a consequence of the predictor being strictly proper whereas the filter possesses a unity feedthrough term and negligible dynamics. The Kalman filter at $\sigma_n^2 = 0.001$is $0.994 + .00372(z-.00372)^{-1}$. Comparing Figure 5.3 (a) and (b) it is seen that

the H_∞ error spectra are seemingly indistinguishable from the Kalman error spectra. The same error components dominate and it turns out that peak errors exhibited by the Kalman predictor and filter are negligibly worse than the H_∞ predictor and filter. At $\sigma_v^2 = 0.001$ the H_∞ filter (at $\gamma = \sigma_v$) is $0.996 + .00239(z-.00239)^{-1}$, hence at dc it follows that the H_∞ filter is better than the Kalman filter at doing nothing. The consequence of $p > \tilde{p}$ is that H_∞ filter has its dynamics placed at higher frequencies with a marginal reduction in peak error at dc. From Figure 5.3 (c) and (d) it is seen that the worse case error occurs at $\sigma_v^2 = 100$ and is dominated by the R_{zw} component. At low SNR the feedthrough term becomes small and the filter transfer functions approaches that of the predictors. Once again, it is not possible to discern any improvement in peak error due to H_∞ from the Figures alone. However, noting that the Kalman filter is given by $0.0025z(z-0.599)^{-1}$ and the H_∞ filter (at $\gamma = 1$) is $0.0037z(z-0.598)^{-1}$, then it can be deduced that the magnitude of the H_∞ filter is closer to 1 at dc.

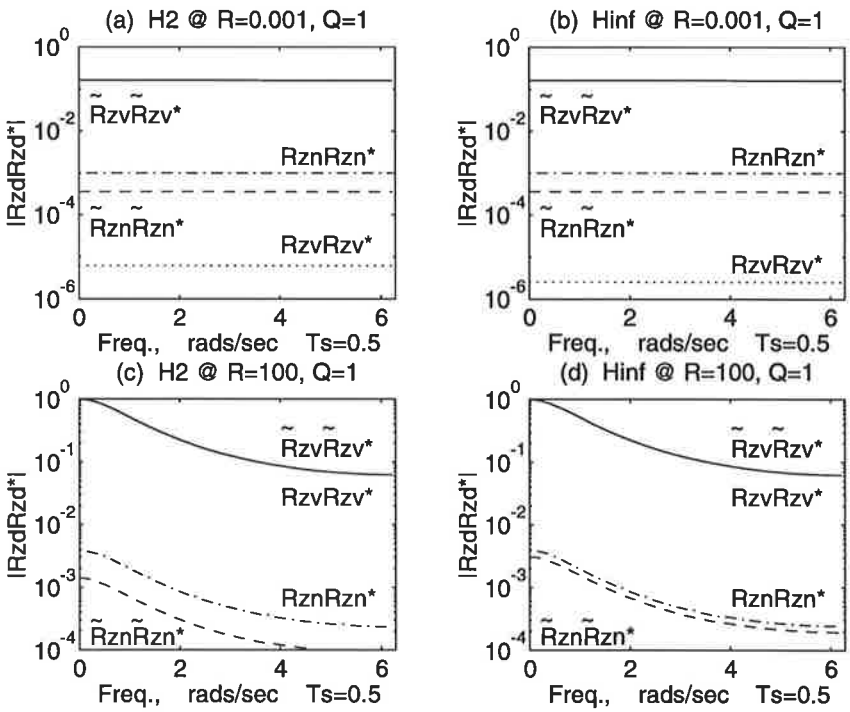

Fig. 5.3. Error spectra for Example 5.5.

It is not at all surprising that the filter exhibits less peak error than the predictor. The predictor ignores the current data point in the determination of the current estimate whereas the filter includes it. Therefore the filter rather than the predictor should be implemented whenever the performance is an issue.

Similar observations pertain to the case when the low-pass plant possesses a direct feedthrough term. The error components that were observed to dominate in Example 5.5 also happen to dominate within the bandwidth of the (proper, low-pass) plant. Beyond the

plant bandwidth, some intersection of the error spectra typically occurs, but for low-pass plants this happens at low amplitudes and is therefore inconsequential.

5.2.3 Stable, known, high-pass plants.

When the plant is high-pass, the reduction in peak error offered by the H_∞ filter can be more significant compared to the Kalman filter. The goal of attaining a high-pass filter response directly opposes the requirement to minimise the MSE. Thus it is hardly surprising that the trade-off between peak error and MSE can be significant when the plant is high-pass. At low SNR, the reduction in peak error by the H_∞ filter compared to the Kalman filter is most apparent. This claim is illustrated by the following example.

Example 5.6. The error spectra resulting for the high-pass plant $4.975(z-0.6)(z+0.99)^{-1}$ at $T_s = 0.5$, $\sigma_w^2 = 1$ and $\sigma_v^2 = 100$ are shown in Figure 5.4. From the transfer function of the H_∞ filter, $0.969 - 0.0295(z+0.0257)^{-1}$ at $\gamma = 10$, it follows that the magnitude is close to unity at high frequencies (z=0) and consequently R_{zd} is dominated by the R_{zv} component. This contrasts with the transfer function of the Kalman filter namely $0.488 - 0.286(z-0.43)^{-1}$, whereupon R_{zw} is not insignificant at z=0, as is shown in Figure 5.4. This example demonstrates the high cost of using peak error as the only a performance criterion. A 1.7 dB reduction in high frequency peak error is achieved at the expense of a 10 dB increase error at dc and about double the MSE.

Next it is demonstrated that the H_∞ filter for known inputs can also be advantageous when the plant is unstable and known.

5.2.4 Unstable, known, low-pass plants.

Example 5.7. For the unstable, low-pass plant $0.335(z+0.99)(z-1.667)^{-1}$, at high SNR the reduction in peak error by the H_∞ filter is negligible compared to the Kalman filter and so the spectra are not shown. At low SNR ($T_s = 0.5$, $\sigma_w^2 = 1$, $\sigma_v^2 = 100$), the improvement is more significant as shown in Figure 5.5. From the figure it is seen that for the H_2 case, the spectrum of R_{zv} and hence the filter, is demonstrably low-pass. This contrasts with the H_∞ solution which does not attempt a stable approximation to the unstable plant but instead minimises R_{zv} via a do nothing filter, namely $(z+1.25*10^{-8})(z+1.87*10^{-5})^{-1}$ at $\gamma = 10$. The magnitude of the R_{zv} component for the H_∞ filter is not shown in Figure 5.5 because it is much less than that of the Kalman filter. The advantage of the H_∞ filter becomes more profound when either the SNR is reduced further or the instability is more severe such as a double pole for example. From Figure 5.5 once again it is seen that the reduction in peak error is attained at the cost of an increase in MSE.

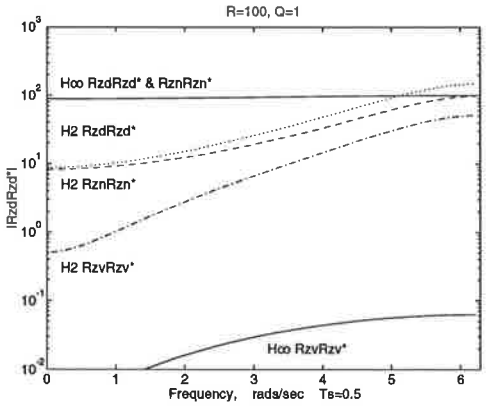

Fig. 5.4. Error spectra for Example 5.6.

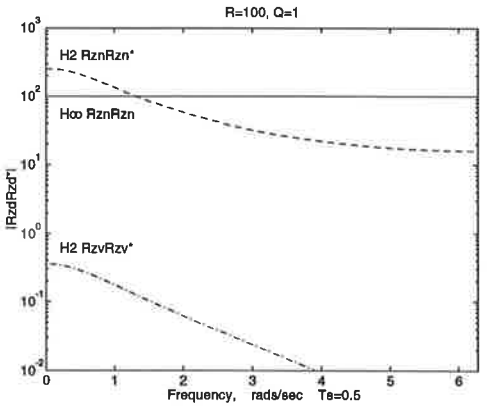

Fig. 5.5 Error spectra for Example 5.7.

5.2.4 Uncertain, low-pass plants.

When the plant uncertainty is not too great, then the H_∞ filter designed to accommodate the uncertainty may reduce the worst case error, at the cost of an increased lower error bound. An illustration is provided via the example that follows. In the case that the inputs are uncorrelated gaussian processes it is possible to simplify the implementation of Lemma 3.1 (and Lemma 3.2) so that the design observation noise variance is

$$\tilde{\sigma}_v^2 = \sigma_v^2 + \gamma^2\delta^2, \tag{5.11}$$

whereas the design process noise variance in Lemma 3.1 may be written as

$$\tilde{\sigma}_w^2 = \frac{\gamma^2\sigma_w^2}{\gamma^2 - 1}. \tag{5.12}$$

Example 5.8 Suppose that $\sigma_w^2 = 1$, $\sigma_v^2 = 1$, the plant is nominally $G_o = 0.2(z+.99)(z-.6)^{-1}$ and there is an uncertainty of $\pm\Delta = \pm 0.5G_o$. This problem may be solved via either an unparametrized additive or a multiplicative uncertainty approach. Since for this example $\|G_o\|_\infty = 1$, identical scaling occurs in the solution of both additive and multiplicative uncertainty problems. Proceeding with $\delta_{nom} = 0.5$, $\gamma_{\min} = 1.01$, the worst case peak error magnitude of about 0.74 occurs when the actual plant is $G_2 + 0.5G_2$. Since Lemmas 3.1 and 3.2 yield a conservative design, it is prudent to explore the performance resulting for various $\gamma > \gamma_{\min}$ and $\delta < \delta_{nom}$. It turns out that a reduced worst case peak error magnitude of about 0.69 can be achieved with $\delta = 0$ in (5.43), yielding $0.54(z+.25)(z-.41)^{-1}$ for the H_∞ filter at $\gamma = 1.02$. The Kalman filter for this example is $0.15(z+.23)(z-.48)^{-1}$. The error spectra that result with the H_∞ filter when the actual plant is varied from $0.5G_2$ through to $1.5G_2$, and also with the Kalman filter at the two extremes, are shown in Figure 5.6. In this example when the actual plant is $1.5G_2$, the H_∞ filter exhibits about 1.9 dB reduction in peak error magnitude, at the cost of about 3.4 dB increase in peak error magnitude when the actual plant is $0.5G_2$.

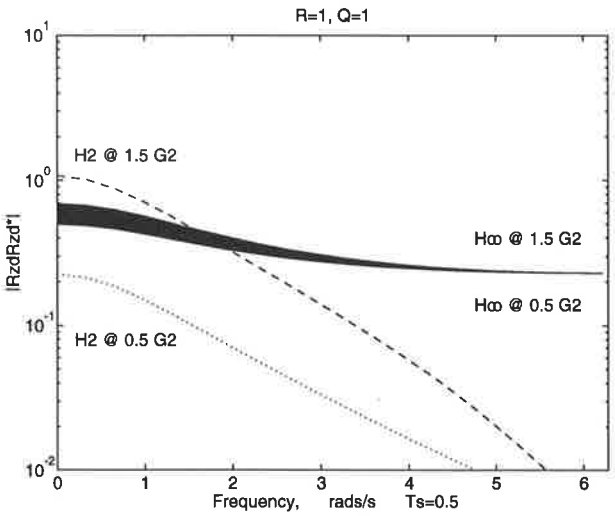

Fig. 5.6. Error spectra for Example 5.8.

It is clear from Figure 5.6, that some robustness to model uncertainty is obtained at the expense of an increased lower error bound. Now consider the possibility of G_2 varying randomly within the stated uncertainty bounds. Although the Kalman filter would exhibit around double the peak error, it may well perform better some of the time. One such application is the extended H_∞ filter described in Chapter 7.

5.3 Continuous-time equalisation.

This section begins by defining the problem and describes how to masquerade equalisation as output estimation. It is observed from a second order example that the H_∞ solution does slightly better than Kalman for minimum phase channels and significantly better in the case of non-minimum phase channels. It is also demonstrated that if the channel is poorly modelled, further advantage may be realised by allowing for some plant uncertainty.

5.3.1 Problem Definition.

In a typical equalisation problem a signal is known to have been distorted by a communications channel and the task is to undo the effect of the channel. A solution is to filter the received signal with an equaliser which is an approximation to the inverse of the channel. Referring to Figure 3.2, suppose that $G_1 = I$ and G_2 is a channel model. Assume momentarily that the problem is completely free of measurement noise. In this case the error spectrum is $R_{zw}R_{zw}^H = (HG_2 - I)Q(G_2^H H^H - I)$, which is clearly minimised by the solution $H = G_2^{-1}$, provided that G_2 is minimum-phase. In applications where the measurement noise is finite consequently the equaliser is likely to be a trade-off between the channel inverse and a filter. The objective of this section is to shed some light on the behaviour of the Kalman and H_∞ filters as solutions to this simple equalisation problem.

In the abovementioned equalisation problem it is desired to specify $G_1 = I\sigma_w$. Although direct feedthrough terms may be accommodated via (3.9) and (3.10), here the attention is confined to the simpler case of strictly proper, SISO plants. In this case $R_{zv} = H\sigma_v$ is the error component due to the observation noise, $R_{zw} = (HG_2 - 1)\sigma_w$ is the error due to the process noise, which may be interpreted as the error in inverting the channel. Here equalisation is masqueraded as an output estimation problem by using $G_1 \approx \varepsilon\,(s+\varepsilon)^{-1}$ where ε is chosen to be suitably large. This raises the question, how large does ε need to be ? If ε is sufficiently small, the problem will revert to output estimation. Clearly ε needs to be large enough so that there is no interaction between the dynamics of G_1 and G_2, say at least an order of magnitude greater than the largest pole or zero of G_2.

Regarding the continuous-time equalisation problem, when the noise convariances are known, the channel model is stable and the observation noise is sufficiently low, it has been observed that:

- In the case of known, minimum phase channels, compared to the Kalman equaliser the H_∞ equaliser exhibits only a marginal reduction in the peak of the error spectrum magnitude.
- When the channel is known and non-minimum phase, the reduction in the peak of the error spectrum magnitude offered by the H_∞ equaliser can be more significant.
- When the channel is known to be minimum phase, the performance of the equaliser tends to be sensitive to model uncertainty. Consequently an equaliser designed to be robust to modelling errors may offer only a marginal advantage.
- When the channel is known to be non-minimum phase and is uncertain, then the H_∞ equaliser is inherently tolerant of modelling errors. Consequently there may not be any need to explicitly design a robust equaliser.

The notation of Section G.1 is used here, in particular, tilded variables denote those specific to Kalman solutions.

5.3.2 Known, minimum-phase channels.

Suppose that the channel is band-pass and has one or more low frequency, minimum phase zeros. It has been observed from studying various numerical examples that the Kalman solution to the equaliser problem behaves quite differently at low observation noise than for high noise. In particular, the observation noise limits how well the equaliser inverts the channel.

The same behaviour has been observed of H_∞ equalisers. Paradoxically at low observation noise, the peak error is dominated by R_{zv}. This arises because at high SNR, the equaliser can be quite successful at inverting the channel. At low observation noise when σ_v^2 is large,

the resulting equaliser is a very low magnitude, low-pass filter, with the result that the maximum of $|R_{zv}R_{zv}^H|$ is much lower than the maximum of $|R_{zw}R_{zw}^H|$. These claims are illustrated via an example that follows.

Example 5.9. Consider the equaliser problem in which $G_2 = (b_1 s + b_0)(s + a)^{-2}$ is minimum-phase with $G_{1=} \varepsilon(s+\varepsilon)^{-1}$ where $b_0>0$, $b_1>b_0$, $a>b_0 b_1^{-1}$, $\varepsilon >> 0$. An solution can be found by writing the problem as an augmented system (3.1) in which

$$A=\begin{bmatrix} -2a & -a^2 & o \\ 1 & 0 & 0 \\ 0 & 0 & -\varepsilon \end{bmatrix}, \quad B_{11}=\begin{bmatrix} 0 & 1 \\ 0 & 0 \\ 0 & 1 \end{bmatrix}, \quad C_{11}^T=\begin{bmatrix} 0 \\ 0 \\ \varepsilon \end{bmatrix}, \quad C_{21}^T=\begin{bmatrix} b_1 \\ b_0 \\ 0 \end{bmatrix}.$$

The equaliser is given by $H = C_1(s-A+KC_2)^{-1}K$ where the gain is $K= PC_2^T R^{-1}$ and P is the solution of the ARE (3.3). Alternatively, consider the transfer function form, obtained via Cramer's rule as $H = \varepsilon k_3(s+a)^2 [(s^2+\beta s+c_\beta)(s+\varepsilon)]^{-1}$ where $K= [k_1,k_2,k_3]^T$ is the gain and $\beta= k_2 b_0 + k_1 b_1 + 2a$, $c_\beta= a^2+ k_1 b_0 + 2a k_2 b_0 - a^2 k_2 b_1$. Factorising the denominator yields

$$H = \varepsilon k_3(s+a)^2 [(s+\beta-\eta)(s+\eta)(s+\varepsilon)]^{-1}, \tag{5.13}$$

where $2\eta= \beta-\sqrt{\beta^2-4c_\beta}$. When σ_v^2 is sufficiently small then it turns out that β is very large resulting in $\eta \approx b_0 b_1^{-1}$ so that the zero of G_2 is cancelled. The Kalman and H_∞ equalisers have been observed to be quite similar, the only difference being that the H_∞ equaliser attains a marginal reduction in the peak of the error spectrum magnitude. This is demonstrated by the following numerical example.

Example 5.10. Consider the equaliser problem in which $G_2= 100(s+0.1)(s+10)^{-2}$and $\varepsilon= 500$, $\sigma_v^2= 100$, $\sigma_w^2= 0.01$, resulting in

$$\tilde{H} = \frac{47600(s+10)^2}{(s+500)(s+10000)(s+.101)} \quad \text{and} \quad H = \frac{54200(s+10)^2}{(s+500)(s+11400)(s+.0962)}$$

at $\gamma = 0.995$. The error spectra are shown in Figure 5.7. From Figure 5.7 (a) and (b) it can be seen that at low frequencies $|R_{zv}R_{zv}^H| > |R_{zw}R_{zw}^H|$ and so the equalisers attempt to invert the channel. The two equalisers are seemingly indiscernable as is evidenced in Figure 2(a). The difference is more apparent by comparing the R_{zw} in Figure 5.7 (b) where it is seen that the magnitude of $(HG_2 - 1)$ is much smaller at dc. Thus compared to the Kalman equaliser, at dc it can be observed that $|R_{zw}R_{zw}^H|$ is considerably reduced, $|R_{zv}R_{zv}^H|$ is slightly increased so that their sum $|R_{zd}R_{zd}^H|$, is only slighty reduced and there is just a marginal benefit.

Example 5.11. If the noise variance is increased to $\sigma_v^2= 10$, the Kalman and H_∞ solutions are

$$\tilde{H}=\frac{612(s+10)^2}{(s+500)(s+317)(s+.33)} \quad \text{and} \quad H=\frac{799(s+10)^2}{(s+500)(s+413)(s+.416)}$$

at $\gamma = 9.535$. It is apparent that they no longer attempt to cancel the low frequency zero of G_2 but instead behave as filters. It turns out that since the equalisers are not greatly different, the error spectra are quite similar.

Example 5.12. If σ_v^2 is sufficiently small so that the equalisers do attempt to invert the channel, then it has been observed that the H_∞ equaliser can be slightly more advantageous when the channel has a higher gain. In respect of Example 5.10, consider increasing the multiplicity of the pole by one and increasing the dc gain by 10, so that the channel model is given by $G_2 = 10000(s+0.1)(s+10)^{-3}$. A H_∞ equaliser design was found at $\gamma = 3.791$ and the error spectra that result are shown in Figure 5.8. It can be seen that $|R_{zw}R_{zw}^H|$ is less than $|\tilde{R}_{zw}\tilde{R}_{zw}^H|$ over the channel bandwidth, in other words the H_∞ equaliser constructs a better inverse because it is less concerned with minimising the MSE.

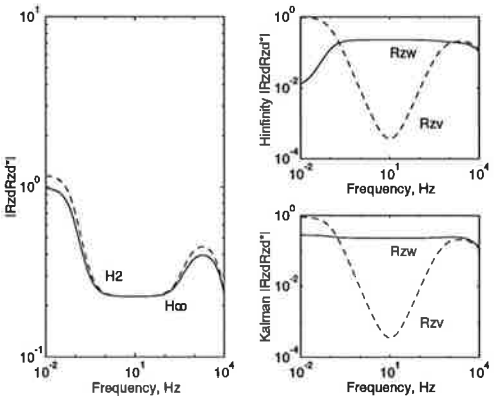

Fig. 5.7. Error spectra for Example 5.10.

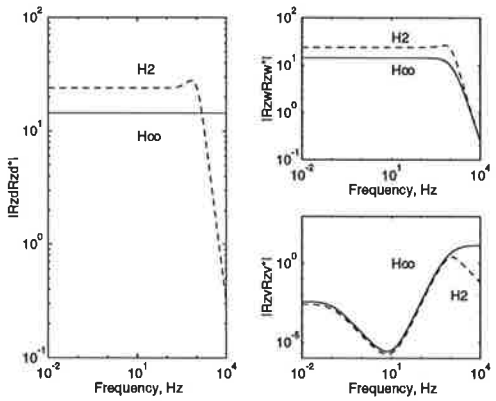

Fig. 5.8. Error spectra for Example 5.12.

5.3.3 Known, non-minimum phase channels.

Suppose that a channel model possesses a causal low frequency zero and that σ_v^2 is sufficiently low so that the equaliser attempts to invert the channel (as in Example 5.10). Consider the model obtained by reflecting the causal zero about the imaginary axis. The exact inverse of non-minimum phase model is unstable, which is obviously inadmissable. Thus the task is to construct some stable approximation to the channel inverse in a way that satisfies the desired optimality criterion. It has been demonstrated previously (in Example 5.7) that the H_∞ filter is better (in a peak error sense) than the Kalman filter, when the underlying model is unstable. Here for unstable equalisation problems, it has been observed that the Kalman solution is approximately the same as for the minimum phase case, whereas the H_∞ solution is a low magnitude, low-pass filter.

Example 5.13. Consider replacing the low frequency causal zero in the model of Example 5.10 by a noncausal zero so that $G_2 = 100(s-0.1)(s+10)^{-2}$. The error spectra that result for the Kalman and H_∞ equalisers at $\gamma = 10$ are shown in Figure 5.9. It is seen that that at dc the H_∞ equaliser is better than the Kalman equaliser for both components of the error. The Kalman solution is the same as for the minimum phase case (to within five significant figures) which does not result in the cancellation of the non-causal factor, hence $\tilde{R}_{zw}\tilde{R}_{zw}^H$ becomes quite large. In contrast, the H_∞ solution does not attempt to invert the channel, instead the roots of the quadratic in the denominator of (5.13) are both large, yielding a low magnitude, low-pass filter. This is apparent from Figure 5.9 where it is seen that the response of the H_∞ equaliser is unlike that of Figure 5.7. A non-minimum phase channel cannot be inverted by a stable filter, hence not much can be done about minimising $R_{zw}R_{zw}^H$. In this case, the H_∞ solution minimises $R_{zv}R_{zv}^H$ via a low magnitude, low-pass filter. In other words, the Kalman equaliser attempts a channel inversion which doesn't work, whereas the H_∞ equaliser minimises the error instead. It can be seen from Figure 5.9 that the H_∞ equaliser attains a peak error reduction of about 3 dB at the cost of around a 3 dB increase in MSE. The advantage of a H_∞ solution lessens with decreasing SNR because the Kalman error is dominated by R_{zw} which reduces with lower observation noise variance.

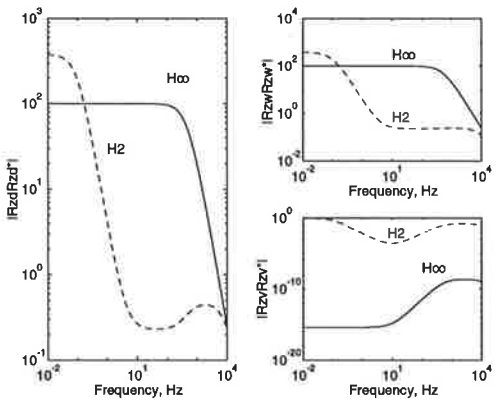

Fig. 5.9. Error spectra for Example 5.13.

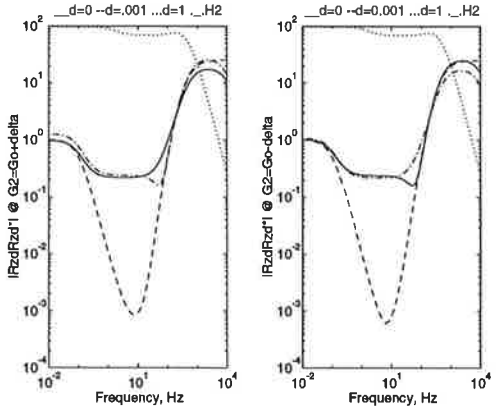

Fig. 5.10. Error spectra for Example 5.14.

5.3.4 Uncertain, minimum phase channels.

If the channel is minimum phase and the nominal channel model differs from the exact channel then the equalisers may perform poorly. The model uncertainty may be routinely accommodated using the approach outlined Section 3.4. For instance the channel may be modelled as $G_2 = G_o \pm \Delta$, where G_o and Δ denote the nominal model and an additive uncertainty respectively. Then a sufficient solution to the uncertain equalisation problem arises via the scalings of (5.43) and (5.44). Clearly it is desirable to minimise uncertainty, otherwise the design will be overly conservative and perform poorly. Equaliser performance can be acutely sensitive to observation noise (including any allowance for modelling

errors), since the noise will be amplified whenever the equaliser has a high magnitude. In the case of low observation noise, uncertain, minimum phase equalisation problems, it is argued that the inclusion of model uncertainty may not always be tractable.

In general, there may be room to accommodate model uncertainty in a particular part of the frequency band, if the equaliser magnitude happens to be at a minimum at that part of the band. For example if $R_{zw}= (HG_o- 1)\sigma_w$ is already small, then $R_{zw}= (HG_2- 1)\sigma_w$ may still be tolerably small. As the observation noise is increased, the equaliser will asymptotically approach a low magnitude, low-pass filter. Therefore a design with an increased σ_v may be more robust to errors in G_o. However the difficulty with low observation noise, band-pass, minimum phase problems, is that the equaliser magnitudes tend to have local maxima occurring at both low and high frequencies; this is certainly apparent from Figures 5.7 and 5.8. Thus there is no inherent robustness to modelling errors. In addition, since the magnitudes are high, the equalisers are sensitive to observation noise.

A convenient approach is to plot the error spectra that result for the robust equaliser at the two extremes, namely $G_2 = G_o+ \Delta$ and $G_2 = G_o- \Delta$. Although the worst case error may well occur at intermediate rather than extremes of the uncertainty, this approach has been found to be satisfactory for low order problems. For band-pass, minimum phase channels, if a two sided uncertainty exists, (ie. $G_2 = G_o \pm \Delta$,) then often it is difficult to improve on the choice of $\delta = 0$. For example, a slight increase in σ_v may result in an slight decrease in $|H|$, although this may be favourable if the channel is underestimated (ie. $G_2= G_o- \Delta$) it is likely to lead to an increase in error if the channel is overestimated (ie. $G_2= G_o+ \Delta$.) Sometimes it may be worthwhile to investigate the merits of solving the modified one-sided uncertainty problem in which $G_0'= G_0- \Delta$ in where $\Delta'= 2\Delta$..

Example 5.14. Assume that in the problem of Example 5.10 there is a high pass modelling uncertainty given by $\Delta = (s+ 1)(s+ 100)^{-1}$. The error spectra that result for the non-robust design ($\delta = 0, \gamma = 0.9952$), a robust design with some arbitrary tuning ($\delta = 0.0001$, $\gamma = 1.0001$), the sufficient design ($\delta = 1$, $\gamma = 10.0001$) and Kalman are shown in Figure 5.10. For the two sided uncertainty it can be seen that the high frequency peak error is the same for the non-robust H_∞ and Kalman equalisers. At high frequencies, the magnitude of the Kalman equaliser is slightly greater than that of H_∞ equaliser and it is observed that the Kalman equaliser is better if $G_2 = G_o- \Delta$, whereas the H_∞ equaliser is better if $G_2 = G_o+ \Delta$. The sufficient design at $\delta = \| \Delta \|_\infty = 1$ yields a peak error of 97.95 (which is guaranteed to be less than $\gamma^2= 100.002$) is obviously too conservative to be useful here. If minimum peak error is the only criterion then clearly $\delta = 0$ is the best choice. However at the expense of an additional 0.02 dB high frequency peak error, at $\delta = 0.0001$ the mid-band error can be reduced by over 20 dB.

It turns out that, the magnitude of the non-robust H_∞ equaliser is slightly greater than G_o. Also the magnitude of the equaliser increases as the design noise variance is increased. Therefore for a particular small increase in design noise variance, in some parts of the frequency band, the equaliser may become a closer approximation to the inverse of G_o. For the example considered here, it so happens that this occurs at $\delta = 0.0001$, so that R_{zw} becomes negligible and the error is entirely due to R_{zv}. Then in the presence of a high frequency model uncertainty, it is seen from Figure 5.11 that the use of $\delta = 0.0001$ continues to be advantageous.

5.3.5 Uncertain, non-minimum phase channels.

If the channel is non-minimum phase and there is some uncertainty associated with the model, then the performance of the Kalman equaliser can degrade severely, whereas the H_∞ equaliser may not be affected at all. Recall that the Kalman equaliser performs poorly even if the non-minimum phase model is known exactly because the non-causal factor cannot be cancelled. The H_∞ solution performs better because it does not try to invert the channel. Instead the error is minimised via a filter having a very low magnitude in the region of the non-causal plant zero.

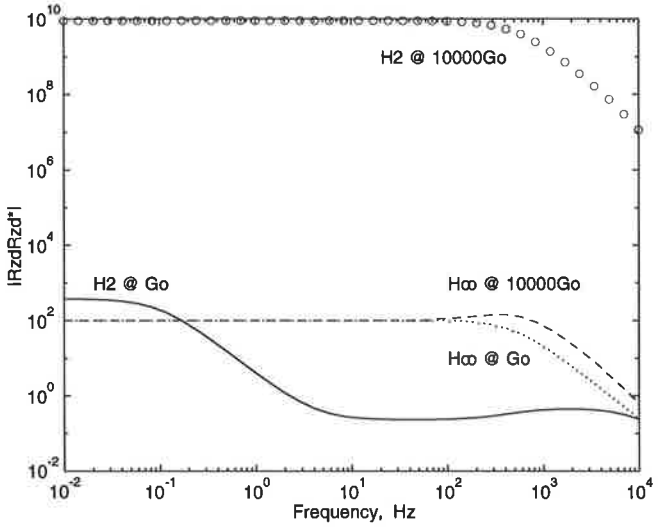

Fig. 5.11. Error spectra for Example 5.13 with channel uncertainty.

In the case of uncertain, non-minimum phase equalisation problems, it is contended that the accommodation of model uncertainty is often superfluous because the H_∞ solution is inherently robust to modelling errors. This arises because the magnitude of the equaliser is very low in the vicinity of the non-causal plant zero, hence $H(G_o + \Delta)$ may remain low, even for quite large uncertainties. Referring to Example 5.13, suppose that there exists a multiplicative channel uncertainty of 40 dB. The error spectra that result for the nominal channel and for 10000 times the nominal channel are shown in Figure 5.11. When the exact channel is $G_2 = 10000G_o$, the peak of the H_∞ error spectrum increases by only 1.3

dB, whereas an increase of 74 dB is exhibited by the Kalman equaliser. Although the non-minimum phase channel H_∞ equaliser generally has some inherent robustness, model uncertainty may nevertheless be explicitly accommodated. This is illustrated for the discrete-time case in Section 5.4.5.

5.4 Discrete-time equalisation

The objective of this section is to shed some light onto the performance benefits of stationary, discrete-time H_∞ equalisers. The section begins by setting out the solution to a scalar problem where γ can be found by solving a quadratic. Scalar, known, low-pass and high-pass channels are examined first, so that some understanding may be gained of band-pass problems which are discussed subsequently. In respect of any channel uncertainties, the H_∞ equaliser possesses some robustness whenever its magnitude is relatively small. This happens if either the channel is non-minimum phase or the channel is minimum phase and the SNR is sufficiently low. This inherent robustness has already been mentioned in the context of continuous-time, non-minimum phase equalisation. Here it is shown how frequency weighted model uncertainty can provide an advantage in the case of poorly identified channel models.

5.4.1. Scalar case.

An equaliser for the discrete-time problem can be found by writing the problem in the regulator framework of (4.1) and solving the Riccati equation (4.14). The H_∞ design arises by (iteratively) determining a minimum γ which ensures that the solution of (4.14) is positive definite. The Kalman equaliser arises by simply taking $\gamma = \infty$ in (4.14). It appears that this equaliser is not well known, for example the minimum MSE equaliser of [KP, (2.43)] is a Wiener formulation. It is likely that the Kalman equaliser would have wider application since it applies also to non-stationary problems.

Consider a stationary, scalar channel having a state space realization $g(s) \stackrel{z}{=} \left[\begin{smallmatrix} a & b \\ c & d \end{smallmatrix}\right]$, then the equalisation problem may be stated as

$$\begin{bmatrix} x_{k+1} \\ z_k \\ y_k \end{bmatrix} \stackrel{z}{=} \begin{bmatrix} a & 0 & b\sigma_w & 0 \\ 0 & 0 & -\sigma_w & 1 \\ c & \sigma_v & d\sigma_w & 0 \end{bmatrix} \begin{bmatrix} x_k \\ v_k \\ w_k \\ u_k \end{bmatrix}. \tag{5.14}$$

The resulting equaliser is denoted by

$$\begin{bmatrix} \hat{x}_{k+1} \\ u_k \end{bmatrix} \stackrel{z}{=} \begin{bmatrix} a - \underline{k}c & \underline{k} \\ -\underline{d}c & \underline{d} \end{bmatrix} \begin{bmatrix} \hat{x}_k \\ y_k \end{bmatrix}, \tag{5.15}$$

where $\underline{k} = \dfrac{bd\sigma_w^2 + apc}{\sigma_v^2 + \sigma_w^2 d^2 + c^2 p}$ and $\underline{d} = \dfrac{d\sigma_w^2}{\sigma_v^2 + \sigma_w^2 d^2 + c^2 p}$ in which p is the solution of the ARE

$$p = a^2 p - l_1^2 + \gamma^2 l_2^2 + b^2\sigma_w^2. \tag{5.15}$$

The quadratic terms of (5.49) are $l_1 = \dfrac{bd\sigma_w^2 + apc}{\sqrt{\sigma_v^2 + \sigma_w^2 d^2 + c^2 p}}$ and $l_2 = \gamma^{-2}\left(\dfrac{b\sigma_w}{w_{12}} + \dfrac{(bd\sigma_w^2 + acp)w_{11}}{w_{21}w_{12}}\right)$

where $\begin{bmatrix} w_{11} & w_{12} \\ w_{21} & 0 \end{bmatrix} = \begin{bmatrix} \dfrac{-d\sigma_w^2}{\sqrt{\sigma_v^2 + \sigma_w^2 d^2 + c^2 p}} & \dfrac{\sqrt{-\gamma^{-2}(\sigma_w^2\sigma_v^2 + c^2 p) + \sigma_v^2 + \sigma_w^2 d^2 + c^2 p}}{\sqrt{\sigma_v^2 + \sigma_w^2 d^2 + c^2 p}} \\ \dfrac{\sqrt{\sigma_v^2 + \sigma_w^2 d^2 + c^2 p}}{} & 0 \end{bmatrix}$.

The notation of Section 5.2 is used here, so that the Kalman predictor and filter gains are denoted by $\tilde{k}$ and $\tilde{d}$ respectively. The ARE for the Kalman solution is simply (5.14) at $\gamma = \infty$, namely

$$\tilde{p} = a^2\tilde{p} - \frac{(bd\sigma_w^2 + a\tilde{p}c)^2}{\sigma_v^2 + \sigma_w^2 d^2 + c^2\tilde{p}} + b^2\sigma_w^2. \tag{5.16}$$

Since $l_2^2 > 0$, it follows immediately from (5.16) and (5.17) that $p > \tilde{p}$. The equaliser (5.15) may be written as a transfer function:

$$h(z) = \frac{-cdk}{z - a + \underline{k}c} + \underline{d} = \frac{\underline{d}z + (-cdk - \underline{d}a)}{z - a + \underline{k}c}. \tag{5.17}$$

Since $p > \tilde{p}$, it can be deduced that $\tilde{d} > \underline{d}$ and $\tilde{k} > \underline{k}$, when σ_w^2 is sufficiently large and σ_v^2 is sufficiently small. Hence $-a + \tilde{k}c < -a + \underline{k}c$ and it can be argued from (5.17) that $\sup_{\omega\in[-\pi,\pi]} |\tilde{h}(e^{j\omega})| > \sup_{\omega\in[-\pi,\pi]} |h(e^{j\omega})|$. This observation is demonstrated in the examples that follow.

Example 5.15. Consider the scalar channel $g(z) = d(z-1)(z-a)^{-1}$, where $-1 < a < 0$. This may be written as $g(z) = d + bc(z-a)^{-1}$ with $d = ad + bc$. It will be shown that the Kalman equaliser, $\tilde{h}(z) = \tilde{d} - c\tilde{d}\tilde{k}(z-a+\tilde{k}c)^{-1} = \tilde{d}(z-a)(z-a+\tilde{k}c)^{-1}$, inverts the channel at high SNR and approaches an open circuit at low SNR. Here high SNR may be defined by $\sigma_v^2 \to 0$ and $\varepsilon = \sigma_v^2\sigma_w^{-2} \to 0$. The solution to (5.16) is given by

$$\tilde{p} = \frac{-\varepsilon(1-a^2) \pm \sqrt{\varepsilon^2(1-a^2) + 4\varepsilon c^2 b^2}}{2c^2\sigma_w^{-2}} \tag{5.18}$$

from which $\lim_{\varepsilon \to 0} \tilde{p} = 0$. It follows that $\lim_{\tilde{p}=0,\, \varepsilon\to 0} \tilde{k} = bd^{-1}$ and $\lim_{\tilde{p}=0,\, \varepsilon\to 0} \tilde{d} = d^{-1}$ which results in $\lim_{\tilde{p}=0,\, \varepsilon\to 0} \tilde{h}(z)g(z) = 1$. Thus at high SNR it is seen that the equaliser inverts the channel. Now low SNR may be defined by $\sigma_v^{-2} \to 0$ and $\varepsilon^{-1} \to 0$. It is argued that the quadratic term within (5.16) vanishes at low SNR, in which case $\lim_{\varepsilon^{-1}\to 0,\, \sigma_v^{-2}\to 0} p = b^2\sigma_w^2(1-a^2)^{-1}$. It follows that

$$\left[\tilde{k}\right]_{\tilde{p}=b^2\sigma_w^2(1-a^2)^{-2}} = \frac{\varepsilon^{-1}bd + \varepsilon^{-1}ac(1-a^2)^{-2}}{1+\varepsilon^{-1}d^2 + \varepsilon^{-1}c^2(1-a^2)^{-1}} \tag{5.19}$$

and

$$\left[\tilde{d}\right]_{\tilde{p}=b^2\sigma_w^2(1-a^2)^{-2}} = \frac{\varepsilon^{-1}d^2}{1+\varepsilon^{-1}d^2 + \varepsilon^{-1}c^2(1-a^2)^{-1}}. \tag{5.20}$$

Clearly $\lim_{\tilde{p}=b^2\sigma_w^2(1-a^2)^{-1},\varepsilon^{-1}\to 0} \tilde{h}(0) = 0$, that is, at low SNR the equaliser approaches an open circuit.

5.4.2. Known, low-pass channels.

Example 5.16. Consider the minimum-phase channel $g(z)= 0.2(z+ 0.99)(z- 0.6)^{-1}$, which corresponds to the bilinear transform of $g(s)= 0.0125(s+ 796)(s+ 1)$ at $F_s = 2$. The equaliser and error spectra for $\sigma_v^2= 0.01$ and $\sigma_w^2= 0.1$ at $\gamma = 0.3185$ are shown in Figure 5.16. It can be seen that the peak error occurs at high frequency. The H_∞ equaliser reduces this by about 1 dB, at the cost of increasing the low frequency error by about 10 dB. This is a consequence of $|\tilde{h}| > |h|$, with the difference reducing at higher frequencies as can be seen in Figure 5.15. At dc, the error is dominated by R_{zw} and since $|\tilde{h}| > |h|$, then $1 > \tilde{h}g > hg$ and it follows that $|\tilde{R}_{zw}\tilde{R}_{zw}^H| < |R_{zw}R_{zw}^H|$. At high frequencies, both error components become significant. At $z = -1$, $|\tilde{R}_{zw}\tilde{R}_{zw}^H| \approx |R_{zw}R_{zw}^H|$ and since $|\tilde{h}| > |h|$ then $|\tilde{R}_{zv}\tilde{R}_{zv}^H| > |R_{zv}R_{zv}^H|$ with the result that $|\tilde{R}_{zd}\tilde{R}_{zd}^H| > |R_{zd}R_{zd}^H|$. When σ_v^2 is decreased sufficiently (eg. $\sigma_v^2= 0.0001$ or less,) the equalisers invert the channel equally well and become indistinguishable. Conversely when σ_v^2 is increased sufficiently (eg. $\sigma_v^2= 10$ or more,) then the difference in error performance also diminishes. This arises because both equalisers become low magnitude filters when σ_v^2 is large, with the result that R_{zw} becomes increasingly dominant and $R_{zd}R_{zd} \approx R_{zw}R_{zw}^H \approx \sigma_w^2 \approx \gamma^2$.

Example 5.17. The zero in G(s) of Example 5.16 is reflected about the imaginary axis yielding the non-minimum phase channel $G(z)= 0.2(z+ 1.0101)(z- 0.6)^{-1}$. The error spectra for the H_∞ equaliser (at $\gamma = 0.3177$) and Kalman equaliser are presented in Figure 5.17. It is seen that the high frequency performance is largely unaffected by the substitution of a non-causal, low frequency zero. However the Kalman equaliser exhibits a greater increase in dc error because it attempts to cancel a noncausal zero with a causal pole. The H_∞ equaliser is better at minimising R_{zw}, since $|\tilde{h}| > |h|$ and $1 >> \tilde{h}g > hg$. If σ_v^2 is increased sufficiently (eg. $\sigma_v^2 = 100$ or more,) the error due to the observation noise becomes more significant than the error in inverting the non-causal zero. Consequently the performance is similar to the minimum phase case.

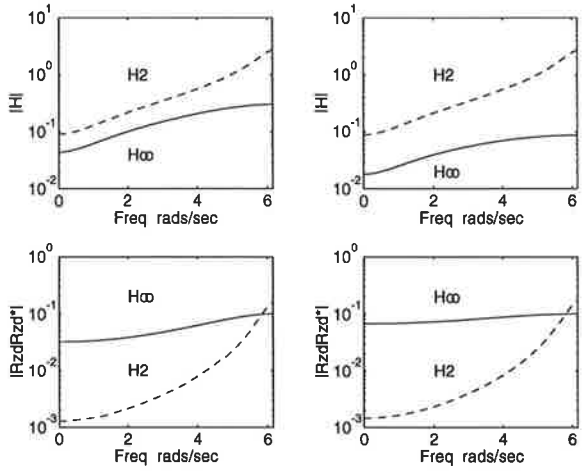

Fig. 5.16. Spectra for Example 5.16. Fig. 5.17. Spectra for Example 5.17.

Examples 5.16 and 5.17 demonstrate that a H_∞ design can be too conservative and can result in a severe performance degradation. In Figures 5.16 and 5.17, it is seen that a small reduction in the peak of the error spectrum is accomplished by severely compromising low frequency performance.

5.4.3. Known, high-pass channels.

Example 5.18. Consider the bilinear transform of the minimum phase channel $G(s) = 80(s+1)(s+796)^{-1}$ at $F_s = 2$, yielding $G(z) = (z-0.6)[2(z+.99)]^{-1}$. The equaliser and error spectra are shown in Figure 5.18. At high frequencies, the error is dominated by the $|R_{zw}R_{zw}^H|$ component, whereupon it can be deduced that $|\tilde{R}_{zw}\tilde{R}_{zw}^H| < |R_{zw}R_{zw}^H|$ from $|\tilde{h}| > |h|$ and $1 > \tilde{h}\,g > hg$. At dc, the contribution of the $|R_{zv}R_{zv}^H|$ components and the observation $|\tilde{R}_{zv}\tilde{R}_{zv}^H| > |R_{zv}R_{zv}^H|$ follows from $|\tilde{h}| > |h|$. Once again it is seen that the reduction in the peak of the error spectrum occurs at the expense of greater mean square error. The performance at low and high observation noise mirrors that of the low-pass minimum phase case. If the observation noise is sufficiently low (eg. $\sigma_v^2 = 0.001$ or less,) the two equalisers become indiscernable as they invert the channel equally well. The H_∞ equaliser offers a marginally reduced peak error at the expense of marginally greater high frequency error. If the measurement noise is sufficiently high (eg. $\sigma_v^2 = 1$ or more,) then it is observed that $|R_{zd}R_{zd}| \approx |R_{zw}R_{zw}^H| \approx \sigma_w^2 \approx \gamma^2$.

Example 5.19. Consider the non-minimum phase channel $G(z) = (0.6z-1)[2(z+.99)]^{-1}$. Compared to Example 2 where the channel was just non-minimum phase, here the zero is placed well outside of the unit circle and the channel is harder to invert. The equaliser and error spectra (at $\sigma_v^2 = 0.01$ $\sigma_w^2 = 0.1$) are shown in Figure 5.19. Not surprisingly, $\sup_{\omega\in\{-\pi,\pi\}}|\tilde{H}(e^{j\omega})| > \sup_{\omega\in\{-\pi,\pi\}}|H(e^{j\omega})|$ and the H_∞ solution exhibits reduced peak error at dc because the contribution due to R_{zv} is smaller. It can be seen that the advantage of H_∞ is

more apparent because the channel is profoundly non-minimum phase. When the SNR is increased (eg. $\sigma^2_{\omega_1}= 0.0001$) , at dc the H_∞ equaliser offers about 1.5 dB less error compared to the Kalman equaliser. An explanation of the comparatively poor performance of the Kalman equaliser is the same as that of the continuous-time channel equaliser problem (Section 5.3.3). The solutions are $\tilde{H}= 1.77(z+0.99)(z-.585)^{-1}$ and $H= 0.000856(z+0.99)(z-0.000425)^{-1}$ at $\gamma = 0.3163$. Thus the Kalman equaliser is an inverse for the minimum phase case whereas the H_∞ solution does not attempt to invert the channel but instead minimizes R_{zw} via a low magnitude equaliser. When the observation noise power is sufficiently high (eg. $\sigma^2_v= 100$), both equalisers behave as filters and exhibit similar performance. For this example $|R_{zd}R^H_{zd}|$ is observed to be flat and due to $|R_{zw}R^H_{zw}|$, with $|R_{zw}R^H_{zw}| \approx \sigma^2_w \approx \gamma^2$.

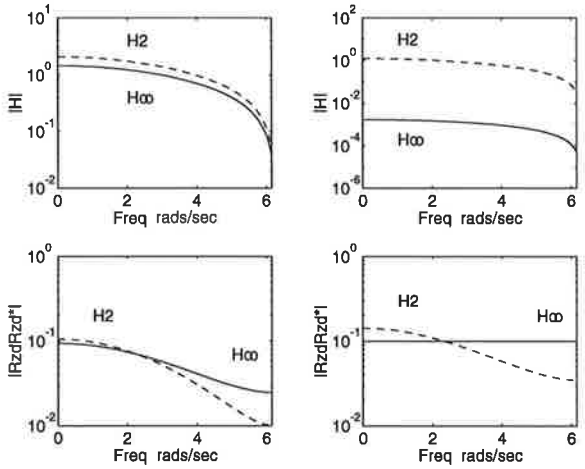

Fig. 5.18. Spectra for Example 5.18.

Fig. 5.19. Spectra for Example 5.19.

For the above examples, it is observed that R_{zd} is dominated by R_{zw} and so $\gamma \approx \sigma_w$. If the noise is white and the model is exact, then it may be difficult to justify the cost incurred by H_∞. Although the H_∞ equaliser does yield lower peak error, the design is very conservative since the peak error occurs out of band and may not be worth the cost. Instead it may be worthwhile to increase γ slightly and obtain an error performance somewhere between the H_∞ and Wiener cases. However, if the disturbance is coloured (say for example that the spectra is similar to the equaliser spectra), then the H_∞ equaliser may offer a slight benefit, by virtue of the slightly lower gain. If the plant is non-minimum phase it is observed that the maximum of the Kalman equaliser spectrum is significantly greater than that of the H_∞ equaliser. Hence it is contended that the H_∞ equaliser is more robust to modelling errors.

This section has begun with a cursory examination of scalar examples because the solution to the discrete-time ARE and hence the equaliser transfer function can be written down *a priori*. It is argued that an awareness of what happens in scalar problems can lead to a

better understanding of equaliser behaviour for second order, band-pass examples. The observations for the above scalar examples are summarised, before moving on to second order problems.

If the channel is low-pass, minimum phase, the exogenous inputs are white and the SNR is sufficiently high then the Kalman equaliser is better most of the time. The H_∞ error spectrum does have a reduced maximum, but this occurs well beyond the channel bandwidth. When the observation noise power is very small, then the two H_∞ equalisers become indistinguisable and invert the channel equally well. When the observation noise power is very large, then the two equalisers yield approximately equal, flat error spectra. Similar trends occur if the channel is high-pass and minimum phase: at low observation noise, the equalisers are approximately equal and at high observation noise, although the equalisers are different, the error spectra are about the same. When the channel is non-minimum phase the H_∞ equaliser is advantageous, provided the observation noise is sufficienty low. In the case of high observation noise, the error performance is comparable to the minimum phase case.

5.4.4 Known, band-pass channels.

It turns out that for second order band-pass channels, the behaviour of equalisers is analogous to that of scalar problems. This is illustrated by two examples.

Example 5.20. Consider the bilinear transform (at $F_s = 2$) of the minimum phase plant $G(s) = 0.0625(s+.1026)(s+156)(s+1)^{-2}$, namely $G(z) = 1.6405(z+0.95)(z-.95)(z-0.6)^{-2}$. It turns out that when the SNR is very high (eg. $\sigma_v^2 = .01$, $\sigma_w^2 = 100$) the two equalisers are approximately equal. When the observation noise is increased (such as $\sigma_v^2 = 10$), although the H_∞ equaliser exhibits about 1 dB less peak error at $z = 1$, the midband error is about 10 dB worse than that of the Kalman solution. This is shown in Figure 5.20. At very low SNRs (eg. $\sigma_v^2 = 10000$ or more), it is observed that $1 >> \sup_{\omega\in[-\pi,\pi]} |\tilde{H}(e^{j\omega})| >> \sup_{\omega\in[-\pi,\pi]} |H(e^{j\omega})|$, in which case the error becomes dominated by R_{zw} and $|R_{zw}R_{zw}^H| \approx \sigma_w^2 \approx \gamma^2$.

Example 5.21. In the case of the non-minimum phase, band-pass channel model of $G(s) = -1.559(z+1.0526)(z-0.95)(z-0.6)^{-2}$, it is found that the minimisation of the peak of the error spectrum is achieved at even greater expense. At very high SNR (such as $\sigma_v^2 = .01$, $\sigma_w^2 = 100$) it so happens that about 1 dB reduction in high frequency peak error is realised at the cost of about 27 dB increase in error at dc. The Kalman and H_∞ error spectra for $\sigma_v^2 = 10$ are shown in Figure 5.20. It can be seen that the H_∞ equaliser trades off MSE for the peak of the error spectrum magnitude. When the observation noise power is very high (eg. $\sigma_v^2 = 10000$ or more,) the equalisers have been observed to behave as filters and the ensuing error spectra are approximately the same as for the high observation noise, minimum phase channel case.

Clearly if the channel models are known exactly and the observation noise is white, then the minimum MSE solution is the better choice. However, if either the channel is minimum phase and the observation noise very high, or if the channel is non-minimum phase then $\sup_{\omega\in[-\pi,\pi]}|\tilde{H}e^{j\omega})| >> \sup_{\omega\in[-\pi,\pi]}|H(e^{j\omega})|$, whereupon the H_∞ equaliser is expected to be more robust to small modelling errors. Furthermore, it is expected that some capacity would exist to explicitly accommodate model uncertainty. This demonstrated in the next section.

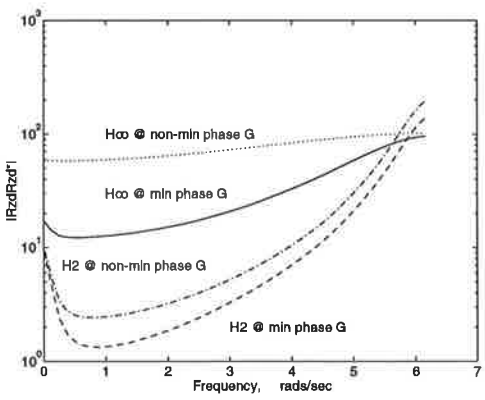

Fig. 5.20. Error spectra for Examples 5.20 and 5.21.

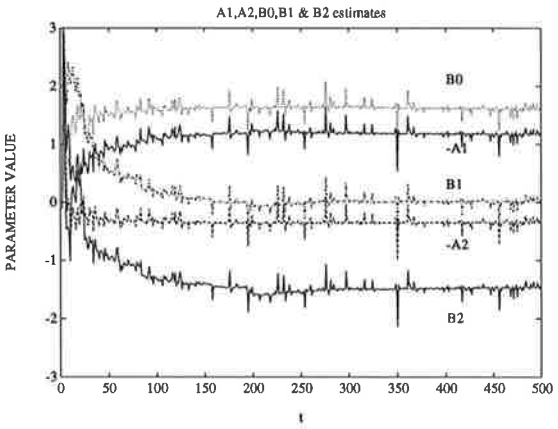

Fig. 5.21. Poorly identified model parameters.

5.4.5 Uncertain, band-pass channels.

The objective of this section is to examine the merits of a robust equaliser that is designed to compensate for an erroneous channel model obtained via some identification procedure. In an approach due to Mayne [S], the Kalman filter may be used to identify the unknown parameters . This method is outlined briefly below. A second order model may be written in terms of the ARMA parameters, that is

$$y_k = -a_1 y_{k-1} - a_2 y_{k-2} + b_0 w_k + b_1 w_{k-1} + b_2 w_{k-2} + v_k. \tag{5.21}$$

Defining $\Theta = [-a_1 \;\; -a_2 \;\; b_0 \;\; b_1 \;\; b_2]$ and $\Phi_k = [y_{k-1} \;\; y_{k-2} \;\; w_k \;\; w_{k-1} \;\; w_{k-2}]$ then (5.21) may be written equivalently

$$y_k = \Theta\, \Phi_k^T + v_k. \tag{5.22}$$

A Kalman filter may be used to produce estimates of Θ from the observations y_k, viz.

$$\hat{\Theta}_{k+1} = \hat{\Theta}_k + K_t(y_k - \Phi_k^T \hat{\Theta}_k), \tag{5.23}$$

where $K_k = \Sigma_k \Phi_k \Omega_k^{-1}$, $\Omega_k = \Phi_k^T \Sigma_k \Phi_k + R$, and

$$\Sigma_{k+1} = \lambda(I - K_{k+1}\Phi_k^T)\Sigma_k + Q. \tag{5.24}$$

This method is convenient to implement because the size of the state vector is a minimum. One disadvantage is that the roots of the denominator of the estimated transfer function are not guaranteed to be inside the unit circle. Consider the task of estimating the ARMA

parameters for the minimum phase plant of Example 5.19. Typical tracks that result for the ARMA coefficients in the case of $\sigma_v^2 = 0.001$, $\sigma_w^2 = 1$, $\lambda = 0.9999$, $Q = 0.00001I$ and $R = 0.001$ are shown in Figure 5.21.

Example 5.22. Consider the model $G_o = (1.428z^2 + .1757z - 1.286)(z^2 - .9384z + .3926)^{-1}$, a particularly erroneous outcome from the above identification method. It has previously been shown (in Examples 5.8 and 5.14) how problems may be solved when the uncertainty is unparametrised. If an estimate for the structure of the uncertainty is available, then a robust design may be found by solving an auxilliary coloured noise problem, as is indicated in the end of Section 3.4.

The procedure that is advocated for accommodating the structured modelling error, is to estimate the worst case uncertainty (denoted by $\Delta(s)$, with $\delta = \|\Delta\|_\infty$) and then explore the error spectra that result for candidate robust designs at various values of γ and δ. Arguably a H_∞ equaliser is conservative, since a small reduction in the peak of the error spectrum is attained at the cost of a substantial increase in MSE. Therefore it may be prudent to increase γ beyond the optimal value. The accommodation of model uncertainty (via Lemma 3.1) arises out of a sufficient condition and it may be beneficial to consider values of δ less than the H_∞-norm bound of the uncertainty.

In practice, the worst case modelling error may occur for some unknown combination of the estimated transfer functions of the nominal model and the worst case uncertainty. In this case it would be advisable to conduct an exhaustive search of combinations of estimated nominal models and uncertainties in order to ascertain the worst case error spectrum. For instance, in Example 5.8 the error spectra were plotted from $G_o - \Delta$ through to $G_o + \Delta$.

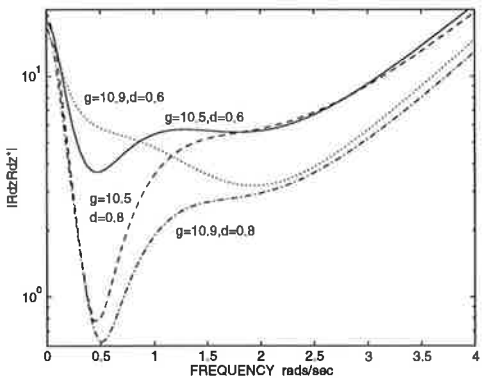

Fig. 5.22. Estimated worst case error spectra.

Suppose that $\Delta = (z \pm 0.99)(z-0.6)^{-2}$ is an additive uncertainty in which case $\|\Delta\|_\infty \approx 3.1$. For convenience, assume that the worst case error occurs when the exact model is given by $G_{ex} = G_o + \Delta$. The task is to compare robust equalisers for various choices of γ and δ.

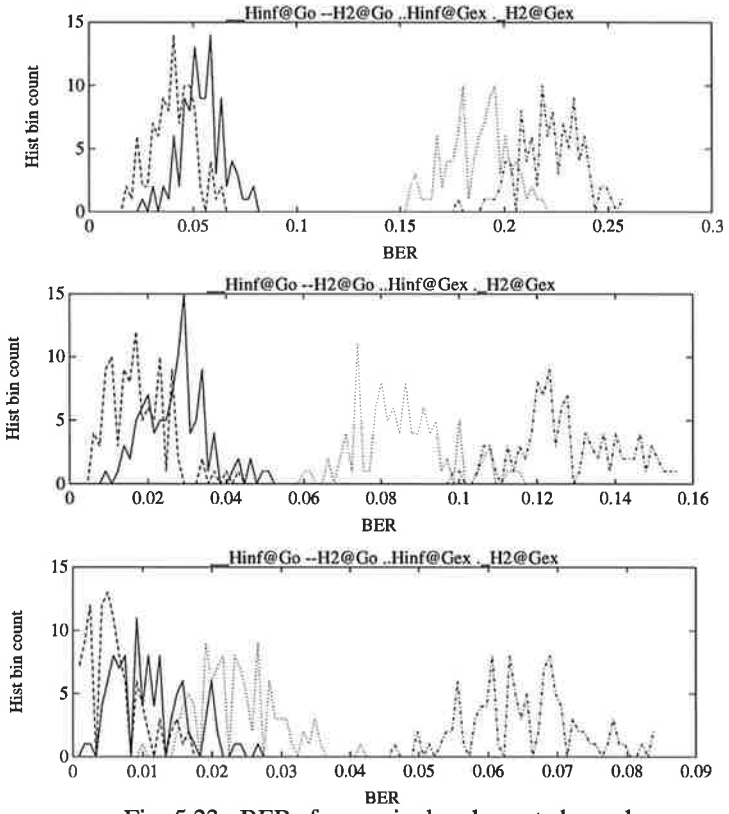

Fig. 5.23. BERs for nominal and exact channels.
18 dB SNR (top), 21 dB SNR (middle) and 24 dB SNR (bottom).

The worst case error spectra for the candidate H_∞ equalisers at $\sigma_v^2 = 10$, $\sigma_w^2 = 100$ for combinations of $\gamma = \{10.5, 10.9\}$ and $\delta = \{0.6, 0.8\}$ are shown in Figure 5.22. It can be seen that the choice of $\gamma = 10.9$ and $\delta = 0.8$ appears to minimise the MSE and in the vicinity of the channel bandwidth. It remains to be demonstrated that the H_∞ equaliser is robust. To this end the results of simulations with binary iid data sequences are presented in Figure 5.23. The simulations of the equalisation of binary data were carried out by inserting a limiter (a nonlinearity that returns the sign of the input) immediately after the equaliser as shown in Figure 2.8. It can be seen at 18 dB SNR, that the Kalman equaliser exhibits marginally less mean bit error rate (BER) than the H_∞ equaliser when the data is generated by the nominal channel, that is when there is no modelling error present. However when the data is generated by the estimate for the exact channel, it is seen that the robust H_∞ equaliser reduces the mean BER. The advantage of the H_∞ equaliser (when the channel is poorly modelled) increases with higher SNRs. With $\sigma_v^2 = 5$ (about 21 dB SNR) for $\delta = 0.85$, from Figure 5.23 the difference in mean BER is seen to be about 1.8 dB. When the observation noise is decreased further ($\sigma_v^2 = 2.5$ is decreased to 2.5 (about 24 dB SNR),

with $\delta = 0.88$, it can be seen from Figure 5.23 that the reduction in mean BER is about 4.8 dB.

This simple example demonstrates that (a) if the uncertainties are modelled, they need to be well characterised, (b) values for the parameters γ and δ may be found iteratively and (c) the cost of robustness is a performance degradation when the uncertainty is not present.

5.5. Conclusions.

The approach taken here is to confine the attention to stationary problems, so that it is meaningful to refer to transfer functions and power spectra. Where possible, scalar problems have been examined so that something may be inferred about higher order problems.

The objective of this chapter is to contribute to an understanding of how and when H_∞ filters offer a performance benefit compared to Kalman filters. It has been observed that when the problem is easy and the Kalman filter works well, then the H_∞ filter does not generally provide any additional benefit. Often the H_∞ filter offers only a marginal reduction in the peak of the error spectrum at the cost of a substantial increase in MSE. However if the problem is difficult and the Kalman filter does not work well, then sometimes a H_∞ design can provide significant reduction in the peak of the error spectrum.

In respect of SISO, output estimation problems:

- When the plant is known and low-pass, at very high SNR the Kalman filter approaches a short circuit, that is, it does nothing. This is reasonably so, since at very high SNR a filter is superfluous. The H_∞ filter is better at doing nothing, that is, it is closer to a short circuit. In other words, the H_∞ filter simply does less and it turns out that this reduces the peak of the error spectrum at the expense of MSE.
- An intuitive explanation of how the H_∞ filter does less follows by examining the scalar case and considering the transfer function description $H(s) = C(sI - A + KC)^{-1}K$. Since $P > \tilde{P}$ and $K = PC^T$, then $KC > \tilde{K}C$ and so the poles of the H_∞ filter are further out than those of the Kalman filter. Alternatively, since $P > \tilde{P}$, the H_∞ filter may be interpreted as a Kalman filter that is designed for a worse case $\tilde{\sigma}_w^2 > \sigma_w^2$.
- If the plant is known, low-pass and stable, then compared to the Kalman filter, the H_∞ filter attains only small reduction in the peak of the error spectrum. This advantage is more profound when the plant is strictly proper and the SNR is high. It can be seen from the H_∞ ARE that when σ_v^2 becomes large, then so does γ^2, in which case it can be deduced that $P \approx \tilde{P}$. Thus at very low SNR, the reduction in the peak of the error spectrum becomes negligible because the H_∞ filter approaches the Kalman filter.

- If the plant is known and high-pass, then the advantage of a H_∞ design can be more substantial. The goal of attaining a high-pass filter response directly opposes the requirement to minimise the MSE. Therefore it is not surprising that the trade-off between the peak of the error spectrum and the area under the error spectrum is more profound when the plant is high-pass.
- When the plant is unstable, the comparative advantage of the H_∞ filter can be more significant. At high SNR, both filters tend to perform similarly whereas at lower SNRs the H_∞ filter offers an increased reduction in peak error of the error spectrum. In contrast to the Kalman filter, the H_∞ solution does not attempt a stable approximation to an unstable plant, rather it just minimises the error via a very low magnitude filter, approaching an open circuit. That is to say, the H_∞ filter is better than the Kalman filter at *doing nothing*. Here *doing nothing* refers to how close a filter approximates an open circuit which ignores the data.
- When the plant model is uncertain, then one may attempt a H_∞ design that is robust to modelling errors. Although the ensuing filter is guaranteed to satisfy a H_∞ optimality criterion, the design may be too conservative and the cost too high. When the uncertainty is small, the robust design may yield an improvement in the peak of the error spectrum at the expense of an increased lower error bound. However when the uncertainty is large, it may not be possible to obtain any improvement.

In respect of SISO, input estimation or equalisation problems:

- The observations stated for known, stable, output estimation problems apply also to equalisation when the plant is known and minimum phase. In particular, a reduction in the peak of the error spectrum is only noteworthy when σ_v^2 is low and can be more apparent when the plant is high-pass. If the plant is low-pass, a major disadvantage of H_∞ equaliser is that an inconsequential reduction in the peak of the error spectrum can be accompanied by a severe degradation in MSE performance.
- When the plant is non-minimum phase, there are some similarities with the unstable output estimation problem. Compared to the Kalman equaliser, the H_∞ equaliser is observed to exhibit increased reductions in the peak of the error spectrum magnitude at lower SNRs. If σ_v^2 is sufficiently small, the Kalman equaliser for a non-minimum phase plant tends to be about the same as the minimum phase case, conversely the H_∞ solution is a low magnitude filter. When σ_v^2 becomes large then the Kalman equaliser becomes a very low magnitude filter, approaching an open circuit, and the H_∞ equaliser is even closer to an open circuit. Actually neither equaliser inverts the plant, but the H_∞ equaliser minimises the peak of the error spectrum instead.

- When the plant is known to be minimum phase, the accommodation of model uncertainty may not be tractable. Solutions to minimum phase equalisation problems are acutely sensitive to modelling errors when σ_v^2 is small. This arises because the contribution of the error component $R_{zw} = (HG_2 - 1)\sigma_w$ becomes significant when $H \neq G_2^{-1}$. Consequently it is necessary to explore the error spectra that result from candidate robust equalisers in order to ascertain if any benefits prevail when the modelling errors are present.
- H_∞ equalisers for non-minimum phase plants are inherently tolerant of modelling errors. Thus when the plant known to be non-minimum phase but the model is not known exactly, there is often no need to explicitly accommodate any uncertainty. This inherent robustness is a virtue of the H_∞ equaliser being a low magnitude filter, so that $HG_2 \approx 0$ and hence $R_{zw} = (HG_2 - 1)\sigma_w \approx \sigma_w$, even when G_2 is uncertain. In a particular example it is argued that H_∞ equaliser is robust to a 30 db uncertainty in the plant magnitude, whereas the peak of the Kalman equaliser error spectrum increases by about 85 db.
- The results of simulations have been presented to demonstrate the advantage of frequency weighted model uncertainty when a channel is poorly modelled.

In respect of cost benefits of a H_∞ design *in lieu* of a Kalman solution:

- If the noise processes are gaussian and the models are known exactly, H_∞ filters *per se* are not necessarily advantageous.
- The H_∞ framework allows the designer to use γ as a tuning parameter and degrade the MSE performance in favour of the peak of the error spectrum.
- Sometimes a H_∞ design can be constructed that may be robust to small modelling errors
- The design effort increases because the optimal choice of γ needs to be determined iteratively. The implementation cost remains unchanged since the order of the solution remains unchanged.

REFERENCES

[EW] Einicke, G. A. and L. B. White, "Performance comparison of H_∞ and Kalman filters", submitted for publication.

[KP] Kassam, S. A. and H. V. Poor, "Robust techniques for signal processing: a survey", *Proc. IEEE*, vol. 73, no. 3, pp. 433-481, Mar. 1985.

[S] Strejc, V., *State space theory of discrete linear control*, Wiley, Chichester, pp. 257-258, 1981.

Chapter 6

Nonlinear observers using fake ARE techniques

This chapter introduces nonlinear filtering problems and shows how the fake ARE technique may be applied in the construction of nonlinear observers for the demodulation of frequency or phase modulated signals.

The contributions of this chapter are the derivation of the nonlinear observer, the use of the fake ARE technique to choose the gains, the determination of the set of gains that guarantee local tracking stability (in the case of known amplitude,) the extensions to multiple signal components and the results of simulations to demonstrate some advantages in frequency tracking problems. The use of the fake ARE technique for the demodulation of single tones has been presented in [EW1] and extensions to the multiple signal component case have been reported in [EW2].

This chapter is organised in 8 sections. The problem is motivated in Section 6.1. The nonlinear observer and the application of the fake ARE technique are described in Sections 6.2 and 6.3 respectively. The application to one signal component, multiple nonharmonic components and multiple harmonic components are described in Sections 6.4, 6.5 and 6.6 respectively. Error stability is addressed briefly in Section 6.7. In Section 6.8 the results of simulations are presented to show performance improvements compared to an extended Kalman filter (EKF).

6.1 Motivation.

The problem of interest is demodulating a signal that is either frequency or phase modulated, and having a slowly varying amplitude. Such signals arise in many applications such as communications, radar and sonar for example. The problem is formulated as a state estimation problem along similar lines to the methods proposed in [AM]. The approach here is different to [AM] in one important respect. In [AM], the extended Kalman

filter is used to produce state estimates. This approach arises by linearising the signal model about the current state estimate, and using the optimal linear (Kalman) filter to derive the state estimate at the next time. This attempts to produce a (locally) optimal filter however it is not, in general, stable. The approach taken in this chapter is to design a nonlinear observer with the nonlinear gain functions chosen to ensure stability of the locally linear system. An approximate criterion for optimality is based on the so-called fake algebraic Riccati techniques due to M. -A. Poubelle, R. R. Bitmead and others [PPGB, BTP, BGW, BG].

In linear H_∞ filtering, some robustness to uncertainties in the inputs is accommodated at the expense of an increase in the state estimation error covariance (Lemmas 3.4 and 4.3). The fake ARE technique was conceived for (linear) problems in which the process noise covariance is uncertain and any robustness to input uncertainty is similarly attained at the cost of MSE (see Section 1.3.1). However the fake ARE technique is more general - it also applies to nonlinear problems, provided that a suitable linearisation can be found. Furthermore, it is shown subsequently that if the error system can be decomposed into a combination of a stable, linear-time-invariant system and a nonlinear part, which is bound within a sector, then stability can be guaranteed. This is demonstrated for the single tone case. Hence the fake ARE technique may be thought of as a method that trades off optimality for stability.

6.2 A nonlinear observer.

Consider the following model, comprising a stable, linear state evolution and a nonlinear output mapping

$$\begin{aligned} x_{k+1} &= Ax_k + Bw_k, \\ y_k &= c(x_k) + v_k, \end{aligned} \tag{6.1}$$

where w_k and v_k are uncorrelated, zero mean, white, l and p order processes with known covariances Q and R respectively. A resursive filter is desired which yields estimates of x_k given measurements y_k for each $k \geq 0$. The filter is required to be unbiased and exhibit good performance in terms of error variance. A nonlinear observer may be constructed having the form

$$\hat{x}_{k+1} = A\hat{x}_k + g_k\left(y_k - c(\hat{x}_k)\right), \tag{6.2}$$

where g_k is a nonlinear gain function to be designed. From (6.1) and (6.2), the state prediction error may be written as

$$\tilde{x}_{k+1} = A\tilde{x}_k - g_k(\varepsilon_k) + Bw_k, \tag{6.3}$$

where $\tilde{x}_k = x_k - \hat{x}_k$ and $\varepsilon_k = y_k - c_k(\hat{x}_k)$ is the output error. The Taylor series expansion of the output mapping to terms linear in the state error yields

$$c(x_k) \approx c(\hat{x}_k) + \left[\frac{\partial c(x)}{\partial x}\right]_{x=\hat{x}_k} \tilde{x}_k. \tag{6.4}$$

Denoting $H_k = \left[\frac{\partial c(x)}{\partial x}\right]_{x=\hat{x}_k}$, then from (6.1) and (6.4) the output error is approximately

$$\varepsilon_k \approx H_k \tilde{x}_k + v_k. \tag{6.5}$$

The objective here is to design the g_k to be a linear function of $\tilde{x}_k$ to first order terms. For certain classes of problems (see Sections 6.4, 6.5 and 6.6) this can be achieved by a suitable choice of a nonlinear D_k (see Sections 6.4, 6.5 and 6.6) resulting in the adaptive gains

$$g_k(\varepsilon_k) = K_k D_k \varepsilon_k, \tag{6.6}$$

where K_k is a gain matrix of appropriate dimensions. In view of (6.6), the error system (6.3) may be written as

$$\tilde{x}_{k+1} = (A - K_k C_k)\tilde{x}_k + K_k D_k v_k + B w_k, \tag{6.7}$$

where

$$C_k = D_k H_k. \tag{6.8}$$

If a bounded function of the states, D_k, can be found, so that C is a constant matrix and if the pair [C,A] is completely observable (namely if $[C, CA, CA^2, \ldots, CA^{n-1}]$ has rank n,) then asymptotic stability can be guaranteed by placing the eigenvalues arbitrarily to ensure $|\lambda(A - K_k C)| < 1$. However this condition does not provide guidance on the optimal K_k. Therefore an approximate equation is written for the estimation error covariance P_k which yields a Lyapunov form of the ARE. Neglecting the cross terms, the approximate equation (for any K_k) is

$$P_{k+1} = (A - K_k C_k) P_k (A - K_k C_k)^T + K_k D_k R D_k^T K_k^T + BQB^T. \tag{6.9}$$

The optimal K_k which minimises P_{k+1} is given by

$$K_k = P_k C_k^T (C_k P_k C_k^T + D_k R D_k^T)^{-1}, \tag{6.10}$$

where P_k is found by solving the Riccati difference equation (RDE)

$$P_{k+1} = A P_k A^T - P_k C_k^T (C_k P_k C_k^T + D_k R D_k^T)^{-1} C_k P_k + BQB^T. \tag{6.11}$$

In general, because of the nonlinear impact of the estimates on (6.11), the solutions are not guaranteed to be positive definite and therefore the resulting error system may not be stable.

6.3 Application of the fake ARE technique.

The fake ARE technique originated from the work of Poubelle, Bitmead *et al* [PPGB] which presents connections between RDE solutions and ARE stability results. The treatment in [PPGB] is rather brief, more constructive discussions are detailed in [BTP]

where the technique is referred to as *covariance setting*. The method was christened the *fake ARE* in [BGW,BG]. Consider the signal model $x_{k+1/k} = Ax_k + Bw_k$, $y_k = Cx_k + v_k$, in which A has its eigenvalues inside the unit circle, [A,C] is observable. If $P = \delta I$ is chosen to be any positive definite matrix and the predictor gain is $K = APC^T(CPC^T + R)^{-1}$, then the matrix $(A - KC)$ has all its eigenvalues strictly inside the unit circle. [BTP,BGW,BG].

Thus for any positive definite matrix $P = \delta I$, the resultant Kalman filter $\hat{x}_{k+1} = (A-KC)\hat{x}_{k/k-1} + Ky_k$ is exponentially asymptotically stable. The first application of the fake ARE is described in [BTP] where (linear) Kalman filters are designed to have desirable properties. Specifically, it is noted that δ serves as a design parameter, allowing convergence rate and noise rejection to be traded off against each other. Now that the fake ARE method has been defined, its application to the nonlinear problem of (6.1) may be set out. Using the approach of [BG,BGW,BTP], the RDE (6.11) may be masqueraded by the fake ARE

$$P = APA^T - PC_k^T (C_kPC_k^T + D_kRD_k^T)^{-1}C_kP + BQB^T. \tag{6.12}$$

Rather than finding a solution to (6.12), instead a fixed positive definite solution Σ is assumed and then the gain may be calculated from (6.10), using Σ in place of P_k.

6.4 One signal component.

Consider a frequency or phase modulated signal which may be modelled by

$$\begin{bmatrix} a_{k+1} \\ \omega_{k+1} \\ \varphi_{k+1} \end{bmatrix} = \begin{bmatrix} 1 & 0 & 0 \\ 0 & 1 & 0 \\ 0 & 1 & 1 \end{bmatrix} \begin{bmatrix} a_k \\ \omega_k \\ \varphi_k \end{bmatrix} + \begin{bmatrix} w_k^{(1)} \\ w_k^{(2)} \\ w_k^{(3)} \end{bmatrix}, \tag{6.13}$$

where $a_k, \omega_k, \varphi_k \in \boldsymbol{R}$, the $w_k^{(1)}, w_k^{(2)}, w_k^{(3)}$ are scalar, zero mean, uncorrelated white noise processes with covariance $Q = diag(\sigma_{w^{(1)}}^2, \sigma_{w^{(2)}}^2, \sigma_{w^{(3)}}^2)$. Let $y_k = y_k^{(1)} + j\, y_k^{(2)}$ denote the (baseband) complex observed signal, which may be written as

$$y_k = a_k\, e^{j\varphi_k} + v_k, \tag{6.14}$$

where $v_k = v_k^{(1)} + j\, v_k^{(2)}$ where the $v_k^{(1)}, v_k^{(2)}$ are uncorrelated white noise processes. The model (6.13) may be written as (6.1) in which $A = \begin{bmatrix} 1 & 0 & 0 \\ 0 & 1 & 0 \\ 0 & 1 & 1 \end{bmatrix}$. Expanding the prediction error to terms linear in the estimation error yields

$$H_k = \begin{bmatrix} \cos\hat{\varphi}_k & 0 & -\hat{a}_k \sin\hat{\varphi}_k \\ \sin\hat{\varphi}_k & 0 & \hat{a}_k \cos\hat{\varphi}_k \end{bmatrix}. \tag{6.15}$$

The form in (6.14) suggests the choice

$$D_k = \begin{bmatrix} \cos\hat{\varphi}_k & \sin\hat{\varphi}_k \\ \dfrac{-\sin\hat{\varphi}_k}{\hat{a}_k} & \dfrac{\cos\hat{\varphi}_k}{\hat{a}_k} \end{bmatrix}, \tag{6.16}$$

since this results in $C = \begin{bmatrix} 1 & 0 & 0 \\ 0 & 0 & 1 \end{bmatrix}$.

Assuming a symmetric positive definite solution to (6.12) of the form $\Sigma = \begin{bmatrix} \Sigma^a & 0 & 0 \\ 0 & \Sigma^{\omega} & \Sigma^{\omega\varphi} \\ 0 & \Sigma^{\varphi\omega} & \Sigma^{\varphi} \end{bmatrix}$ with $\Sigma^a, \Sigma^{\omega}, \Sigma^{\varphi\omega}, \Sigma^{\varphi} \in \boldsymbol{R}$ and choosing the gains according to (6.10) yields

$$K_k = \begin{bmatrix} K_k^a & 0 \\ 0 & K_k^{\omega} \\ 0 & K_k^{\varphi} \end{bmatrix} \quad \text{where} \quad K_k^a = \frac{\Sigma^a}{\Sigma^a + \sigma_v^2}, \quad K_k^{\omega} = \frac{\Sigma^{\omega\varphi}}{\Sigma^{\varphi} + \sigma_v^2 \hat{a}_k^{-2}}, \quad K_k^{\varphi} = \frac{\Sigma^{\varphi}}{\Sigma^{\varphi} + \sigma_v^2 \hat{a}_k^{-2}}. \tag{6.17}$$

The nonlinear observer then becomes

$$\begin{aligned} \hat{a}_{k+1} &= \hat{a}_k + \frac{\Sigma^a (x_k \cos\hat{\varphi}_k + y_k \sin\hat{\varphi}_k - \hat{a}_k)}{\Sigma^a + \sigma_v^2}, \\ \hat{\omega}_{k+1} &= \hat{\omega}_k + \frac{\Sigma^{\omega\varphi} (y_k \cos\hat{\varphi}_k - x_k \sin\hat{\varphi}_k)}{\hat{a}_k \Sigma^{\varphi} + \sigma_v^2 \hat{a}_k^{-1}}, \\ \hat{\varphi}_{k+1} &= \hat{\varphi}_k + \hat{\omega}_k + \frac{\Sigma^{\varphi} (y_k \cos\hat{\varphi}_k - x_k \sin\hat{\varphi}_k)}{\hat{a}_k \Sigma^{\varphi} + \sigma_v^2 \hat{a}_k^{-1}}. \end{aligned} \tag{6.18}$$

The conventional solution to nonlinear filtering problems is the EKF and a derivation is alluded to in [AM]. By way of comparison, the EKF for the system (6.13) and (6.14) is given by [AM, (2.4)-(2.8)]:

$$\begin{aligned} \begin{bmatrix} a_{k/k} \\ \omega_{k/k} \\ \varphi_{k/k} \end{bmatrix} &= \begin{bmatrix} a_{k/k-1} \\ \omega_{k/k-1} \\ \varphi_{k/k-1} \end{bmatrix} + L_k \varepsilon_k, \\ L_k &= \tilde{P}_k H_k^T (H_k \tilde{P}_k H_k^T + R)^{-1}, \\ \begin{bmatrix} a_{k+1/k} \\ \omega_{k+1/k} \\ \varphi_{k+1/k} \end{bmatrix} &= A \begin{bmatrix} a_{k/k} \\ \omega_{k/k} \\ \varphi_{k/k} \end{bmatrix}, \\ \tilde{P}_{k/k} &= \tilde{P}_{k/k-1} - L_k H_k \tilde{P}_{k/k-1}, \\ \tilde{P}_{k+1/k} &= A \tilde{P}_{k/k} A^T + Q. \end{aligned} \tag{6.19}$$

It is well known that the steady state EKF approximates a phase-locked loop. For the system (6.13), a single recursion for the EKF state update is $\hat{x}_{k+1/k} = A\hat{x}_{k/k-1} + AL_k\varepsilon_k$, in which the gain AL_k is amplitude dependent. Similarly, from (6.17) it is seen that the frequency and phase gain terms of the nonlinear observer become small when the amplitude becomes small. It is contended that the nonlinear observer may be interpreted as a phase-locked loop having a more direct form of automatic gain control.

6.5 Multiple nonharmonic components.

The problem of estimating signals that contain periodic components arises in many applications, including fault detection in rotating machinery, radar, sonar and communication signal processing. It is contended that the occurrence of pure sinusoids is quite rare, rather it is the superposition of multiple signal components (some of which may be harmonically related), that generally arises in practice.

Suppose that measurements of a multitone signal are available. It is assumed that there exist n tones which are not necessarily harmonically related. An augmented state vector may be constructed, namely $\boldsymbol{x_k} = [x_k^{(1)},x_k^{(2)},...,x_k^{(n)}]^T$ where $x_k^{(i)} =[a_k^{(i)},\omega_k^{(i)},\varphi_k^{(i)}]^T$ and

$$\boldsymbol{A} = diag[A,A,...,A] \text{ where } A = \begin{bmatrix} 1 & 0 & 0 \\ 0 & 1 & 0 \\ 0 & 1 & 1 \end{bmatrix}. \tag{6.20}$$

The $c(x_k)$ in (6.1) is then given by

$$c(x_k) = [a_k^{(1)}\cos\varphi_k^{(1)} + ...+ a_k^{(n)}\cos\varphi_k^{(n)} \quad a_k^{(1)}\sin\varphi_k^{(1)} + ...+ a_k^{(n)}\sin\varphi_k^{(n)}], \tag{6.21}$$

which results in $\boldsymbol{H_k} = [H_k^{(1)}, H_k^{(2)},..., H_k^{(n)}]$ where

$$H_k^{(i)} = \left[\frac{\partial c(x)}{\partial x}\right]_{x=\hat{x}_k^{(i)}} = \begin{bmatrix} \cos\hat{\varphi}_k^{(i)} & 0 & -\hat{a}_k^{(i)}\sin\hat{\varphi}_k^{(i)} \\ \sin\hat{\varphi}_k^{(i)} & 0 & \hat{a}_k^{(i)}\cos\hat{\varphi}_k^{(i)} \end{bmatrix}. \tag{6.22}$$

This form suggests the choice of $\mathbf{D_k^T} = [D_k^{(1)},D_k^{(2)},...,D_k^{(n)}]^T$ where

$$D_k^{(i)} = \begin{bmatrix} \cos\hat{\varphi}_k^{(i)} & \sin\hat{\varphi}_k^{(i)} \\ \dfrac{-\sin\hat{\varphi}_k^{(i)}}{\hat{a}_k^{(i)}} & \dfrac{\cos\hat{\varphi}_k^{(i)}}{\hat{a}_k^{(i)}} \end{bmatrix}. \tag{6.23}$$

A convenient choice for the fake ARE solution is

$$\Sigma = diag[\Sigma^{(1)},\Sigma^{(2)},...,\Sigma^{(n)}] \text{ where } \Sigma^{(i)} = \begin{bmatrix} \Sigma_a^{(i)} & 0 & 0 \\ 0 & \Sigma_\omega^{(i)} & \Sigma_{\omega\varphi}^{(i)} \\ 0 & \Sigma_{\omega\varphi}^{(i)} & \Sigma_\varphi^{(i)} \end{bmatrix}. \tag{6.24}$$

However the linearization $\boldsymbol{C_k} = \boldsymbol{D_k H_k}$ does not result in perfect decoupling. While the diagnol blocks reduce to $C^{(i,i)} = \begin{bmatrix} 1 & 0 & 0 \\ 0 & 0 & 1 \end{bmatrix}$, the off diagonal blocks possess time varying quantities, namely

$$C_k^{(i,j)} = \begin{bmatrix} \cos(\varphi_k^i - \varphi_k^j) & 0 & a_k^{(j)}\sin(\varphi_k^i - \varphi_k^j) \\ -\dfrac{1}{a_k^{(i)}}\sin(\varphi_k^i - \varphi_k^j) & 0 & \dfrac{a_k^{(j)}}{a_k^{(i)}}\cos(\varphi_k^i - \varphi_k^j) \end{bmatrix}, \tag{6.25}$$

which account for coupling between the components. For a single tone, the denominator of (6.10) is diagonal in which case it is easy to arrive at expressions for the filter gain. Here the existence of the nonzero couplings (6.25) prevents the adaptive gain from being easily written down *a priori*. Instead (6.10) may be evaluated at each instant in time.

The EKF for the multitone problem is [AM, (2.4) - (2.8)] applied to (6.20), (6.21) using (6.22). The elements of the state noise covariance in [AM, (2.8)] are tuning parameters and one convenient choice is $Q = diag[Q^{(1)},Q^{(2)},...,Q^{(n)}]$ where $Q^{(i)} = diag[\sigma_w^{2(1)},\sigma_w^{2(2)},\sigma_w^{2(3)}]$.

6.6 Multiple harmonic components.

If some of the signal components are harmonically related then those frequencies can be deleted from the state vector and the corresponding entries in the state transition matrix replaced by the particular multiples of the fundamental. For convenience it is assumed here that all the tones are harmonically related. The use of the EKF for this problem has been reported in [AP,PA].

The augmented state vector may be written as $\boldsymbol{x}_k = [a_k^{(1)},\omega_k^{(1)},\varphi_k^{(1)},a_k^{(2)}, \varphi_k^{(2)},...,a_k^{(n)},\varphi_k^{(n)}]^T$ and

$$A = \begin{bmatrix} 1 & 0 & 0 & 0 & 0 \\ 0 & 1 & 0 & 0 & 0 \\ 0 & 1 & 1 & 0 & 0 \\ 0 & 0 & 0 & 1 & 0 \\ 0 & 2 & 0 & 0 & 1 \\ \cdot & \cdot & \cdot & \cdot & \cdot \\ 0 & 0 & 0 & 0 & 0 \\ 0 & n & 0 & 0 & 0 \end{bmatrix} \begin{matrix} 0 \\ 0 \\ 0 \\ 0 \\ 0 \\ \cdot \\ 1 \\ 0 \end{matrix}.$$

In this case $H_k^{(2)}$ through to $H_k^{(n)}$ of (6.22) have the second column deleted and the choice of (6.23) remains appropriate.

6.7 Error stability.

6.7.1 Single tone.

In this section the objective is to identify the set of gains, K, sufficient for the error system to be asymptotically stable, where stability is defined as $\tilde{x} \in l_2$, that is, the energy of the error is bounded. The analysis to follow mirrors that usually applied to the phase-locked loop stability. The attention is restricted to the case where amplitude is known. Neglecting the observation noise, the error system is

$$\begin{bmatrix} \tilde{\omega}_{k+1} \\ \tilde{\varphi}_{k+1} \end{bmatrix} = \begin{bmatrix} 1 & 0 \\ 1 & 1 \end{bmatrix} \begin{bmatrix} \tilde{\omega}_k \\ \tilde{\varphi}_k \end{bmatrix} - \begin{bmatrix} K^{\omega} \\ K^{\varphi} \end{bmatrix} \sin \tilde{\varphi}_k + w_k \tag{6.26}$$

for constant K^{ω}, K^{φ}. Stability is argued by appealing to passivity theory and making use of the discrete-time Popov criterion [DV].

Theorem 6.2 [DV] *Consider the system depicted in Figure 6.1 where* $e_1 = u - Ge_2$ *and* $e_2 = \gamma(e_1)$. *Let* $\gamma(x) : \mathbf{R} \to \mathbf{R}$ *belong to the sector* $[\alpha, \beta]$ *with* $0 \le \alpha \le \beta$, *that is,* $\alpha x^2 < x\gamma(x) < \beta x^2$. *Let G be causal, linear-time-invariant and map* $l_2 \to l_2$. *Assume that G has a z transform* $\tilde{g}(z)$ *which is bounded on the unit circle. Suppose that for some* $q \ge 0$, *there is a* $\delta > 0$ *such that*

$$\mathrm{Re}\{\, 1 + q(1 - z^{-1})\,\}\tilde{g}(z) + 1/\beta \ge \delta, \text{ for } z = e^{j\theta},\ 0 \le \theta \le \pi \tag{6.27}$$

If $\alpha > 0$ *and if* $\delta - (q\beta/4\alpha^2) > 0$, *then* $u \in l_2 \Rightarrow e_1, e_2 \in l_2$.

An interpretation of this theorem is that if the linear part is bounded and the maximum slope of the nonlinear part satisfies a test condition, then the internal and output signals will be bounded. The use of Theorem 6.2 requires that the system (6.26) is reformulated as a combination of a linear part and a nonlinear part:

$$\begin{bmatrix} \tilde{\omega}_{k+1} \\ \tilde{\varphi}_{k+1} \end{bmatrix} = G \begin{bmatrix} \tilde{\omega}_k \\ \tilde{\varphi}_k \end{bmatrix} + \gamma\left([0\ \ 1] \begin{bmatrix} \tilde{\omega}_k \\ \tilde{\varphi}_k \end{bmatrix} \right) + w_k, \tag{6.28}$$

where $G = \begin{bmatrix} 1 & -K^{\omega} \\ 1 & 1 - K^{\varphi} \end{bmatrix}$ and $\gamma(x) = x - \sin x$.

Expanding out (6.28) yields

$$\begin{aligned} \tilde{\omega}_{k+1} &= \tilde{\omega}_k - K^{\omega}[(\tilde{\varphi}_k - \sin\tilde{\varphi}_k) - \tilde{\varphi}_k], \\ \tilde{\varphi}_{k+1} &= \tilde{\varphi}_k + \tilde{\omega}_k - K^{\varphi}[(\tilde{\varphi}_k - \sin\tilde{\varphi}_k) - \tilde{\varphi}_k]. \end{aligned} \tag{6.29}$$

Hence the linear part is

$$\begin{aligned} \tilde{\omega}_{k+1} &= \tilde{\omega}_k - K^{\omega}\tilde{\varphi}_k, \\ \tilde{\varphi}_{k+1} &= \tilde{\varphi}_k + \tilde{\omega}_k - K^{\varphi}\tilde{\varphi}_k, \end{aligned} \tag{6.30}$$

from which it follows that

$$\tilde{g}(z) = \frac{K^{\varphi} z + K^{\varphi} + K^{\omega}}{z^2 + (K^{\varphi} - 2)z + K^{\omega} + 1 - K^{\varphi}}. \tag{6.31}$$

The maximum of $\frac{\gamma(x)}{x} = \frac{x - \sin x}{x}$ yields $\beta = 1.217$. Candidate gains may be assessed by checking that $\tilde{g}(z)$ is stable and then applying the condition (6.27). The resulting gain space which ensures the stability of (6.26) is shown in Figure 6.2.

Now the solution to (6.26) also can be written as the sum of a "natural part" due to non zero initial error and the remaining "forced part" due to state noise. (In a linear-time-invariant system for example, the "forced part" of the output is the input process convolved with the impulse response.) Clearly the "forced part" is in l_2 from the passivity argument. Since the "natural part" can be written as a product of the initial conditions and some function of the delta function, clearly the "natural part" is in l_2 . Thus the location of the

(K^{ω}, K^{φ}) within the region of Figure 6.2 is sufficient for (6.26) to be asymptotically stable, independent of initial conditions.

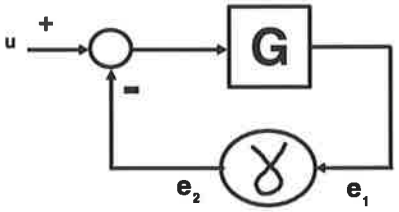

Fig. 6.1. Nonlinear error model.

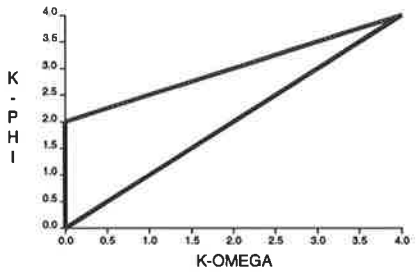

Fig. 6.2. Gain space for stable error.

6.7.2 Harmonic tones.

When multiple harmonic components exist and their amplitudes are known, a suitable state vector is $\boldsymbol{x}_k = [\,\omega_k, \varphi_k^{(1)}, \varphi_k^{(2)}, \ldots, \varphi_k^{(n)}]^T$ in which case

$$A = \begin{bmatrix} 1\,0\,0 & .0 \\ 1\,1\,0 & .0 \\ 2\,0\,1 & .0 \\ \cdots & \cdots \\ n\,0\,0 & .1 \end{bmatrix}. \tag{6.32}$$

It is easily shown that

$$\mathbf{D_k\varepsilon_k} = \begin{bmatrix} \sin \tilde{\varphi}_k^{(1)} \\ \sin \tilde{\varphi}_k^{(2)} \\ \cdot \\ \sin \tilde{\varphi}_k^{(n)} \end{bmatrix}. \tag{6.33}$$

The error system is given by

$$\tilde{x}_{k+1} = A\tilde{x}_k - \boldsymbol{K_k D_k \varepsilon_k}, \tag{6.34}$$

which is indeed similar to (6.26), except that the gain is a $(n+1) \times n$ matrix and the nonlinearity is a n-vector. Therefore it is expected that the discrete-time Popov criterion may be applied to calculate the gain space which ensures that (6.34) is stable. That is, one needs to find the range of gain components for which the linear system is stable and then apply a test condition (arising out of Theorem 6.2).

6.7.3 Continuous-time.

In continuous-time, a single tone signal may be modelled as $\dot{x}(t) = A\,x(t) + w(t)$ where $x(t) = [a(t), \omega(t), \varphi(t)]^T$, $w(t) = [w^{(1)}(t), w^{(2)}(t), w^{(3)}(t)]^T$ and $A = \begin{bmatrix} 0\,0\,0 \\ 0\,0\,0 \\ 0\,1\,0 \end{bmatrix}$. A formulation for the nonlinear observer follows readily from the continuous-time analogy of Section 6.2. In the case of known amplitude and fixed gains the error system is

$$\begin{bmatrix}\dot{\omega}(t)\\ \dot{\varphi}(t)\end{bmatrix}=\begin{bmatrix}0&0\\1&0\end{bmatrix}\begin{bmatrix}\omega(t)\\ \varphi(t)\end{bmatrix}-\begin{bmatrix}K^{\omega}\\ K^{\varphi}\end{bmatrix}\sin\varphi(t)+\ w(t) \tag{6.35}$$

In order to determine the set of gains sufficient for (6.31) to be asymptotically stable, passivity theory may be appealed to. The error system may be formulated as a combination of a linear part and a nonlinear part shown in the configuration of Figure 6.3. The continuous-time Popov criterion [DV] may similarly be used here. It turns out that the linear part is stable for $K^{\varphi}, K^{\omega} > 0$, theorem of [DV, pp. 186-187] is true for the region shown in Figure 6.4, in which case $u, \dot{u}, \in L_2 \Rightarrow y_1, y_2 \in L^2, L^{\infty}$.

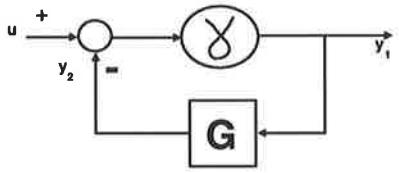

Fig. 6.3 Continuous-time nonlinear error model.

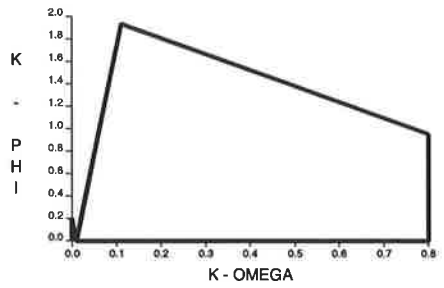

Fig. 6.4. Continuous-time gain space for stable error

6.8 Simulations.

6.8.1 Single tone estimation.

For the single tone estimation problem, the variance of either the nonlinear observer or the EKF frequency estimate can be made arbitrarily small (with a commensurate increase in convergence time) by selecting the state covariances to be suitably small. The approach here is to tune the estimators to give approximately equal transient performance and then look at their asymptotic behaviour. In the case of zero initial conditions, the two methods have been observed to exhibit somewhat different transient behaviour. The nonlinear observer tends to approach the asymptotic value in a mononotonic fashion, the EKF converges in an oscillatory manner. Furthermore, it appears that the EKF initial phase estimate is required to be within about $\pi/4$ of the actual value, otherwise divergent behaviour can result. In contrast, the fake ARE method is observed to converge successfully, irrespective of the initial values. Regarding the problem of estimating a constant tone with zero initial conditions, at an SNR of 5 dB, both estimators are found to exhibit about the same convergence rate and output variance for $\Sigma^{a}= 0.1, \Sigma^{\omega\varphi}= 0.11, \Sigma^{\varphi}= 0.33$ and $\sigma_u^2= 0.1, \sigma_v^2= 0.027, \sigma_w^2= 0.03$. Then the variance of the frequency estimates (with known initial conditions) is examined, for 500 realizations of 1000 data points. In Figure 6.3 the lower and upper bounds of the output variance are plotted. As the SNR is reduced below 5 dB, the EKF upper bound of the variance is seen to increase more rapidly than that of the nonlinear observer (NLO). Thus the fake ARE method can have a better sub-threshold

estimation capability and appears to have some robustness with regard to parameter selection. However the sub-threshold capability occurs at the expense of convergence rate. This is illustrated in Figure 6.4 where the convergence rates are plotted, namely the 1σ limits of the number of data points required until the estimate attains 1/e of the actual value. From (6.17) it clear that the gains reduce with increasing noise variance and, from (6.26), it is seen this results in a decrease in convergence rate.

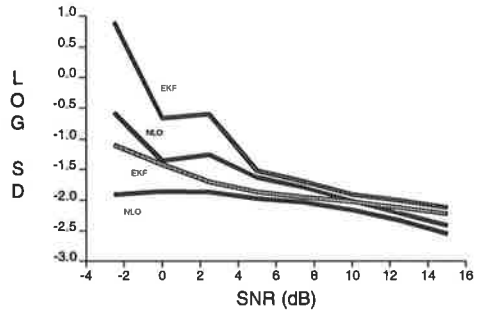

Fig. 6.3. Output variance for tone estimation.

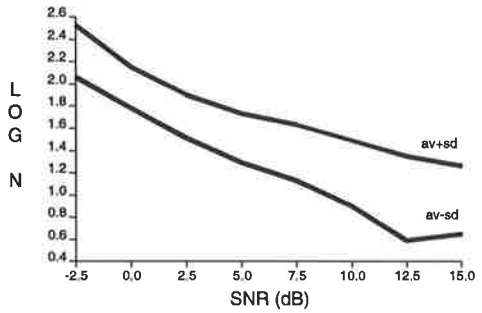

Fig. 6.4. Convergence rate for tone estimation.

6.8.2 Tone estimation during amplitude fade.

A 6 dB cosinusoidal fade is imposed on the amplitude such that the SNR is 10 dB at t=0, t=500 and 4 dB at t=250. The resulting mean square errors for the constant tone estimation problem is shown in Figure 6.5. At the extremes both estimators yield similar performance. However near the peak of the fade the nonlinear observer is seen to exhibit less error. Although the gain in both (6.17) and (6.19) includes the current amplitude estimate, evidently the form of (6.17) is better able to adapt to amplitude variation.

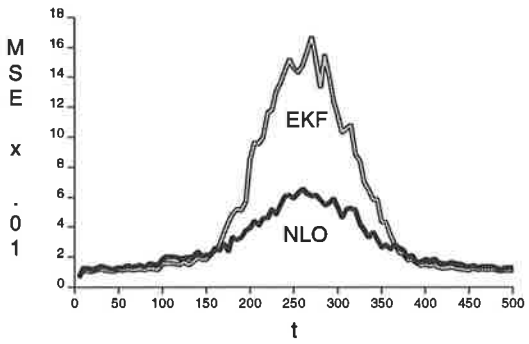

Fig. 6.5. Fade during tone estimation.

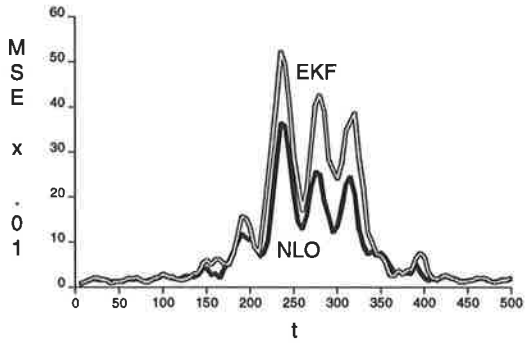

Fig. 6.6. Fade during frequency tracking.

6.8.3 Frequency tracking during amplitude fade.

In the above threshold, constant amplitude, frequency tracking problem, both methods can be tuned in an attempt to optimize mean square error and have been observed to give

approximately equal performance. Therefore the effect of a slow amplitude fade is examined. A 6 dB fade is imposed on the amplitude while tracking a sinusoidal frequency message signal given by 0.5+ 0.5cos 0.079t. The resulting mean square error is shown in Figure 6.6. It can be seen once again, that at the peak of the fade there is some improvement over the EKF. Arguably the use of the nonlinear observer would be advantageous in the presence of amplitude uncertainty, due to say modelling error or interference such as fading. Above threshold (such as t=0, 500,) it is seen that that both methods perform similarly.

6.8.4 Two harmonic components.

Consider a signal comprising two in-phase, unity amplitude, harmonic components with n=1 and n=2 in Section 6.6. With a nominal SNR of 10 dB, the effect of a 20 dB cosinusoidal amplitude fade is examined, so that at t= 0,500 the SNR is 10 dB and at t= 250 the SNR is -10 dB. Both the nonlinear observer and EKF are tuned to have comparable error variance and mean square error at 10 dB SNR. This is accomplished by choosing $\Sigma_a^{(1,2)}$= 0.01, $\Sigma_\varphi^{(1,2)}$= 0.009, $\Sigma_\omega^{(1,2)}$= 0.008, $\Sigma_{\omega\varphi}^{(1,2)}$= 2$E$–5 and $\sigma_a^{2\,(1,2)}$= 0.001, $\sigma_\varphi^{2\,(1,2)}$= 1$E$–6, $\sigma_\omega^{2\,(1,2)}$= 2.5E–9. The state vectors were initialised with the correct values and both filters were run for a hundred data points at 10 dB SNR, prior to each fade. The NLO and EKF fundamental frequency estimates for one typical realisation is shown in Figure 6.7. It can be seen that compared to the EKF, the NLO estimate does not deviate as far from the nominal frequency. Furthermore the NLO frequency estimate appears to exhibit less variation during the peak of the fade. Evidently the NLO has comparatively less gain near the peak of the fade and is better able to smooth out the noise.

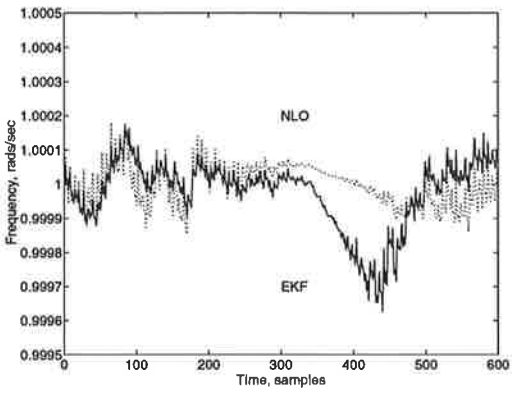

Fig. 6.7. Frequency track during amplitude fade.

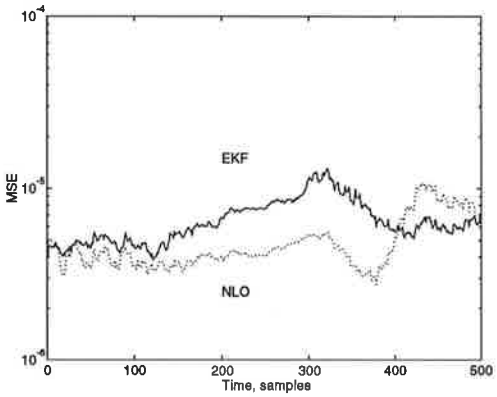

Fig. 6.8. MSE during amplitude fade.

The resulting MSE of the fundamental frequency estimate over 100 realizations, each of 500 points is shown in Figure 6.8. It can be seen that at the peak of the fade, the gain of the NLO is a minimum with the result that the mean square error is about 3 dB less than for the EKF. The NLO is seen to be slower to recover from the fade since it exhibits about

2 dB higher mean square error in the vicinity of t= 450. It is possible to obtain some improvement in MSE by rejecting outliers in the frequency estimates [AP,PA]. However this was not found to alter the fade recovery problem exhibited by the NLO, around 20% of the time. One possible solution is to reinitialise the NLO after a fade has been detected.

6.8.5 Non-harmonic Components.

Consider the problem of estimating two in-phase, unity amplitude tones with constant angular frequencies of $\omega^{(1)}$= 1 and $\omega^{(2)}$= 1.2. By way of an example, the nominal SNR is set to 10 dB and a 15 dB cosinusoidal fade is imposed. With the choices $\Sigma_a^{(1,2)}$= 0.02, $\Sigma_\varphi^{(1,2)}$= 0.006, $\Sigma_\omega^{(1,2)}$= 0.01, $\Sigma_{\omega\varphi}^{(1,2)}$= 5$E$–5, $\sigma_a^{2\,(1,2)}$= 0.001, $\sigma_\varphi^{2\,(1,2)}$= 1$E$–6, $\sigma_\omega^{2\,(1,2)}$= 2.5E–8, both estimators where found to exhibit similar performance in the absence of a fade. The average of the mean square error of the two frequency estimates, calculated over 100 realizations, is shown in Figure 6.9. Once again it is seen that the NLO exhibits dramatically less error during the fade but performs comparatively poorly immediately afterwards.

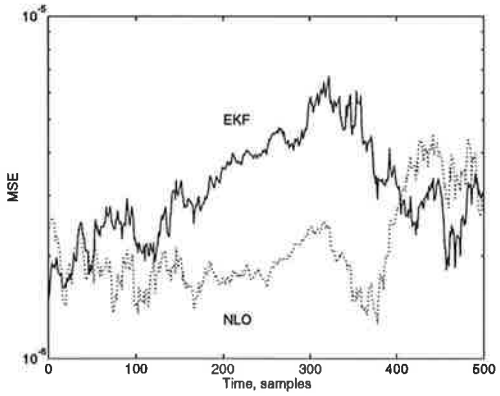

Fig. 6.9. Two tone estimation during a fade.

6.9 Conclusions.

The chapter has introduced the problems of frequency and phase demodulation. Typically the amplitudes, frequencies and phases evolve from linear models, but the in-phase and quadrature observations are nonlinear, requiring the application of nonlinear filters. The conventional solution to the frequency or phase demodulation problem is the EKF. When more than one signal component is present, the resultant filters are akin to a number of coupled phase-locked loops, each simultaneously tracking the frequencies and phases of the individual signal components. The contribution of this chapter is the application of the fake ARE technique in the development of a nonlinear observer and the performance comparisons with the EKF.

The nonlinear observer developed herein is novel in the following respects:

- The manner by which the amplitude estimates adjust the estimator gain term which

differs somewhat from the usual EKF approach. An interpretation from (6.18) is that the nonlinear observer possesses some form of automatic gain control.

- In the single tone known amplitude case, the gain space which yields an asymptotically stable error system has been identified (see Figure 6.2).
- In the known amplitude, multiple harmonic case, in view of the error system (6.34) it is contended that similar procedure applies for the calculation of the gain space which ensures error stability.

It is claimed that compared to the EKF, the nonlinear observer exhibits the following advantages

- Improved robustness to initial conditions.
- Sub-threshold tracking capability (see Figure 6.3), albeit at the expense of convergence rate.
- Improved robustness to amplitude uncertainty (see Figures 6.5 to 6.9).

A disadvantage of the nonlinear observer is that it adapts poorly immediately after a fade. A few possible remedies are mentioned here, but further investigations have not yet been carried out. One possible solution is to reinitialise the error covariance after a fade has been detected. Alternatively the stable gain space could be precalculated which could be used to censure the gains. For convenience block diagonal solutions have been assumed for the fake ARE. It is expected that performance improvements may be realised if off-diagonal terms were included to account for coupling between the signal components.

REFERENCES

[AM] Anderson, B. D. O. and J. B. Moore, *Optimal Filtering*, Prentice Hall, Englewood Cliffs, NJ, 1979.

[AP] Anderson, B. D. O. and P. P. Parker, "Frequency Tracking of Periodic Signals in Noise", *Aust. Symp. Signal Processing and Applications*, Adelaide Australia, pp. 263-267, 1989.

[BG] Bitmead, R. R. and M. Gevers, Riccati difference and differential equations: convergence, monotonicity and stability, in: S. Bittanti, A. J. Laub, J. C. Willems, Eds., *The Riccati Equation*, Springer Verlag, ch. 10.8.1, 1991.

[BGW] Bitmead, R. R., M. Gevers and V. Wertz, *Adaptive optimal control*, Prentice Hall, Sydney, pp. 86-87, 1990.

[BTP] Bitmead, R. R., A.-C. Tsoi and P. J. Parker, "Kalman Filtering Approach to Short Time Fourier Analysis", *IEEE Trans. Acoustics, Speech and Signal Processing*, v. 34, no. 6, pp. 1493-1501, 1986.

[DV] C. A. Desoer and M. Vidyasagar, *Feedback Systems : Input - Output Properties*, Academic Press, N.Y., 1975.

[EW1] Einicke, G. A. and L.B. White, "Estimation of Frequency and Phase Modulated Signals Using Fake Algebraic Riccati Techniques", *Proc. 3rd ISSPA*, Gold Coast, Australia, vol. 2, pp. 339-343, 1992.

[EW2] Einicke, G. A. and L. B. White, "A class of nonlinear filters for periodic signals", *IEEE Int. Symp. CAS*, Chicago, IL, vol. 1, pp. 144-147, May 1993.

[PA] Parker, P. P. and B.D.O. Anderson, "Frequency Tracking of Nonsinsoidal Periodic Signals in Noise", *Signal Processing*, Vol. 20, pp. 127-152, 1990.

[PBG] Poubelle, M. -A., R. R. Bitmead, M. Gevers, "Fake Algebraic Riccati Techniques and Stability", *IEEE Trans. Automatic Contr.*, vol. 33, pp. 379-381, 1988.

[S] Snyder, D. L., *The State-Variable Approach to Continuous Estimation with Applications to Analog Communications Theory*, Cambridge, MA., MIT Press, 1969.

Chapter 7

The extended H_∞ filter

This chapter describes a new approach to make the extended Kalman filter (EKF) robust to linearisation errors. The problem is motivated in Section 7.1 and the EKF is described in Section 7.2. The robust EKF, dubbed *the extended H_∞ filter*, is introduced in Section 7.3 and the results of simulation studies are presented in Section 7.4. A continuous-time formulation is proposed in Section 7.5. An extension to plants possessing nonzero direct feedthrough terms is detailed in Section 7.6.

7.1 Motivation.

The use of the EKF is heavily entrenched in nonlinear signal processing applications. Well known applications include navigation and system identification, see [HA,CCC] for example. Despite the fact that the EKF has been in use for decades, some understanding of its tracking performance has only reported recently [LB]. The EKF works well when the measurement noise is negligible and the underlying (known) signal model is almost linear. Otherwise the EKF is suboptimal [AM]. There are two sources of error:

- imperfect linearisation, which is compounded by
- measurement noise.

The EKF depends upon the solution of a RDE having the form

$$\Sigma_{k+1} = A_k\Sigma_k A_k^T - A_k\Sigma_k C_k^T(C_k\Sigma_k C_k^T + R)^{-1}C_k\Sigma_k A_k^T + B_k Q B_k^T, \tag{7.1}$$

where A_k, B_k, C_k are state estimate dependent. It has been shown in Chapter 6 that, compared to the EKF, the fake ARE technique can be advantageous when the nonlinearity is confined to the output mapping and the SNR is low. The fake ARE technique can offer error stability by masquerading (7.1) as a fake ARE in which the elements of Q are regarded

as tuning parameters. It is argued in [LB] that the elements of Q in (7.1) may also be tuned: if Q is too small than this can lead to filter divergence, whereas if Q satisfies some sufficient conditions, then the errors of the EKF remain bounded.

The technique described in this chapter does have some connections to [LB], namely there is (amongst other things) a tampering of the Q and the worst case performance is bounded provided that some sufficient conditions are satisfied. The solution described here is motivated by recognising that imperfect linearisation is a modelling error problem, which may be accommodated via the use of H_∞ techniques.

The EKF is derived via a linearisation procedure which is presented in [AM]. Briefly, the nonlinear model describing the measurements is successively linearised about each current state estimate and the (linear) Kalman filter is then applied to produce the next state estimate. Suboptimal behaviour can arise when there are large deviations of the estimated state trajectory from the nominal trajectory. In this case, the nonlinear signal model is less accurately approximated by the Taylor series expansion about the conditional mean and the higher order terms become more significant. However in the EKF, the higher order terms are ignored. Instead of neglecting the higher order terms of the Taylor series expansions, they may be regarded as model uncertainties which are functions of the state estimation error and the exogenous inputs and are assumed to have bounded H_∞ norm. This approach naturally leads to a minimax estimation problem which can be treated using standard H_∞ methods of chapters 3 and 4. The chosen norm bounds cannot in general be precomputed, so are regarded as "tuning" parameters for the resulting filter. The choice of zero as the norm bound results in the standard EKF.

A conventional approach that attempts to mitigate against linearisation errors is the *second order EKF* [SM,G]. This filter arises by retaining second order terms of the Taylor series expansions of the plant parameters about the conditional mean. Another approach is the *iterated filter* where the EKF recursions are iterated at each observation until it is deemed that better estimates have been obtained [SM,Ja,G]. Both of these methods increase the computational overhead, whereas the procedure outlined herein does not.

An approach which seeks to improve low SNR EKF performance via smoothing is set out in Appendix H. Briefly, the smoother arises by combining estimates from a forward and adjoint EKF. Although it is possible to frame the problem of Appendix H in a H_∞ framework, at this stage, applications where this may be advantageous are not known.

The use of H_∞ techiques to solve nonlinear problems is certainly not novel, see [V,J,GT] for example. The work described in this chapter has been published in [EW,EW2] and is claimed to be the first account of making an EKF robust to linearisation errors via the use of the linear H_∞ methods.

7.2 The extended Kalman filter.

Consider an output estimation problem (where $G_1 = G_2$ in Figure 3.2) and suppose that plants are nonlinear and the observations may be modelled by

$$\begin{aligned} x_{k+1} &= a_k(x_k) + b_k(x_k)w_k, \\ y_k &= c_k(x_k) + v_k, \end{aligned} \tag{7.2}$$

where $x_k \in \mathbf{R}^N$, $w_k \in \mathbf{R}^M$, $z_k, v_k \in \mathbf{R}^P$, a, b, and c are sufficiently smooth functions of appropriate dimension; w_k and v_k are uncorrelated, zero mean, white noise processes having covariances Q and R respectively. The objective is to arrive at a causal filter that produces approximate conditional mean estimates of x_k given measurements of z_k. The nonlinear functions a, b and c can be expanded in Taylor series about the filtered and predicted estimates $\hat{x}_{k/k}$ and $\hat{x}_{k/k-1}$ as

$$\begin{aligned} a_k(x_k) &= a_k(\hat{x}_{k/k}) + Da_k(\hat{x}_{k/k})(x_k - \hat{x}_{k/k}) + \Delta_1(x_k - \hat{x}_{k/k}), \\ b_k(x_k) &= b_k(\hat{x}_{k/k}) + \Delta_2(x_k - \hat{x}_{k/k}), \\ c_k(x_k) &= c_k(\hat{x}_{k/k-1}) + Dc_k(\hat{x}_{k/k-1})(x_k - \hat{x}_{k/k-1}) + \Delta_3(x_k - \hat{x}_{k/k-1}), \end{aligned} \tag{7.3}$$

where D denotes the derivative. Here, Δ_i, $i = 1,2,3$ are assumed to be continuous operators from $l_2 \to l_2$ with induced norms bounded by δ_i respectively. The Δ_i represent the higher order terms of the Taylor series expansions which have not been explicitly included in the formulation of the EKF. Denoting the filter state error $x_k - \hat{x}_{k/k}$ by $\tilde{x}_{k/k}$ and the predictor state error $x_k - \hat{x}_{k/k-1}$ by $\tilde{x}_{k/k-1}$ and substituting (7.3) into (7.2) gives (at time k)

$$\begin{aligned} x_{k+1} &= A_k x_k + B_k w_k + p_k + \Delta_1(\tilde{x}_{k/k}) + \Delta_2(\tilde{x}_{k/k})w_k, \\ y_k &= C_k x_k + v_k + q_k + \Delta_3(\tilde{x}_{k/k-1}), \end{aligned} \tag{7.4}$$

where $A_k = Da_k(\hat{x}_{k/k})$, $B_k = b_k(\hat{x}_{k/k})$, $C_k = Dc_k(\hat{x}_{k/k-1})$, the known inputs are $p_k = a_k(\hat{x}_{k/k}) - A_k\hat{x}_{k/k}$ and $q_k = c_k(\hat{x}_{k/k-1}) - C_k\hat{x}_{k/k-1}$. The EKF arises by determining the Kalman filter for the linearised problem (7.4) with the higher order terms (namely the Δ_i) set to zero. The linearised problem is depicted in Figure 7.1.

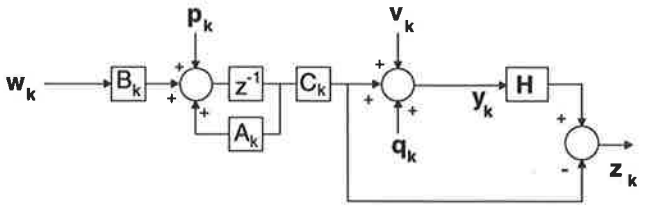

Fig. 7.1. The linearised filtering problem.

The resulting equations in predictor-corrector form are as follows. The corrector part is

$$\begin{aligned} \hat{x}_{k/k} &= \hat{x}_{k/k-1} + L_k(y_k - c_k(\hat{x}_{k/k-1})), \\ L_k &= \Sigma_{k/k-1} C_k (C_k^T \Sigma_{k/k-1} C_k + R_k)^{-1}, \\ \Sigma_{k/k} &= \Sigma_{k/k-1} - L_k C_k^T \Sigma_{k/k-1}. \end{aligned} \tag{7.5}$$

The predictor part is

$$\begin{aligned} \hat{x}_{k+1/k} &= a_k(\hat{x}_{k/k}), \\ \Sigma_{k+1/k} &= A_k \Sigma_{k/k} A_k^T + B_k Q_k B_k^T. \end{aligned} \tag{7.6}$$

These iterations need to be suitably initialised at $k = 0$.

7.3 An evolution of the extended H_∞ filter.

The EKF arises by applying the Kalman filter for deterministic inputs to the linearised signal model (7.4). In order to proceed similarly with a H_∞ design, the filter structure for deterministic inputs is required, this is established via a linearity argument.

Proposition 7.1 *Consider the linear signal model and observation with deterministic inputs p_k and q_k*

$$\begin{aligned} x'_{k+1} &= A_k x'_k + B_k w_k + p_k, \\ y'_k &= C_k x'_k + v_k + q_k. \end{aligned} \tag{7.7}$$

Suppose that there exists a linear filter corresponding to (7.7) where the gain K_k is determined in some optimal way and the update for the state estimate is given by

$$\hat{x}'_{k+1} = A_k \hat{x}'_k + p_k + K_t(y'_k - C_k \hat{x}'_k - q_k). \tag{7.8}$$

Then from identical initial conditions, the state errors arising from (7.7) and (7.8) are the same as for the case when $p_k = q_k = 0$.

Proof. From (7.7) and (7.8) the state error is

$$\tilde{x}'_k = x'_k - \hat{x}'_k = A_k x'_k + B_k w_k - A_k \hat{x}'_k - K_k(C_k x'_k + v_k - C_k \hat{x}'_k),$$

which is the same as is obtained when $p_k = q_k = 0$. ∇

Thus if a signal model has deterministic inputs p_k and q_k in the state and observation updates respectively, then the H_∞ filter has the same structure as the corresponding Kalman filter.

Now the nonlinear output estimation problem of Section 7.2 may be addressed. Denote the inputs by $d_k = \begin{bmatrix} v_k \\ w_k \end{bmatrix}$. The objective is to design a filter that produces a state estimate $\hat{x}_k$ from the noisy observations $y_k = c_k(x_k) + v_k$ such that the state error $\tilde{x}_k = \hat{x}_k - x_k$ satisifies

$$\|\tilde{x}_k\|^2 \leq \gamma^2(\sigma_w^{-2}\|w_k\|^2 + \sigma_v^{-2}\|v_k\|^2), \tag{7.9}$$

for all uncertainties Δ_1, Δ_2 and Δ_3 satisfying their respective norm bounds. The approach here is to accommodate the uncertainties via the two part procedure described in Section 3.4. Firstly, the inputs and outputs of the uncertainties may be regarded as inputs and outputs to an auxiliary H_∞ problem. Secondly, the multiple output problem may be converted into a single output problem by appropriately scaling the inputs. Consider the auxiliary problem defined by

$$\begin{aligned} x_{k+1} &= A_k x_k + B_k w_k + p_k + s_k, \\ \tilde{x}_k &= \hat{x}_k - x_k, \\ y_k &= C_k x_k + v_k + q_k + t_k, \end{aligned} \tag{7.10}$$

where $B_k s_k = \Delta_1(\tilde{x}_{k/k}) + \Delta_2(\tilde{x}_{k/k}) w_k$ and $t_k = \Delta_3(\tilde{x}_{k/k})$ are additional inputs satisfying

$$\|s_k\|^2 \leq \beta_1^2 \|\tilde{x}_{k/k}\|^2 + \beta_2^2 \|w_k\|^2, \tag{7.11}$$

$$\|t_k\|^2 \leq \delta_3^2 \|\tilde{x}_{k/k}\|^2 \leq \delta_3^2 \|\tilde{x}_{k/k-1}\|^2. \tag{7.12}$$

A sufficient solution to this auxiliary problem arises by scaling the inputs as shown in Figure 7.2.

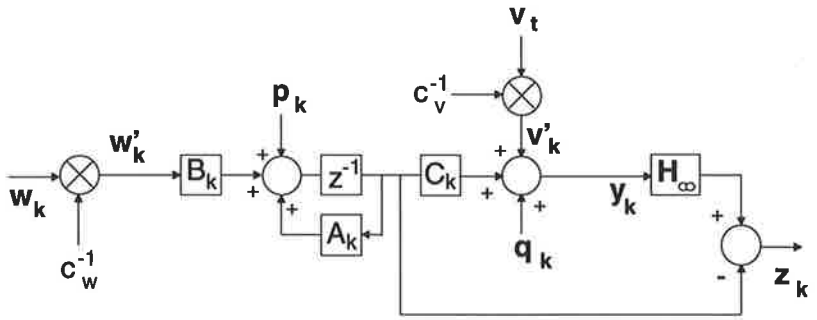

Fig. 7.2. A scaled auxiliary filtering problem.

Lemma 7.2. *The solution of the scaled auxiliary H_∞ optimisation problem shown in Figure 7.2, where v_t is scaled by*

$$c_v^2 = 1 - \gamma^2 \beta_1^2 - \gamma^2 \delta_3^2 \tag{7.13}$$

and w_t is scaled by

$$c_w^2 = c_v^2 (1 + \beta_2^2)^{-1}, \tag{7.14}$$

is sufficient for the solution of the auxiliary H_∞ optimisation problem (7.10) which possesses the additional inputs $B_k s_k$ and t_k.

Proof. If the H_∞ problem (7.10) has been solved then a γ has been found such that

$$\begin{aligned}
\|\tilde{x}_k\|^2 &\le \gamma^2(\|w_k\|^2 + \|s_k\|^2 + \|t_k\|^2 + \|v_k\|^2) \\
&\le \gamma^2(\|w_k\|^2 + \beta_1^2\|\tilde{x}_k\|^2 + \beta_2^2\|w_k\|^2 + \delta_3^2\|\tilde{x}_k\|^2 + \|v_k\|^2) \\
\Rightarrow \quad & (1 - \gamma^2\beta_1^2 - \gamma^2\delta_3^2)\|\tilde{x}_k\|^2 \le \gamma^2((1 + \beta_2^2)\|w_k\|^2 + \|v_k\|^2) \\
\Rightarrow & \|\tilde{x}_k\|^2 \le \gamma^2(c_w^{-2}\|w_k\|^2 + c_v^{-2}\|v_k\|^2) \quad \nabla.
\end{aligned}$$

The resulting extended H_∞ filter arises by applying the discrete-time H_∞ filter (of Section 4.2) to the problem (7.10) and may be written in predictor-corrector form as follows. The corrector part is

$$\begin{aligned}
\hat{x}_{k/k} &= \hat{x}_{k/k-1} + L_k(y_k - c_t(\hat{x}_{k/k-1})), \\
\hat{x}_{k+1/k} &= a(\hat{x}_{k/k}), \\
L_k &= \Sigma_{k/k-1}C_k^T(C_k\Sigma_{k/k-1}C_k^T + R)^{-1}, \\
\Sigma_{k/k} &= \Sigma_{k/k-1} - \Sigma_{k/k-1}\begin{bmatrix} -C_k^T \\ C_k^T \end{bmatrix}\begin{bmatrix} C_k\Sigma_{k/k-1}C_k^T - \gamma^2 I & -C\Sigma_{k/k-1}C_k^T \\ -C_k\Sigma_{k/k-1}C_k^T & C\Sigma_{k/k-1}C_2^T + R_k \end{bmatrix}^{-1}[-C_k \;\; C_k]\Sigma_{k/k-1},
\end{aligned} \tag{7.15}$$

The predictor part is

$$\begin{aligned}
\hat{x}_{k+1/t} &= a_k(\hat{x}_{k/k}), \\
\Sigma_{k+1/k} &= A_k\Sigma_{k/k}A_k^T + B_kQ_kB_k^T.
\end{aligned} \tag{7.16}$$

Proposition 7.3. *When the state error is negligibly small and the process noise power is small, then at $\gamma = \infty$, the extended H_∞ filter reverts to the EKF.*

Proof. The approximations in the EKF are reasonable when the state error is small (so that $\Delta_1(\tilde{x}_{k/k}) \approx 0$ and $\Delta_3(\tilde{x}_{k/k-1}) \approx 0$) and the process noise power is small (so that $\Delta_2(\tilde{x}_{k/k})w_k \approx 0$). Thus for the linearised signal model, with $\beta_1 = \beta_2 = \delta_3 = 0$ in (7.12, 7.13), the extended H_∞ filter (7.14, 7.15) is simply the linear H_∞ filter which reverts to the Kalman filter at $\gamma = \infty$. ∇

Remark The above scaling arises out of a sufficient rather than a necessary condition. The design may be too conservative and it is prudent to explore the merits of using values for β_1, β_2 and δ_3 less than the norm bounds on the respective model uncertainties. The use of the optimal γ can also be too conservative - too much emphasis may be placed in accommodating the worst case input conditions at the cost of MSE. It can be advantageous to choose a γ greater than optimal and realise a compromise between MSE and H_∞ error performance.

7.4 Extensions to nonlinear plant feedthroughs.

Suppose that the observations may be modelled by

$$\begin{aligned}
x_{k+1} &= a_k(x_k) + b_k(x_k)w_k, \\
y_k &= c_k(x_k) + d_k(x_k)w_k + v_k,
\end{aligned} \tag{7.17}$$

where $d_k(x_k)$ is a nonlinear direct feedthrough function which may be expanded in a Taylor series about the predicted estimate as

$$d_k(x_k) = d_k(\hat{x}_{k/k-1}) + \Delta_4(x_k - \hat{x}_{k/k-1}). \tag{7.18}$$

Substituting (7.3) and (7.18) into (7.17) yields the linearised system

$$\begin{aligned} x_{k+1} &= A_k x_k + B_k w_k + p_k + \Delta_1(\tilde{x}_{k/k}) + \Delta_2(\tilde{x}_{k/k})w_k, \\ y_k &= C_k x_k + D_k w_k + v_k + q_k + \Delta_3(\tilde{x}_{k/k-1}) + \Delta_4(\tilde{x}_{k/k-1})w_k, \end{aligned} \tag{7.19}$$

where $D_k = d_k(\hat{x}_{k/k-1})$. The EKF corresponding to (7.17) arises by determining the Kalman filter for (7.19) with the Δ_i set to zero. The predictor step comes about by substituting for p_k and q_k into (D.24) which gives

$$\hat{x}_{k+1/k} = a(\hat{x}_{k/k}) + B_k Q_k D_k^T \bar{R}_k^{-1}(y_k - c_k(\hat{x}_{k/k})), \tag{7.20}$$

where $\bar{R}_k = R_k + D_k Q_k D_k^T$. It is easily shown [AM, (5.12), p. 117] that the approximate error covariance prediction is given by

$$\Sigma_{k+1/k} = (A_k - B_k Q_k D_k \bar{R}_k^{-1} C_k)\Sigma_{k/k}(A_k - B_k Q_k D_k \bar{R}_k^{-1} C_k)^T + B_k(Q_k - B_k Q_k \bar{R}_k^{-1} Q_k B_k^T)B_k^T. \tag{7.21}$$

The corrector step is unchanged viz.

$$\begin{aligned} \hat{x}_{k/k} &= \hat{x}_{k/k-1} + L_k(y_k - c(\hat{c}_{k/k})), \\ \Sigma_{k/k} &= \Sigma_{k/k-1} - L_k C_k^T \Sigma_{k/k-1}. \end{aligned} \tag{7.22}$$

The filter output similarly follows from (D.25), ie.

$$u_k = c(\hat{x}_{k/k}) + D_k Q_k D_k^T \bar{R}_k^{-1}(y_k - c_k(\hat{x}_{k/k})). \tag{7.23}$$

An extended H_∞ filter for the problem of (7.17) may be constructed by approximating (7.19) by an auxiliary problem defined by

$$\begin{aligned} x_{k+1} &= A_k x_k + B_k w_k + p_k + s_k, \\ z_k &= \hat{x}_k - x_k, \\ y_k &= C_k x_k + D_k w_k + v_k + q_k + t_k, \end{aligned} \tag{7.24}$$

where t_k is an additional input satisfying

$$\|t_k\|^2 \leq \beta_3^2 \|\tilde{x}_{k/k}\|^2 + \beta_4^2 \|w_k\|^2. \tag{7.25}$$

Lemma 7.4. *The solution of a scaled auxiliary H_∞ optimisation problem in which v_k is scaled by*

$$c_v^2 = 1 - \gamma^2\beta_1^2 - \gamma^2\beta_3^2, \tag{7.26}$$

and w_k is scaled by

$$c_w^2 = c_n^2(1 + \beta_2^2 + \beta_4^2)^{-1}, \tag{7.27}$$

is sufficient for the solution of the auxiliary H_∞ optimisation problem (7.24) which possesses the additional inputs s_k and v_k.

Proof. Same as proof for Lemma 7.2 using (7.25) instead of (7.12).

Thus one possible way of accommodating nonlinear direct feedthrough functions is to apply the scalings of (7.26) and (7.27) in which β_1, β_2, β_3, β_4 and γ are tuning parameters that need to be found.

7.5 Signal demodulation examples.

The purpose of this section is to show how the extended H_∞ filter may be applied and to illustrate that benefits can arise when the problems are sufficiently nonlinear.

Example 7.1. The EKF is commonly applied to demodulate frequency modulated (FM) signals [SM]. For this application the signal is usually modelled such that the signal nonlinearity is present only in the output mapping. Here the pure integrator within the signal models of Chapter 6 is replaced with a saturating nonlinearity in an endeavour to better approximate some practical systems. The FM model is given by (7.28). When σ_w^2 is small, the model output is an FM signal. Alternatively when σ_w^2 is sufficiently large, the model output resembles a phase shift keyed (PSK) signal.

$$\begin{aligned} \omega_{k+1} &= \mu\omega_k + w_k, \\ \varphi_{k+1} &= \arctan(\lambda\varphi_k + \omega_k), \\ y_k^{(1)} &= \cos\varphi_k + v_k^{(1)}, \\ y_k^{(2)} &= \sin\varphi_k + v_k^{(2)}. \end{aligned} \tag{7.28}$$

The objective is to estimate the frequency message ω_k, from the noisy in-phase and quadrature observations $y_k^{(1)}$ and $y_k^{(2)}$. A conventional EKF solution arises via (7.5,7.6) in which the choice $x_k = \begin{bmatrix} \varphi_k \\ \omega_k \end{bmatrix}$ yields $a_k(\hat{x}_k) = \begin{bmatrix} \arctan(\lambda\hat{\varphi}_k + \hat{\omega}_k) \\ \mu\hat{\omega}_k \end{bmatrix}$, $C_k(\hat{x}_k) = \begin{bmatrix} \cos(\hat{\varphi}_k) & 0 \\ \sin(\hat{\varphi}_k) & 0 \end{bmatrix}$, $A_k = \begin{bmatrix} \dfrac{\lambda}{(\lambda\varphi_k + \omega_k)^2 + 1} & \dfrac{1}{(\lambda\varphi_k + \omega_k)^2 + 1} \\ 0 & \mu \end{bmatrix}$ and $C_k(\hat{x}_k) = \begin{bmatrix} -\sin(\hat{\varphi}_k) & 0 \\ \cos(\hat{\varphi}_k) & 0 \end{bmatrix}$. This EKF attempts a full state reconstruction. In contrast with the extended H_∞ filter (EH$_\infty$F), particular states can be specified to satisfy the optimality criterion (7.9). Here it is appropriate to define the augmented blocks $\overline{B} = \begin{bmatrix} 0 & 0 & 0 \\ 0 & c_w\sigma_w & 0 \end{bmatrix}$, $\overline{C} = \begin{bmatrix} C_1 \\ C_k(\hat{x}_k) \end{bmatrix}$, $\overline{D} = \begin{bmatrix} 0 & 0 & 1 \\ c_v\sigma_v & 0 & 0 \\ 0 & c_v\sigma_v & 0 \end{bmatrix}$ in which $C_1 = \begin{bmatrix} 0 & 0 \\ -1 & -1 \end{bmatrix}$. The RDE (4.14) may be written in predictor-corrector form as

$$\begin{aligned} \Sigma_{k/k} &= \Sigma_{k/k-1} - \Sigma_{k/k-1}\overline{C}^T S^{-1}\overline{C}\Sigma_{k/k-1}, \\ \Sigma_{k+1/k} &= A_k\Sigma_{k/k}A_k^T + \overline{B}J\overline{B}^T \end{aligned} \tag{7.29}$$

and, the filter gain is calculated as $K_k = \Sigma_{k/k-1} C_k^T S_3^{-1}$, where S_3 is the (2,2) partition of $S = \overline{D} J \overline{D}^T + \overline{C} \Sigma_{k/k-1} \overline{C}^T$ in which $J_{32} = \begin{bmatrix} I_3 & 0 \\ 0 & \gamma^2 I_2 \end{bmatrix}$.

Simulations were conducted with $\mu = 0.9$, $\lambda = 0.99$ and $\sigma_v^2 = 0.0032$. For $\sigma_w < 0.1$, where the state behaviour is quite linear, the tuning of the extended H_∞ filter (EH$_\infty$F) parameters was not found to result in a performance benefit compared to the EKF. In this case the use of the fake ARE has previously been found to be advantageous. However when $\sigma_w^2 = 1$, the state behaviour is substantially nonlinear, then the EH$_\infty$F may offer some robustness to linearisation errors which can plague the EKF. A robust design was implemented using $\beta_1 = 0.03$, $\beta_2 = 5.3$ and $\delta_3 = 0.001$. It was found that $\gamma = 1.42$ is sufficient for Σ_k of (7.16) to be always positive definite. A histogram of the mean square error in the frequency estimate is shown in Figure 7.3. Although both filters were observed to yield frequency outliers, those of the EKF, while infrequent, are seen to be more severe. For 1000 realisations of 1000 data points each, the EKF is observed to produces outliers which are up to 8.1 dB worse than the EH$_\infty$F. Thus the H_∞ design provides some robustness to outliers, there is a price however - from Figure 7.3 it is seen that the EKF is better on average. Here the MSE exhibited by the EH$_\infty$F is 0.2 dB worse than the EKF.

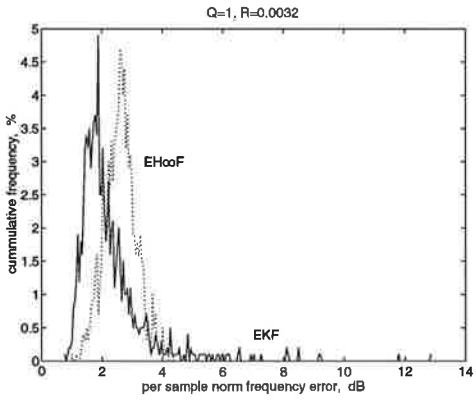

Fig. 7.3. Error histogram for Example 7.1.

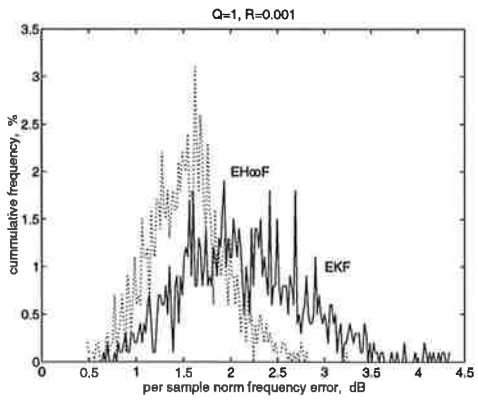

Fig. 7.4. Error histogram for Example 7.2.

Example 7.2. The SNR is increased from 25 dB to 30 dB and a robust design was implemented using $\beta_1 = 0.1$, $\beta_2 = 4.5$, $\delta_3 = 0.001$ and $\gamma = 1.38$. A histogram of the frequency estimation errors is shown in Figure 7.3 and it appears that the robust design is more advantageous at higher SNRs. Compared to the EKF, the EH$_\infty$F is observed to exhibit a reduction in worst case error and MSE of 1.1 dB and 0.5 dB respectively.

Example 7.3. As the problem becomes more nonlinear, there is a commensurate increase in linearisation errors. This is demonstrated by the choice of $\sigma_w^2 = 100$, $\sigma_v^2 = 0.001$, whereupon the output of the model (7.28) resembles a phase shift keyed (PSK) signal. The error histograms corresponding to $\sigma_v^2 = 0.001$, $\beta_1 = 0.19$, $\beta_2 = 5$ and $\gamma = 8.5$ are shown in

Figure 7.4. It can be seen that while both filters suffer from increased linearisation errors, the worst case errors for the $EH_\infty F$ can be constrained by a suitable choice of tuning parameters. Here the $EH_\infty F$ is seen to exhibit an improvement of 5 dB and 6.4 dB in MSE and peak error respectively.

Evidently when the EKF works reasonably well, the robust design offers only a slight improvement in MSE (as in Example 7.2) or a slight degradation (as in Example 7.1). However when the problem is more nonlinear (as in Example 7.3) so that the linearisation is less successful, then there is a greater opportunity to realise an advantage with the $EH_\infty F$.

Example 7.4. If the nonlinearity operates only on frequency, ie.

$$\begin{aligned} \omega_{k+1} &= \mu\omega_k + v_k, \\ \varphi_{k+1} &= \nu\varphi_k + {}^{2k}/_{\pi}\, arctan\, \lambda\omega_k + w_k, \end{aligned} \tag{7.29}$$

then the model output can resemble a frequency shift keyed (FSK) signal. It is claimed that a robust demodulator based on (7.29) can sometimes provide a performance improvement compared to a conventional FSK demodulator based on the model

$$\begin{aligned} \omega_{k+1} &= \mu\omega_k + v_k, \\ \varphi_{k+1} &= \nu\varphi_k + \omega_k + w_k. \end{aligned} \tag{7.30}$$

Suppose that the ω_k data is an i.i.d. binary sequence and that a limiter exists to quantise the output of the demodulator as depicted in Figure 2.8. For the case of $\sigma_v^2 = 0.32$, $\omega_k = \{\pm 0.3\}$, it was found that the choice $Q = \begin{bmatrix} 0.1 & 0.07 \\ 0.07 & 0.6 \end{bmatrix}$ ensures that an EKF based on (7.30) attains close to the minimum possible MSE. Similarly a $EH_\infty F$ based on (7.29) is defined by $Q = \begin{bmatrix} 0.5 & 0.01 \\ 0.01 & 0.1 \end{bmatrix}$, $\beta_1 = 0.04$, $\beta_2 = 1$, $\delta_3 = 0.001$, $k = 0.8$ and $\gamma = 0.95$. The results of simulations are shown in Figure 7.6 and it is seen that the $EH_\infty F$ reduces the mean BER by about 0.15 dB and the peak BER by 0.14 dB.

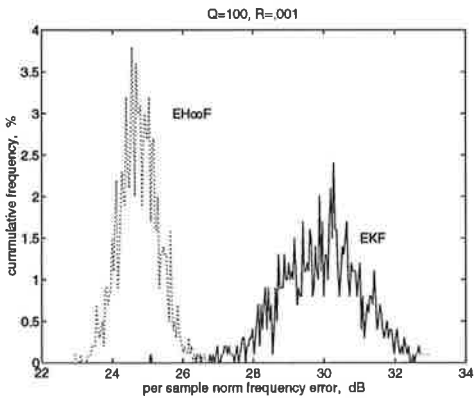

Fig. 7.5. Error histogram for Example 7.3.

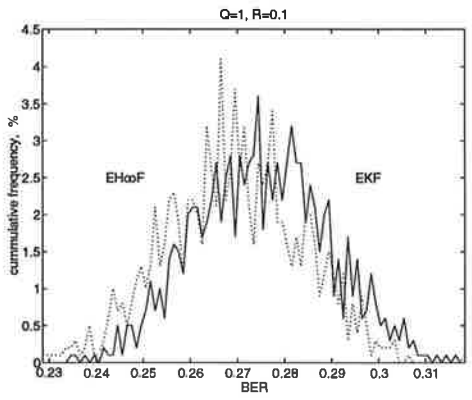

Fig. 7.6. Error histogram for Example 7.4.

Example 7.5. In respect of high SNR, linear equalisation problems (see Sections 5.3 and 5.4), the Kalman solution inverts the channel when the channel zeros are causal, whereas it is not successful when the zeros are non-causal. In Example 5.20 it is shown that if a channel has a high frequency, non-causal zero, then compared to the Kalman equaliser, the H_∞ equaliser can exhibit a reduction in the magnitude of the error spectrum at high frequencies. Consider the channel model $G(z) = 14(z+ 1.29)(z- .95)(z+.6)^{-2}$ which possesses a low frequency, non-causal zero. This model may be written in state-space as

$$\begin{aligned} x_{k+1} &= \begin{bmatrix} 1.2 & -.36 \\ 1 & 0 \end{bmatrix} x_k + \begin{bmatrix} 1 \\ 0 \end{bmatrix} w_k, \\ y_k &= [12.1 \;\; -22.1] x_k + 14 w_k. \end{aligned} \tag{7.31}$$

The error spectra that result for the H_∞ and Kalman equaliser for $\sigma_v^2 = 1$, $\sigma_w^2 = 100$ and $\gamma = 10.1$ are shown in Figure 7.7. It can be seen that the H_∞ equaliser offers a comparative reduction in the dc error spectrum magnitude.

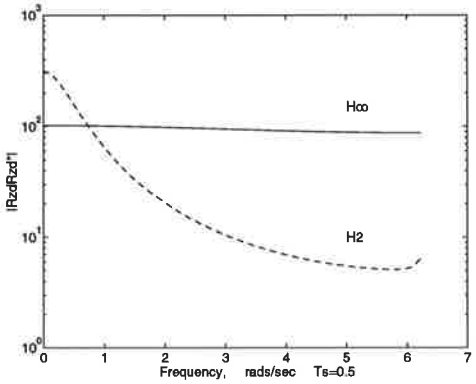

Fig. 7.7 Error spectra for equalising (7.31).

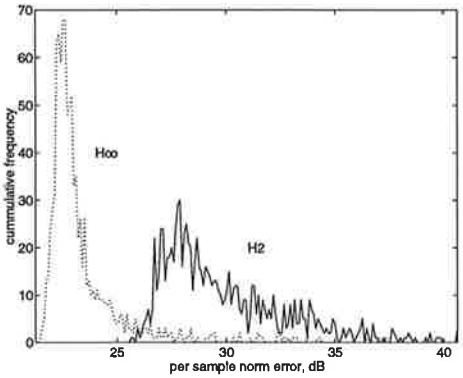

Fig. 7.8 Error histogram for Example 7.5.

Now consider instead a nonlinear channel having the state space realisation

$$\begin{aligned} x_{k+1} &= \begin{bmatrix} 1.2 & -.36 \\ 1 & 0 \end{bmatrix} x_k + \begin{bmatrix} 1 \\ 0 \end{bmatrix} w_k, \\ y_k &= [12.1 \;\; -22.1] x_k + 14 \; arctan \; ([0 \;\; 1] x_k) \; w_k. \end{aligned} \tag{7.32}$$

Actually (7.32) is obtained by multiplying the feedthrough term within (7.31) by a nonlinear function of the state. The problem of equalising (7.32) is more difficult than for (7.31) because the $D_k = d_k(\hat{x}_{k/k-1})$ of (7.20), (7.21) and (7.23) depends on the state estimate which can be error prone when the channel is non-minimum phase. The results of simulations with $\gamma = 10.1$, $\beta_3 = 0$ and $\beta_4 = .008$ are shown in Figure 7.8. It turns out that for a 1000 realisations of 1000 data points each, the MSE exhibited by the H_∞ equaliser is about 6 dB less than that of the Kalman equaliser. For this malicious example at least, the extended H_∞ filter is advantageous for two reasons. Firstly, the linear H_∞ equaliser is comparatively better for non-minimum phase equalisation (see Figure 7.7). Secondly, it

has extra parameters (namely γ, β_3 and β_4) which may be tuned to optimise the performance.

7.6 Conclusions.

The EKF arises by successively linearising a nonlinear model about each current state estimate and then applying the Kalman filter to obtain the next state estimate. It has been demonstrated that when the underlying model is particularly nonlinear, the EKF can exhibit both a high MSE and severe peak errors, for example see Figure 7.3. The contribution of this Chapter is to propose a new method to make the EKF robust to linearisation errors.

In summary, the robust EKF came to fruition by:

- Formulating a signal model that accounted for the truncated higher order (Taylor series) terms.
- Motivating the pursuit of a robust EKF as a model uncertainty task, by posing an H_∞ auxiliary problem possessing additional inputs in lieu of the uncertainties.
- Arriving at input scalings that are sufficient for the solution of the H_∞ auxiliary problem.
- Using the discrete-time H_∞ filter developed in Chapter 4 and a linearity argument to obtain a so-called extended H_∞ filter in predictor-corrector form.
- Specifying a particular state (about which the linearisation is performed) which is required to satisfy the H_∞ optimality criterion (7.9).
- Accommodating nonlinear feedthrough functions via the application of the Kalman and H_∞ filters to a linearised plant.
- Presenting some examples that demonstrate a performance benefit.

The success (or otherwise) of the robust EKF depends on how closely the assumed mixed norm uncertainty bounds the residuals. It has been observed that when the state equation is linear then the EKF and robust design can yield similar performance. Conversely, when the problem is sufficiently nonlinear the so-called extended H_∞ filter may offer a performance benefit.

Signal demodulation examples have been described and it has been shown how to set up the problem in a robust framework. It turns out for the examples considered here, when the state is nonlinear and the observation noise is power is small, then the robust EKF may reduce both the peak error and the mean square error. It has also been demonstrated that the performance of a conventional FSK demodulator can be improved via the inclusion of a saturating nonlinearity in the signal model.

The extended H_∞ filter possesses additional tuning parameters which need to be determined by trial and error. These parameters may be used to control the trade-off between peak

error and mean square error and the scaling of the inputs in order to accommodate linearisation errors. Since the H_∞ filter has the same structure as the Kalman filter, it is not surprising that the extended H_∞ filter has the precisely the structure of the EKF. Unlike conventional measures to mitigate linearisation errors, such as the iterated EKF or the second order EKF, here the computational overheads are not affected since the order of the problem remains unchanged.

REFERENCES

[AM] Anderson, B. D. O. and J.B. Moore, *Optimal Filtering*, Prentice-Hall, Englewood Cliffs NJ, 194-195, 1979.

[CCC] Chui, C. K., G. Chen and H. C. Chui, "Modified extended Kalman filtering and a real time parallel algorithm for system parameter identification", *IEEE Trans. Automat. Contr*, vol. 35, no. 1, pp. 100-104, Jan. 1990.

[EW] Einicke, G. A. and L.B. White, "The extended H_∞ filter - a robust EKF", *Proc. ICASSP*, Adelaide, Australia, vol. 4, pp. 181-184, 1994.

[EW2] Einicke, G. A. and L.B. White, "Robust nonlinear filtering using a H_∞ performance criterion", submitted for publication.

[G] Gelb, A., *Applied optimal estimation*, M.I.T. Press, Cambridge MA., pp. 190-192, 1974.

[GT] Gurov, I. R. and G. Tadmor, "On the robustness of H_∞ state feedback control to nonlinear perturbations", *Automatica*, vol. 30, no. 3, pp. 499-502, 1994.

[HA] Hostetler, L. D. and R. D. Andreas, "Nonlinear Kalman filtering techniques for terrain-aided navigation", *IEEE Trans. Automat. Contr.*, vol. 28, no. 3, pp. 315-322, Mar. 1983.

[J] James, M. R., "Computing the H_∞ norm for nonlinear systems", *Proc. 12th Cong. IFAC*, vol. 4, pp. 343-346, July 1993.

[Ja] Jazwinski, A. H., *Stochastic processes and filtering Theory*, Academic Press, N.Y., pp. 279-281, 1970.

[LB] La Scala, B. F. and R. B. Bitmead, "Design of an extended Kalman filter frequency tracker", *Proc. ICASSP*, Adelaide, Australia, vol. 3, pp. 525-527, 1994.

[SM] Sage, A. P. and J. L. Melsa, *Estimation theory with applications to communications and control,* McGraw-Hill, N.Y., pp. 465-472, 1973.

[V] Van der Schaft, A. J., "On a state space approach to nonlinear H_∞ control", *Sys. Cont. Lett.*, vol. 16, pp. 1-8, 1991.

Chapter 8

Summary

This chapter begins by summarising what has been tackled, touches on what else could be done and concludes by recapitulating the performance benefits of robust filters.

8.1 Achievements.

The first contribution [EW] is the derivation of a discrete-time formulation for the interpolation solution of [S]. Previously in [GE], the benefits of a H_∞ approach was argued exclusively by observing a reduction in the peak of the error spectrum. Here advantages have also been demonstrated via performance criteria such as the input to error energy ratio and bit error rate. The results of simulation studies have been presented. The use of frequency weighted error has been illustrated in a continuous-time, output estimation problem. The use of the discrete-time H_∞ solution has shown to be advantageous in a high SNR, linear, channel equalisation problem.

Initially it was desired to similarly derive the discrete-time version of the game theoretic H_∞ filter of [LS], however the results had already been worked out in a control context [LGW]. Thus, a discrete-time H_∞ filter was obtained by simplifying the results of [LGW] and has been shown to have precisely the structure of the Kalman filter. Some performance trends have been observed by examining the error spectra that result for various scalar problems. In particular, the problems of output estimation and equalisation have been addressed in both continuous-time and discrete-time contexts. A performance comparison of H_∞ and Kalman filters has been summarised in [EW2].

Robust solutions to nonlinear filtering problems were first investigated via the application of a false ARE technique. The construction of nonlinear observers for the demodulation of single tone and multitone signals is detailed in [EW3,EW4].

It was recognised that the linearisation errors which occur in an EKF is a modelling error problem which can be handled quite naturally in a H_∞ framework. The extended H_∞ filter was borne out of the step-wise linearisation akin to the EKF combined with a H_∞ filter designed to be robust with respect to the errors introduced by truncating the Taylor series expansions beyond the linear term. Conventional measures to overcome linearisation errors such as the *second order EKF* or the *iterated EKF* [G,SM] increase the computational cost but here the order of the solution remains the same. The extended H_∞ filter does possess extra tuning parameters which need to be determined by trial and error. The results of simulations demonstrate an advantage in demodulation applications and have been reported in [EW5,EW6].

PROBLEM	ADVANTAGE	ILLUSTRATION
Filtering stable, known, low-pass plant.	Small at high SNR, negligible at low SNR.	Examples 5.2, 5.3, 5.5.
Filtering stable, known, high-pass plant.	Greater at high SNR, negligible at low SNR.	Example 5.6.
Filtering known, unstable plant.	Negligible at high SNR, moderate at low SNR.	Example 5.7.
Filtering uncertain, stable, low-pass plant.	Can be moderate at high SNR, negligible at low SNR.	Example 5.8.
Equalising known, minimum phase, low-pass plant.	Marginal at high SNR, negligible at low SNR.	Examples 5.10, 5.11, 5.12, 5.16.
Equalising known, non-minimum phase, low-pass plant.	Small at high SNR, negligible at low SNR.	Example 5.13, 5.17.
Equalising known, minimum phase and non-minimum phase, high-pass plant.	Small at high SNR, negligible at low SNR.	Example 5.18, 5.19.
Equalising uncertain, minimum phase plant.	Small. Only a small margin may exist to accommodate uncertainties.	Example 5.14.
Equalising uncertain, non-minimum phase plant.	Inherently robust to modelling errors.	Section 5.3.5.
Equalising known, minimum phase, band-pass plant.	Negligible at high SNR, small but costly at low SNR.	Example 5.20.
Equalising known, non-minmimum phase, band-pass plant.	Small but costly at high SNR.	Example 5.21.
Equalising minimum phase, band-pass plant mis-modelled as non-minimum phase.	Can be moderate but costly at high SNR.	Example 5.22.

Table 8.1. Performance summary of H_∞ filters and equalisers.

8.2 H_∞ filters and equalisers.

When the Kalman filter works well, it is most difficult to improve on as, after all, it is "optimum among all linear processors" [AM]. Throughout this thesis, "improvement" refers to a reduction in the peak of the error spectrum at the expense of an increase in MSE. It turns out, that for easy problems, the Kalman filter performs well in the abovementioned peak error sense. Consider the known, stable, minimum phase, low-pass plant filtering problem: clearly minimising the MSE is not in direct opposition to minimising the peak error. For this easy problem, it has been demonstrated via examples, that only a small reduction in peak error can be accomplished at the cost of a substantial increase in MSE. Conversely, when the goal of attaining a minimum MSE directly opposes that of minimising the peak error, the trade off provided by a H_∞ design can be more significant.

Consequently, for more difficult problems such as filtering unstable or high-pass plants and non-minimum phase equalisation, the reduction in peak error can be more apparent but once again, at the cost of MSE.

The performance of H_∞ filters and equalisers compared to Kalman filters and equalisers is summarised in Table 8.1. When the plant model is known exactly, the comparative advantage of H_∞ filters tends to be quite small and the cost can be high. Consequently, it is concluded that if everything about the problem is known exactly, there is no intrinsic value in H_∞ designs. However, if the plant model is uncertain, then a robust H_∞ design can be advantageous provided that the uncertainty is not too great.

8.3 Robust nonlinear observers designed via the fake ARE.

The fake ARE technique was originally used in the design of linear Kalman filters [BTP] where the solution for the fake ARE is assumed to be a constant (parameter) times the identity matrix; this parameter permits convergence rate and noise rejection to be traded off against each other. The contribution of [EW3,EW4] is the design of nonlinear observers via an approximate linearisation followed by the use of the fake ARE technique. Here the components of the assumed fake ARE solution are treated as tuning parameters. The following advantages are claimed for the nonlinear observer:

- Improved robustness to initial conditions.
- Sub-threshold tracking capability.
- Robustness to amplitude uncertainty.
- Error stability.

The apparent robustness to initial conditions was observed during the course of conducting simulations. The fake ARE comes about by sacrificing some optimality in exchange for error stability. A proof for asymptotic error stability has been set out for a known amplitude case, which does not rely on any assumptions regarding the initial conditions.

The sub-threshold capability refers to a reduction in the (low SNR) error variance for the tone tracking problem, as is evidenced in Figure 6.3. The robustness to amplitude uncertainty is demonstrated by Figures 6.5 to 6.9 where an amplitude fade is imposed during either tone tracking or frequency tracking.

These performance improvements are incurred at the expense of convergence rate and MSE. The reduction in convergence rate can be argued by observing that the components of the gain become small when the signal amplitude becomes small. The increase in MSE is apparent by comparing the solution of the actual RDE with that of the fake ARE. In conclusion, the use of the nonlinear observers (proposed herein) may offer a reduction in

MSE when the amplitude is uncertain at the expense of convergent rate and a higher MSE when no uncertainty is present.

8.4 The extended H_∞ filter.

The use of the linear H_∞ filter can be advantageous when model uncertainties are present, the so-called extended H_∞ filter arises precisely as one such application. The EKF works well if the filtering problem is substantially linear, in which case the extended H_∞ filter does not offer any performance benefits. In fact the EKF reverts to the Kalman filter which is optimal when the problem is exactly linear. Otherwise, when the problem is highly nonlinear, the EKF performance tends to degrade severely and the robust design can be beneficial.

The fake ARE approach for nonlinear observer design has been fruitful at low SNRs, where the observation noise has tended to dominate the filtering problem. This contrasts with the extended H_∞ filter, which has been found to be beneficial when the problem is dominated by linearisation errors. In Examples 7.1 and 7.2, it is demonstrated that the use of an extended H_∞ filter can offer both a reduction in MSE and peak error, if an EKF were used to demodulate a highly nonlinear FM signal. The performance benefit reduces if the signal model is more linear such as Example 7.4. These examples demonstrate that when the EKF does not work well, a robust approach can be better.

8.5 Open Questions.

8.5.1 Noncausal filters.

Regarding non-minimum phase equalisation problems, it has been argued that a H_∞ equaliser achieves a comparative reduction in the peak of the error spectrum because it is better at ignoring the data. Although the equalisers do minimise the error, they do not invert the channel. Clearly a delay needs to be built into the equaliser specification. Regarding filtering *per se*, Van Trees [VT] gives an exposition of the advantage of unrealisable Wiener filters and remarks that a delay of several times the plant's dominant time-constant will usually result in the minimum possible MSE. In order to exploit the high throughputs offered by the lastest digital signal processing technology, the data is invariably pipelined and then processed one block at a time. It is contended that noncausal filters may be implemented quite naturally (in a block processing context).

While the design of optimum noncausal filters may not be tractable, it is likely that filters possessing some delay may still be advantageous. The following avenues may be worth exploring:

- In [VK] the solution for continuous-time H_∞ controllers is set out for the Pritchard-Salamon class of problems in which delays may be specified. It may be worthwhile to produce a derivation and explore the merits of a discrete-time analogy.
- In [Ba] a dynamic game is proposed where the two players are endowed with a delay. The virtues of this approach could be investigated.
- Perhaps the simplest approach is to explore the possibility of adding a delay in the same way that frequency weighting is applied in [LS].

8.5.2 Nonlinear smoothing.

It has been noted that the EKF performance degrades when the measurement noise power increases. One possible remedy is the design of a nonlinear smoother. In Appendix H, an extended Kalman smoother is proposed for problems in which the state evolution is linear and the output mapping is nonlinear. (A solution for the more general problem remains outstanding.) However, a simulation study shows that only a small performance improvement is obtained. Another approach is to use an EKF in the usual way and then run an EKF on the reversed data. The results of the forward filter with a backward predictor may be combined via the approach of Fraser and Potter [FP]. This approach can be successful when the data is iid as in Example 7.4. However, an EKF is not expected to perform as well on the reversed data if the data is actually generated by a stochastic model. Alternatively, the competitive approach of Niedzwiecki et al [NS] may be applied, in which either a forward estimate, a backward estimate or the linear combination of [FP] is selected by evaluating a cost function over a sliding window.

8.5.3 μ-synthesis.

The accommodation of modelling errors discussed in Chapters 3, 5 and 7 has been via an unstructured uncertainty approach. The application of structured approaches such as μ-synthesis [Mo] to communications filtering has yet to be investigated.

8.6 Concluding remarks.

Before this work began, although the theoretical aspects of H_∞ filters were largely known, not a great deal was known about any performance benefits. The work described herein is an attempt to plug that (knowledge) gap.

Grimble was among the first to demonstrate that H_∞ filters can be advantageous in applications where particular parts of the frequency spectrum are accorded a weighting [GE]. Here, it has been found that small benefits (in a peak-error-spectrum sense) can arise provided that the SNR is sufficiently high. Although it is possible to write down sufficient conditions for when the "SNR is sufficiently high", they do not lend themselves to interpretation and the performance analysis tends to be anecdotal. It turns out that the

H_∞ filter can be slightly more beneficial when it is required to have a high-pass response or to be a stable approximation of an unstable plant. More tangible benefits arise when small modelling errors are accommodated, however considerable effort can be required to optimise the design. The construction of a solution that is robust with respect to model uncertainties is not always tractable, for example robust minimum phase equalisation can be problematic. Conversely, non-minimum phase H_∞ equalisers have been found to be inherently robust to mismodelling.

The present work has been bought to fruition in the development of the extended H_∞ filter for which desirable attributes have been established at high SNR. At low SNR, nonlinear observers designed via the fake ARE technique appears to be promising. Many open questions remain, for example the design of robust nonlinear smoothers and robust noncausal filters are unsolved problems.

REFERENCES.

[AM] Anderson, B. D. O. and J. B. Moore, *Optimal filtering*, Prentice-Hall, Englewood Cliffs, New Jersey, p. 108, 1979.

[Ba] Basar, T., "A dynamic game approach to controller design: disturbance rejection in discrete-time", *IEEE Trans. Automat. Contr.*, vol. 36, no. 8, pp. 936-952, 1991.

[BTP] Bitmead, R. R., A. -C. Tsoi and P. J. Parker, "Kalman filtering approach to short time Fourier analysis", *IEEE Trans. Acoustics, Speech and Signal Processing*, v. 34, no. 6, pp. 1493-1501, 1986.

[EW] Einicke, G. A. and L. B. White, "The use of H_∞ filters for linear demodulation and equalisation", *IEEE Int. Symp. CAS.*, San Diego, CA, vol. 4, pp. 1721-1724, May 1992.

[EW2] Einicke, G. A. and L. B. White, "Performance comparison of H_∞ and Kalman filters ", submitted for publication.

[EW3] Einicke, G. A. and L. B. White, "Estimation of frequency and phase modulated signals using false algebraic Riccati techniques", *Proc. 3rd ISSPA*, Gold Coast, Aust., vol. 2, pp. 339-343, Aug. 1992.

[EW4] Einicke, G. A. and L. B. White, "A class of nonlinear filters for periodic signals", *IEEE Int. Symp. CAS*, Chicago, IL, vol. 1, pp. 144-147, May 1993.

[EW5] Einicke, G. A. and L. B. White, "The extended H_∞ filter - a robust EKF", *Proc. ICASSP*, Adelaide, Aust., vol. 4, pp. 181-184, Apr. 1994.

[EW6] Einicke, G. A. and L. B. White, "Robust nonlinear filtering using a H_∞ performance criterion", submitted for publication.

[FP] Fraser, D. C., and J. E. Potter, "The optimum linear smoother as a combination of two optimum linear filters", *IEEE Trans. Automat. Contr.*, pp. 387-390, Aug. 1969.

[G] Gelb, A., *Applied Estimation Theory*, M.I.T. Press, Cambridge, MA, pp. 200-203, 1974.

[GE] Grimble, M. J., and A. El Sayed, "Solution of the H_∞ optimal linear filtering problem for discrete-time systems", *IEEE Trans. ASSP., vol. 38, no. 7, pp. 1092-1104, July 1990.*

[LS] Limebeer, D. J. N. and U. Shaked, "Minimax terminal state estimation and H_∞ filtering", submitted to *IEEE Trans. Automat. Contr.*

[LGW] Limebeer, D. J. N., M. Green and D. Walker, "Discrete-time H_∞ control", *Proc. 28th CDC*, Tampa, Fl., vol. 1, pp. 392-396, Dec. 1989.

[Mo] Moser, A. N., "Designing controllers for flxible structures with H_∞/μ-synthesis", *IEEE Contr. Sys. Mag.*, pp. 79-89, 1993.

[NW] M. Niedzwiecki and W. A. Sethares, "Smoothing of Discontinuous Signals, The Competitive Approach", *IEEE Trans. SP*, vol. 43, no. 1, pp. 1-13, Jan. 1995

[SM] Sage, A. P., and J. L. Melsa, *Estimation theory with applications to communications and control*, McGraw-Hill Book Company, New York, 1971.

[S] Shaked, U., "H_∞-minimum error state estimation of linear stationary processes", *IEEE Trans. Automat. Contr.*, vol. 34, no. 5, pp. 554-558, May 1990.

[VK] Van Keulen, B., *H_∞-control for distributed parameter systems: a state space approach*, Birkhauser, Boston, 1993.

[VT] Van Trees, H. L., *Detection, estimation and modulation theory*, Wiley, New York, ch. 6, 1968.

Appendix A

The Wiener filter

The purpose of this appendix is to define the Wiener filter and to demonstrate an equivalence between the various formulations that appear in the literature. The determination of the causal parts of transfer functions are also outlined, as this can be required in some Wiener formulations. The Wiener filter set out herein, is used in the performance comparisons of Chapter 2.

A.1 The continuous-time Wiener filter.

Consider the filtering problem of Chapter 2 together with the simplifications $N = I$, $W = I$ and $G_2 = G_1 = G$, the error power spectral density matrix from (2.3) is

$$R_{zd}R_{zd}^H = (H\Delta - GG^H\Delta^{-H})(\Delta^H H^H - \Delta^{-1}GG^H) + \Phi_1, \tag{A.1}$$

in which $\Delta\Delta^H = GQG^H + R$. An optimal filter H, which minimises the square of the error, follows from $H\Delta = GG^H\Delta^{-H}$. However this filter is non-causal and unrealisable because it contains the factor Δ^{-H} which possesses poles in the right-hand-plane (RHP). A suboptimal realisable filter can be obtained by taking the causal part of $GG^H\Delta^{-H}$, namely

$$\tilde{H} = \left\{GG^H\Delta^{-H}\right\}_+ \Delta^{-1}. \tag{A.2}$$

Thus an expression for the Wiener filter can be deduced via a simple completing the squares argument. This form of the Wiener filter arises as a component of H_∞ filter in [Sh3]. A formal derivation [Sh] arises via a calculus of variations approach to minimise the cost function $tr\frac{1}{2\pi j}\int_{-j\infty}^{j\infty} R_{zd}R_{zd}^H(s)\,ds$. A Wiener-Hopf derivation is detailed in [Pa].

A.2 The causal part of a continuous-time transfer function.

The causal part of a transfer function may be found by summing any constants plus the partial fractions having left-hand-plane (LHP) poles and excluding those having RHP poles. Consider for some $a > 0$, the LHP pole $(s + a)^{-1}$, which is really $(a + j2\pi f)^{-1}$, then the inverse Fourier transform is $u(t)e^{-at}$, where $u(t)$ is the unit step function. Clearly $u(t)e^{-at}$ is zero for $t < 0$. Now consider the RHP pole $(s - a)^{-1}$, that is $-(a - j2\pi f)^{-1}$, the inverse Fourier transform yields $u(-t)e^{at}$ which is non-zero for $t < 0$.

A.3 The discrete-time Wiener filter.

For the case of discrete-time plants, the Wiener filter is also given by (A.2), however the determination of the causal part is different. A derivation appears in [Sh2].

A.4 The causal part of a discrete-time transfer function.

Consider the SISO plant $G(z) = c_0 + G_{iuc}(z) + G_{ouc}(z)$ where $G_{iuc}(z) = \sum_{i=1}^{n} \frac{c_i}{z - a_i}$, $|a_i| < 1$, is the sum of partial fractions having inside-unit-circle poles and $G_{ouc}(z) = \sum_{i=1}^{m} \frac{d_i}{z - b_i}$, $|b_i| > 1$, is the sum of partial fractions having outside-unit-circle poles. Previously in continuous-time, the convention is to define constants to be causal. This is consistent with ensuring that the non-causal part of the discrete-time plant is zero at $t = 0$. Therefore in the above example, the non-causal part is $\{G(z)\}_- = G_{oucp}(z) - G_{oucp}(0)$ and the causal part is whatever remains: $\{G(z)\}_+ = G(z) - \{G(z)\}_-$. Some numerical examples are given in [Pa].

A.5 Equivalent discrete-time formulations.

From the definition $\Delta\Delta^H = GQG^H + R$, it follows that $GQG^H\Delta^{-H} = \Delta - R\Delta^{-H}$ and taking the causal part yields $\{\Delta - R\Delta^{-H}\}_+ = \Delta(z) - R\Delta^{-H}(0)$. Therefore the discrete-time Wiener filter may be written equivalently as

$$\tilde{H} = \{\Delta - R\Delta^{-H}\}_+\Delta^{-1} = \mathrm{I} - \{R\Delta^{-H}\}_+\Delta^{-1} = \mathrm{I} - R\Delta^{-H}(0)\Delta^{-1}(z). \tag{A.3}$$

In [Sh2,Pa] it is recognised that $\Delta^{-H}(0) = \lim_{z\to\infty} \Delta(z)$ which results in

$$\tilde{H} = I - R\Omega^{-1/2}\Delta^{-1}, \tag{A.4}$$

where $\Omega^{1/2} = \lim_{z\to\infty} \Delta(z)$. Incidentally the one-step-ahead predictor [Pa] is given by

$$\tilde{H}_{k|k-1} = I - \Omega^{1/2}\Delta^{-1}. \tag{A.5}$$

The filter may also written in terms of state space parameters using (1.7) and (1.8). It is easily shown (see [Sh2,AM] for the case of strictly proper plants) that the factorization of $\Delta\Delta^H$ yields $\Delta = [I + C(zI-A)^{-1}K]\Omega^{1/2}$ where $\Omega = CPC^T + DQD^T + R$, P is the solution of $P = BQB^T + APA^T - K\Omega K^T$ and $K = (APC^T + BQD^T)\Omega^{-1}$.

Substituting Δ into (A.4) and applying a special case of the matrix inversion lemma, namely $[I + C(zI - A)^{-1}K]^{-1} = I - C(zI - (A - KC))^{-1}K$, leads to the formulation

$$\tilde{H} = R\Omega^{-1}C(zI - A + KC)^{-1}K + I - R\Omega^{-1}, \tag{A6}$$

where the filter feedthrough is $I - R\Omega^{-1} = (CPC^T + DQD^T)\Omega^{-1}$. In fact (A.6) is the Kalman filter for time-invariant plants possessing a direct feedthrough term. Similarly it is easily shown that an equivalent representation of (A.5) is

$$\tilde{H}_{k/k-1} = C(zI - A + KC)^{-1}K, \tag{A.7}$$

which is also happens to be the transfer function of the Kalman (one-step-ahead) predictor.

A.6 Equivalent continuous-time formulations.

In the continuous-time case it is usual to restrict the problem to strictly proper plants. Hence it follows from $\Delta\Delta^H = GQG^H + R$ that $\lim_{s \to \infty} \Delta = R^{1/2}$ and so another formulation for the Wiener filter is [Sh]:

$$\tilde{H} = I - \left\{R\Delta^{-H}\right\}_+ \Delta^{-1} = I - R^{1/2}\Delta^{-1}. \tag{A.8}$$

A state-space formulation can be found by substituting $G = C(sI - A)^{-1}B$ into $\Delta\Delta^H$ and factorizing to obtain $\Delta = R^{1/2} + C(sI - A)^{-1}KR^{1/2}$. Here $K = PC^TR^{-1}$ and P is the solution of the ARE $0 = AP + PA^T - KRK^T + BQB^T$. From (A.7) and the application of the matrix inversion lemma leads to [SM]:

$$\tilde{H} = C(sI - A)^{-1}KR^{1/2}\Delta^{-1} = C(sI - A + KC)^{-1}K, \tag{A.9}$$

which is recognisable as the transfer function of the Kalman filter.

REFERENCES

[AM] Anderson, B.D.O. and J.B. Moore, *Optimal Filtering*, Prentice Hall, Englewood Cliffs, N.J., ch. 4, 1979.

[Pa] Papoulis, A., *Probability, random variables and stochastic processes,* Mc-Graw-Hill, 2nd Ed., ch. 13, 1989.

[Sh] Shaked, U., "A general transfer-function approach to the steady-state linear quadratic Gaussian stochastic control problem", *Int. J. Contr.*, vol. 24, no. 6, pp. 771-800, 1976.

[Sh2] Shaked, U., "A transfer function approach to the linear discrete stationary filtering and the steady-state discrete optimal control problems", *Int. J. Contr.*, vol. 29, no. 2, pp. 279-291, 1979.

[Sh3] Shaked, U., " H_∞-minimum error state estimation of linear Stationary Processes", *IEEE Trans. Automat. Contr.,* vol. 35, no. 5, pp. 554-558, May 1990.

[SM] Sage, A. P. and J. L. Melsa, *Estimation theory with applications to communications and control,* McGraw-Hill, N.Y., ch. 7, 1973.

Appendix B

A frequency domain H_∞ filter.

The inclusion of specified noise covariances, coloured noise and frequency weighted error reported in [EW] is a natural extension of [Sh4] and consequently the discussion herein is kept brief. The appendix begins with the role of the inner transfer function matrix and follows the treatment of [Sh4] quite closely. The salient aspects of an interpolation solution [Sh] are quoted in Section B.2. Some remarks regarding the optimal value of γ are mentioned in Section B.2. Section B.4 outlines the use of the Bilinear transform in the solution of discrete-time interpolation problems. The appendix concludes with a discussion of some implementation considerations.

B.1 The role of the inner function.

From (2.3) and (2.7) it follows that a filter is desired which satisfies

$$W(H\Delta - \tilde{G}_1\tilde{G}_2^H\Delta^{-H})(\Delta^H H^H - \Delta^{-1}\tilde{G}_2\tilde{G}_1^H)W^H = \gamma^2 I - \Phi_1, \tag{B.1}$$

The solution is not unique since an inner U, satisfying $UU^H = I$, may be factored into the right-hand-side of (B.1), that is

$$\gamma^2 I - \Phi_1 = W\tilde{G}_1\Delta_2 UU^H\Delta_2^H\tilde{G}_1^H W^H. \tag{B.2}$$

It is seen that the optimal filter follows from

$$W(H\Delta - \tilde{G}_1\tilde{G}_1^H\Delta^{-H}) = WG_1\Delta_2 U \tag{B.3}$$

and is given by

$$H^\infty = W^{-1}(\tilde{G}_1\Delta_2 U + \tilde{G}_1\tilde{G}_2^H\Delta^{-H})\Delta^{-1}. \tag{B.4}$$

which is equivalent to (2.8). Thus the filtering problem is an inner design problem and is also known as an interpolation problem. The role of U is to ensure that the noncausal part

of $\tilde{G}_1\Delta_2 U + \tilde{G}_1\tilde{G}_2^H\Delta^{-H}$ is zero. Since G_1 is assumed to be stable, U is required to cancel the poles of $\tilde{G}_2^H\Delta^{-H}$. In [Sh4] it is assumed that G_1 and G_2 have the same dynamics. In this case the poles of G_1^H are cancelled by the zeros of Δ^{-H} and so the task of U is to cancel the poles of Δ^{-H}, or equivalently the zeros of Δ^H. In order to factor out Δ^{-H} from U, it is necessary to factor out an all-pass quantity $\tilde{\Delta}^H\Delta^{-H}$ so that U is all-pass. Thus the inner of [Sh4] is defined as $U = U_1\tilde{\Delta}^H\Delta^{-H}$ where $\tilde{\Delta}\,\tilde{\Delta}^H = \Delta\Delta^H$ and $\tilde{\Delta}$ has its zeros all in the RHP. It follows from (B.3) that the optimal H_∞ filter arises by solving the so-called interpolation problem of

$$W(H\Delta\Delta^H - \tilde{G}_1\tilde{G}_2^H) = W\tilde{G}_1\Delta_2 U_1\tilde{\Delta}^H, \tag{B.5}$$

at the zeros of Δ^H, where U_1 is an inner is required to be found. In the case of SISO plants, the quantities in (B.5) are polynomial fractions. If (B.5) is evaluated at the zeros of Δ^H, denoted by s_i, $i = 1,\ldots, p$, the first term is zero and dividing through by $W(s_i)\tilde{G}(s_i)$, (assuming this is non-zero,) yields the interpolation constraints

$$-\Delta_2^{-1}(s_i)G_2^H(s_i) = U_1(s_i)\tilde{\Delta}^H(s_i). \tag{B.6}$$

Assuming that the s_i are distinct, a solution may be found via the method of [Sh]. In the event that the s_i have multiplicities, the interpolation method of [Sh3] may be employed.

B.2 Statement of a continous-time vector interpolation solution.

Using the notation of [Sh], the interpolation contraints are written as $\tilde{U} = [u_1,\ldots, u_p]$ and $W = [w_1,\ldots, w_p]$ where $u_i = \tilde{\Delta}^H(s_i)$ and $w_i = -\Delta_2^{-1}(s_i)G^H(s_i)$. The continuous-time vector interpolation solution of [Sh3] is defined as a function of an arbitrary inner matrix Θ such that $\Theta^H\Theta = I$. The choice of $\Theta = I$ yields

$$U_1(s) = [I - \tilde{C}(sF + \tilde{A})^{-1}\tilde{C}^H], \tag{B.7}$$

where $\tilde{C} = \tilde{U} - W$, $\tilde{A} = \tilde{C}^H\tilde{U} - F\Lambda_s$, $f_{ij} = (s_i^H + s_j)^{-1}(u_i^H u_j - w_i^H w_j)$ and $F = \{f_{ij}\}$.

B.3 Summary of the solution procedure.

From (B.2) it follows that a minimum value for γ, denoted by $\gamma_{\min}$, is required to be found so that the spectral factorization

$$\Delta_2\Delta_2^H = \gamma^2\tilde{G}_1^{-1}W^{-1}W^{-H}\tilde{G}_1^{-H} - (I + \tilde{G}^H N^{-H}R^{-1}N^{-1}\tilde{G})^{-1}, \tag{B.8}$$

yields a stable and minimum phase Δ_2. From (2.3) it follows for SISO plants that a lower bound for γ^2 can be calculated as $\gamma = \|\Phi_1\|_\infty$. A convenient upper bound can be found by calculating the maximum magnitude of Wiener error spectrum. The $\gamma_{\min}$ generally needs to be determined iteratively, one method is start at this upper bound and progressively bisect the distance to the lower bound. The problem can have a tendency to be ill-condi-

tioned when γ is close to γ_{min}. Indeed in [Sh2] it is argued that at $\gamma = \gamma_{min}$, a pole of the inner tends to infinity. Therefore it is prudent to choose $\gamma > \gamma_{min}$ and check that (a) a reduced order solution for $U(s)$ is obtained, (b) the noncausal part of $\tilde{G}_1\Delta_2 U + \tilde{G}_1\tilde{G}_2^H\Delta^{-H}$ is zero, and (c) the solution satisfies (2.7).

B.4 Extension to discrete-time.

The formulation of the Wiener filter (2.6) is equally applicable in the discrete-time case with appropriate definitions of causality. Similarly the H_∞ filter of (2.8) or (B.4) also applies for discrete-time plants, except that a discrete-time inner needs to found. Denoting the p zeros of Δ^H as z_i, the discrete-time interpolation constraints are

$$-\Delta_2^{-1}(z_i)G_2^H(z_i) = U_1(z_i)\tilde{\Delta}^H(z_i). \tag{B.9}$$

The continuous-time interpolation conditions may be obtained via the Bilinear transform as $s_i = 2(z_i - 1)(z_i + 1)^{-1}$ at $T_s = 1$. The continuous-time U_1 is calculated from (B.7) and the discrete-time version follows by again applying the Bilinear transform. Finally the optimal filter (2.6) is calculated using the z-domain definition of the causal part (described in Appendix A).

B.5 Some implementation considerations.

Some *Matlab*® routines were written so that the optimal H_∞ filter can be found when G_1 and G_2 are of arbitrary order. The calculation of $(sF + \tilde{A})^{-1}$ in (B.7) requires matrices to be inverted symbolically - the use of Cramers rule (dividing adjoints by determinants) was found to be satisfactory. Performing spectral factorisations such as (B.8) can be error prone because the roots of polynomials are calculated with finite precision - it is a good practice to check that the difference between a spectral factor times its adjoint, and the polynomial being factorised, is sufficiently small. Cancelling common factors in polynomial fractions, such as those within (B.4), tends to be problematic - it can be useful to at least compare the transfer functions evaluated at $s = \infty$ and at $s = 0$. The errors that accumulate as a result of approximate factorisation and cancellation, appear to increase with the order of the polynomials; consequently the use of frequency domain methods is only recommended for low order problems. Indeed in [SM] it is concluded that the "the Kalman algorithm is computationally superior to the Wiener algorithm" owing to the difficulty with spectral factorisations, particularly for higher order problems.

REFERENCES

[EW] Einicke, G.A. and L.B. White, "The use of H_∞ filters for linear demodulation and equalisation", *IEEE ICAS.*, vol. 4, pp. 1721-1724, May 1992.

[Sh] Shaked, U., " The explicit structure of inner matrices and its application in H_∞-optimization", *IEEE Trans. Automat. Contr.,* vol. 34, no. 7, pp. 734-738, Jul. 1989.

[Sh2] Shaked, U., "A two-sided interpolation approach to H_∞ optimization problems", *IEEE Trans. Automat. Contr.,* vol. 34, no. 12, pp. 1285-1290, Dec. 1989.

[Sh3] Shaked, U., "The structure of inner matrices that satisfy multiple directional interpolation requirements", *IEEE Trans. Automat. Contr.,* vol. 34, no. 12, pp. 1293-1296, Dec. 1989.

[Sh4] Shaked, U., " H_∞-minimum error state estimation of linear Stationary Processes", *IEEE Trans. Automat. Contr.,* vol. 35, no. 5, pp. 554-558, May 1990.

[SM] Sage A. P. and J. L. Melsa, *Estimation theory with applications to communications and control,* McGraw-Hill, N.Y., 1973.

Appendix C

Continuous-time, all-pass scaling

In the frequency domain approaches to H_∞ filtering discussed in Chapter 2, the error spectrum is designed to be all-pass. This contrasts with the game-theoretic approach discussed in Chapter 3, where it is usual to to assume a minimum entropy solution, which results in a low pass error. This appendix shows how the continuous-time, game-theoretic H_∞ filter can be scaled to yield all-pass error.

This appendix begins with a definition of an all-pass transfer function. A scaling due to [Gr] is then defined which ensures that the open loop system is pass. Finally a closed loop formulation is introduced which is shown to exhibits an all-pass error.

Theorem C.1. *([GLDKS] thm. 4.1(b)). Consider the plant* $G \overset{s}{=} \left[\begin{smallmatrix} A & B \\ C & D \end{smallmatrix}\right]$, *if* $D'D = \sigma^2 I$ *and* $CP + DB^T = 0$ *where* $P = P^T$ *is the controllability gramian given by* $AP + PA^T + BB^T = 0$. *then* $GG^H = \sigma^2 I$.

C.1 The open loop error system.

The controller for *problems of the second kind* ([LAKG], thm. 3.3), may be scaled by replacing $\nu = \boldsymbol{U}r$ with $\gamma\nu = \boldsymbol{U}\gamma r$. This scaling is stated to yield all-pass error in [Gr]. In the filtering problems, there is usually no path from the controller to the plant and so $B_2 = 0$.

Theorem C.2. *Consider the time-invariant, filtering problem described by*

$$\begin{bmatrix} \dot{x} \\ z \\ y \end{bmatrix} \overset{s}{=} \begin{bmatrix} A & B_1 & 0 \\ C_1 & 0 & 1 \\ C_2 & D_{21} & 0 \end{bmatrix} \begin{bmatrix} x \\ d \\ u \end{bmatrix}, \tag{C.1}$$

where $x = \begin{bmatrix} x_2 \\ x_1 \end{bmatrix}$, $d = \begin{bmatrix} r \\ w \end{bmatrix}$ *and* $D_{21} = [1\ \ 0]$.

Then the set of filters such that $R_{zd}R_{zd}^H = \gamma^2$ *is parametrised by*

$$\begin{bmatrix} \dot{\hat{x}} \\ u \\ v \end{bmatrix} \overset{s}{=} \begin{bmatrix} A - B_1D_{21}^TC_2 - PC_2^TC_2 & -B_1D_{21}^T - PC_2^T & -\gamma^{-1}PC_1^T \\ C_1 & 0 & \gamma \\ C_2 & \gamma & 0 \end{bmatrix} \begin{bmatrix} \hat{x} \\ y \\ r \end{bmatrix}, \tag{C.2}$$

$$v = Ur, \tag{C.3}$$

in which $\gamma^{-1}U$ *is a causal, contractive operator and where P is the solution of the ARE*

$$(A - B_1D_{21}^TC_2)P + P(A - B_1D_{21}^TC_2)^T - P(C_2^TC_2 - \gamma^{-2}C_1^TC_1)P + B_1D_\perp{}^TD_\perp B_1^T = 0, \tag{C.4}$$

and $D_\perp = \begin{bmatrix} 0 \\ 1 \end{bmatrix}$ *is an orthogonal extension to* D_{21}.

An operator X is contractive if $\|X\|_\infty \leq 1$. Causality is discussed in Appendix A.

Proof. Observing that $\hat{x}$ estimates $-x$, the error may be written as $e = x + \hat{x}$ and it is easy to show that R_{zd} corresponding to (C.2) is given by

$$\begin{bmatrix} \dot{e} \\ z \\ \gamma v \end{bmatrix} \overset{s}{=} \begin{bmatrix} A - B_1D_{21}^TC_2 - PC_2^TC_2 & -B_1D_{21}^TD_{21} - PC_2^TD_{21} & -\gamma^{-1}PC_1^T \\ C_1 & 0 & \gamma \\ C_2 & \gamma D_{21} & 0 \end{bmatrix} \begin{bmatrix} e \\ y \\ v \end{bmatrix}. \tag{C.5}$$

For convenience (C.5) is written as $\begin{bmatrix} \dot{e} \\ z \\ \gamma v \end{bmatrix} \overset{s}{=} R_{zd} \begin{bmatrix} \hat{x} \\ y \\ v \end{bmatrix}$ where $R_{zd} \overset{s}{=} \begin{bmatrix} A_{zd} & B_{zd} \\ C_{zd} & C_{zd} \end{bmatrix}$. Now Theorem C.1 may be used to argue that (C.5) is all-pass. The controllability gramian pertaining to (C.5) is

$$\begin{aligned} &(A - B_1D_{21}'C_2)P + P(A - B_1D_{21}'C_2)' + B_1B_1' - B_1D_{21}'D_{21}B_1' - B_1D_{21}'C_2P - B_1D_{21}'D_{21}B_1' \\ &+ B_1D_{21}'D_{21}D_{21}'D_{21}B_1' + B_1D_{21}'D_{21}D_{21}D_{21}'C_2P - PC_2'D_{21}B_1' + PC_2'D_{21}D_{21}'D_{21}B_1' \\ &+ PC_2'D_{21}D_{21}'D_{21}B_1' + PC_2'D_{21}D_{21}'C_2P + \gamma^{-2}PC_1'C_1P = 0 \end{aligned} \tag{C.6}$$

Since $D_{21}D_{21}' = [1\ \ 0]$ and equating (C.6) to (C.4) yields $I - D_{21}'D_{21} = D_\perp'D_\perp$ which is true. Thus the solution of the ARE (C.4) equals the controllability gramian. By direct substitution it can be shown that $C_{zd}P + D_{zd}B_{zd} = 0$. Since $D_{R_{zd}}D_{R_{zd}}^H = \gamma^2 I$, the result follows. ∇

The conditions that are sufficient for the open loop system (C.5) to be all-pass will be required in showing that a closed loop system is all-pass. For convenience R_{zd} is written as $\begin{bmatrix} A + \alpha_1 + \alpha_2 & \beta_1 & \beta_2 \\ C_1 & 0 & \gamma \\ C_2 & \delta & 0 \end{bmatrix}$, where $\alpha_1 = B_1D_{21}^TC_2$ and $\beta_1 = -B_1D_{21}^TD_{21} - PC_2^TD_{21}$ etc. Then equating the solution of (C.4) to controllability gramian yields

$$-\alpha_2 P - P\alpha_2^T - P(C_2^T C_2 - \gamma^{-2} C_1^T C_1)P + B_1 D_\perp{}^T D_\perp B_1^T - \beta_1\beta_1^T - \beta_2\beta_2^T = 0 \qquad \text{(C.7)}$$

and $C_{zd}P + D_{zd}B_{zd} = 0$ results in

$$C_1 P + \gamma\beta_2^T = 0, \qquad \text{(C.8)}$$

$$C_2 P + \delta\beta_1^T = 0, \qquad \text{(C.9)}$$

the conditions for the open loop system to be all-pass. Now a sufficient condition can be stated for the closed loop controller to be all-pass.

C.2 The closed loop error system.

Theorem C.3. *The choice of* $U = \gamma^{-1}$ *in the filter of theorem C.2 results in* $R_{zd}R_{zd}^H = \gamma^2 I$.

Proof. Substituting $U = \gamma^{-1}$ into (C.5) yields the closed loop system

$$\begin{bmatrix} \dot{e} \\ z \end{bmatrix} \overset{s}{=} \begin{bmatrix} A + \alpha_1 + \alpha_2 + \gamma^{-1}\beta_2\varepsilon_2 & \beta_1 + \beta_2\delta \\ C_1 + C_2 & \delta \end{bmatrix} \begin{bmatrix} e \\ d \end{bmatrix}. \qquad \text{(C.10)}$$

Now using (C.7) the design ARE can be written as

$$(A + \alpha_1 + \alpha_2 + \gamma^{-1}\beta_2\varepsilon_2)P + P(A + \alpha_1 + \alpha_2 + \gamma^{-1}\beta_2\varepsilon_2)^T - \gamma^{-1}\beta_2\varepsilon_2 P - \gamma^{-1}P\varepsilon_2^T\beta_2^T + \beta_1\beta_1^T + \beta_2\beta_2^T = 0. \qquad \text{(C.11)}$$

From (C.8) and (C.9), the controllability gramian can be shown to be identical to (C.11). Also $C_{zd}P + D_{zd}B_{zd}^T = 0$ via (C.8) and (C.9). Since $D_{R_{zd}}D_{R_{zd}}^H = \gamma^2 I$, the result follows. ∇

REFERENCES

[GLDKS] Glover, K., D.J.N. Limebeer, J.C. Doyle, E.M. Kasenally and M.G. Safonov, "A characterization of all solutions to the four block general distance problem", *SIAM J. Contr. Optim.*, vol. 29, no. 2, pp. 283-324, Mar. 1991

[Gr] Green, M., *Optimal H_∞ control course*, Faculty of Engineering and Information Technology, Dept. of Systems Engineering, Australian National University, 3rd - 7th Feb., 1992.

[LAKG] Limebeer, D.J.N., B.D.O. Anderson, P.P. Khargonekar and M. Green, "A game theoretic approach to H^∞ control for time-varying systems", *SIAM J. Control Optim.*, vol. 30, no. 2, pp. 262-283, Mar. 1992.

Appendix D

A review of the Kalman filter and predictor

This Appendix reviews the Kalman filter and predictor for the problem of Figure 3.2 where there are two different plants which may possess a nonzero direct feedthrough term. It is assumed that the two plants G_1, G_2 are linear with state space representations denoted by $\begin{bmatrix} A & B_1 \\ C_1 & D_1 \end{bmatrix}$ and $\begin{bmatrix} A & B_2 \\ C_2 & D_2 \end{bmatrix}$ respectively. (If G_1 and G_2 have different dynamics one may proceed similary by defining $\overline{A} = diag\,[A_1, A_2]$,$\overline{C}_1 = [0\ C_1]$ and $\overline{C}_2 = [C_2\ 0]$.) The v_k and w_k are assumed to be zero mean, stationary, white noise processes with $E\{v_k v_k^T\} = R$, $E\{w_k w_k^T\} = Q$ and $E\{n_k v_k^T\} = 0$. The objective is to arrive at a linear, causal, stable filter H that estimates the output of G_1 from noisy measurements of G_2 such that the error z_k is optimum in a minimum variance sense.

The Kalman filter and predictor, for the case of proper plants are set out in Section D.1. Extensions to problems containing feedthrough terms and deterministic inputs are detailed in Sections D.2 and D.3 respectively; these formulations are used to generalise the EKF in Chapter 7.

D.1 Strictly proper plants.

The approach of [G; BGW, Sec. 3.4] is set out here, where an augmented plant model is contructed so that the Kalman recursions can be applied to obtain the filtered and predicted estimates. Consider initially the state estimation problem when $G_1 = G_2 \stackrel{z}{=} \begin{bmatrix} A & B_2 \\ C_2 & 0 \end{bmatrix}$

$$\begin{bmatrix} x \\ \xi \end{bmatrix}_{k+1} = \begin{bmatrix} A & 0 \\ I & 0 \end{bmatrix}_k \begin{bmatrix} x \\ \xi \end{bmatrix}_k + \begin{bmatrix} B_2 w \\ 0 \end{bmatrix}_k, \qquad (D.1)$$

$$y_k = [C_2 \quad 0]_k \begin{bmatrix} x \\ \xi \end{bmatrix}_k + v_k. \tag{D.2}$$

The x_k and ξ_k correspond to the current state and a one step delayed state of G_2 respectively. Application of the Kalman predictor recursions [AM] yields

$$\begin{bmatrix} \hat{x} \\ \hat{\xi} \end{bmatrix}_{k+1/k} = \begin{bmatrix} A_2 & 0 \\ I & 0 \end{bmatrix}_k \begin{bmatrix} \hat{x} \\ \hat{\xi} \end{bmatrix}_{k/k-1} + \begin{bmatrix} K \\ D \end{bmatrix}_k \left(y_k - [C_2 \quad 0]_k \begin{bmatrix} \hat{x} \\ \hat{\xi} \end{bmatrix}_{k/k-1} \right) \tag{D.3}$$

in which

$$\begin{bmatrix} K \\ D \end{bmatrix}_k = \begin{bmatrix} A_2 & 0 \\ I & 0 \end{bmatrix}_k \begin{bmatrix} P & P_{21}^T \\ P_{21} & P_{22} \end{bmatrix}_k \begin{bmatrix} C_2^T \\ 0 \end{bmatrix}_k \Omega_k^{-1}, \tag{D.4}$$

$$\begin{bmatrix} P & P_{21}^T \\ P_{21} & P_{22} \end{bmatrix}_{k+1} = \begin{bmatrix} A_2 & 0 \\ I & 0 \end{bmatrix}_k \begin{bmatrix} P & P_{21}^T \\ P_{21} & P_{22} \end{bmatrix}_k \begin{bmatrix} A_2 & 0 \\ I & 0 \end{bmatrix}_k^T - \begin{bmatrix} K \\ D \end{bmatrix}_k \Omega_k \begin{bmatrix} K \\ D \end{bmatrix}_k^T + \begin{bmatrix} B_2 Q B_2^T & 0 \\ 0 & 0 \end{bmatrix}_k \tag{D.5}$$

and

$$\Omega_k = [C_2 \quad 0]_k \begin{bmatrix} P & P_{21}^T \\ P_{21} & P_{22} \end{bmatrix}_k [C_2 \quad 0]_k^T + R_k. \tag{D.6}$$

From now on, the k-dependence is omitted except where it is felt that confusion may arise. The (1,1) partition of (D.5) is $P_{k+1} = AP_kA^T - K_k\Omega_kK_k^T + B_2QB_2^T$ where $\Omega_k = C_2P_kC_2^T + R$. The predictor recursion is

$$\hat{x}_{k+1/k} = A\hat{x}_{k/k-1} + K_k(y_k - C_2\hat{x}_{k/k-1}), \tag{D.7}$$

in which $\hat{x}_{k+1/k}$ is the estimate of $x_{k/k-1}$ given the data $\{y_k, y_{k-1}, y_{k-2}\ldots\}$ and K_k is the one step ahead predictor gain. The corrector recursion is

$$\hat{x}_{k/k} = \hat{x}_{k/k-1} + D_k(y_k - C_2\hat{x}_{k/k-1}). \tag{D.8}$$

Since $\hat{\xi}_{k+1/k} = \hat{x}_{k/k-1}$ is an estimate of x_k given the observations, D_k is the filter gain (and also happens to be a feedthrough term). Now suppose that $G_1 \stackrel{z}{=} \begin{bmatrix} A & B_1 \\ C_1 & 0 \end{bmatrix}$, then the objective is to estimate the output of G_1 from noisy observations of G_2. The predicted and filtered output estimates are denoted as $u_{k/k-1} = C_1\hat{x}_{k/k-1}$ and $u_{k/k} = C_1\hat{x}_{k/k}$ respectively. Equivalently

$$\begin{bmatrix} \hat{x}_{k+1/k} \\ u_{k/k-1} \\ u_{k/k} \end{bmatrix} = \begin{bmatrix} A - KC_2 & K \\ C_1 & 0 \\ C_1 - DC_2 & D \end{bmatrix}_k \begin{bmatrix} \hat{x}_{k/k-1} \\ y_k \end{bmatrix}. \tag{D.9}$$

It is seen that compared to the Kalman predictor, the Kalman filter possesses a direct feedthrough term. Denoting the prediction error as $y_k - C_2\hat{x}_{k/k-1}$, allows (D.9) to be expressed as

$$\begin{bmatrix} \hat{x}_{k+1/k} \\ u_{k/k-1} \\ u_{k/k} \end{bmatrix} = \begin{bmatrix} A & K \\ C_1 & 0 \\ C_1 & D \end{bmatrix}_k \begin{bmatrix} \hat{x}_{k/k-1} \\ y_k - C_2\hat{x}_{k/k-1} \end{bmatrix}. \tag{D.10}$$

D.2 Plants containing feedthroughs.

Extensions to problems where the plants possess a nonzero direct feedthrough term follow by solving a correlated noise problem. Consider the model with a direct feedthrough:

$$x_{k+1} = Ax_k + B_2 w_k, \tag{D.11}$$

$$y_k = C_2 x_k + D_2 w_k + v_k. \tag{D.12}$$

This is a correlated noise problem since (D.12) may be written equivalently as

$$y_k = C_2 x_k + \bar{v}_k, \tag{D.13}$$

where $cov\left\{\begin{bmatrix} w_k \\ \bar{v}_k \end{bmatrix}[w_k^T \ \bar{v}_k^T]\right\} = \begin{bmatrix} Q & S \\ S^T & \bar{R} \end{bmatrix}$ in which $\bar{R} = R + D_2 Q D_2^T$ and $S = QD_2^T$ [AM, Prob. 4.3, p. 114]. This correlated noise problem can be converted into a problem where the noise processes are uncorrelated by defining

$$\bar{w}_k = w_k - S_k \bar{R}^{-1} \bar{v}_k, \tag{D.14}$$

where $cov\left\{\begin{bmatrix} \bar{w}_k \\ \bar{v}_k \end{bmatrix}[\bar{w}_k^T \ \bar{v}_k^T]\right\} = \begin{bmatrix} \bar{Q} & 0 \\ 0 & \bar{R} \end{bmatrix}$ in which $\bar{Q} = Q - S\bar{R}^{-1}S^T$ [AM, p. 115]. Substituting for w_k of (D.14) into (D.11) and (D.12) yields

$$x_{k+1/k} = Ax_{k/k} + B_2 \bar{w}_k + B_2 S \bar{R}^{-1}(y_k - C_2 x_{k/k}). \tag{D.15}$$

Since the best estimate of $\bar{w}_k$ from observations of y_k is 0, the predicted state may be estimated by

$$\hat{x}_{k+1/k} = A\hat{x}_{k/k} + B_2 Q D_2^T \bar{R}^{-1}(y_k - C_2 \hat{x}_{k/k}) \tag{D.16}$$

and the filtered state estimate may be obtained from (D.8). Substituting (D.8) into (D.16) and rearranging yields

$$x_{k+1/k} = Ax_{k/k-1} + (AP_k C_2 + B_2 S)(C_2 P C_2^T + \bar{R})^{-1}(y_k - C_2 \hat{x}_{k/k-1}). \tag{D.17}$$

Thus in the case of direct feedthrough terms, the prediction (D.7) remains valid and the one-step-ahead predictor gain is given by

$$K_k = (AP_k C_2 + B_2 Q D_2^T)\Omega_t^{-1}, \tag{D.18}$$

where $\Omega_k = C_2 P_k C_2^T + D_2 Q D_2^T + R$. Since (D.16) provides an estimate of $A_2 x_k + B_2 w_k$, then a filtered estimate of $C_1 x_k + D_1 w_k$ can be obtained from

$$u_{k/k} = C_1 \hat{x}_{k/k} + D_1 Q D_2^T \bar{R}^{-1}(y_k - C_2 \hat{x}_{k/k}). \tag{D.19}$$

Therefore (D.8) also defines the correction when feedthroughs exist. The filter gain is calculated as

$$D_k = (C_1 P_k C_2^T + D_1 Q D_2^T)\Omega_t^{-1}. \tag{D.20}$$

D.3 Deterministic inputs.

Consider the signal model

$$x_{k+1} = Ax_k + B_2 w_k + p_k, \tag{D.21}$$

$$y_k = C_2 x_k + D_2 w_k + \bar{v}_k + q_k, \tag{D.22}$$

where p_k and q_k are known inputs. Then substituting for w_k of (D.14) into (D.21) and (D.22) results in

$$x_{k+1/k} = Ax_{k/k} + B_2\bar{w}_k + p_k + B_2 S\bar{R}^{-1}(y_k - C_2\hat{x}_{k/k} - q_k). \tag{D.23}$$

It follows from (D.23) that a prediction recursion for $\hat{x}_{k+1/k}$ is

$$\hat{x}_{k+1/k} = A\hat{x}_{k/k} + p_k + B_2 Q D_2^T \bar{R}^{-1}(y_k - C_2\hat{x}_{k/k} - q_k), \tag{D.24}$$

where $\hat{x}_{k/k}$ is obtained from (D.8). Similarly it is easily shown the filter output is given by

$$u_{k/k} = C_1\hat{x}_{k/k} + q_k + D_1 S\bar{R}^{-1}(y_k - C_2\hat{x}_{k/k} - q_k). \tag{D.25}$$

REFERENCES

[AM] Anderson, B. D. O. and J. B. Moore, *Optimal Filtering*, Prentice-Hall, Englewood Ciffs, N.J., 1979.

[BGW] Bitmead, R. B., M. Gevers and V. Wertz, *Adaptive Optimal Control, The Thinking Man's GPC*, Prentice-Hall, Australia, 1990.

[G] Green, M., Personal communication, Faculty of Engineering and Information Technology, Dept. of Systems Engineering, Australian National University, 6th Oct. 1994.

Appendix E

A derivation of the H_∞ filter

The game theoretic solution to the general discrete-time H_∞ control problem is set out in [LGW,Gr]. As is the case for continuous-time problems of the third kind where neither of D_{12} or D_{21} is invertable, the design of the controller requires the solution of two RDEs. Here the results of [LGW] are simplified for filtering problems where $D_{12} = I$. In particular, the arguments of [LAKG,Gr2] are used to set out a solution for discrete-time problems of the second kind. The resulting H_∞ filter requires the solution of just one RDE and has precisely the structure of the Kalman filter.

E.1 Perfect information control.

In the perfect information control problem it is assumed that the inputs and the states are available. The plant is assumed to have a time-varying state-space realisation

$$\begin{matrix} n \\ p \\ l \end{matrix}\begin{bmatrix} x_{k+1} \\ z_k \\ y_k \end{bmatrix} = \begin{matrix} n & l & m \\ \multicolumn{3}{c}{\begin{bmatrix} A & B_{11} & B_{12} \\ C_{11} & D_{11} & D_{12} \\ 0 & I & 0 \end{bmatrix}}_k \end{matrix}\begin{bmatrix} x_k \\ d_k \\ u_k \end{bmatrix}. \qquad (E.1)$$

For convenience of notation the k-dependence is omitted, except where confusion may arise. The problem may be reformulated in a J-factorization framework [GGLD,Gr] by defining $\tilde{B} = [B_1\ B_2]$, $\tilde{C} = \begin{bmatrix} C_1 \\ 0 \end{bmatrix}$, $\tilde{D} = \begin{bmatrix} D_{11} & D_{12} \\ I_l & 0 \end{bmatrix}$, $J_{pl} = \begin{bmatrix} I_p & 0 \\ 0 & -\gamma^2 I_l \end{bmatrix}$ and $J_{ml} = \begin{bmatrix} I_m & 0 \\ 0 & -\gamma^2 I_l \end{bmatrix}$. The objective is to find a minimum γ and a controller to satisfy the cost function

$$\|z\|^2 - \gamma^2\|d\|^2 = \|u - u^*\|^2 - \gamma^2\|d - d^*\|^2, \qquad (E.2)$$

for any input sequence d_k and any control sequence u_k, where d_k^* is the worst case input sequence and u_k^* is the best case control sequence. The saddle point conditions, namely the identification of d_k^* and u_k^* are reported in [LGW,Gr].

Theorem E.1. *Suppose for every input sequence d_k, there exists a $\overline{S}_k > 0$ and a $\overline{M}_k$ such that $\overline{M}_k^T \overline{S}_k^{-1} \overline{M}_k > 0$ for all k, where*

$$\overline{S} = \tilde{D}^T J_{pl} \tilde{D} + \tilde{B}^T X_k \tilde{B}, \tag{E.3}$$

$$\overline{M} = \tilde{C}^T J_{pl} \tilde{C} + A^T X_k \tilde{B}, \tag{E.4}$$

in which X_k satisifies the RDE

$$X_k = \tilde{C}^T J_{pl} \tilde{C} + A^T X_{k+1} A - M^T S^{-1} M \tag{E.5}$$

and $X_N = 0$. Then

$$\begin{bmatrix} i_k \\ j_k \end{bmatrix} = \overline{W} \begin{bmatrix} d_k \\ u_k \end{bmatrix} + \overline{L}^T x_k \tag{E.6}$$

satisifies (E.2) where

$$\overline{W}^T J_{ml} \overline{W} = \overline{S} \text{ with } \overline{W} = \begin{bmatrix} \overline{W}_{11} & \overline{W}_{12} \\ \overline{W}_{21} & 0 \end{bmatrix} \tag{E.7}$$

$$\text{and } \overline{L} = \begin{bmatrix} \overline{L}_1 \\ \overline{L}_2 \end{bmatrix} = J_{ml}^{-1} \overline{W}^{-T} \overline{M}. \tag{E.8}$$

Proof. See [LGW, Thm. 2.2, p. 394]

The saddle point conditions may be written

$$i_k = \overline{W}_{11} d_k + \overline{W}_{12} u_k + \overline{L}_1 x_k, \tag{E.9}$$

$$j_k = \overline{W}_{21} d_k + \overline{L}_2 x_k. \tag{E.10}$$

Now suppose that imperfect state measurements are available, namely the observations

$$y_k = C_{21} x_k + d_k. \tag{E.11}$$

Then the task is to combine the perfect information controller together with an observer that attempts to reconstruct the state. Since d_k is not accessible, the observer can only be driven by u_k and y_k. Consider the observer

$$\hat{x}_{k+1} = A\hat{x}_k + B_{11} d_k + B_{12} u_k . \tag{E.12}$$

Substituting for d_k from (E.11) into (E.9) results in

$$u_k = \overline{W}_{12}^{-1} (i_k - \overline{W}_{11} y_k - \overline{W}_{11} C_{21} x_k - \overline{L}_1 x_k) \tag{E.13}$$

and similarly (E.10) yields

$$j_k = \overline{W}_{21} y_k - \overline{W}_{21} C_{21} x_k + \overline{L}_2 x_k. \tag{E.14}$$

Substituting for d_k and u_k into (E.12) yields the controller

$$\begin{bmatrix} \hat{x}_{k+1} \\ u_k \\ j_k \end{bmatrix} \overset{s}{=} \begin{bmatrix} A - B_{11}C_{21} + B_2\overline{W}_{12}^{-1}\overline{W}_{11}C_{21} - B_{12}\overline{W}_{12}^{-1}\overline{L}_1 & B_{11} - B_{12}\overline{W}_{12}^{-1}\overline{W}_{11} & B_{12}\overline{W}_{12}^{-1} \\ \overline{W}_{12}^{-1}\overline{W}_{11}C_{21} - \overline{W}_{12}^{-1}\overline{L}_1 & -\overline{W}_{12}^{-1}\overline{W}_{11} & \overline{W}_{12}^{-1} \\ -\overline{W}_{21}C_{21} + \overline{L}_2 & \overline{W}_{21} & 0 \end{bmatrix} \begin{bmatrix} \hat{x}_k \\ y_k \\ i_k \end{bmatrix}. \tag{E.15}$$

This controller corresponds to (E.11), that is $D_{21} = I$, whereas in filtering problems $D_{12} = I$. The solution to this dual problem can be found using the arguments of [Gr2,IG], by taking the inverse adjoint of the controller for the adjoint problem. The map of the controller for the adjoint problem may be written as

$$\begin{bmatrix} A^T - C_{11}^T B_{12}^T + C_{21}^T W_{21}^{-T} W_{11}^T B_{12}^T - C_{21}^T W_{12}^{-T} L_1^T & -C_{11}^T + C_{21}^T W_{12}^{-T} W_{11}^T & -C_{21}^T W_{21}^{-T} \\ -W_{21}^{-T} W_{11}^T B_{21}^T + W_{21}^{-T} L_1^T & -W_{21}^{-T} W_{11}^T & W_{21}^{-T} \\ W_{12}^T B_{12}^T - L_2^T & W_{12}^T & 0 \end{bmatrix}, \tag{E.16}$$

where

$$S = WJ_{qm}W^T = \overline{D}\, J_{lm}\overline{D}^T + \overline{C}\, P_k \overline{C}^T, \tag{E.17}$$

$$M = \overline{B}\, J_{lm}\overline{D}^T + AP_k\overline{C}^T, \tag{E.18}$$

$$L = [L_1 \;\; L_2] = M(J_{qm}W^T)^{-1}, \tag{E.19}$$

in which $\overline{B} = [B_{11} \;\; 0]$, $\overline{C} = \begin{bmatrix} C_{11} \\ C_{21} \end{bmatrix}$, $\overline{D} = \begin{bmatrix} D_{11} & I \\ D_{21} & 0 \end{bmatrix}$, $J_{qm} = \begin{bmatrix} I_q & 0 \\ 0 & -\gamma^2 I_m \end{bmatrix}$ and P_k satisifes the RDE

$$P_{k+1} = \overline{B}\, J_{lm}\overline{B}^T + AP_kA^T - MS^{-1}M^T. \tag{E.20}$$

The inverse adjoint of (D.16) is

$$\begin{bmatrix} A - B_{12}C_{11} + B_{12}W_{11}W_{21}^{-1}C_{21} - L_1W_{12}^{-1}C_{21} & B_{21}W_{11}W_{21}^{-1} - L_1W_{21}^{-1} & L_2 - B_{12}W_{12} \\ C_{11} - W_{11}W_{12}^{-1}C_{21} & -W_{11}W_{21}^{-1} & W_{12} \\ W_{21}^{-1}C_{21} & W_{21}^{-1} & 0 \end{bmatrix}. \tag{E.21}$$

As in the continuous-time case, i_k and j_k are scaled by γ, this ensures that the closed loop system is all-pass (a proof is given in Appendix F). The resulting open loop filter is given by the map

$$\begin{bmatrix} A - B_{12}C_{11} + B_{12}W_{11}W_{21}^{-1}C_{21} - L_1W_{12}^{-1}C_{21} & B_{21}W_{11}W_{21}^{-1} - L_1W_{21}^{-1} & \gamma(L_2 - B_{12}W_{12}) \\ C_{11} - W_{11}W_{12}^{-1}C_{21} & -W_{11}W_{21}^{-1} & \gamma W_{12} \\ \gamma W_{21}^{-1}C_{21} & \gamma W_{21}^{-1} & 0 \end{bmatrix}. \tag{E.22}$$

REFERENCES

[GGLD] M. Green, K. Glover, D. J. N. Limebeer, and J. C. Doyle, "A J-spectral factorization approach to H_∞ control", *Siam J. Control Optim.*, vol. 28, no. 6, pp. 1350-1371, Nov. 1990.

[GLDKS] K. Glover, D.J.N. Limebeer, J.C. Doyle, E.M. Kasenally and M.G. Safonov, "A characterization of all solutions to the four block general distance problem", *SIAM J. Contr. Optim.*, vol. 29, no. 2, pp. 283-324, Mar. 1991

[Gr] M. Green, "H_∞ controller synthesis by J-lossless coprome factorization", *Siam J. Contr. Optim.*, vol. 30, no. 3, pp. 522-547, May 1992.

[Gr2] M. Green, *Optimal H_∞ control course*, Faculty of Engineering and Information Technology, Dept. of Systems Engineering, Australian National University, 3rd - 7th Feb., 1992.

[IG] Iglesias, P. I. and K. Glover, "State space approach to discrete-time H_∞ control", *Int. J. Contr.*, vol. 54, pp. 1031-1073, 1991.

[LAKG] D.J.N. Limebeer, B.D.O. Anderson, P.P. Khargonekar and M. Green, "A game theoretic approach to H^∞ control for time-varying systems", *SIAM J. Contr. Optim.*, vol. 30, no. 2, pp. 262-283, Mar. 1992.

Appendix F

Discrete-time, all-pass error scaling

This Appendix reports a negative result, namely that a scalar contractive operator cannot be found which ensures that the closed loop filter exhibits all-pass error. Firstly the required definition of all-pass error system, namely the dual of [IG, Lem. 2.7, p. 1042] is stated. Next it is shown that the open loop filter (4.15) yields all-pass error and finally the closed loop case is addressed.

Lemma F.1. *Let* $R \overset{z}{=} \begin{bmatrix} A & B \\ C & D \end{bmatrix}$ *with (C,A) detectable, suppose that* $P = P^T$ *satisfies*

$$P = APA^T + BB^T. \tag{F.1}$$

Then

$$RR^H = DD^T + CPC^T \tag{F.2}$$

if

$$DB^T + CPA^T = 0. \tag{F.3}$$

Proof. Writing $R = C(zI - A)^{-1}B + D$, expanding out the terms of RR^H, substituting for P and using (F.3) results in (F.2). ∇

F.1 The open loop error system.

Lemma F.2. *The error system corresponding to the open loop filter (4.15) is all-pass.*

Proof. Defining $e_{k+1} = x_{k+1} + \hat{x}_{k+1}$, then it can be shown that R_{zd} is given by

$$\begin{bmatrix} e_{k+1} \\ z_k \\ s_k \end{bmatrix} \overset{z}{=} \begin{bmatrix} A-L_1W_{21}^{-1}C_2 & -L_1W_{21}^{-1} & B_1-L_1W_{21}^{-1}D_2 & \gamma L_2 \\ C_1-W_{11}W_{21}^{-1}C_2 & -W_{11}W_{21}^{-1} & D_1-W_{11}W_{21}^{-1}D_2 & \gamma W_{12} \\ \gamma W_{21}^{-1}C_2 & \gamma W_{21}^{-1} & \gamma W_{21}^{-1}D_2 & 0 \end{bmatrix} \begin{bmatrix} e_k \\ n_k \\ v_k \\ r_k \end{bmatrix}. \qquad (F.4)$$

The second row of condition (F3) for the system (F.4) yields

$$\gamma W_{21}^{-1}(-W_{12}^{-1}L_1^T + D_2B_1^T - D_2D_2^TW_{12}^{-1}L_1^T + C_2PA^T - C_2PC_2^TW_{12}^{-1}L_1^T) = 0. \qquad (F.6)$$

By equating the infinite horizon solution of (4.14) to the controllability gramian (F.1) and using (B.3) results in

$$L_1 = (APC_2^T + B_2QD_2^T)W_{12}^{-1}. \qquad (F.7)$$

Substituting (4.18) into (4.13) also yields (F.7) and the result follows. ∇

In the continuous-time (Appendix C), the conditions yielding an all-pass open loop system were used to find a scalar value for U. The same strategy is attempted here. For brevity (F.4) may be written as

$$R_{zd} \overset{z}{=} \begin{bmatrix} A+\alpha_1 & \beta_1 & \beta_2 & \beta_3 \\ \varepsilon_1 & \delta_1 & \delta_2 & \delta_3 \\ \varepsilon_2 & \delta_4 & \delta_5 & 0 \end{bmatrix}, \qquad (F.8)$$

where $\alpha_1 = -L_1W_{21}^{-1}C_2$, $\beta_1 = -L_1W_{21}^{-1}$, $\varepsilon_1 = C_1 - W_{11}W_{21}^{-1}C_2$ and $\delta_1 = -W_{11}W_{21}^{-1}$ etc. Applying the all-pass condition (F.3) to the system (F.8) results in

$$\delta_1\beta_1^T + \delta_2\beta_2^T + \delta_3\beta_3^T + C_1P(A+\alpha_1)^T = 0, \qquad (F.9)$$

$$\delta_4\beta_1^T + \delta_5\beta_2^T + C_2P(A+\alpha_1)^T = 0. \qquad (F.10)$$

Equating the infinite horizon solution of (4.14) to the controllability gramian (F.1) for (F.8) yields

$$-\alpha_1PA^T - AP\alpha_1 - \alpha_1P\alpha_1^T + B_2QB_2^T - MS^{-1}M^T = \beta_1\beta_1^T + \beta_2\beta_2^T + \beta_3\beta_3^T. \qquad (F.11)$$

This result will be used in an analysis of the closed loop system.

F.2 The closed loop error system.

Proposition F.3. *It is not possible to find a scalar for U which ensures that the system (F.4) is all-pass.*

Proof. By substituting $U = k$ into (F.4) yields the closed loop system

$$\begin{bmatrix} e_{k+1} \\ z_k \end{bmatrix} = \begin{bmatrix} A+\alpha_1+k\beta_3\varepsilon_2 & \beta_1+k\beta_3\delta_4 & \beta_2+k\beta_3\delta_5 \\ \varepsilon_1+k\delta_3\varepsilon_2 & \delta_1+k\delta_3\delta_4 & \delta_2+k\delta_3\delta_5 \end{bmatrix} \begin{bmatrix} e_k \\ n_k \\ v_k \end{bmatrix}. \qquad (F.12)$$

By equating the infinite horizon solution of the (4.14) to the controllability gramian (F.1) for (F.12) and simplifying via (F.9) and (F.10) results in the following condition for the scalar

$$k^2 = (\delta_4\delta_4^T + \delta_5\delta_5^T + C_2PC_2^T)^{-1}. \tag{F.13}$$

For the error system (F.12) to be all-pass, condition (F.3) needs to be met, this leads to

$$\tau_1 + \tau_2 + \tau_3 + \tau_4 = 0, \tag{F.14}$$

where

$$\begin{aligned}
\tau_1 &= \delta_1\beta_1^T + \delta_2\beta_2^T + C_1PA^T + C_1P\alpha_1^T + \delta_3\beta_3^T, \\
\tau_2 &= k\delta_3(\delta_4\beta_1^T + \delta_5\beta_2^T + C_2PA^T + C_2P\alpha_1^T), \\
\tau_3 &= k^2\delta_3\delta_4\delta_4^T\beta_3^T + k^2\delta_3\delta_5\delta_5^T\beta_3^T + k^2\delta_3C_2PC_2^T\beta_3^T - \delta_3\beta_3^T, \\
\tau_4 &= k^2\delta_3\delta_5\delta_4^T\beta_3^T + k\delta_1\delta_4^T\beta_3^T + k\delta_2\delta_4'\beta_3^T + kC_1PC_2^T\beta_3^T - k^2\delta_3\delta_5\delta_5^T\beta_3^T.
\end{aligned} \tag{F.15}$$

Now $\tau_1 = 0$ via (F.9), $\tau_2 = 0$ via (F.10). Also from (F.13,) it follows that $\tau_3 = 0$ and therefore (F.14) implies $\tau_4 = 0$. Thus the scalar needs to simultaneously satisfy (F.13) and $\tau_4 = 0$. It is argued that in general a solution for k cannot be found unless conditions are imposed on the plant. ∇

REFERENCE

[IG] Iglesias, P. I. and K. Glover, "State space approach to discrete-time H_∞ control", *Int. J. Cont.*, vol. 54, no. 5, pp. 1031-1073, 1991.

Appendix G

High SNR Conditions

Consider the stationary output estimation problem in which the signal model is known, the input noises are zero mean, gaussian white processes with known covariances. It turns out that compared to the Kalman filter, H_∞ filter exhibits a small reduction in the maximum of the error spectrum magnitude, provided that the SNR is sufficiently high. The objective of this appendix is to quantify conditions for when "the SNR is sufficiently high".

The error spectrum has two components, the part due to the process noise and the part due to the observation noise. The approach taken here is to report which error component is observed to dominate and then attempt to define sufficient conditions for this to be the case. Conventionally SNR is defined as either the signal to observation noise ratio or the ratio of the signal plus noise to noise ratio. Here the reference to SNR is quite loose. Rather, an attempt is made to identify when certain observations prevail. It is contended that an examination the error spectra does contribute to an understanding of how and when the H_∞ filter offers a reduction in the maximum of the magnitude of the error spectrum. However the ensuing conditions are stated in terms of filter gain or the solution of an ARE, which do not lend themselves to be easily interpreted.

G.1 Continuous-time output Estimation.

G.1.1 Notation.

The stationary plants of Figure 3.2 are assumed to have known state space representations denoted by $G_2 = G_1 \stackrel{s}{=} \begin{bmatrix} A & B \\ C & 0 \end{bmatrix}$. The observations may be modelled as

$$\dot{x} = Ax + BQ^{1/2}w, \quad y = Cx + R^{1/2}v \tag{G.1}$$

where $v(t)$, $w(t)$ are zero mean, gaussian, white processes and $E\{vv^T\} = I$, $E\{ww^T\} = I$. The Kalman filter is denoted by

$$\begin{bmatrix} \dot{\hat{x}} \\ u \end{bmatrix} \overset{s}{=} \begin{bmatrix} A - \tilde{K}C & \tilde{K} \\ C & 0 \end{bmatrix} \begin{bmatrix} \hat{x} \\ y \end{bmatrix}, \tag{G.2}$$

where the filter gain is given by $\tilde{K} = \tilde{P}C^T$ and $\tilde{P}$ arises from the ARE

$$0 = A\tilde{P} + \tilde{P}A^T - \tilde{P}C^T R^{-1} C\tilde{P} + BQB^T. \tag{G.3}$$

The output error is denoted as $z = Ce$, where the state error is defined as $e = x - \hat{x}$. Then from (G.1) and (G.2) the map from $d = \begin{bmatrix} v \\ w \end{bmatrix}$ to z is given by

$$\begin{bmatrix} \dot{e} \\ z \end{bmatrix} \overset{s}{=} \begin{bmatrix} A - \tilde{K}C & -\tilde{K}R^{1/2} & BQ^{1/2} \\ C & 0 & 0 \end{bmatrix} \begin{bmatrix} e \\ v \\ w \end{bmatrix}. \tag{G.4}$$

This error system may also be written as $z = \tilde{R}_{zv}v + \tilde{R}_{zw}w$, where $\tilde{R}_{zv} \overset{s}{=} \begin{bmatrix} A - \tilde{K}C & -\tilde{K}R^{1/2} \\ C & 0 \end{bmatrix}$ and $\tilde{R}_{zw} \overset{s}{=} \begin{bmatrix} A - \tilde{K}C & BQ^{1/2} \\ C & 0 \end{bmatrix}$. These error components may be written equivalently as transfer functions, namely $\tilde{R}_{zv} = -C(sI - A + \tilde{K}C)^{-1}\tilde{K}R^{1/2}$ and $\tilde{R}_{zw} = C(sI - A + \tilde{K}C)^{-1}BQ^{1/2}$. The error spectrum is given by $\tilde{R}_{zd}\tilde{R}_{zd}^H = \tilde{R}_{zv}\tilde{R}_{zv}^H + \tilde{R}_{zw}\tilde{R}_{zw}^H$, in which

$$\tilde{R}_{zv}\tilde{R}_{zv}^H = C(sI - A + \tilde{K}C)^{-1}\tilde{K}R\tilde{K}^T(sI - A + \tilde{K}C)^{-H}C^T, \tag{G.5}$$

$$\tilde{R}_{zw}\tilde{R}_{zw}^H = C(sI - A + \tilde{K}C)^{-1}BQB^T(sI - A + \tilde{K}C)^{-H}C^T. \tag{G.6}$$

The H_∞ filter for known input covariances is denoted by

$$\begin{bmatrix} \dot{\hat{x}} \\ u \end{bmatrix} \overset{s}{=} \begin{bmatrix} A - KC & K \\ C & 0 \end{bmatrix} \begin{bmatrix} \hat{x} \\ y \end{bmatrix}, \tag{G.7}$$

where the filter gain is given by $K = PC^T$ and P arises from the ARE

$$0 = AP + PA^T - PC^T(R^{-1} - \gamma^{-2}I)CP + BQB^T. \tag{G.8}$$

The H_∞ error components are similarly given by (5.9) and (5.10)

$$R_{zv}R_{zv}^H = C(sI - A + KC)^{-1}KRK^T(sI - A + KC)^{-H}C^T, \tag{G.9}$$

$$R_{zw}R_{zw}^H = C(sI - A + KC)^{-1}BQB^T(sI - A + KC)^{-H}C^T. \tag{G.10}$$

G.1.2 Known plants.

If $G(s)$ is a known, stable plant, a real positive definite solution to (G.3) has been found and $0 > \tilde{P}A^T + A\tilde{P}$, then it is claimed that

$$|\tilde{R}_{zw}\tilde{R}^H_{zw}(j\omega)|^2 > |\tilde{R}_{zv}\tilde{R}^H_{zv}(j\omega)|^2 \quad \forall\omega\varepsilon\mathbf{R}. \tag{G.11}$$

This can be seen by writing the Kalman ARE (G.3) as

$$BQB^T = \tilde{K}R\tilde{K}^T - \tilde{P}A^T - A\tilde{P}. \tag{G.12}$$

From the above-mentioned condition, and (G.12) it follows that $BQB^T > \tilde{K}R\tilde{K}^T$. The claim (G.11) follows from the sum of (G.5) and (G.6). That is, at high SNR the error component due to the measurement noise is small and, the Kalman error spectrum is dominated by the error component due to the process noise.

The converse is true in the case of a H_∞ filter, namely at high SNR, the maximum magnitude of the error component due to the measurement noise is observed to dominate. Suppose that $G(s)$ is a stable plant, a γ has been found to ensure $P > 0$ and the SNR is sufficiently high such that

$$\gamma^{-2}PC^TCP + PA^T + AP > 0, \tag{G.13}$$

then

$$|R_{zv}R^H_{zv}(j\omega)|^2 > |R_{zw}R^H_{zw}(j\omega)|^2 \quad \forall\omega\varepsilon\mathbf{R}. \tag{G.14}$$

This can be seen by writing the H_∞ ARE (G.8) may be written as

$$KRK^T = BQB^T + PA^T + AP + \gamma^{-2}PC^TCP. \tag{G.15}$$

From the condition (G.13) and (G.15), $KRK^T > BQB^T$. The claim follows from the sum of (G.9) and (G.10).

The H_∞ filter exhibits a comparative reduction in the peak of the error spectrum magnitude because the peak magnitude of $\tilde{R}_{zw}\tilde{R}^H_{zw}(s)$ is greater than that of $R_{zv}R^H_{zv}(s)$ and the peak magnitude of $\tilde{R}_{zv}\tilde{R}^H_{zv}(s)$ is greater than that of $R_{zw}R^H_{zw}(s)$. In particular if

$$\sup_{\omega\varepsilon\mathbf{R}} |\tilde{R}_{zw}\tilde{R}^H_{zw}(j\omega)|^2 > \sup_{\omega\varepsilon\mathbf{R}} |R_{zv}R^H_{zv}(j\omega)|^2 \tag{G.16}$$

and the SNR is sufficiently high such that

$$\sup_{\omega\varepsilon\mathbf{R}} |\tilde{R}_{zv}\tilde{R}^H_{zv}(j\omega)|^2 > \sup_{\omega\varepsilon\mathbf{R}} |R_{zw}R^H_{zw}(j\omega)|^2, \tag{G.17}$$

then

$$\sup_{\omega\varepsilon\mathbf{R}} |\tilde{R}_{zd}\tilde{R}^H_{zd}(j\omega)|^2 > \sup_{\omega\varepsilon\mathbf{R}} |R_{zd}R^H_{zd}(j\omega)|^2. \tag{G.18}$$

The claim (G.18) follows from the sum of (G.16) and (G.17).

It is somewhat more enlightening to consider low-pass plants which may be defined as follows.

Definition. A transfer function $G(s)$ is low-pass if $\exists\ \omega_0 > 0$ such that $|G(j\omega)| \to 0$ monotonically as $\omega \to 0$, $\omega > \omega_0$. Further, it is said to be strictly low-pass if $\omega_0 = 0$.

If R_{zd} and $\tilde{R}_{zd}$ are strictly low-pass with

$$(-A+\tilde{K}C)^{-1}BQB^T(-A+\tilde{K}C)^{-T} > (-A+KC)^{-1}KRK^T(-A+KC)^{-T} \tag{G.19}$$

and the SNR is sufficiently high such that

$$(-A+\tilde{K}C)^{-1}\tilde{K}R\tilde{K}^T(-A+\tilde{K}C)^{-T} > (-A+KC)^{-1}BQB^T(-A+KC)^{-T}, \tag{G.20}$$

then

$$|\tilde{R}_{zd}\tilde{R}^H_{zd}(j\omega)|^2_{\omega=0} > |R_{zd}R^H_{zd}(j\omega)|^2_{\omega=0}. \tag{G.21}$$

This follows by premultiplying (G.19) by C and postmultiplying by C^T yielding

$$|\tilde{R}_{zw}\tilde{R}^H_{zw}(j\omega)|^2_{\omega=0} > |R_{zv}R^H_{zv}(j\omega)|^2_{\omega=0}, \tag{G.22}$$

and similary at dc (G.18) is equivalent to

$$|\tilde{R}_{zv}\tilde{R}^H_{zv}(j\omega)|^2_{\omega=0} > |R_{zw}R^H_{zw}(j\omega)|^2_{\omega=0}. \tag{G.23}$$

The claim (G.21) follows from the sum of (G.23) and (G.22).

With the error defined by $z = C(x - \hat{x})$, it follows from Figure 3.2 that if the plants are SISO, the error components may also be expressed as

$$R_{zv}(s) = -\sigma_v H(s), \tag{G.24}$$

$$R_{zw}(s) = -\sigma_w(H(s) - 1)G(s). \tag{G.25}$$

The high SNR observation (G.14) states that the maximum of $|R_{zv}(s)|$ is greater than the maximum of $|R_{zw}(s)|$. Further, suppose that the SNR is very high such that the $|R_{zw}(s)|$ is insignificant compared to $|R_{zv}(s)|$. Clearly $|R_{zw}(s)|$ is minimised by the choice of $|H(s)| \approx 1$, in which case $|R_{zd}R^H_{zd}(s)| \approx \sigma_v^2$. Since the H_∞ filter is designed such that $|R_{zd}R^H_{zd}(s)| \leq \gamma^2$, then it follows that a convenient *a priori* choice is $\gamma \approx \sigma_v$. From (G.8) it is seen that this yields a $P > 0$, provided that $AP + PA^T < 0$.

Thus at very high SNR the optimum H_∞ solution is a "do nothing filter", this is more apparent in the scalar case (see Examples 5.1, 5.2 and 5.3).

G.2 Discrete-time output estimation.

G.2.1 Notation.

The stationary plants of Figure 3.2 are assumed to have known state space representations denoted by $G_2 = G_1 \stackrel{s}{=} \begin{bmatrix} A & B \\ C & D \end{bmatrix}$. In the case that $D = 0$, the observations may be modelled as

$$x_{k+1} = Ax_k + BQ^{1/2}w_k, \quad y_k = Cx_k + R^{1/2}v_k, \tag{G.26}$$

where the v_k, w_k are zero mean, gaussian white noise processes and $E\{vv^T\} = I$, $E\{ww^T\} = I$. The Kalman predictor is denoted by

$$\begin{bmatrix} \hat{x}_{k+1/k} \\ u_{k/k-1} \end{bmatrix} \stackrel{z}{=} \begin{bmatrix} A - \tilde{K}C & \tilde{K} \\ C & 0 \end{bmatrix} \begin{bmatrix} \hat{x}_{k/k-1} \\ y_k \end{bmatrix}, \tag{G.27}$$

where the one-step-ahead predictor gain is given by $\tilde{K} = A\tilde{P}C^T(C\tilde{P}C^T + R)^{-1}$ and $\tilde{P}$ arises from the ARE

$$\tilde{P} = A\tilde{P}A^T - A\tilde{P}C^T(C\tilde{P}C^T + R)^{-1}C\tilde{P}A^T + BQB^T. \tag{G.28}$$

The output prediction error is denoted by $z_{k/k-1} = Ce_{k/k-1}$ where $e_{k/k-1} = x_k - \hat{x}_{k/k-1}$ is the state prediction error. Then from (5.31) and (5.32) the map from $d_k = \begin{bmatrix} v_k \\ w_k \end{bmatrix}$ to $z_{k/k-1}$ is given by

$$\begin{bmatrix} e_{k/k-1} \\ z_{k/k-1} \end{bmatrix} \stackrel{z}{=} \begin{bmatrix} A - \tilde{K}C & -\tilde{K}R^{1/2} & BQ^{1/2} \\ C & 0 & 0 \end{bmatrix} \begin{bmatrix} e_k \\ v_k \\ w_k \end{bmatrix}. \tag{G.29}$$

This error system may also be written as $z_{k/k-1} = \tilde{R}_{zv}v_k + \tilde{R}_{zw}w_k$, where $\tilde{R}_{zv} \stackrel{z}{=} \begin{bmatrix} A - \tilde{K}C & -\tilde{K}R^{1/2} \\ C & 0 \end{bmatrix}$ and $\tilde{R}_{zw} \stackrel{z}{=} \begin{bmatrix} A - \tilde{K}C & BQ^{1/2} \\ C & 0 \end{bmatrix}$. These error components may be written equivalently as transfer functions, namely $\tilde{R}_{zv} = C(zI - A + \tilde{K}C)^{-1}\tilde{K}R^{1/2}$ and $\tilde{R}_{zw} = C(zI - A + \tilde{K}C)^{-1}BQ^{1/2}$. The error spectrum is given by $\tilde{R}_{zd}\tilde{R}_{zd}^H = \tilde{R}_{zv}\tilde{R}_{zv}^H + \tilde{R}_{zw}\tilde{R}_{zw}^H$, in which

$$\tilde{R}_{zv}\tilde{R}_{zv}^H = C(zI - A + \tilde{K}C)^{-1}\tilde{K}R\tilde{K}^T(zI - A + \tilde{K}C)^{-H}C^T, \tag{G.30}$$

$$\tilde{R}_{zw}\tilde{R}_{zw}^H = C(zI - A + \tilde{K}C)^{-1}BQB^T(zI - A + \tilde{K}C)^{-H}C^T. \tag{G.31}$$

The Kalman filter is denoted by

$$\begin{bmatrix} x_{k+1/k} \\ u_{k/k} \end{bmatrix} \stackrel{z}{=} \begin{bmatrix} A - \tilde{K}C & \tilde{K} \\ C - \tilde{D}C & \tilde{D} \end{bmatrix} \begin{bmatrix} x_{k/k-1} \\ y_k \end{bmatrix}, \tag{G.32}$$

where the filter gain is given by $\tilde{D} = C\tilde{P}C^T(C\tilde{P}C^T + R)^{-1}$. The H_∞ filter for known input covariances is denoted by

$$\begin{bmatrix} \underline{x}_{k+1/k} \\ \underline{u}_{k/k} \end{bmatrix} \stackrel{z}{=} \begin{bmatrix} A - \underline{K}C & \underline{K} \\ C - \underline{D}C & \underline{D} \end{bmatrix} \begin{bmatrix} \underline{x}_{k/k-1} \\ y_k \end{bmatrix}, \tag{G.33}$$

where $\underline{K} = AP\,C^T(CP\,C^T + R)^{-1}$ is the predictor gain, $\underline{D} = CP\,C^T(CP\,C^T + R)^{-1}$ is the filter gain and P arises from the ARE

$$P = APA^T - AP\begin{bmatrix} -C^T \\ C^T \end{bmatrix}\begin{bmatrix} CP_kC^T - \gamma^2 \mathrm{I} & -CPC^T \\ -CPC^T & CPC^T + R \end{bmatrix}^{-1}[-C \;\; C]PA^T + BQB^T. \tag{G.34}$$

For convenience (5.34) may be written as

$$P = APA^T - L_1L_1^T + \gamma^2 L_2L_2^T + BQB^T, \tag{G.35}$$

in which $L_1L_1^T = APC^T(CPC^T + R)^{-1}CPA^T$ and L_2 is defined within Section 4.2.

G.2.2 Known plants.

It is claimed that (i) If $G(z)$ is a stable plant, a real positive definite solution to (G.28) has been found and $0 > A\tilde{P}A^T - \tilde{P}$ then

$$\sup_{\omega\in\{-\pi,\pi\}} |\tilde{R}_{zw}\tilde{R}_{zw}^H(e^{j\omega})|^2 > \sup_{\omega\in\{-\pi,\pi\}} |\tilde{R}_{zv}\tilde{R}_{zv}^H(e^{j\omega})|^2 \tag{G.36}.$$

(ii) If in addition, the SNR is sufficiently high such that $\gamma^2 L_2L_2^T + APA^T - P > 0$, then

$$\sup_{\omega\in\{-\pi,\pi\}} |R_{zv}R_{zv}^H(e^{j\omega})|^2 > \sup_{\omega\in\{-\pi,\pi\}} |R_{zw}R_{zw}^H(e^{j\omega})|^2. \tag{G.37}$$

(iii) If $\sup_{\omega\in\{-\pi,\pi\}} |\tilde{R}_{zw}\tilde{R}_{zw}^H(e^{j\omega})|^2 > \sup_{\omega\in\{-\pi,\pi\}} |R_{zv}R_{zv}^H(e^{j\omega})|^2$ and the SNR is sufficiently high such that $\sup_{\omega\in\{-\pi,\pi\}} |\tilde{R}_{zv}\tilde{R}_{zv}^H(e^{j\omega})|^2 > \sup_{\omega\in\{-\pi,\pi\}} |R_{zw}R_{zw}^H(e^{j\omega})|^2$, then

$$\sup_{\omega\in\{-\pi,\pi\}} |\tilde{R}_{zd}\tilde{R}_{zd}^H(e^{j\omega})|^2 > \sup_{\omega\in\{-\pi,\pi\}} |R_{zd}R_{zd}^H(e^{j\omega})|^2. \tag{G.38}$$

(iv) If R_{zd} and $\tilde{R}_{zd}$ are low-pass with

$$(I - A + \tilde{K}C)^{-1}BQB^T(I - A^T + \tilde{K}C)^{-T} > (I - A + \underline{K}C)^{-1}\underline{K}R\underline{K}^T(I - A^T + \underline{K}C)^{-T}$$

and the SNR is sufficiently high such that

$$(I - A + \tilde{K}C)^{-1}\tilde{K}R\tilde{K}^T(I - A^T + \tilde{K}C)^{-T} > (I - A + \underline{K}C)^{-1}BQB^T(I - A^T + \underline{K}C)^{-T},$$

then

$$|\tilde{R}_{zd}\tilde{R}_{zd}^H(e^{j\omega})|_{\omega=0}^2 > |R_{zd}R_{zd}^H(e^{j\omega})|_{\omega=0}^2. \tag{G.39}$$

Since the structures of the one-step-ahead predictors are the same as the continuous-time filters, it is not at all surprising that the same observations arise. An understanding of how and when the H_∞ filter minimises the peak of the error spectrum magnitude may be obtained by observing which error components dominate. It is easy to verify (G.36) through to (G.39) via the approach of the previous section. The observation (G.39) is included here to emphasise that in the stationary case, the problem can be investigated *a priori*.

The key observation is (G.38), namely at high SNR the H_∞ filter minimises $|R_{zw}R_{zw}^H(z)|$ via a do nothing filter. Unfortunately it is not possible to set out the high SNR conditions without reference to the solution of an ARE, in which case the actual error spectra may just as well be examined. To this end, some scalar examples are presented in Section 5.2.

G.3 Equalisation.

The discussion pertaining to equalisation problems uses the same notation introduced in Section G.1. In particular, tilded variables denote those specific to Kalman solutions.

Suppose that the channel is band-pass and has one or more low frequency, minimum phase zeros. It has been observed from studying various numerical examples that the Kalman solution to the equaliser problem behaves quite differently at low observation noise than for high noise. In particular, the observation noise limits how well the equaliser inverts the channel.

In respect of the equaliser problem, if the observation noise is sufficiently small so that

$$\sup_{\omega \in \mathbf{R}} |\tilde{R}_{zw}\tilde{R}_{zw}^H(j\omega)|^2 < \sup_{\omega \in \mathbf{R}} |\tilde{R}_{zv}\tilde{R}_{zv}^H(j\omega)|^2, \tag{G.40}$$

then the Kalman solution attempts to invert the channel, that is $\tilde{H}(s) \approx G^{-1}(s)$ and irrespective of how much σ_w^2 is increased, the error will be due to both $\tilde{R}_{zv}(s)$ and $\tilde{R}_{zw}(s)$. Conversely if the observation noise is sufficiently large so that

$$\sup_{\omega \in \mathbf{R}} |\tilde{R}_{zw}\tilde{R}_{zw}^H(j\omega)|^2 >> \sup_{\omega \in \mathbf{R}} |\tilde{R}_{zv}\tilde{R}_{zv}^H(j\omega)|^2, \tag{G.41}$$

then the Kalman solution behaves like a filter and does not invert the channel, that is $\sup_{\omega \in \mathbf{R}} |\tilde{H}G_2(j\omega)| << 1$ and irrespective of how much σ_v^2 is increased, the peak error will be dominated by the $\tilde{R}_{zw}(s)$ component.

The same behaviour has been observed of H_∞ equalisers. Paradoxically at low observation noise, the peak error is dominated by $R_{zv}(s)$. This arises because at high SNR, the equaliser can be quite successful at inverting the channel. At low observation noise when σ_v^2 is large, the resulting equaliser is a very low magnitude, low-pass filter, with the result that the maximum of $|R_{zv}R_{zv}^H(s)|$ is much lower than the maximum of $|R_{zw}R_{zw}^H(s)|$. These claims are illustrated via the examples in Sections 5.3 and 5.4.

Appendix H

An extended Kalman smoother

The objective of this appendix is to seek improvements in the performance of FM demodulators. The demodulator that is often implemented in FM receivers is the phase-locked loop (PLL). A digital PLL is usually tuned for one operating point: typically an integrated circuit has connections for external components which allow the selection of the VCO centre frequency and loop filter. It turns out that the extended Kalman filter (EKF) reverts to the PLL under some simplifying assumptions.

There are two reasons why an EKF design can exhibit performance improvements compared to the PLL. Firstly, the time-varying EKF (which has an adaptive gain) generally outperforms the time invariant EKF [AM]. Secondly, while the PLL is conventionally tuned to one operating point, *a priori* modelling information (such as the measurement noise power for example) is easily encorporated into the EKF design.

It is well known that the performance of EKFs degrades with increasing measurement noise power. This appendix is intended to contribute to an understanding of EKF performance and, demonstrate that an extended Kalman smoother can be used to provide an improvement. The contents of this appendix is as follows. Section 1 reviews some smoothing literature that is relevant to Kalman filters (and potentially EKFs). A proposed formulation for an extended Kalman smoother is developed in Section 2. The results of some simulation studies are presented in Section 3.

H.1. A review of some smoothing techniques.

An survey of early smoothing contributions was compiled by Meditch [Me] in which the citations include the work of Kepler, Gauss, Kolmogorov, Wiener, Kalman, Bucy, Levinson, Bode and Shannon. Of particular interest here are smoothers that are potentially

applicable to the FM demodulation problem, in which a model nonlinearity appears in the output mapping, viz

$$\begin{aligned} x_{k+1} &= A_k x_{k)} + B_k w_k, \\ y_k &= c_k(x_{k)} + v_k. \end{aligned} \tag{1}$$

While nonlinear, continuous-time smoothing and linear, discrete-time smoothing have been dealt with extensively, for example see [LPS,L,RTS,Ma,FP,Me,Mo,C,NK], the subject of nonlinear, discrete-time smoothers appears to have received somewhat scant attention. Fixed interval and fixed point smoothing solutions for the continuous-time analogy of (1) have been detailed by [LPS] and [L] respectively. Some key results for discrete-time, linear, smoothing problems include [RTS,Ma,FP,Mo]. The Rauch-Tung-Striebel recursions rely on storing filtered estimates and then proceeding in reverse time [RTS]. Mayne's approach for fixed interval smoothing uses "Kalman's filtering theory to obtain an estimate using past observations, and optimal control theory to obtain an estimate using future observations". Mayne's fixed interval smoother formulation uses a linear combination of the past and future estimates which was presented again by Fraser and Potter [FP]. A standard formula is used for the optimum combination of two independent estimates, $\hat{x}_1$ (covariance Σ_1) and $\hat{x}_2$ (covariance Σ_2), namely

$$\begin{aligned} \hat{x} &= (\Sigma_1^{-1} + \Sigma_2^{-1})(\Sigma_1^{-1}\hat{x}_1 + \Sigma_2^{-1}\hat{x}_2), \\ \Sigma &= (\Sigma_1^{-1} + \Sigma_2^{-1})^{-1}. \end{aligned} \tag{2}$$

In a subsequent analysis [C] it is shown that the fixed interval smoother of [Ma,FP] can be derived without assuming that the forward and backward estimation errors are independent.

Moore obtained fixed lag smoothers by augmenting the state transition matrix and applying the Kalman filter [Mo]; further discussions of fixed point smoothers are detailed in [AM]. A lag 1 smoother arises by applying the Kalman filter to the model

$$\begin{aligned} \begin{bmatrix} x_{k+1} \\ \xi_{k+1} \end{bmatrix} &= \begin{bmatrix} A_k & 0 \\ I & 0 \end{bmatrix} \begin{bmatrix} x_k \\ \xi_k \end{bmatrix} + \begin{bmatrix} B_k \\ 0 \end{bmatrix} w_k, \\ y_k &= [C_k \;\; 0] \begin{bmatrix} x_k \\ \xi_k \end{bmatrix} + v_k. \end{aligned} \tag{3}$$

Approaches for nonlinear, discrete-time smoothing are discussed in [G] and [SM]. Gelb describes a continuous-discrete, linear Kalman filter and defines a backward signal model; these are used in fixed interval smoothing where a backward estimate (obtained by a backwards linearisation about each forward estimate), is combined with the forward estimate [G].

Sage and Melsa acknowledge stability problems with reverse-time solutions and evolve an adjoint state in their fixed interval smoother [SM]. They minimise a cost function for a linear, discrete-time, two point boundary value problem and obtain a Hamiltonian (that

is, canonical equations relating the forward and adjoint states). In the nonlinear case, they make use of forward linearisations and forward estimates in a recursion for a smoothed estimate.

More recently, Nagpal and Khargonekar describe a continuous-time, linear, fixed interval smoother in a H_∞ framework [NK]. Theodor, Shaked and de Souza [TSdS] have addressed linear, discrete-time, H_∞ smoothing problems. In particular, a H_∞ formulation for fixed lag smoother (using the model of [Mo]) is described in [TSdS]. Substituting $\gamma = \infty$ into the fixed interval H_∞ smoother of [TSdS], yields,

$$\begin{aligned} \hat{x}_{k+1} &= A_k\hat{x}_k + A_kP_kC_k(C_kP_kC_k + R)^{-1}(y_k - C_k\hat{x}_k), \\ \hat{\xi}_k &= (I + C_kR^{-1}C_kP_k^{-1})(A_k - B_kC_k^TR^{-1}C_k)^T\hat{\xi}_{k+1} + C_kR^{-1}(y_k - C_k\hat{x}_k), \end{aligned} \tag{4}$$

in which $\hat{\xi}_k$ is the adjoint state estimate, $\hat{x}_k$ is the forward state estimate and P_k is the forward error covariance. The fixed interval, smoothed estimate is given by $C_k(\hat{x}_k + P_k\hat{\xi}_k)$.

It turns out that Mayne's reverse time estimates arise from an adjoint model, even though this was not explicitly stated in [Ma]. Consider the system $x_{k+1} = A_kx_k + B_kw_k$, $y_k = Cx_k$, then an adjoint system is described by

$$\begin{aligned} \xi_k &= A_{k+1}^T\xi_{k+1} + C_{k+1}^Ty_{k+1}, \\ \Gamma_k &= B_k^T\xi_k. \end{aligned} \tag{5}$$

When observation noise is present, ie. $y_k = Cx_k + v_k$, with $E\{v_kv_k^T\} = R_k$, a standard approach is to whiten the observations, that is $\hat{\xi}_k = A_{k+1}^T\hat{\xi}_{k+1} - C_{k+1}^TR_{k+1}^{-1}y_{k+1}$. Optimal adjoint state estimates can be obtained by applying the Kalman filter recursions to (5), bearing in mind that the deterministic input $-C_{k+1}^TR_{k+1}^{-1}y_{k+1}$ is added to the predicted state, and that the outputs Γ_k are not available. The corrected estimates are

$$\hat{\xi}_{k/k} = \hat{\xi}_{k/k+1} - \kappa_kB_k\hat{\xi}_{k/k+1}, \tag{6}$$

$$\Theta_{k/k} = \Theta_{k/k+1} - \kappa_kB_k^T\Theta_{k/k+1}, \tag{7}$$

where $\kappa_{k+1} = \Theta_{k+1/k+1}B_{k+1}(I + B_{k+1}^T\Theta_{k+1/k+1}B_{k+1})^{-1}$ is the gain, and

$$\hat{\xi}_{k/k+1} = A_{k+1}^T\hat{\xi}_{k+1/k+1} - C_{k+1}^TR_{k+1}^{-1}y_{k+1}, \tag{8}$$

$$\Theta_{k/k+1} = A_{k+1}^T\Theta_{k+1/k+1}A_{k+1} + C_{k+1}^TR^{-1}C_{k+1}, \tag{9}$$

are the predicted estimates. Actually (6) and (8) are equivalent to (33) of [Ma]; (7) and (9) are equivalent to (32) of [Ma].

H.2. The development of an extended Kalman smoother.

A standard solution for the problem (1) is the EKF [AM], in which the output linearisation is given by

$$C_k = \left[\frac{\partial c_k(x)}{\partial x}\right]_{x=\hat{x}_{k-1}}. \tag{10}$$

The application of the EKF to an FM demodulation problem is described in Section 3.

In [G] the philosophy is to produce a backward prediction from each forward correction and combine them via (2). A backwards version of $x_{k+1} = Ax_k + Bw_k$ is given by $x_k = A^{-1}(x_{k+1} - Bw_k)$. If the plant is stable (ie. A's eigenvalues are inside the unit circle), then the backwards plant (having a state transition matrix of A^{-1}) is not. For example in a linear FM model, $A = \begin{bmatrix} \mu & 0 \\ 1 & \lambda \end{bmatrix}$ with $0 < \mu < 1$, $0 < \lambda < 1$, clearly the backwards plant with $A^{-1} = \begin{bmatrix} \mu^{-1} & 0 \\ -\mu^{-1}\lambda^{-1} & \lambda^{-1} \end{bmatrix}$ is unstable. This approach was also attempted for the FM demodulation problem. It was found that the backward predictions diverged markedly from the forward corrected estimates (because A^{-1} is unstable), with the result that there was no improvement on the EKF.

In contrast to Gelb's method, in Mayne's approach the adjoint transition matrix is stable. Therefore an adjoint version of the forward EKF is required. The adjoint state and forward state estimates may then be combined via the smoothing formula (2). One possible technique is to retain the linearisations (10) from a forward EKF and then apply the adjoint Kalman filter (6)-(9), to produce estimates of the adjoint states. However, it turned out for the FM problem, that the adjoint estimates were too erroneous for the smoother to improve on a EKF. This method is unsatisfactory because the output mapping in (1) is a nonlinear function of the state, so swapping the parameters $[A_k, B_k, C_k]$ with $[A_k^T, -C_k^T, -B_k^T]$ does not necessarily result in an adjoint system.

A better approach arises by recasting the problem so that the output mapping is decoupled from the state, that is by defining $y_k = C_k x_k + v_k$ and

$$C_k = \frac{c_k(x_k)}{x_k}. \tag{11}$$

The above linearisation allows the direct application of the adjoint Kalman filter (6) - (9) and the subsequent construction of a smoother. This technique can result in some success at low SNRs, but the linearisation (11) must be applied carefully. For example in an FM problem (see Section 3), although $\frac{\sin\varphi}{\varphi}$ is finite at $\varphi = 0$, $\frac{\cos\varphi}{\varphi}$ has a singularity at $\varphi = 0$, consequently a different observation, namely $1 - \cos\varphi$, needs to be considered in lieu of

cos φ. However this solution has been found to be unsatisfactory at high SNRs. The difficulty is that the approximate linearisation (11) can lead to a poor state reconstruction, even when the measurement noise is low; any linearisation inaccuracies are then amplified by the factor R^{-1} in (9).

An evolution for the adjoint state of (1), which can sometimes lead to successful smoother performance is

$$\hat{\xi}_k = A_{k+1}^T \hat{\xi}_{k+1} - [c_{k+1}^{-1}(y_{k+1})]^T, \tag{12}$$

in which it is convenient to introduce $c_k^{-1}(c_k(x_k)) = x_k$, provided that $c_k^{-1}(\,.\,)$ exists and is well defined. Suppose that there is no measurement noise, then substituting $y_{k+1} = c_{k+1}(x_{k+1})$ into (12) yields $\xi_k = A_{k+1}^T \xi_{k+1} - x_{k+1}$, which dispenses with the need for any linearisation.

An extended Kalman smoother for the problem (1) therefore comprises: evolving adjoint state estimates via (6), (7), (12), from the observed data, obtaining forward state estimates via an EKF and, calculating the smoothed estimates using (2).

H.3. An example.

This section begins with a brief examination of a linear filtering problem in order to provide some insight into a FM demodulation problem. Consider the linear system

$$x_{k+1} = Ax_k + Bw_k\,, \quad y_k = Cx_k + v_k \tag{13}$$

in which $A = \begin{bmatrix} \mu & 0 \\ 1 & \lambda \end{bmatrix}$, $B = \begin{bmatrix} 1 \\ 0 \end{bmatrix}$, $C = [0 \;\; 1]$. Since $[C^T, A^T C^T] = \begin{bmatrix} 0 & 1 \\ \rho & \lambda \end{bmatrix}$ is nonsingular provided $\rho \neq 0$, the system (13) is observable, that is, the states can be recovered from the observations. Let $x_k = \begin{bmatrix} \omega_k \\ \varphi_k \end{bmatrix}$ where ω_k and φ_k denote the instantaneous frequency and phase respectively. The phase update in (13) is given by

$$\varphi_k = \lambda\varphi_{k-1} + \hat{\omega}_{k-1}. \tag{14}$$

Consider the stationary filtering problem for the system (13), in the absence of phase errors and observation noise. Substituting $P = \begin{bmatrix} p & 0 \\ 0 & 0 \end{bmatrix}$ into the Riccati equation for the Kalman filter corresponding to (13) yields $p \approx \sigma_\omega^2$. It follows that the correction in the frequency estimate is given by

$$\hat{\omega}_{k/k} \approx \hat{\omega}_{k/k-1} + \mu(\varphi_k - \hat{\varphi}_{k/k-1}), \tag{15}$$

in which φ_k denotes the zero phase error measurement. The phase prediction is

$$\hat{\varphi}_{k/k-1} = \lambda\hat{\varphi}_{k-1/k-1} + \hat{\omega}_{k-1/k-1}. \tag{16}$$

Subtracting (16) from (14) yields $\varphi_k - \hat{\varphi}_{k/k-1} \approx \omega_{k-1} - \hat{\omega}_{k-1/k-1}$ and substitution into (15) leads to $\hat{\omega}_{k/k} \approx \mu\omega_{k-1}$. Thus the frequency estimate lags one time step behind the phase estimate and an appropriate definition for the frequency estimation error is

$$\tilde{\omega}_k = \omega_{k-1} - \hat{\omega}_{k/k}. \tag{17}$$

It is possible to compare the error spectra for the optimal causal filter and, for the optimal noncausal filter, having a transfer function $H = (\Delta - R\Delta^{-H})\Delta^{-1}$, where $\Delta\Delta^H = GQG^H + R$ and $G = C(zI - A)^{-1}B$. It is easily confirmed that the noncausal filter provides a reduction in mean square error. Therefore it is expected that fixed interval smoothing would be of some benefit.

Now consider instead the nonlinear system

$$\omega_{k+1} = \mu\omega_k + w_k, \tag{18}$$

$$\varphi_{k+1} = \lambda\varphi_k + \rho\omega_k, \tag{19}$$

$$y_k^{(1)} = \cos\varphi_k + v_k^{(1)}, \tag{20}$$

$$y_k^{(2)} = \sin\varphi_k + v_k^{(2)}, \tag{21}$$

in which the $y_k^{(1)}$ and $y_k^{(2)}$ denote the real and imaginary measurements. From an analysis of a sampled continuous-time, narrow-band, FM voice problem [W], it was determined that suitable parameters values are $\mu = 0.75$, $\lambda = 1$, $\rho = 0.25$ and $\sigma_w = 0.4$.

In the case of (20), (21), the output mapping is $c_k = \begin{bmatrix} \cos\hat{\varphi}_{k/k-1} \\ \sin\hat{\varphi}_{k/k-1} \end{bmatrix}$ and the linearisation for the forward EKF is $C_k = \begin{bmatrix} -\sin\hat{\varphi}_{k/k-1} \\ \cos\hat{\varphi}_{k/k-1} \end{bmatrix}$. In this example, it turns out that the EKF is difficult to improve upon. For example the iterated-EKF [J], a standard approach for reducing the effect of linearisation errors, was not found to offer any advantage for this problem. Even at negative SNRs the EKF was observed to be phase-locked (that is the phase errors were very small). Indeed, when the problem is locally linear, the EKF reverts to the Kalman filter, which is the optimum filter from the set of all possible linear filters [AM].

An extended Kalman smoother was constructed in which the adjoint state prediction is given by

$$\hat{\xi}_{k/k+1} = A^T\hat{\xi}_{k+1/k+1} + \begin{bmatrix} 0 \\ \sigma_v^{-2}(\arccos y_{k+1}^{(1)} + \arcsin y_{k+1}^{(2)}) \end{bmatrix}, \tag{22}$$

in which the $y_k^{(i)}$ are amplitude limited to ensure that $| y_k^{(i)} | \leq 1$. It was found that while this met with some success, better performance was obtained via

$$\hat{\xi}_{k/k+1} = A^T\hat{\xi}_{k+1/k+1} + \sigma_v^{-2}\begin{bmatrix} \hat{\varphi}_{k+1} \\ \hat{\omega}_{k+1} \end{bmatrix}, \tag{23}$$

where the state estimates $\hat{\varphi}_{k+1}$, $\hat{\omega}_{k+1}$, arise from a forward EKF. While the use of σ_v^2 in (23) is conservative, it was found that a reduction in the design observation noise results in a performance degradation.

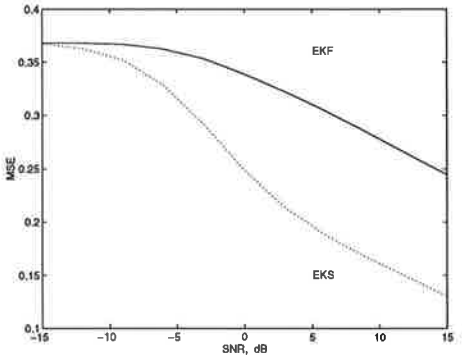

Fig. H.1. Performance using criterion (24).

Simulations were conducted with SNRs in 3 dB steps, from -15 db to 15 dB, for 500 realisations of 500 data points each. The error in the frequency estimate may defined conventionally as

$$\tilde{\omega}_k = \omega_k - \hat{\omega}_{k/k}. \tag{24}$$

A plot of the observed mean square error per realisation versus SNR is shown in Figure H.1. In this example, it has been observed that the EKF remains phase-locked, even at -15 dB SNR. Furthermore, when the EKF is phase-locked, the frequency estimate lags one time step behind the phase estimate. Therefore the criterion (24) does not reflect the actual EKF performance. The mean square error per realisation was recalculated according to (17) and is shown in Figure H.2. From a comparison with Figure H.1, it can be seen for this example that the use of the criterion (24) leads to a conservative perception of filter and smoother performance.

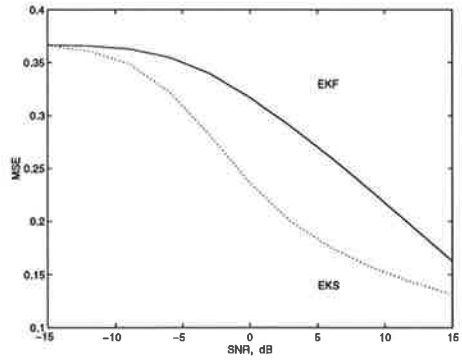

Fig. H.2. Performance using criterion (17).

It can be seen that smoothing can be beneficial at intermediate SNRs but diminishes for both very low and very high SNRS. At 3 dB SNR, it turns out that the extended Kalman smoother (EKS) provides a performance improvement of 5 dB compared to the EKF. In

general, a filter has a reduced gain (and a commensurately increasing lag), as the measurement noise is increased. Since the smoother combines the lagging and leading estimates, a benefit can occur, provided that both estimates are reasonably good. At very low SNR, the estimates become erroneous (they may well have opposite polarity), in which case smoothing is not effective. Conversely, at very high SNR, the estimates are already good and smoothing is superfluous.

An approach which may yield low SNR performance improvements is to combine the philosophy of gaussian sums [AM] together with the competitive smoothing approach of [NS]. In particular, it may be useful to evaluate a cost function over a sliding window in order to select between differently initialised extended Kalman smoothers.

H.4. Conclusions.

A discrete-time, fixed-interval, extended Kalman smoother is described, which reverts to the Kalman smoother when the model is linear. The smoother arises by combining forward estimates from the EKF, with the adjoint estimates, via the so-called Fraser-Potter smoother. Although a backward recursion is proposed for evolving the adjoint states from the measurements, in practice it is better use forward state estimates as inputs to the adjoint system.

The results of a simulations study show that the benefits of smoothing are negligible at both very high and ver low SNRs. However at 3 dB SNR, the extended Kalman smoother provides a 5 dB reduction in mean square error. Comparisons with actual FM voice data will be undertaken in ongoing work.

It would appear that the performance of fixed interval smoothers is not as good as the optimal noncausal filter which arises in Wiener filtering. Therefore the pursuit of a time-varying formulation for the optimal, noncausal, nonlinear filter will be a subject of ongoing research.

Acknowledgements.

The author is grateful to Lang White and Brian Anderson, who analysed the sampled data problem and provided the discrete-time model used herein.

REFERENCES.

[AM] Anderson, B. D. O. and J. B. Moore, *Optimal filtering*, Prentice-Hall, Englewood Cliffs, New Jersey, p. 108, 1979.

[C] Catlin, D. E., "The independence of forward and backward estimation errors in the two-filter form of the fixed interval Kalman smoother", *IEEE Trans. Automat. Contr.*, vol. AC-25, no. 6, pp. 1111-1115, Dec. 1980.

[FP] Fraser, D. C., and J. E. Potter, "The optimum linear smoother as a combination of two optimum linear filters", *IEEE Trans. Automat. Contr.*, vol. AC-14, pp. 387-390, Aug. 1969.

[G] Gelb, A., *Applied Estimation Theory*, M.I.T. Press, Cambridge, MA, pp. 200-203, 1974.

[J] Jazwinski, A. H., *Stochastic processes and filtering Theory*, Academic Press, N.Y., pp. 279-281, 1970.

[L] Lee, G. M., "Nonlinear interpolation", *IEEE Trans. Inform. Theory*, vol. IT-17, no. 1, pp. 45-49, Jan. 1971.

[LPS] Leondes, C. T., J. B. Peller and E. B. Stear, "Nonlinear smoothing theory", *IEEE Trans. Sys. Sci. Cyb*, vol. SSC-6, pp. 63-71, Jan. 1970.

[Ma] Mayne, D. Q., "A solution of the smoothing problem for linear dynamic systems", *Automatica*, vol. 4, pp. 73-92, 1966.

[Me] Meditch, J. S., "A survey of data smoothing for linear and nonlinear dynamic systems", *Automatica*, vol. 9, pp. 151-162, 1973

[Mo] Moore, J. B., "Discrete-time fixed-lag smoothing algorithms", *Automatica*, vol. 9, pp. 163-173, 1973.

[NK] Nagpal, K. M. and P. P. Khargonekar, "Filtering and smoothing in an H_∞ setting", *IEEE Trans. Automat. Contr.*, vol. 36, no. 2, pp. 152-166, Feb. 1991.

[NS] M. Niedzwieki and W. A. Sethares, "Smoothing of discontinuous signals: the competitive approach", *IEEE Trans. Sig. Proc.*, vol. 43, no. 3, pp. 1 - 13, Jan. 1995.

[RTS] H. E. Rauch, F. Tung and C. T. Striebel, "Maximum likelihood estimates of linear dynamic systems", *AIAA*, vol. 3, pp. 1445-1450, 1965.

[SM] Sage, A. P., and J. L. Melsa, *Estimation theory with applications to communications and control*, McGraw-Hill Book Company, New York, 1971.

[TSdS] Theodor, Y., U. Shaked and C. E. de Souza, "A game theory approach to robust discrete-time H_∞ -estimation", *IEEE Trans. Sig. Proc., vol. 42, no. 6, pp. 1486 - 1495, Jun. 1994.*

[W] White, L. B., "A comparison of digital FM demodulators", SA/95/05U, Communications Division, DSTO Australia, May 1995.